



**This electronic thesis or dissertation has been
downloaded from Explore Bristol Research,
<http://research-information.bristol.ac.uk>**

Author:
Redfern, Jonathan

Title:
The sedimentology and stratigraphy of the permo-carboniferous Grant group, Barbwire Terrace, Canning Basin, Western Australia.

General rights

Access to the thesis is subject to the Creative Commons Attribution - NonCommercial-No Derivatives 4.0 International Public License. A copy of this may be found at <https://creativecommons.org/licenses/by-nc-nd/4.0/legalcode>. This license sets out your rights and the restrictions that apply to your access to the thesis so it is important you read this before proceeding.

Take down policy

Some pages of this thesis may have been removed for copyright restrictions prior to having it been deposited in Explore Bristol Research. However, if you have discovered material within the thesis that you consider to be unlawful e.g. breaches of copyright (either yours or that of a third party) or any other law, including but not limited to those relating to patent, trademark, confidentiality, data protection, obscenity, defamation, libel, then please contact collections-metadata@bristol.ac.uk and include the following information in your message:

- Your contact details
- Bibliographic details for the item, including a URL
- An outline nature of the complaint

Your claim will be investigated and, where appropriate, the item in question will be removed from public view as soon as possible.

**THE SEDIMENTOLOGY AND STRATIGRAPHY OF THE PERMO-CARBONIFEROUS
GRANT GROUP, BARBWIRE TERRACE, CANNING BASIN,
WESTERN AUSTRALIA.**

**Volume 2
Figures, Plates and Appendices**

JONATHAN REDFERN

A thesis submitted to the University of Bristol
in accordance with the requirements for the degree
of Doctor of Philosophy in the Faculty of Science,
Department of Geology, August 1990.

LIST OF FIGURES

- Figure 1. Map of Australia, with inset of the United Kingdom for size comparison.
- Figure 2. Permo-Carboniferous sedimentary basins of Australia.
- Figure 3. The Canning Basin, location map and main structural elements.
- Figure 4. Schematic structural cross section across the Canning Basin.
- Figure 5. Study area location map, displaying WMC licence areas.
- Figure 6. Location map, highlighting cored wells incorporated in the study.
- Figure 7. Structural framework of the study area.
- Figure 8. Detailed tectonics elements map for the north Canning Basin, displaying possible en-echelon transfer faults.
- Figure 9. Regional Bouguer gravity anomaly contour map over the study area.
- Figure 10. Base Grant Unconformity structure in time contour map
- Figure 11. Generalised stratigraphic column for the Canning Basin.
- Figure 12. Reconstruction of the northwest margin of Australia during the Late Carboniferous to Early Triassic.
- Figure 13. Reconstruction of the northwest margin of Australia during the Triassic and Early Jurassic.
- Figure 14. A model for continental ice sheet margin fluctuations
- Figure 15. Periodicity of ice sheet fluctuations.
- Figure 16. Reconstruction of Gondwanan palaeogeography from the Late Devonian to Early Permian, showing inferred major ice centres.
- Figure 17. Continental reconstruction showing the relative position of Australia in the Late Devonian, Early Permian, Late Jurassic and Tertiary.
- Figure 18. Flow lines for the Antarctic ice sheet, displaying multiple ice centres.
- Figure 19. Distribution of major ice centres in Australia during the Permo-Carb.
- Figure 20. Solid geology of the study area.
- Figure 21. Composite stratigraphy for the Grant Group of the Canning Basin.
- Figure 22. Dating of the Permo-Carboniferous Grant Group.
- Figure 23. Location of the type sections for the Wye Worry and Millajiddee Members.
- Figure 24. A detailed section of graded beds recorded from the Wye Worry Member.
- Figure 25. Section of cross bedded and ripple laminated sandstone of the Millajiddee Member.

- Figure 26. Stratigraphic Framework of the Grant Group on the Barbwire Terrace.
- Figure 27. Stratigraphic correlation between Hoya 1, Calytrix 1, Clianthus 1 and Melaleuca 1.
- Figure 28. Stratigraphic correlation between Drosera 1, Caladenia 1, Halganina 1 and Melaleuca 1
- Figure 29. Stratigraphic correlation between Eremophila 1, 2, 3 and Ficus 1.
- Figure 30. Stratigraphic correlation between Kunzea 1, Drosera 1, Goodenia 1 and Aristida 1A.
- Figure 31. Detailed facies correlation of Hoya 1, Calytrix 1 and Clianthus 1
- Figure 32. Detailed facies correlation between Eremophila 1, 2 and 3.
- Figure 33. Seismic line 82-20A.
- Figure 34. Pre-Grant structure and the variability of subcropping formations.
- Figure 35. Interpretation of two regional seismic lines running SW to NE across the Fitzroy Graben.
- Figure 36. Summary correlations between the Barbwire Terrace stratigraphy, Lake Betty 1 and St. George Range 1
A. Correlation of the Barbwire Terrace stratigraphy with the previously defined stratigraphy for Lake Betty 1, extended to St George Range 1.
B. Proposed revision to the stratigraphy for St George Range 1, and its correlation to Lake Betty 1 and the Barbwire Terrace.
- Figure 37. Correlation between the Barbwire Terrace Grant Group stratigraphy defined in this thesis and the published stratigraphy for Lake Betty 1.
- Figure 38. Correlation between the Grant Group section on the Barbwire Terrace, and that recorded from Lake Betty 1 and St. George Range 1.
- Figure 39. The main elements of the sequence stratigraphic depositional model.
- Figure 40. Comparison of the 'Depositional Sequence' with the 'Genetic Sequence'.
- Figure 41. The main elements of seismic acquisition.
- Figure 42. A. Reflection relationships within an idealised seismic sequence.
B. Examples of diagnostic reflection configurations.
- Figure 43. Base Grant Unconformity Structure in Time Map for the Eremophila area.
- Figure 44. Depth to Base Grant Unconformity for the Eremophila area.
- Figure 45. Detail of seismic line 82-24 (see Enclosure 2) and large mounded feature was cored by Drosera 1.
- Figure 46. Regional interpretation of the 'mounded seismic facies'.
- Figure 47. Proposed depositional environment for the sandstones encountered in Drosera 1 and Kunzea 1.
- Figure 48. Detail of seismic line 82-20A.

- Figure 49. Sequence stratigraphic interpretation for the Grant Group .
- Figure 50. Classification of glacial deposits.
- Figure 51. Key to facies log annotation.
- Figure 52. Typical facies logs for the Basal Diamictite Facies Association (BD).
- Figure 53. Detail of the Base Grant Unconformity in Hoya 1.
- Figure 54. A section of the Hoya Formation from Eremophila 3.
- Figure 55. Models for deposition from ice sheets with base at melting point.
- Figure 56. Typical facies logs for the diamictite facies.
- Figure 57. Detail of a stratified diamictite from Aristida 1.
- Figure 58. The relationship and gamma-ray log character of Sandstone Facies 1 and Sandstone Facies 2 from Drosera 1.
- Figure 59. Typical facies logs for the Hoya sandstone facies.
- Figure 60. The stability field for different bedforms in water depths of 20cm.
- Figure 61. A. Block diagram illustrating the deposition of sheet sandstones within a braided river system.
B. Definition diagram for different bar types on a sandy river bed.
- Figure 62. Typical facies logs for Hoya Formation Sandstone Facies 4 to 7.
- Figure 63. Structures and textures of deposits from mass-gravity-flows.
- Figure 64. A. The divisions of the idealised 'Bouma' sequence.
B. Idealised change in turbidite character due to waning flow for proximal and distal locations.
- Figure 65. Detail of Sandstone Facies 2 in Drosera 1
- Figure 66. Depositional model for an ice marginal locations, applicable to much of the Hoya Formation.
- Figure 67. Summary depositional model for the Hoya Formation.
- Figure 68. Facies distribution and classification in the subglacial and supraglacial environment.
- Figure 69. Facies distribution and classification at the margins of an ice sheet.
- Figure 70. A schematic representation of the wide variety of facies deposited proximal to an ice sheet.
- Figure 71. Two models for ice marginal sedimentation.
- Figure 72. Possible ice advance and retreat cycles recorded in the Hoya Formation of Eremophila 3.
- Figure 73. Possible mechanism for the formation of isolated shelf sandbodies.

- Figure 74. Typical facies logs for the Cliaanthus Formation.
A. Sandstone facies
B. Heterolithic facies.
- Figure 75. Characteristics of wave-generated ripples.
- Figure 76. Combined summary depositional model for the Calytrix and Cliaanthus Formations.
- Figure 77. A model for the evolution of the Grant Group sedimentary package in relation to the ice sheet dynamics and changes in relative sea level.
- Figure 78. Map showing the various stages in the retreat of the Laurentide ice sheet.
- Figure 79. Map to show the size of the Ross ice sheet.
- Figure 80. Comparison in size between the Canning Basin and the Ross Ice shelf of Antarctica.
- Figure 81. Schematic model for the distribution of ice in the Canning Basin area during the Perm-Carboniferous

LIST OF APPENDICES

APPENDIX 1 Facies Logs.

1. Aristida 1
2. Aristida 1A
3. Caladenia 1
4. Calytrix 1
5. Drosera 1
6. Eremophila 1
7. Eremophila 2
8. Eremophila 3
9. Ficus 1
10. Halgania 1
11. Hoya 1
12. Kunzea 1
13. Melaleuca 1
14. Triodia 1

APPENDIX 2 Well Data Sheets

1. Aristida 1
2. Aristida 1A
3. Caladenia 1
4. Calytrix
5. Clianthus
7. Drosera 1
8. Eremophila 1
9. Eremophila 2
10. Eremophila 3
11. Ficus 1
12. Goodenia
13. Halgania 1
14. Hoya 1

15. Kunzea 1

16. Melaleuca 1

17. Triodia 1

APPENDIX 3 MICROPALAEONTOLOGICAL ANALYSIS (V. Palmieri)

ENCLOSURE 1 GEOSEISMIC INTERPRETATION OF LINE 82-24 (East)

ENCLOSURE 2 GEOSEISMIC INTERPRETATION OF LINE 82-24 (West)

FIGURES

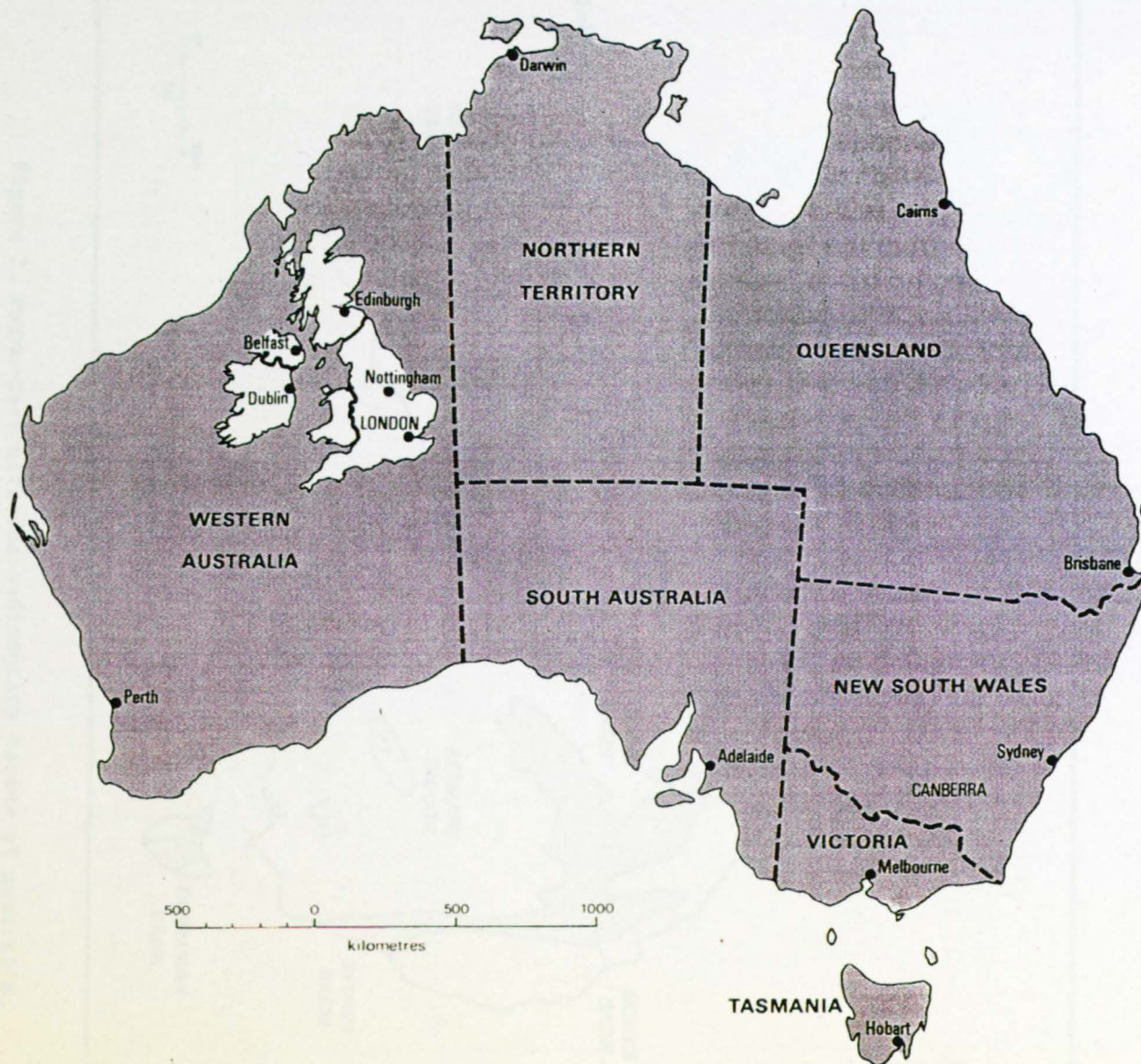


Figure 1. Map of Australia, with inset of the United Kingdom for size comparison.

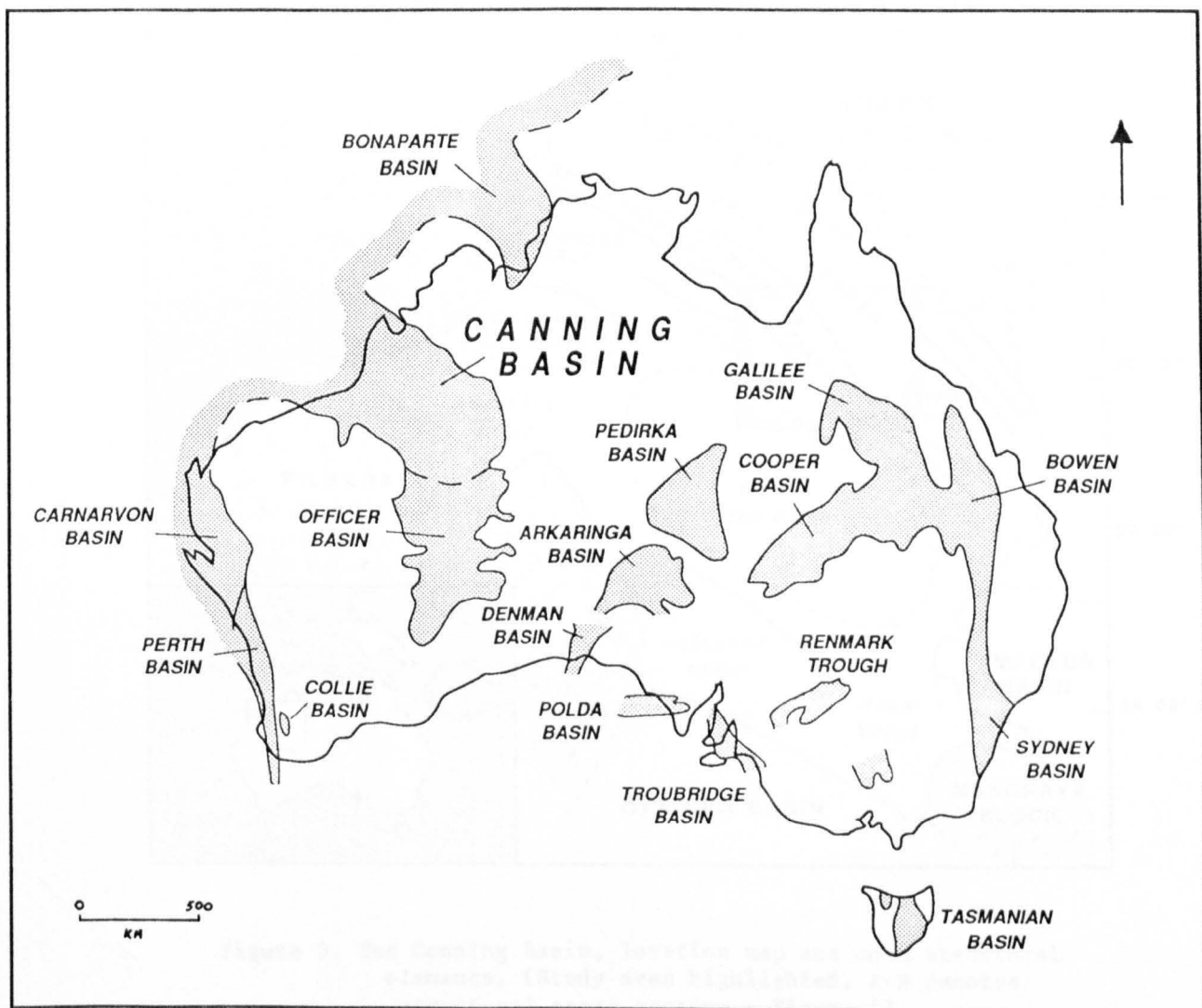


Figure 2. Permo-Carboniferous sedimentary basins of Australia.

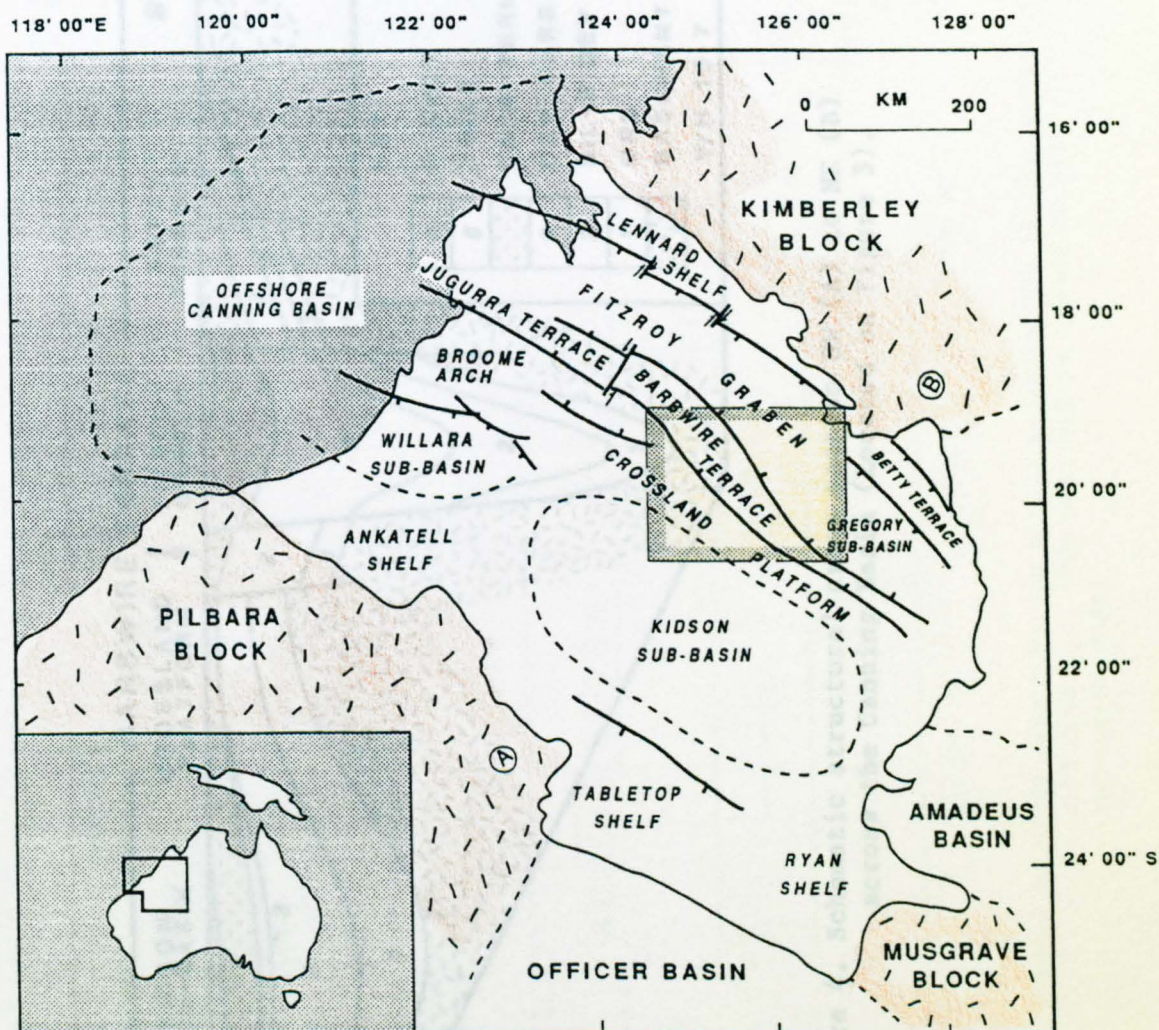


Figure 3. The Canning Basin, location map and main structural elements. (Study area highlighted, A-B denotes structural cross section - Figure 4).

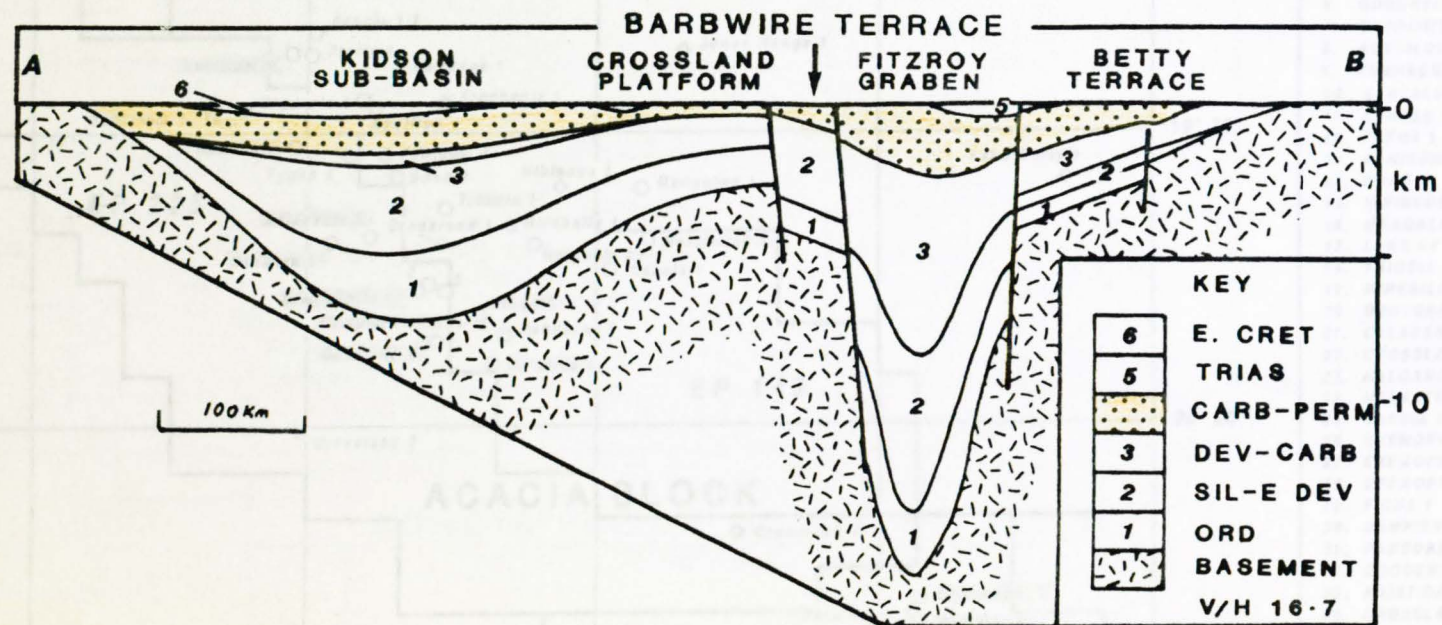


Figure 4. Schematic structural cross section SW (A) to NE (B) across the Canning Basin (Located on Figure 3).

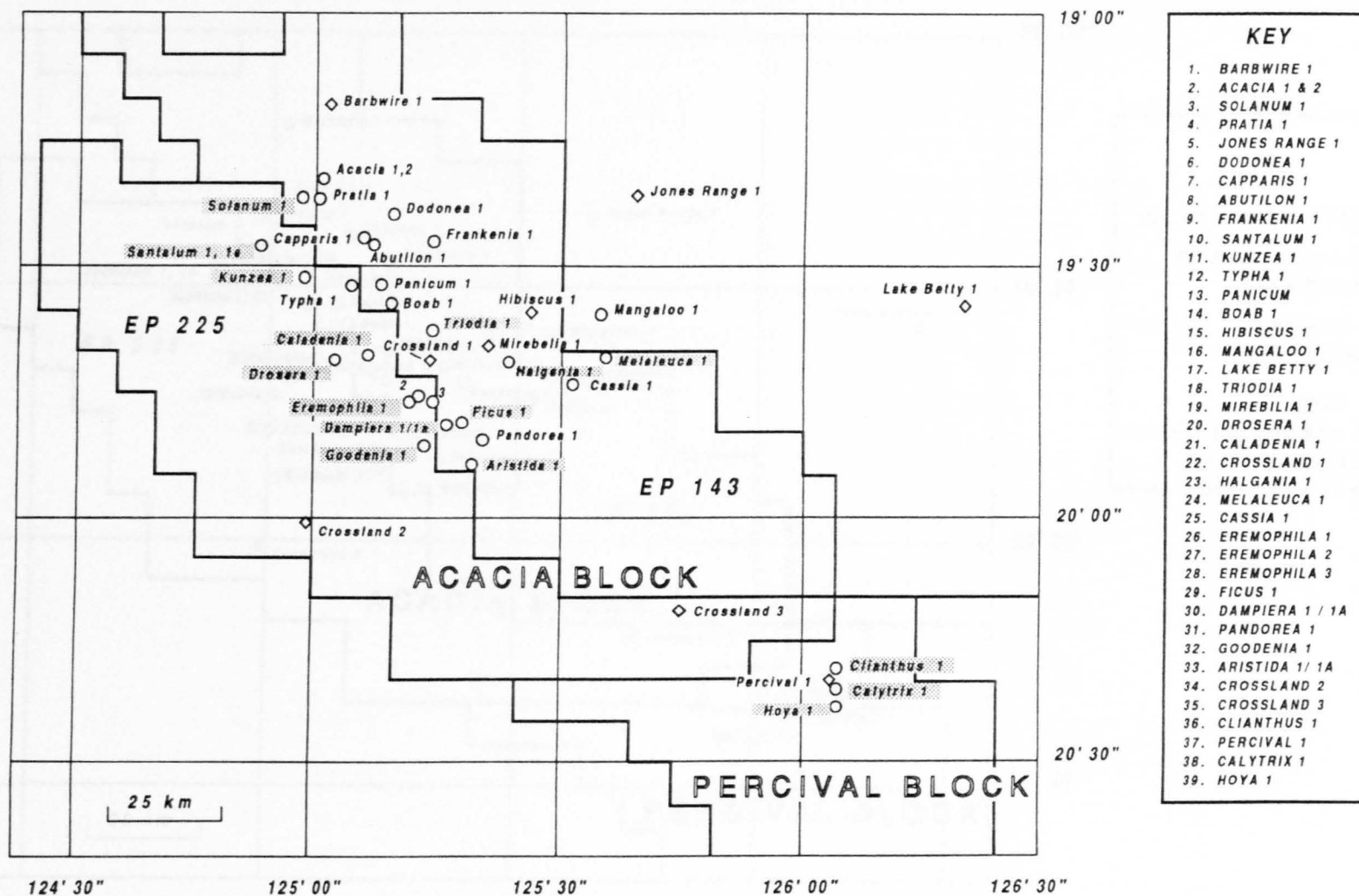


Figure 5. Study area location map, displaying WMC licence areas and well coverage. (The well key is common to all subsequent maps)

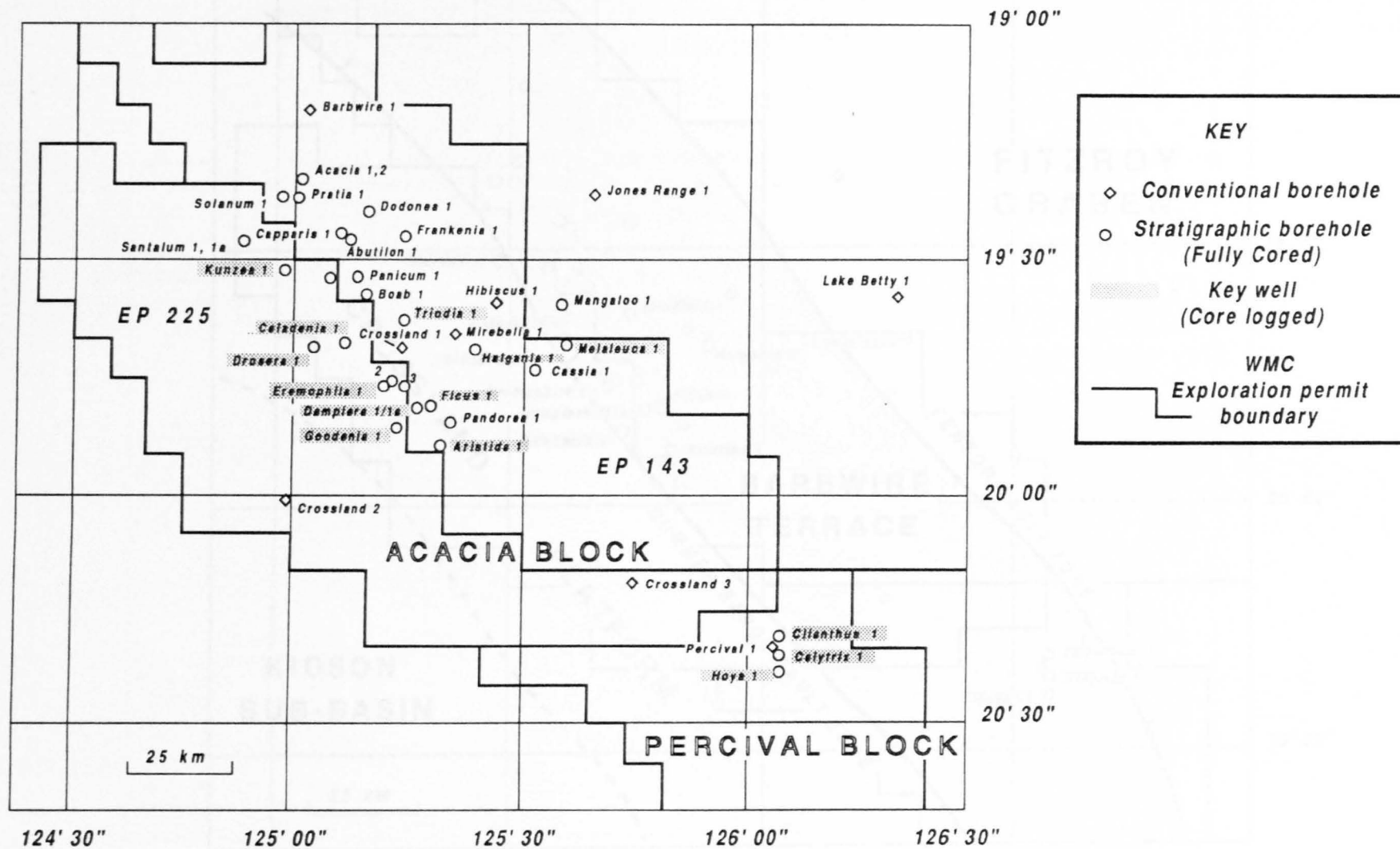


Figure 6. Location map, highlighting cored wells incorporated in the study. (The wells symbols are common to all subsequent maps)

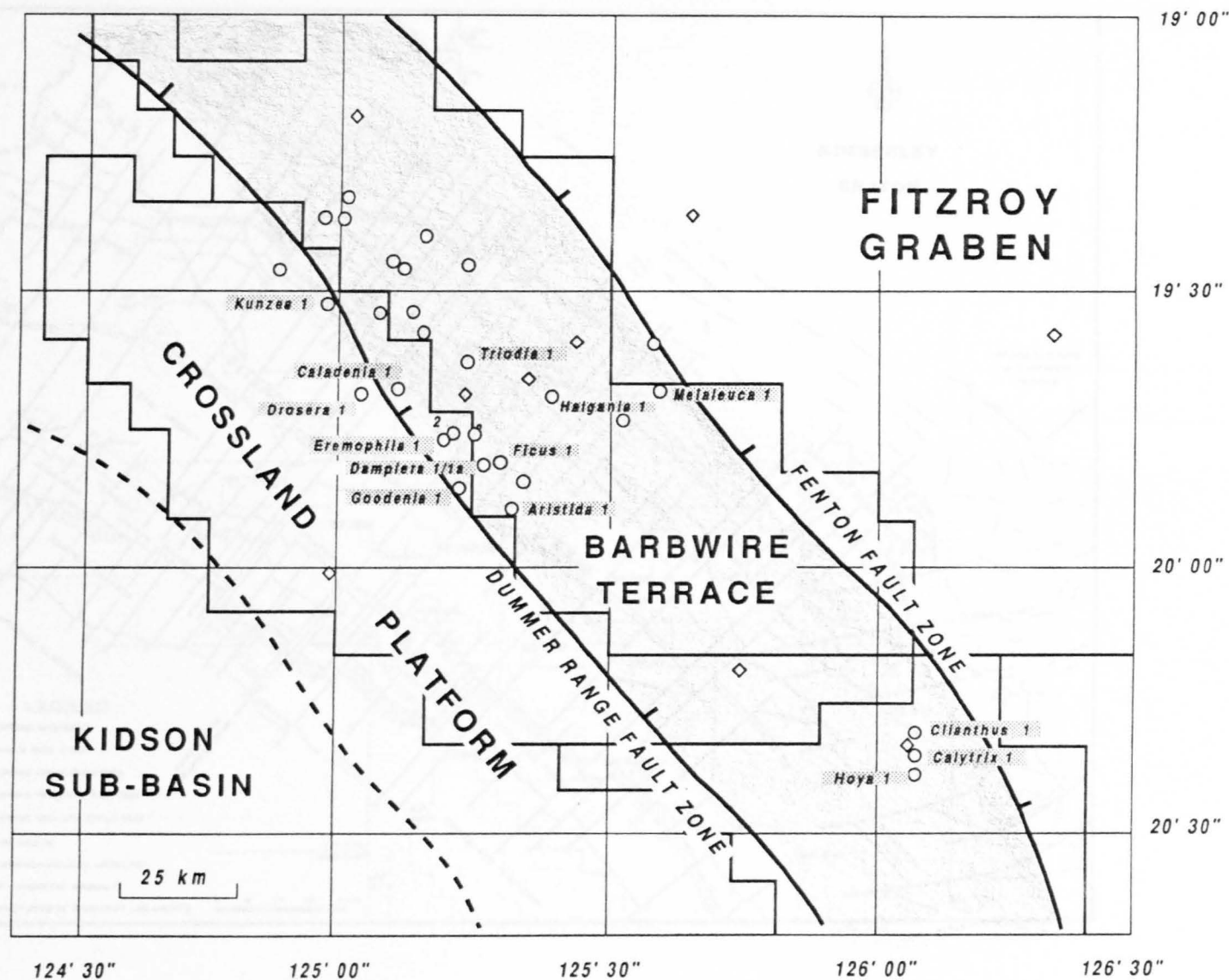


Figure 7. Structural Framework of the study area.

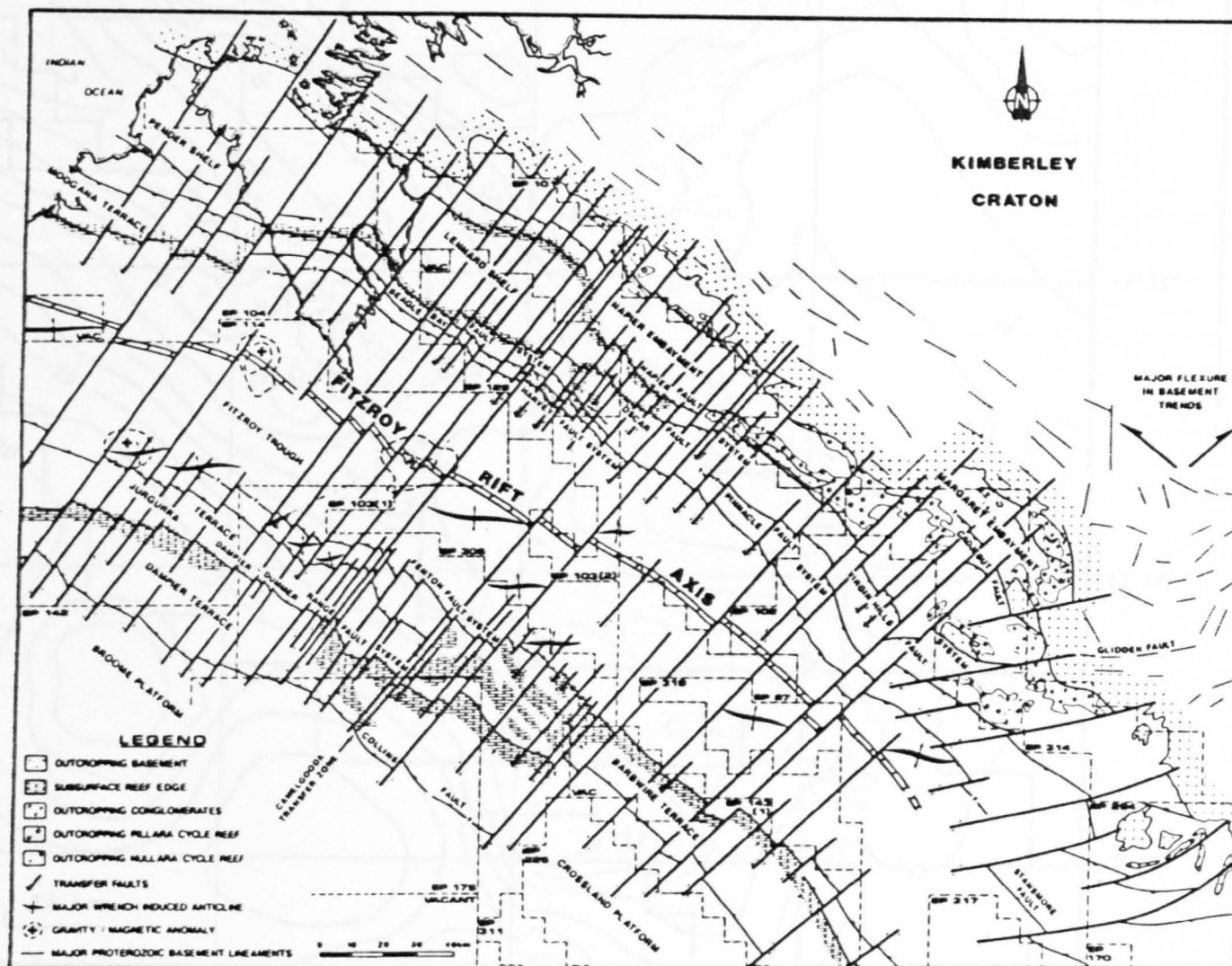


Figure 8. Detailed tectonics elements map for the north Canning Basin, displaying possible en-echelon transfer faults. (From Begg 1987)

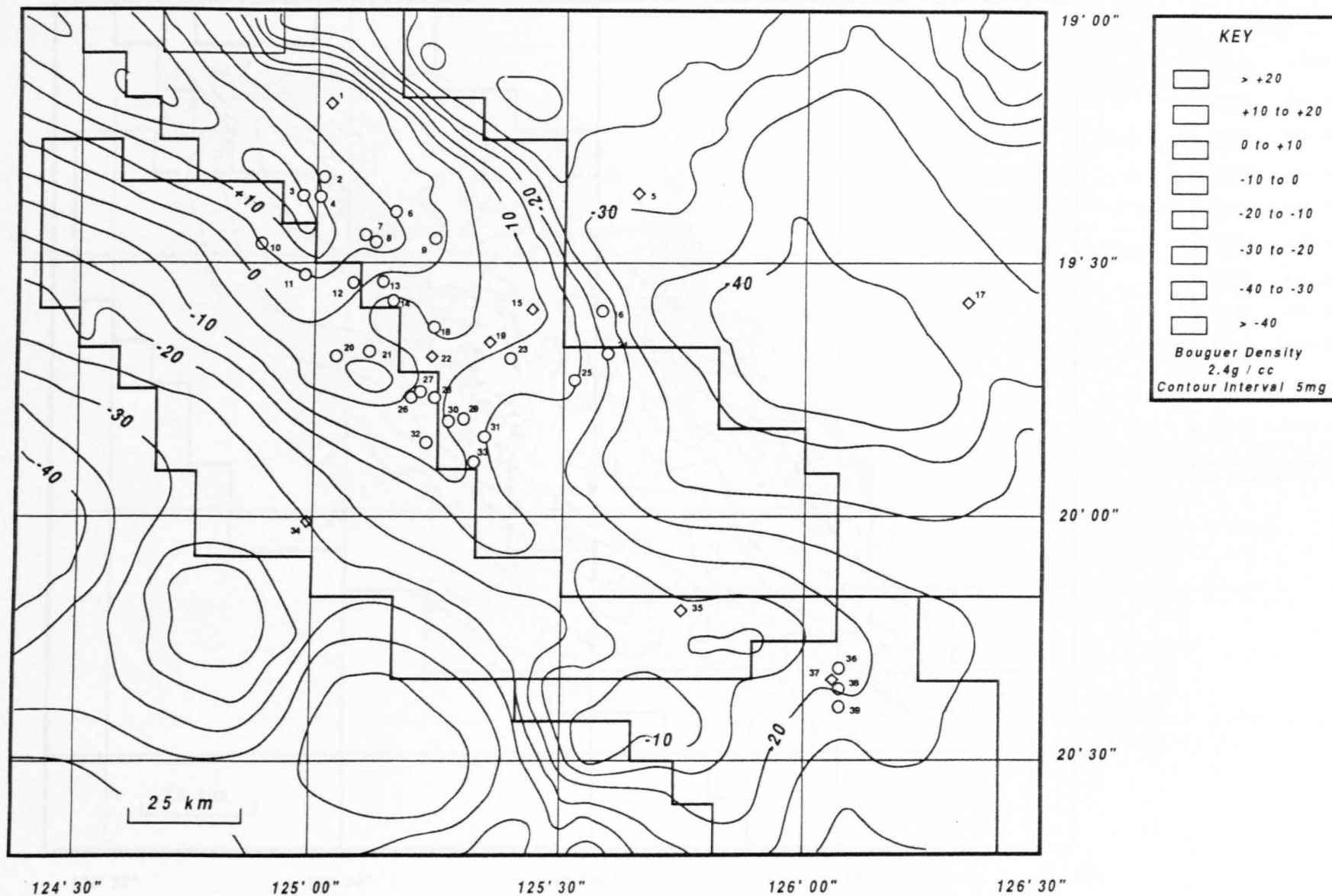


Figure 9. Regional Bouguer gravity anomaly contour map over the study area. (from WMC proprietry data)

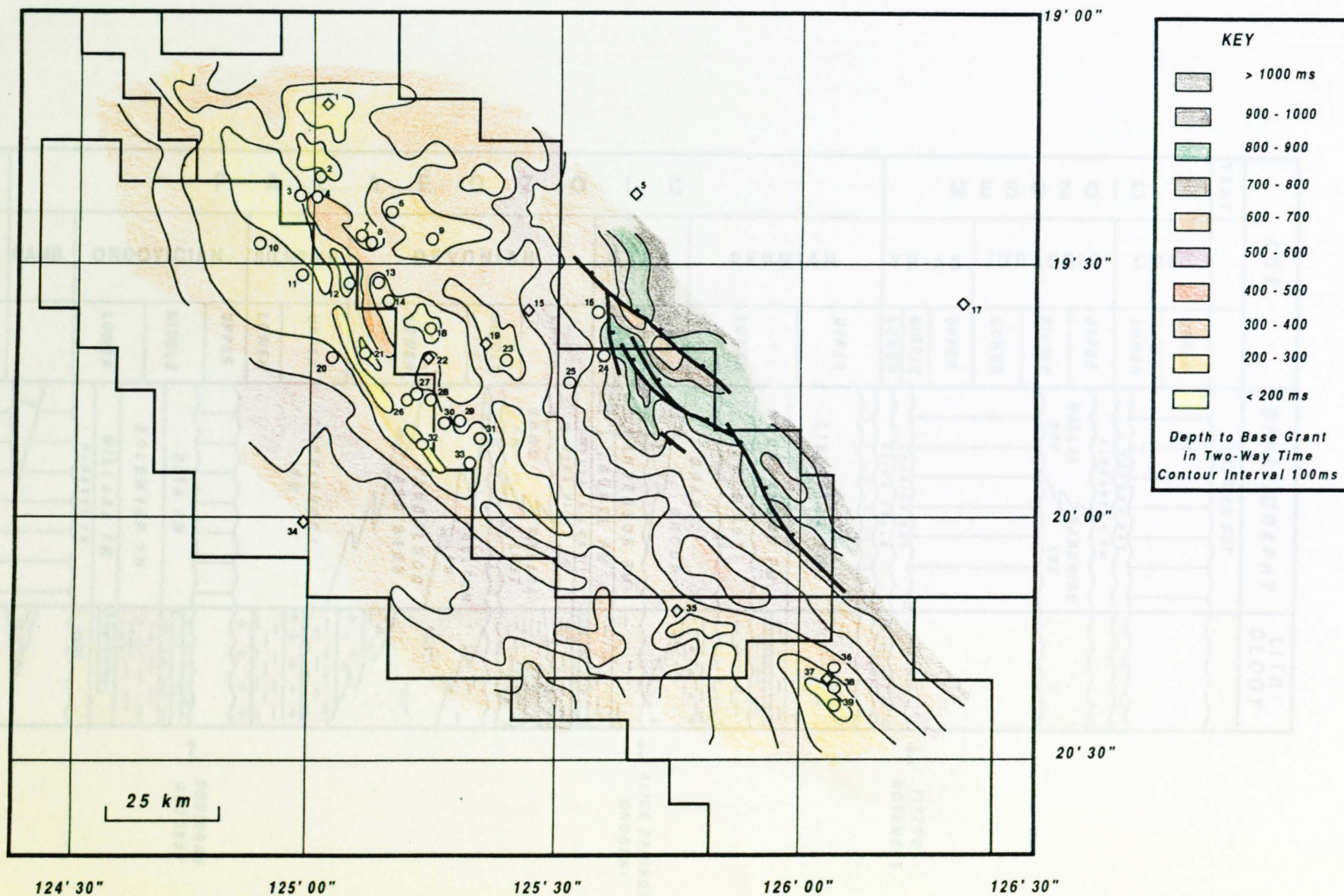


Figure 10. Base Grant Unconformity structure in time contour map

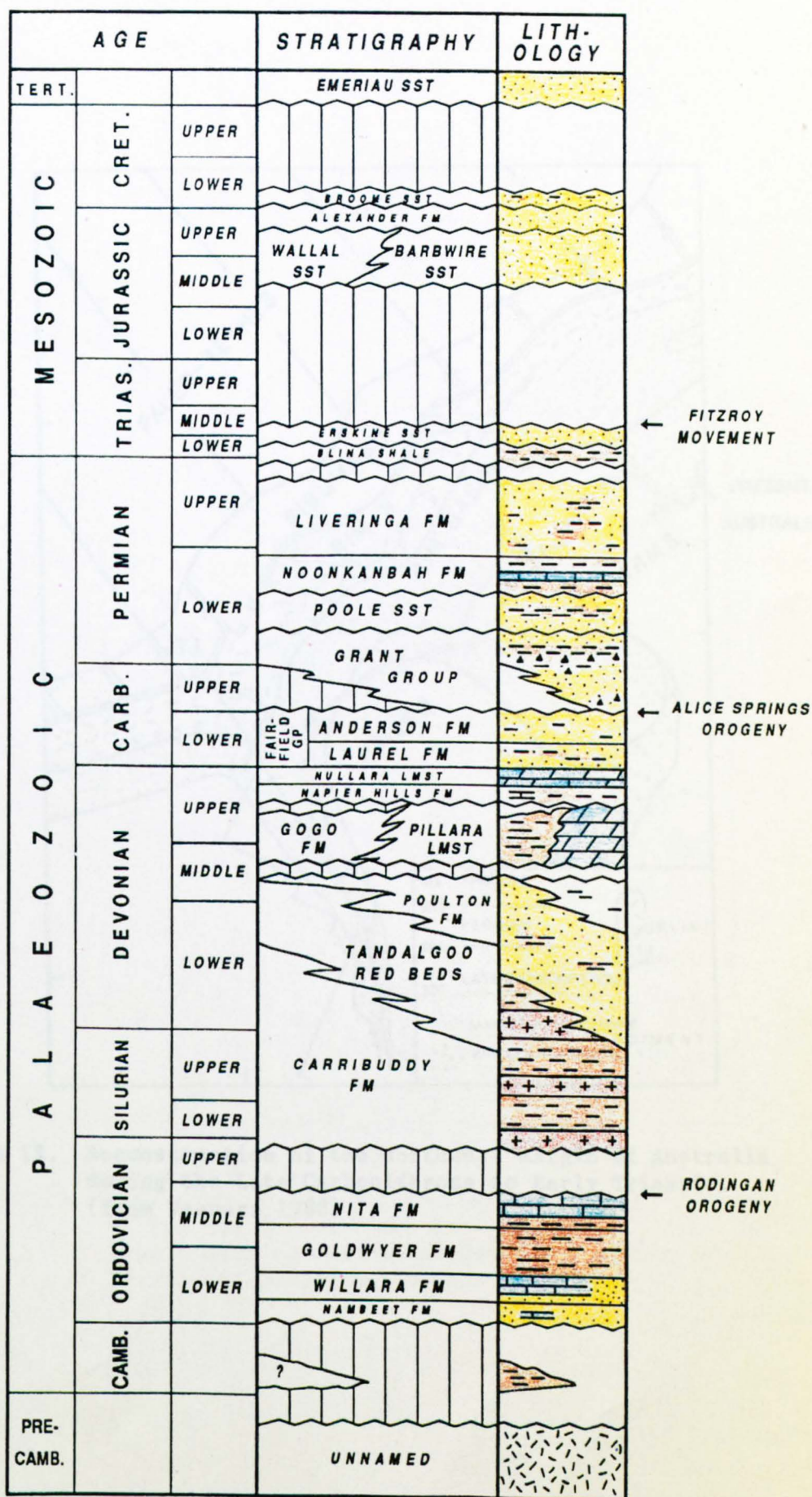


Figure 11. Generalised stratigraphic column for the Canning Basin.
(after Purcell 1984, Begg 1987)

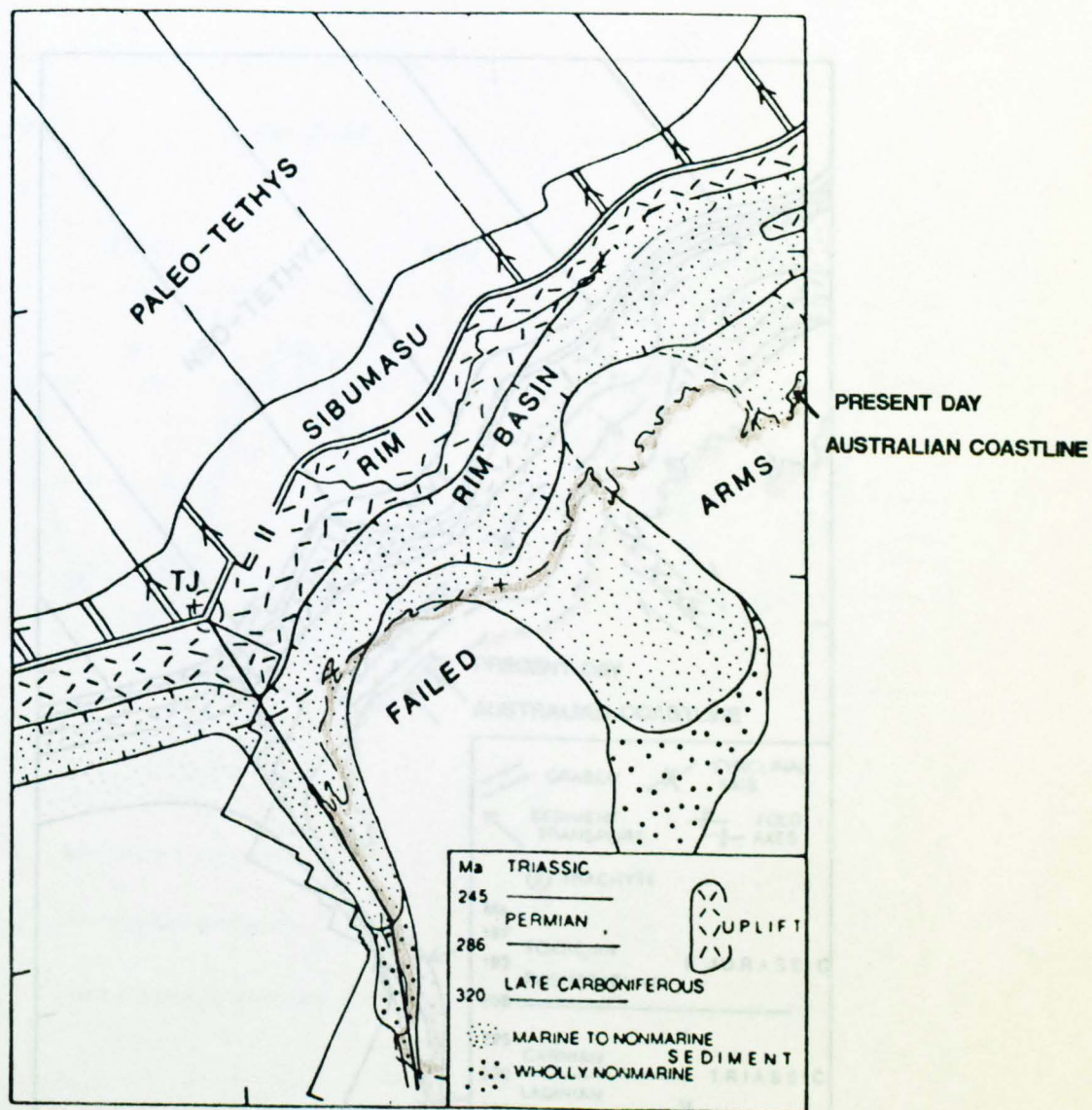


Figure 12. Reconstruction of the northwest margin of Australia during the Late Carboniferous to Early Triassic. (from Veevers 1988)

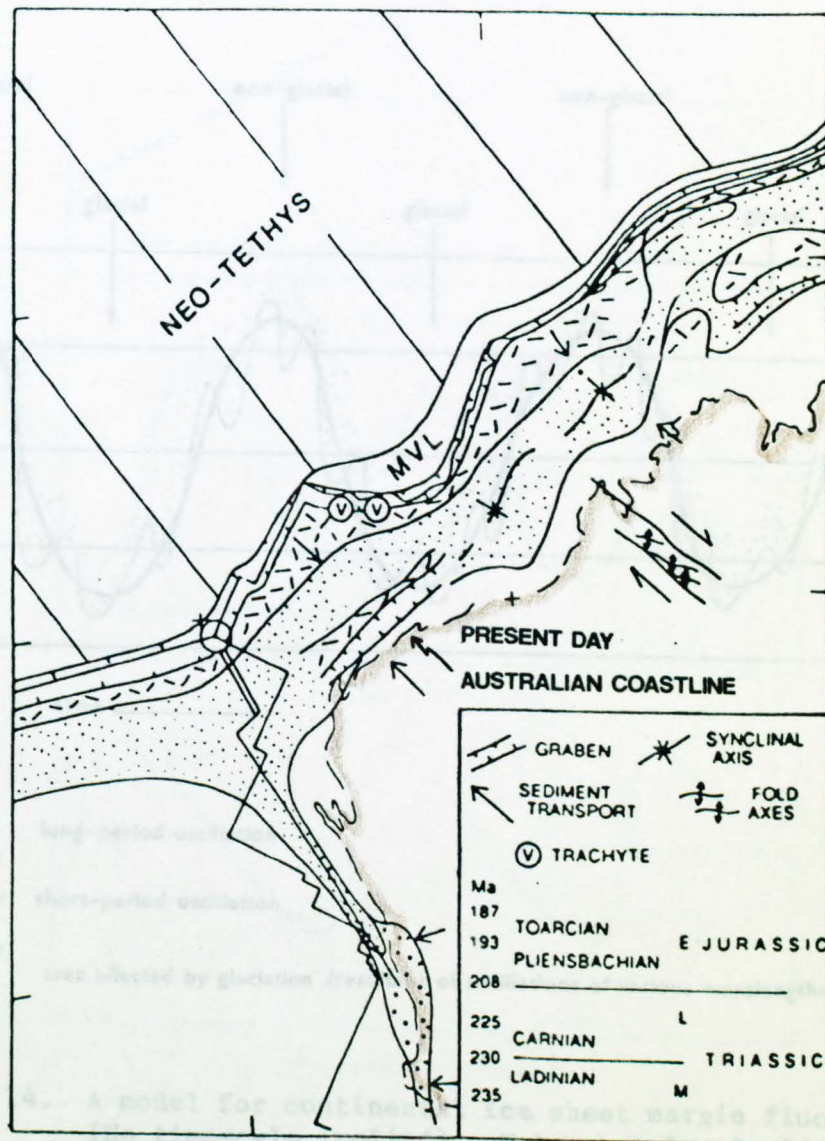


Figure 13. Reconstruction of the northwest margin of Australia during the Triassic and Early Jurassic. Note the development of wrench related folds within the Fitzroy Graben (from Veevers 1988).

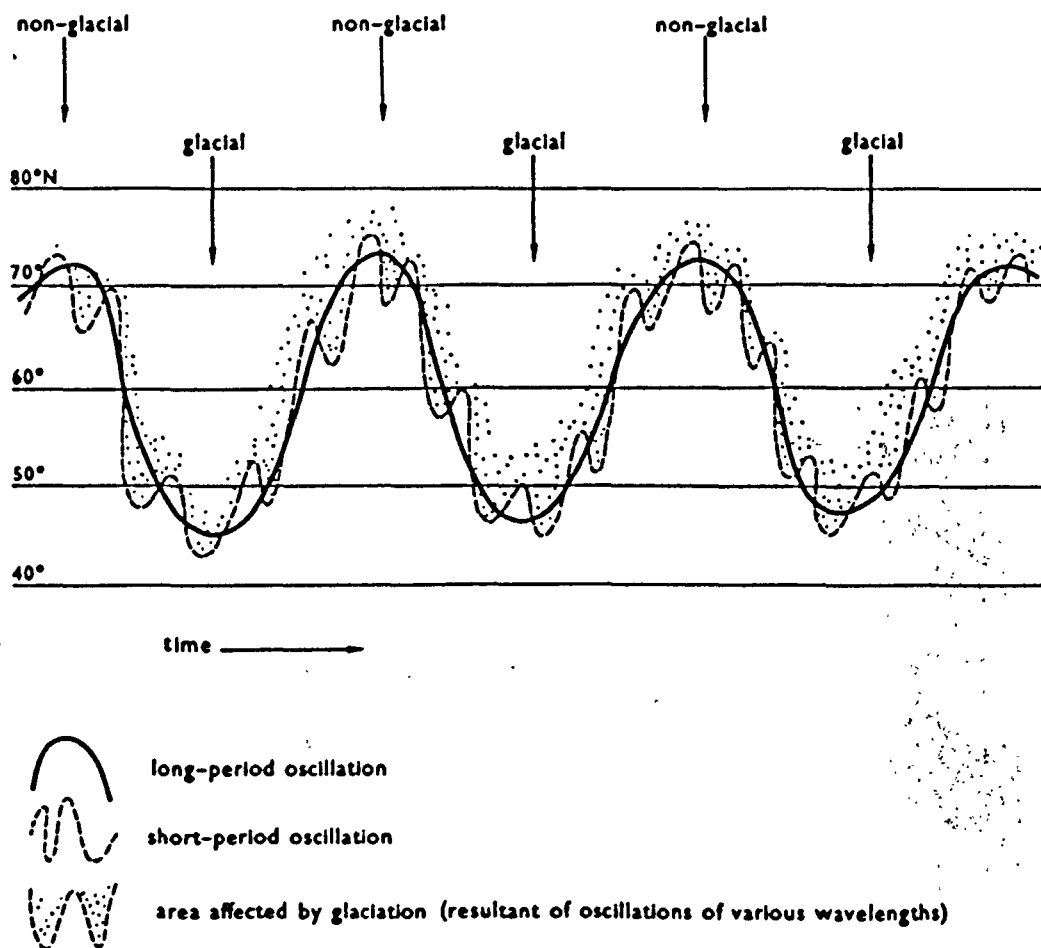


Figure 14. A model for continental ice sheet margin fluctuations (No timescale implied). Note that low latitudes display more discrete glacial advance and retreat cycles. (from Sugden and John 1985)

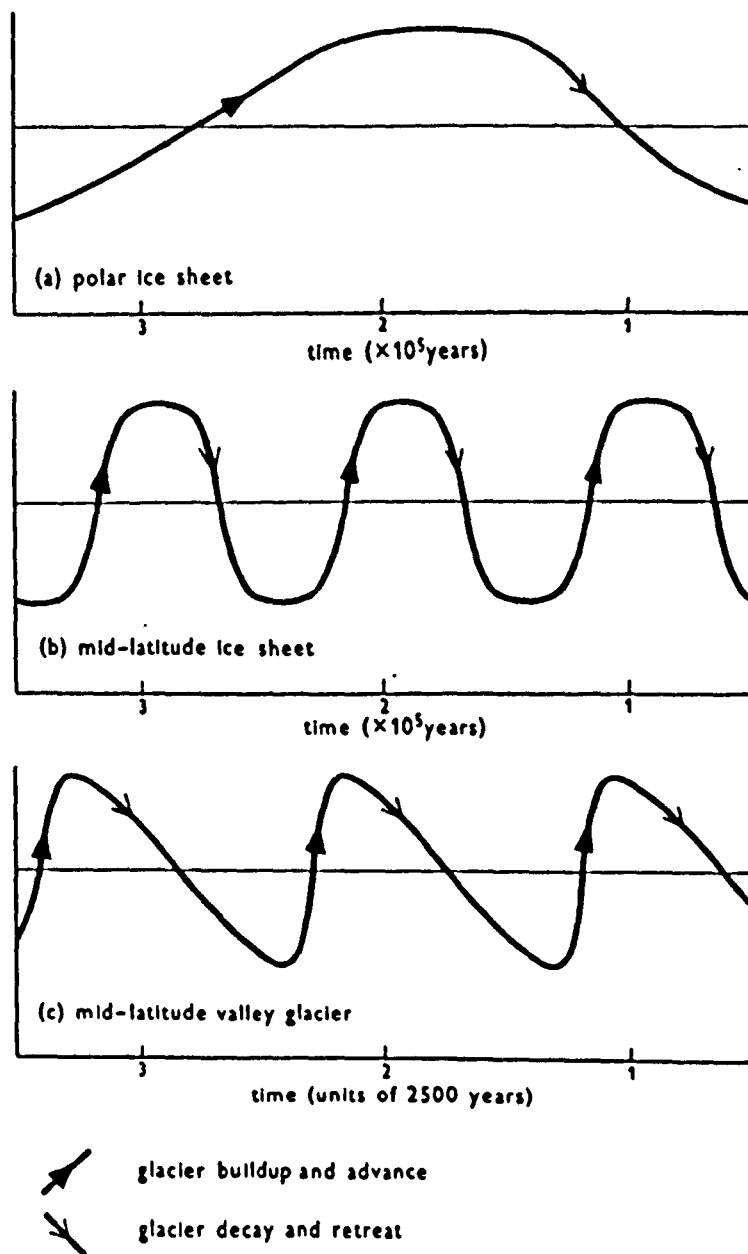


Figure 15. Periodicity of ice sheet fluctuations.
(from Sugden and John 1985)

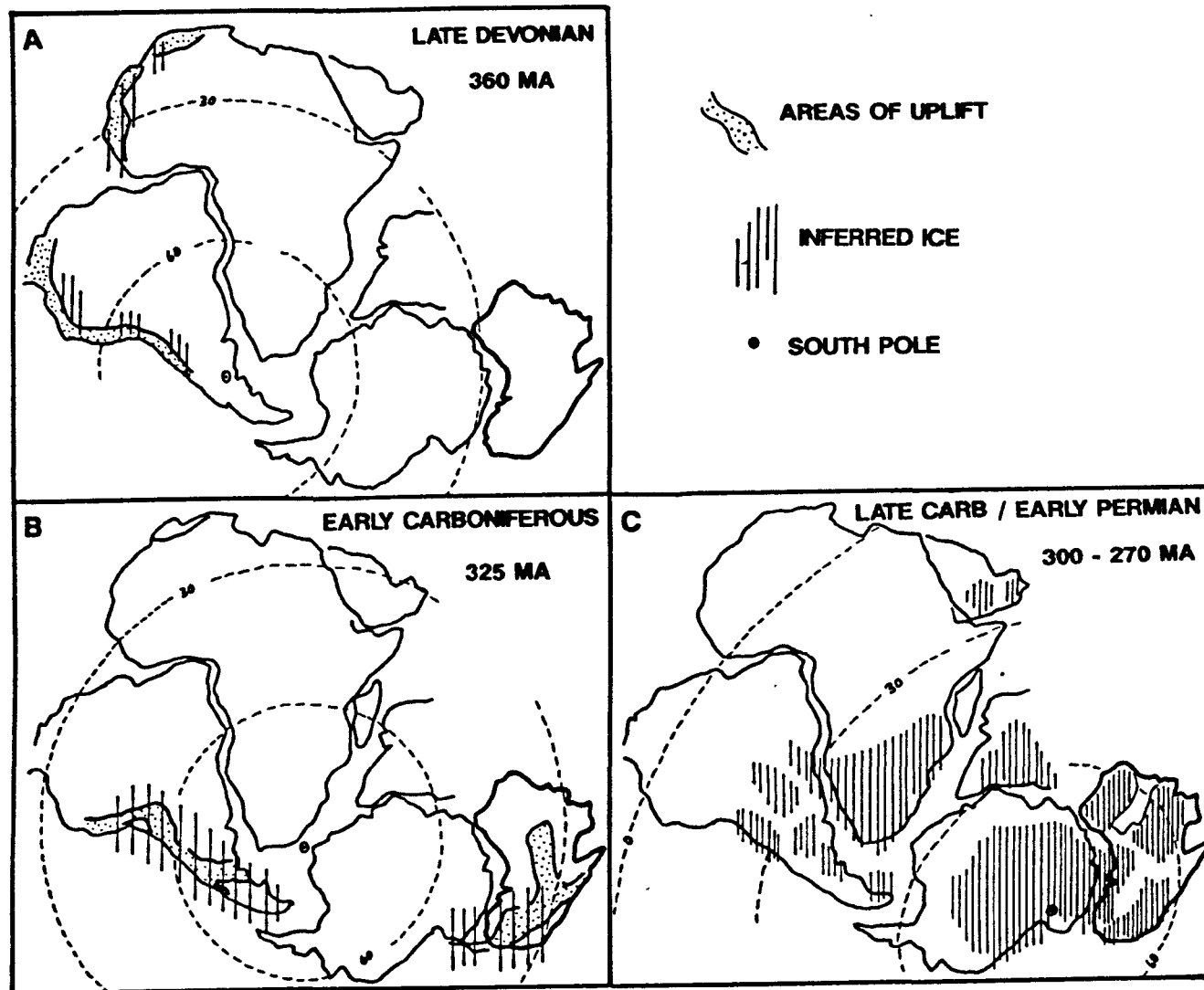


Figure 16. Reconstruction of Gondwanan palaeogeography from the Late Devonian to Early Permian, showing inferred major ice centres. (after Powell and Veevers 1987)

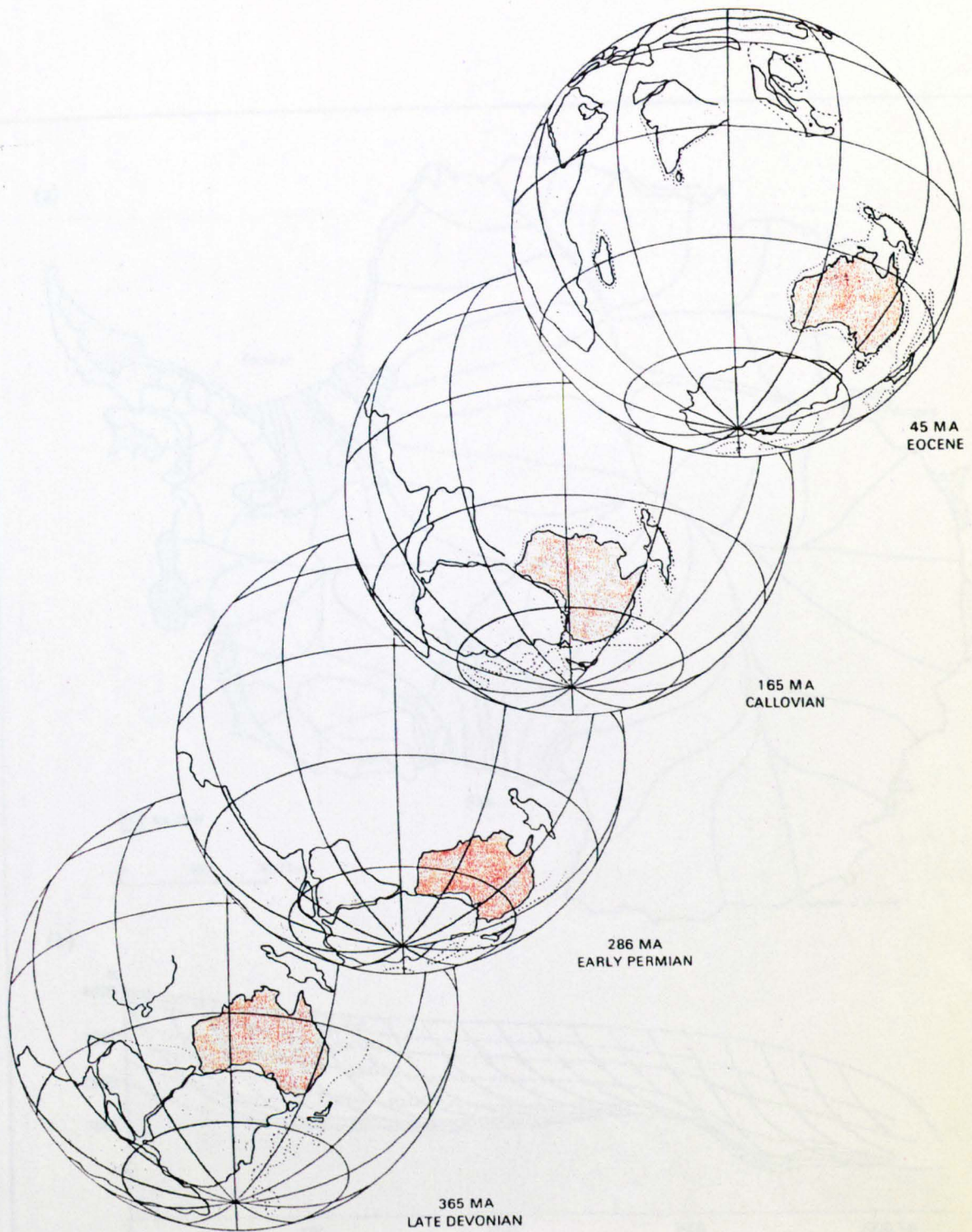


Figure 17. Continental reconstruction showing the relative position of Australia in the Late Devonian, Early Permian, Late Jurassic and Tertiary. (after Scotese 1986)

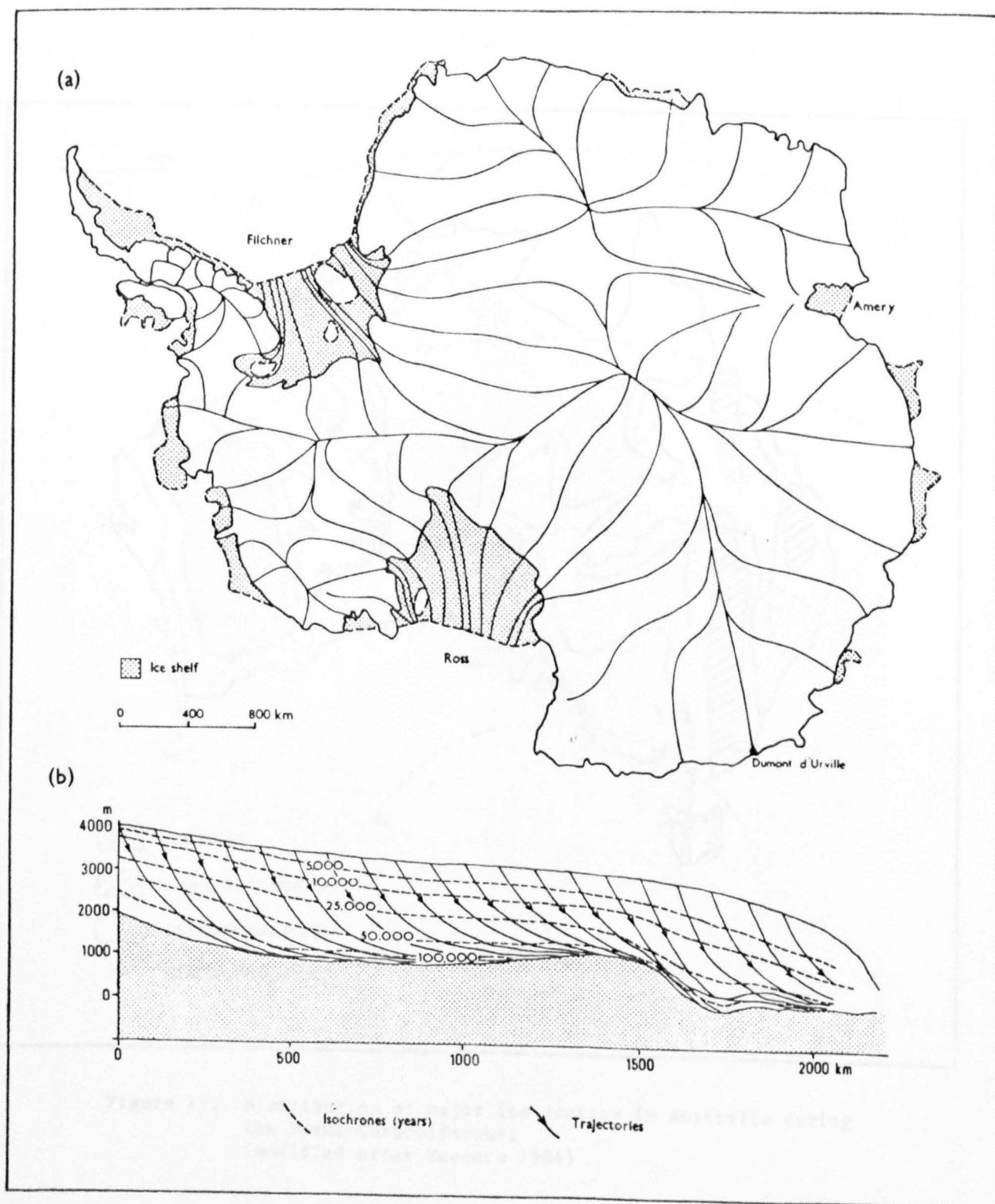


Figure 18. Flow lines for the Antarctic ice sheet, displaying multiple centres or 'domes', which act as independent ice sheet accumulation and dispersal locations. (from Budd *et al.* 1971)

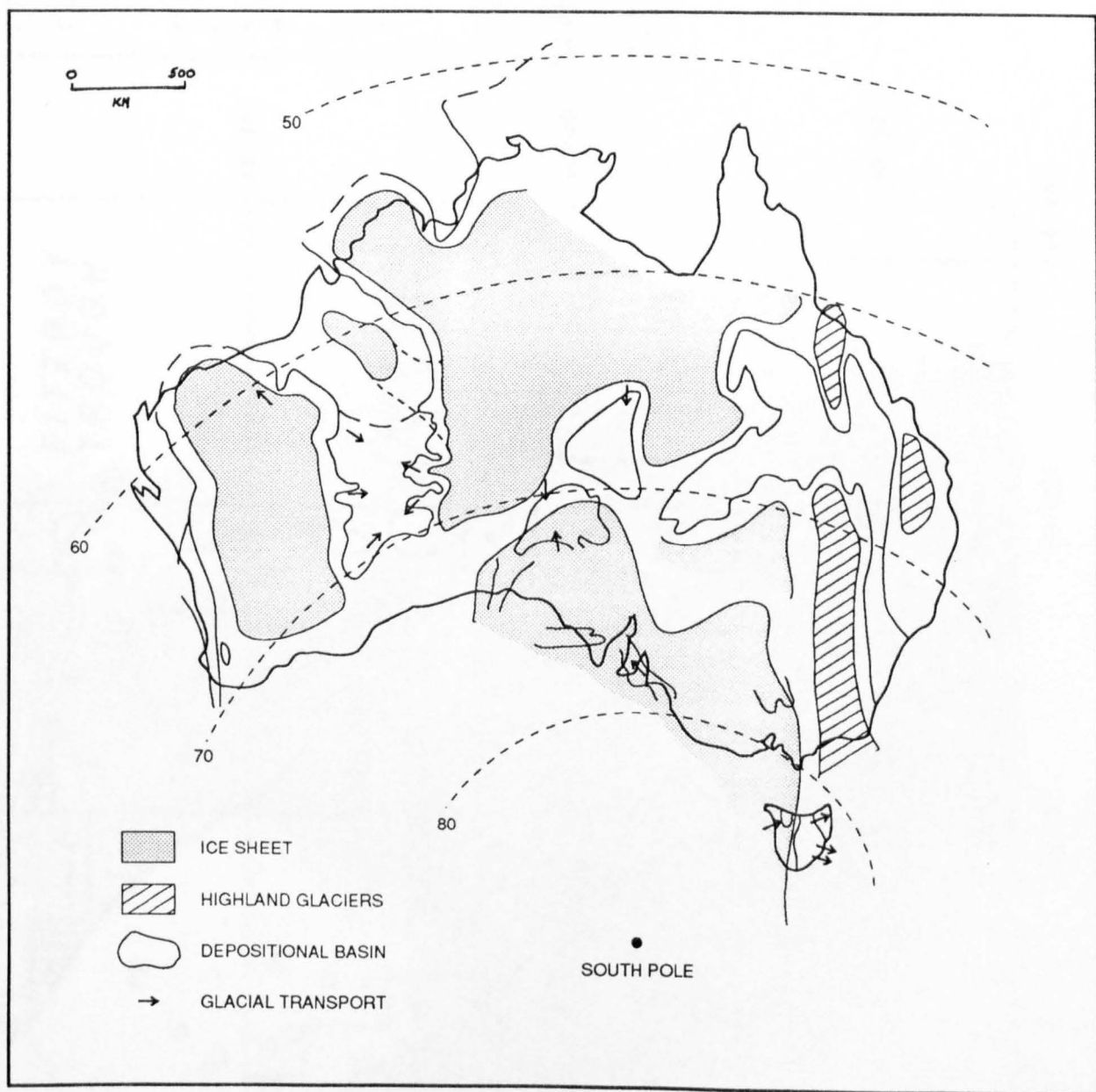


Figure 19. Distribution of major ice centres in Australia during the Permo-Carboniferous.
(modified after Veevers 1984)

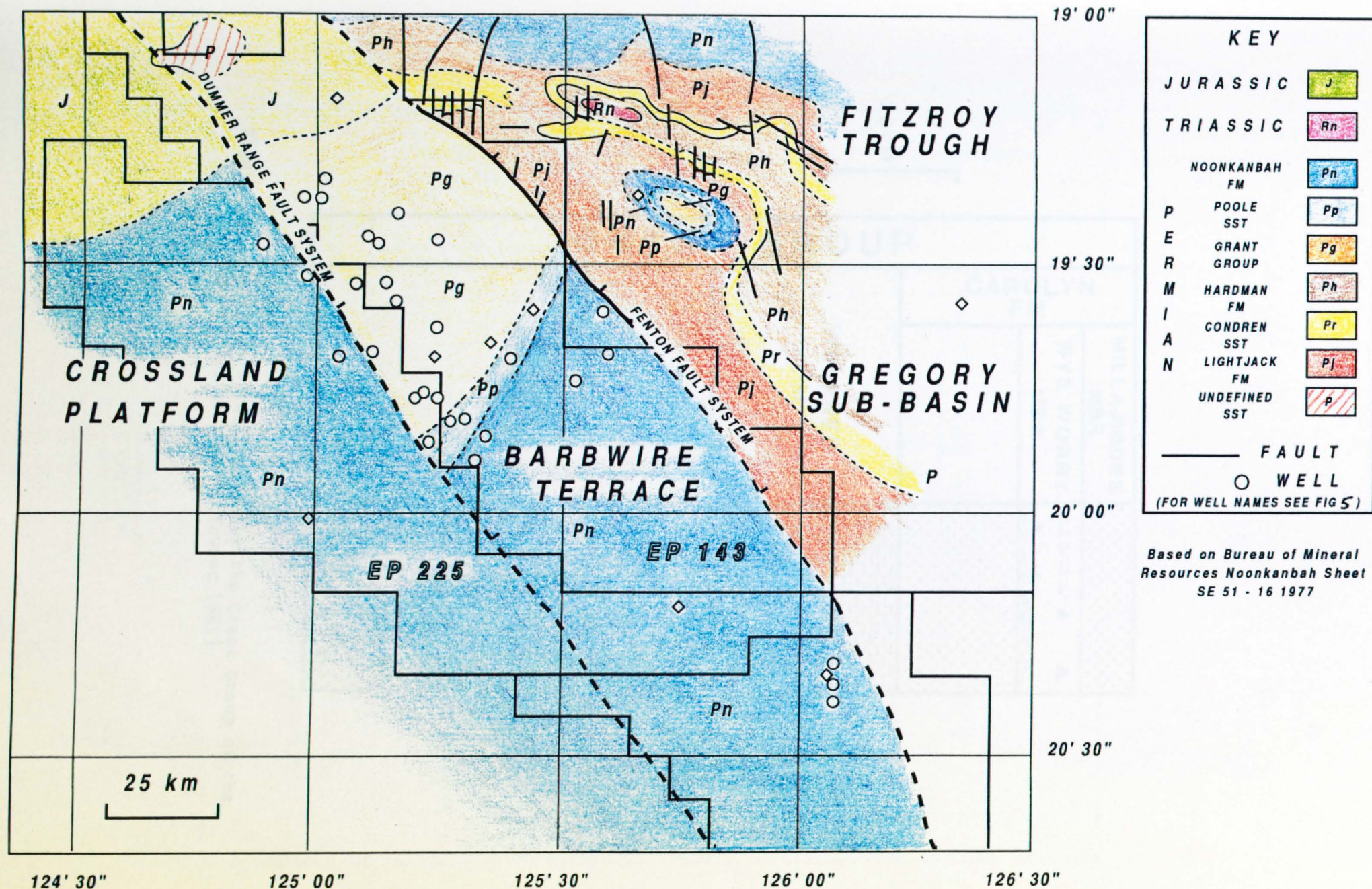


Figure 20. Solid geology of the study area. Dashed lines indicate uncertain boundaries. (modified from BMR Sheet SE51-16 compiled by Towner, Wyborn and Walton, 1977)

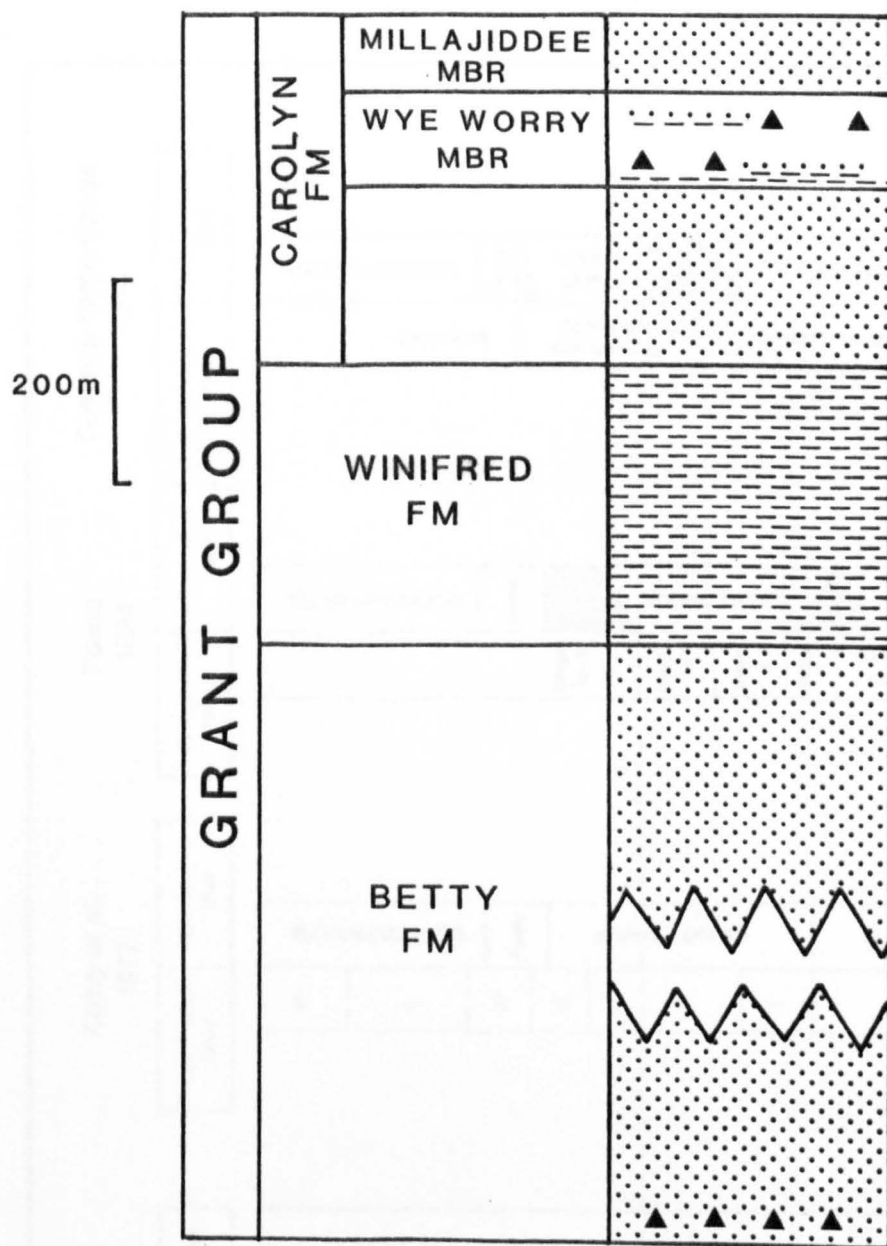


Figure 21. Composite stratigraphy for the Grant Group of the Canning Basin. (after Towner 1981)

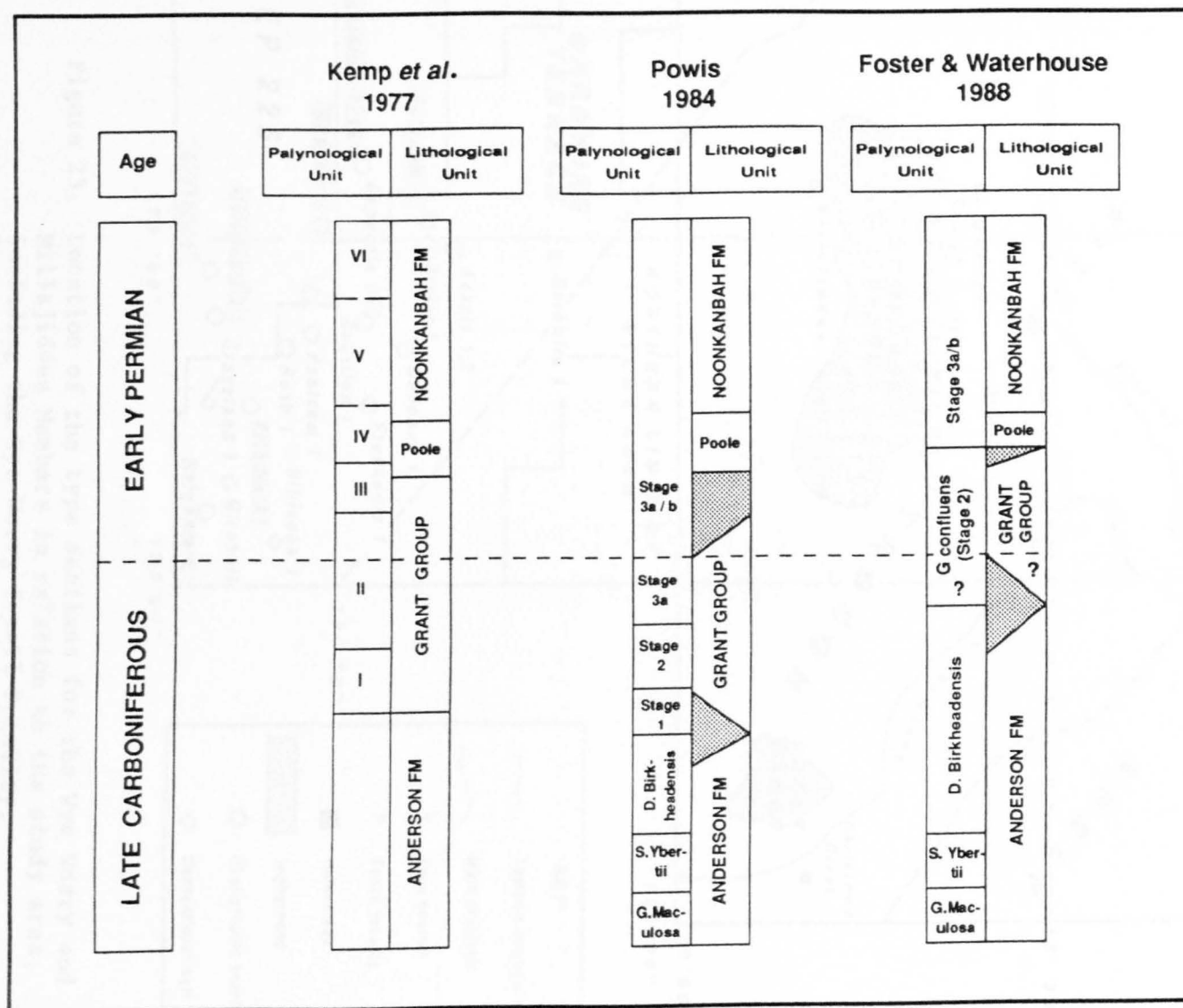


Figure 22. Dating of the Permo-Carboniferous Grant Group.
A comparison of the proposed range of the Grant Group
from recent publications.

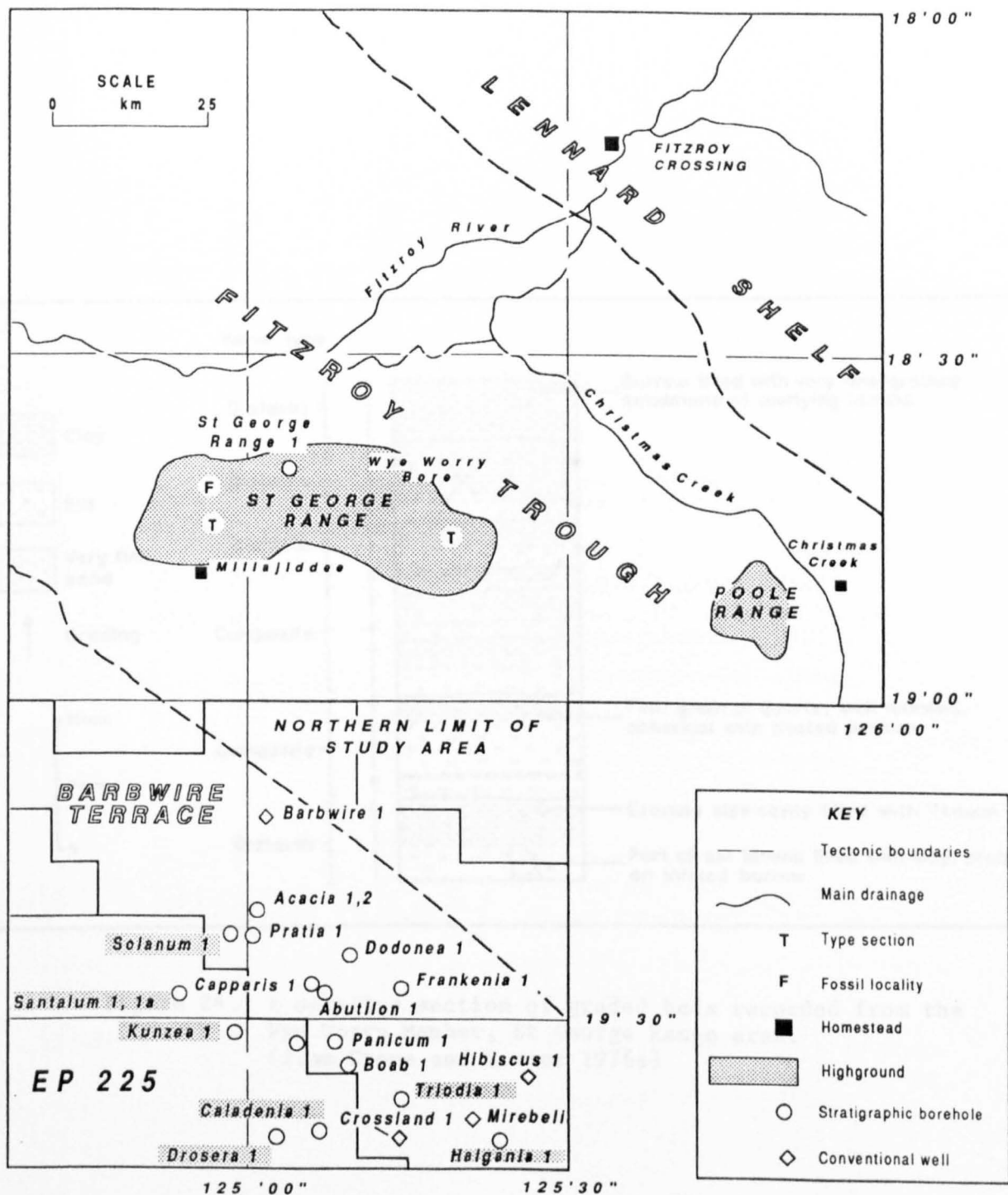


Figure 23. Location of the type sections for the Wye Worry and Millajiddee Members in relation to the study area, including the Wye Worry fossil locality.
(Based on Crowe and Towner 1976c, Dickens et al. 1977)

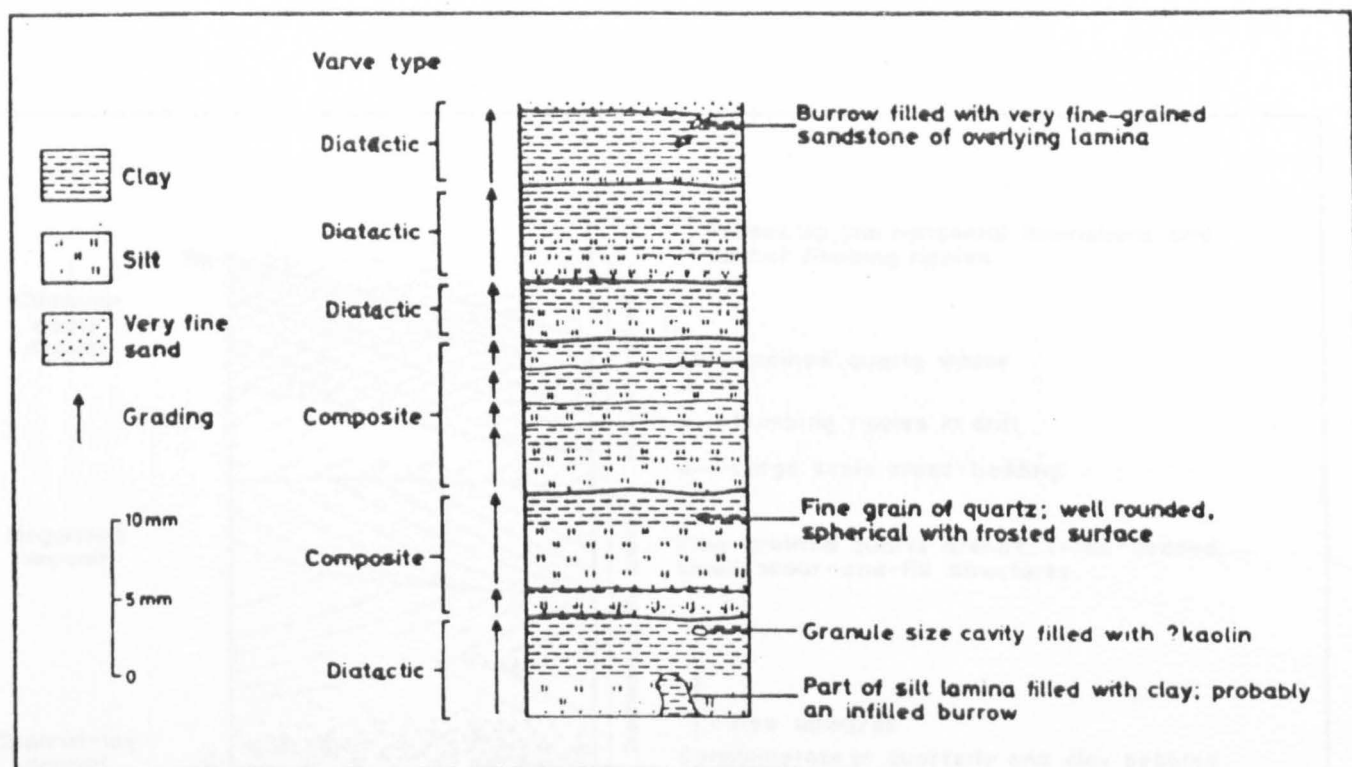


Figure 24. A detailed section of graded beds recorded from the Wye Worry Member, St George Range area. (from Crowe and Towner 1976a)

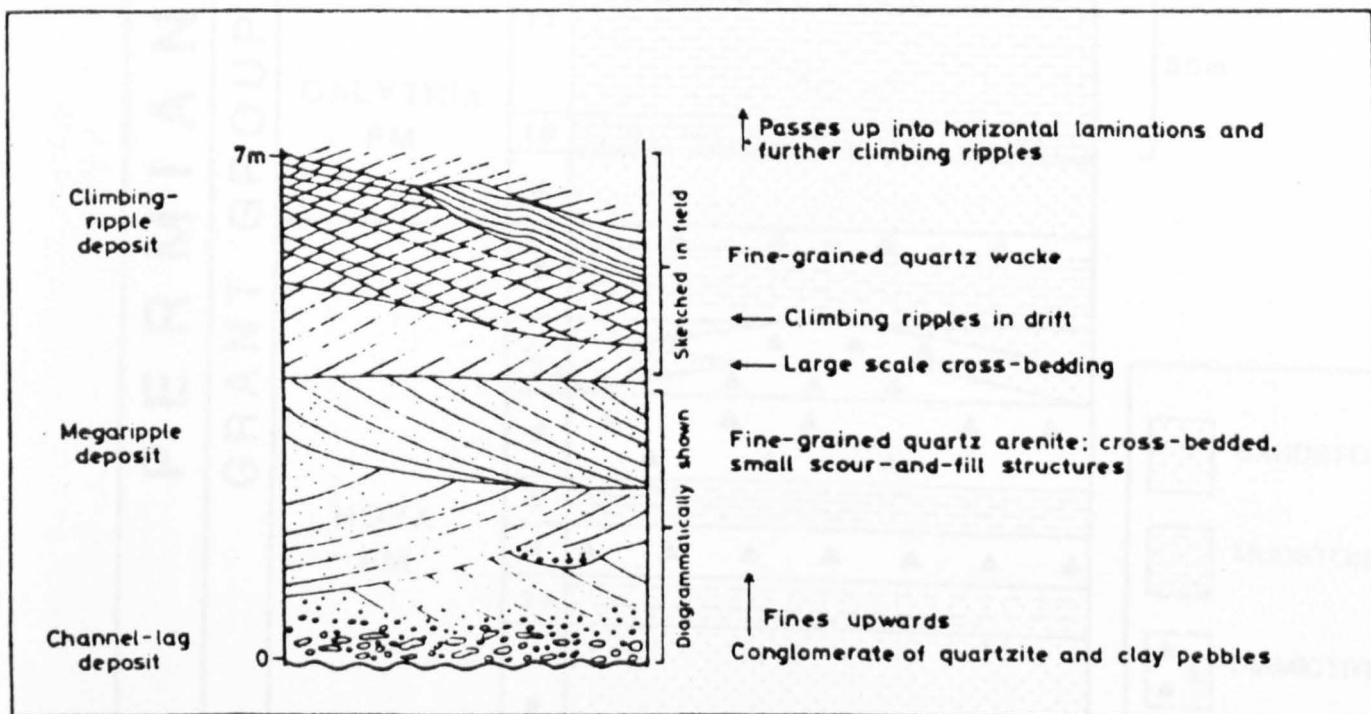


Figure 25. Section of cross bedded and ripple laminated sandstone of the Millajiddee Member from the eastern part of the St George Range. (from Crowe and Towner 1976a)

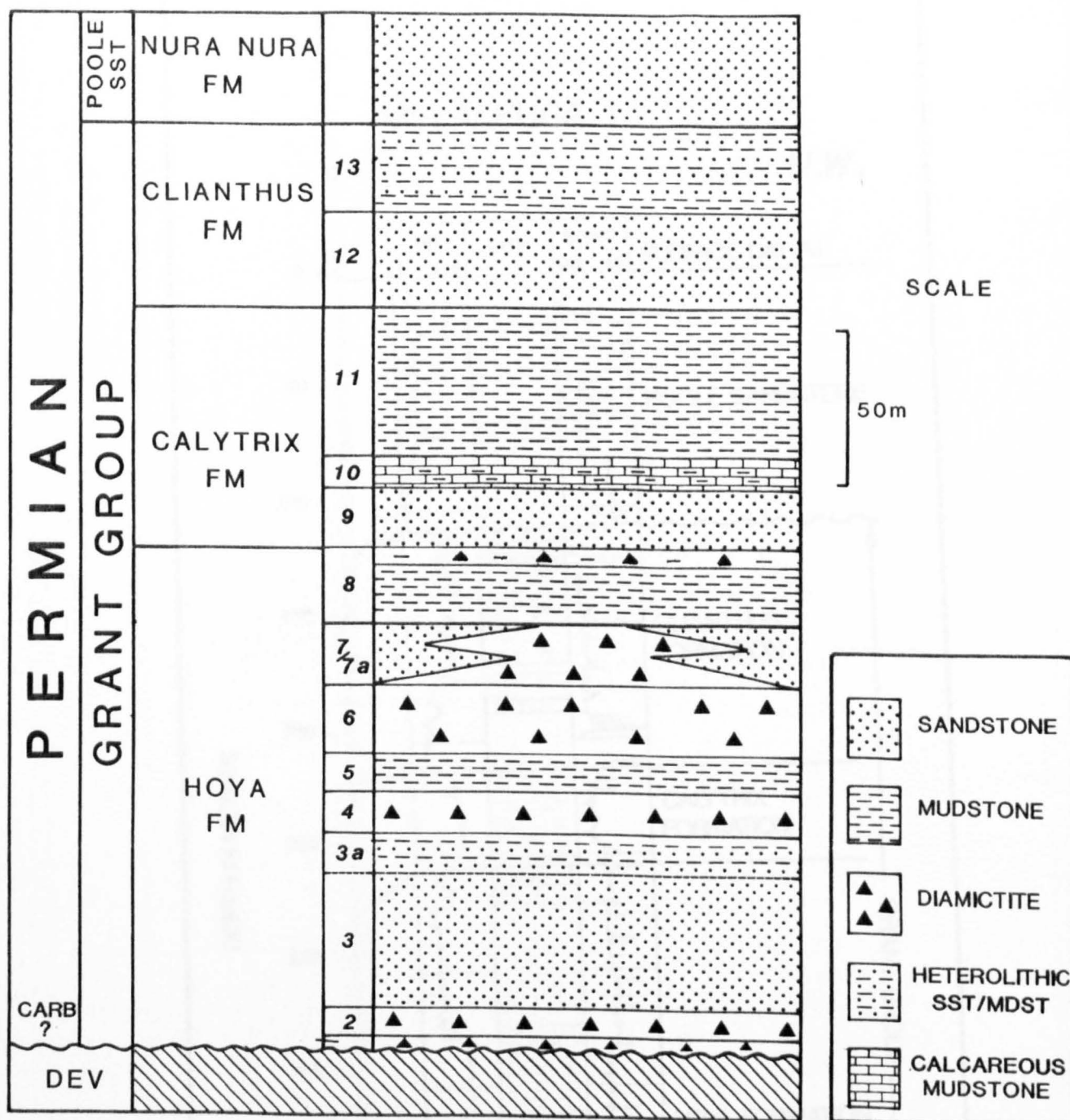


Figure 26. Stratigraphic Framework of the Grant Group on the Barbwire Terrace (Defined in this thesis).

STRATIGRAPHIC CORRELATION 1

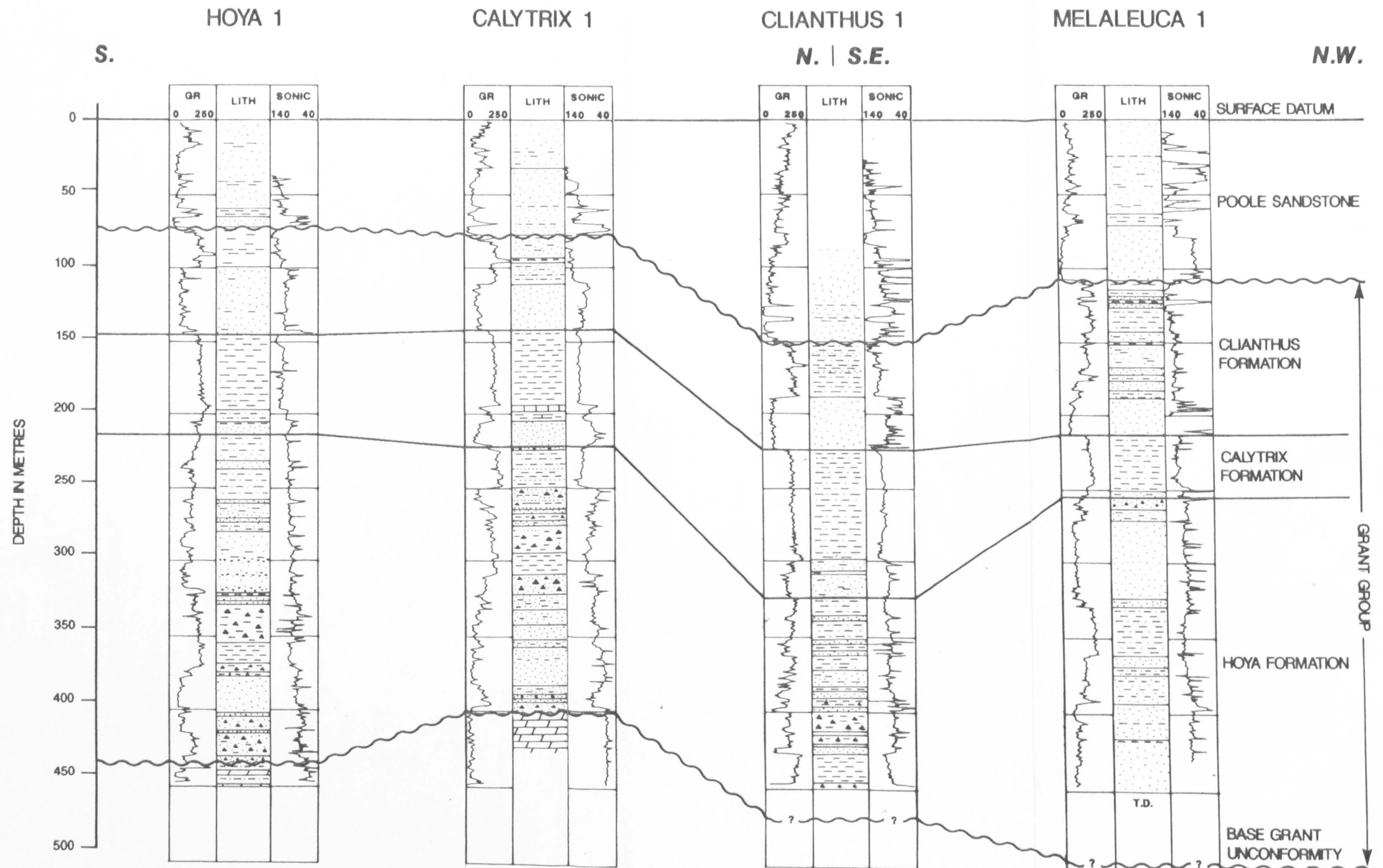


Figure 27. Stratigraphic correlation between Hoya 1, Calytrix 1, Clianthus 1 and Melaleuca 1.

STRATIGRAPHIC CORRELATION 2

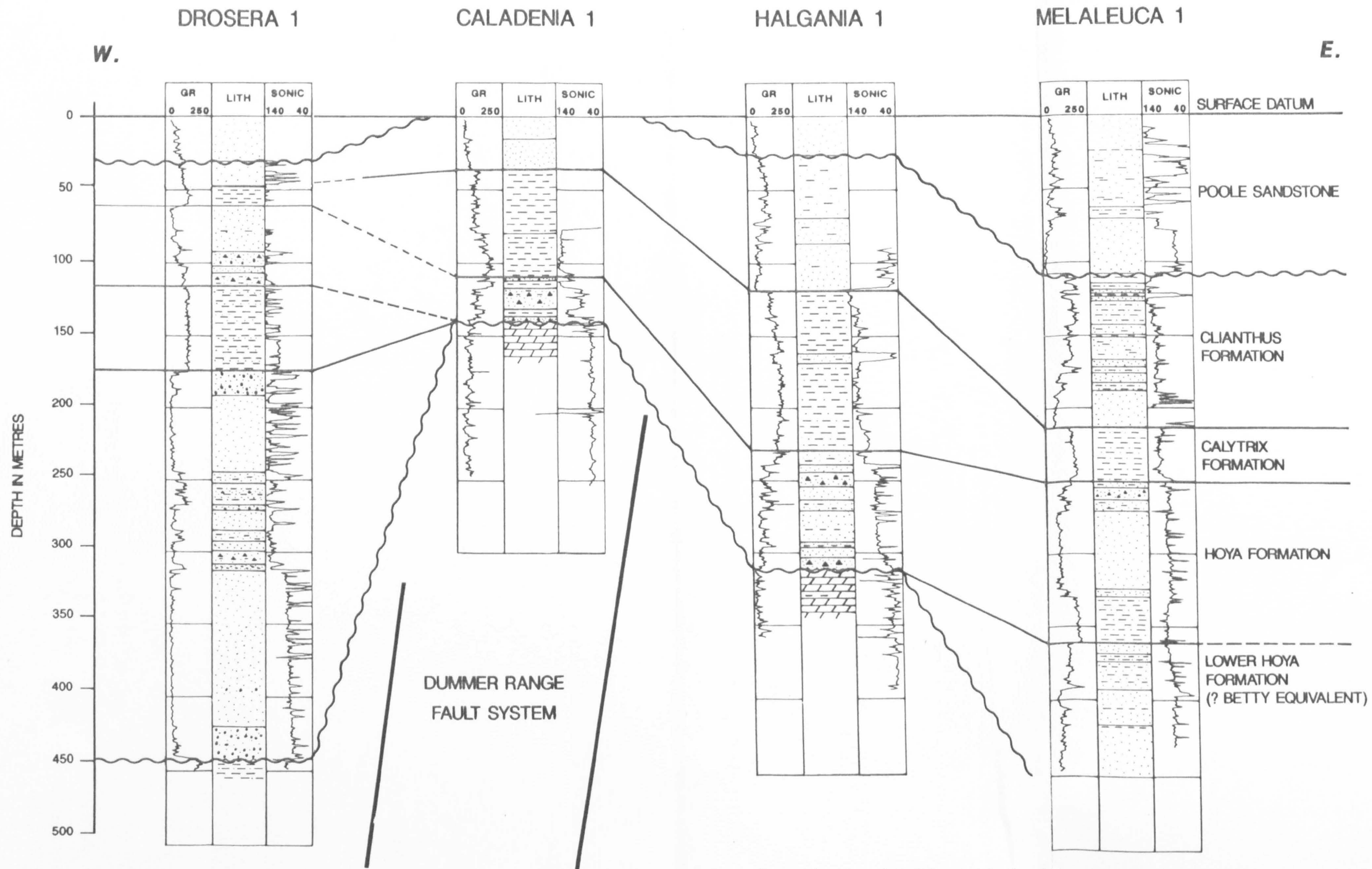


Figure 28 Stratigraphic correlation between Drosera 1, Caladenia 1, Halgania 1 and Melaleuca 1

STRATIGRAPHIC CORRELATION 3

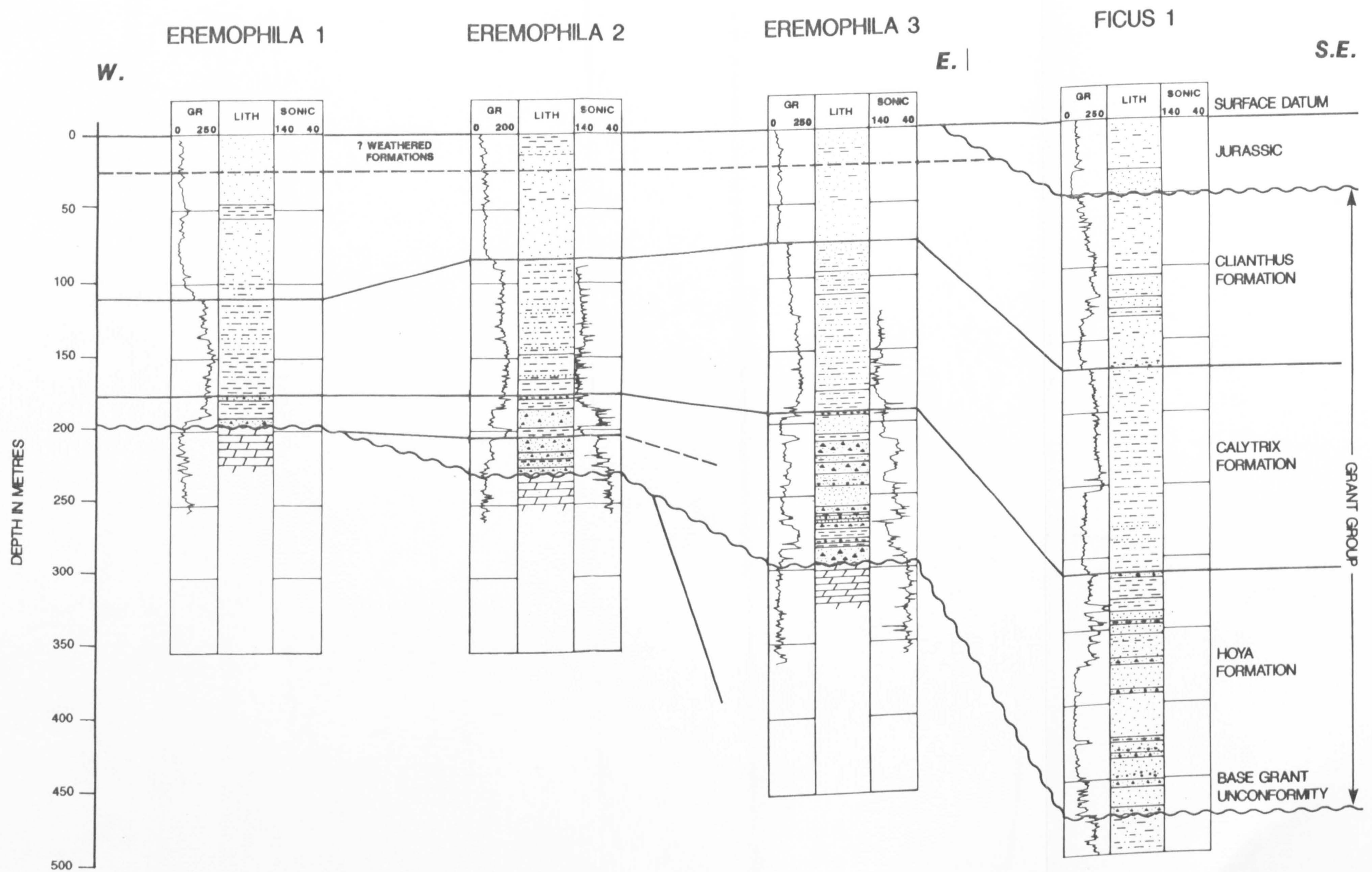


Figure 29 Stratigraphic correlation between Eremophila 1, 2, 3 and Ficus 1.

STRATIGRAPHIC CORRELATION 4

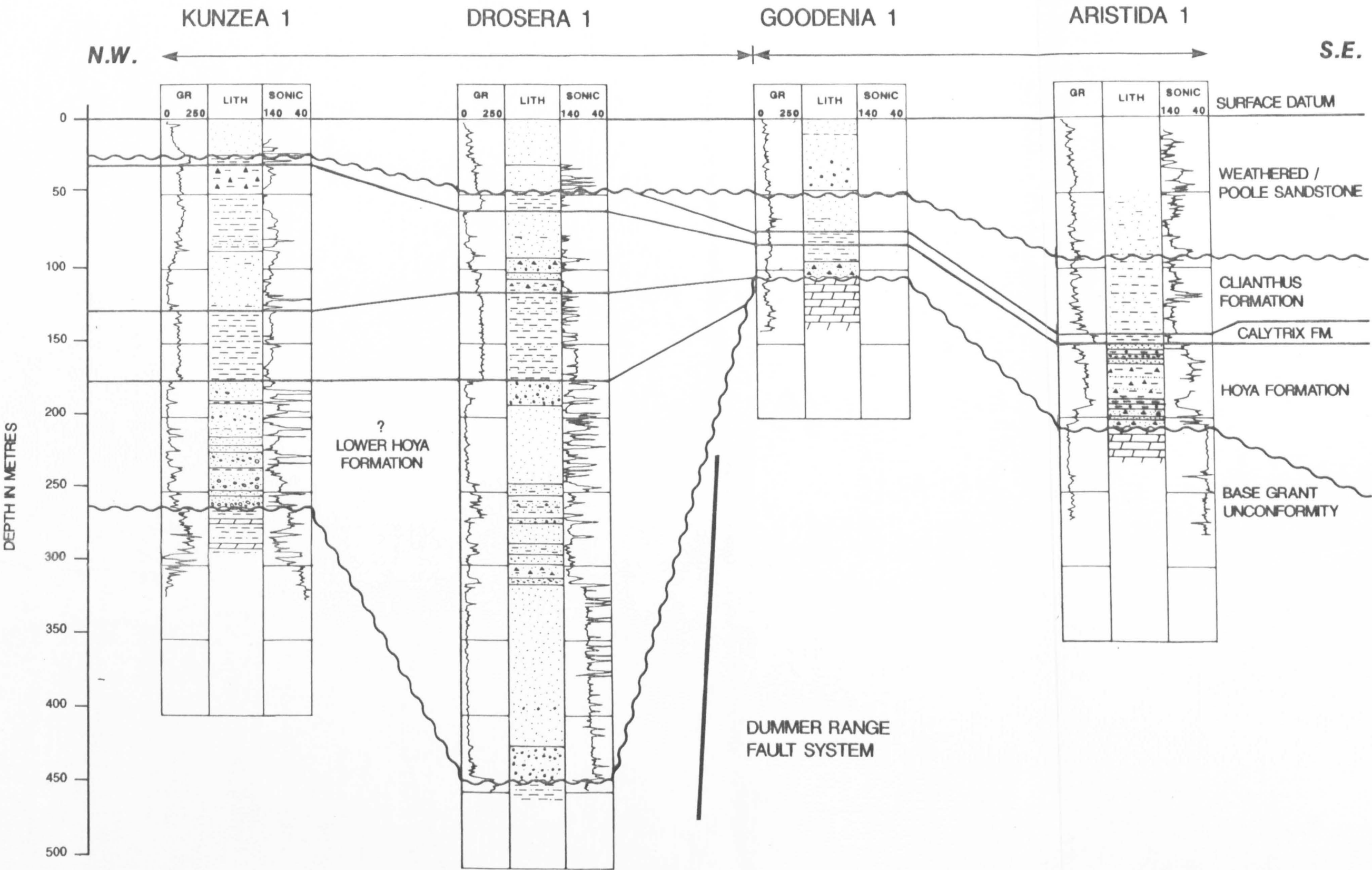


Figure 30 Stratigraphic correlation between Kunzea 1, Drosera 1, Goodenia 1 and Aristida 1A.

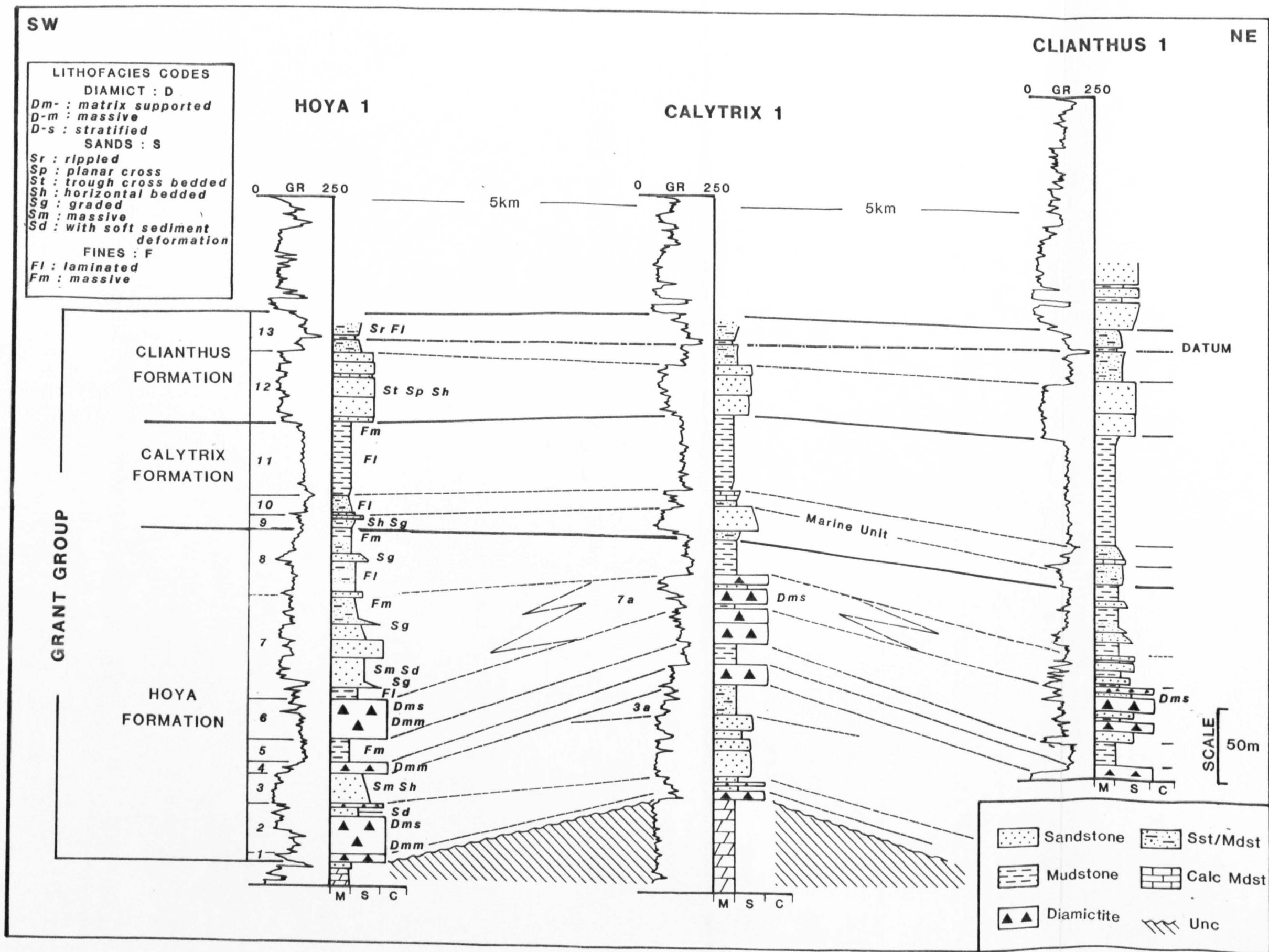


Figure 31. Detailed facies correlation of Hoya 1, Calytrix 1 and Clianthus 1

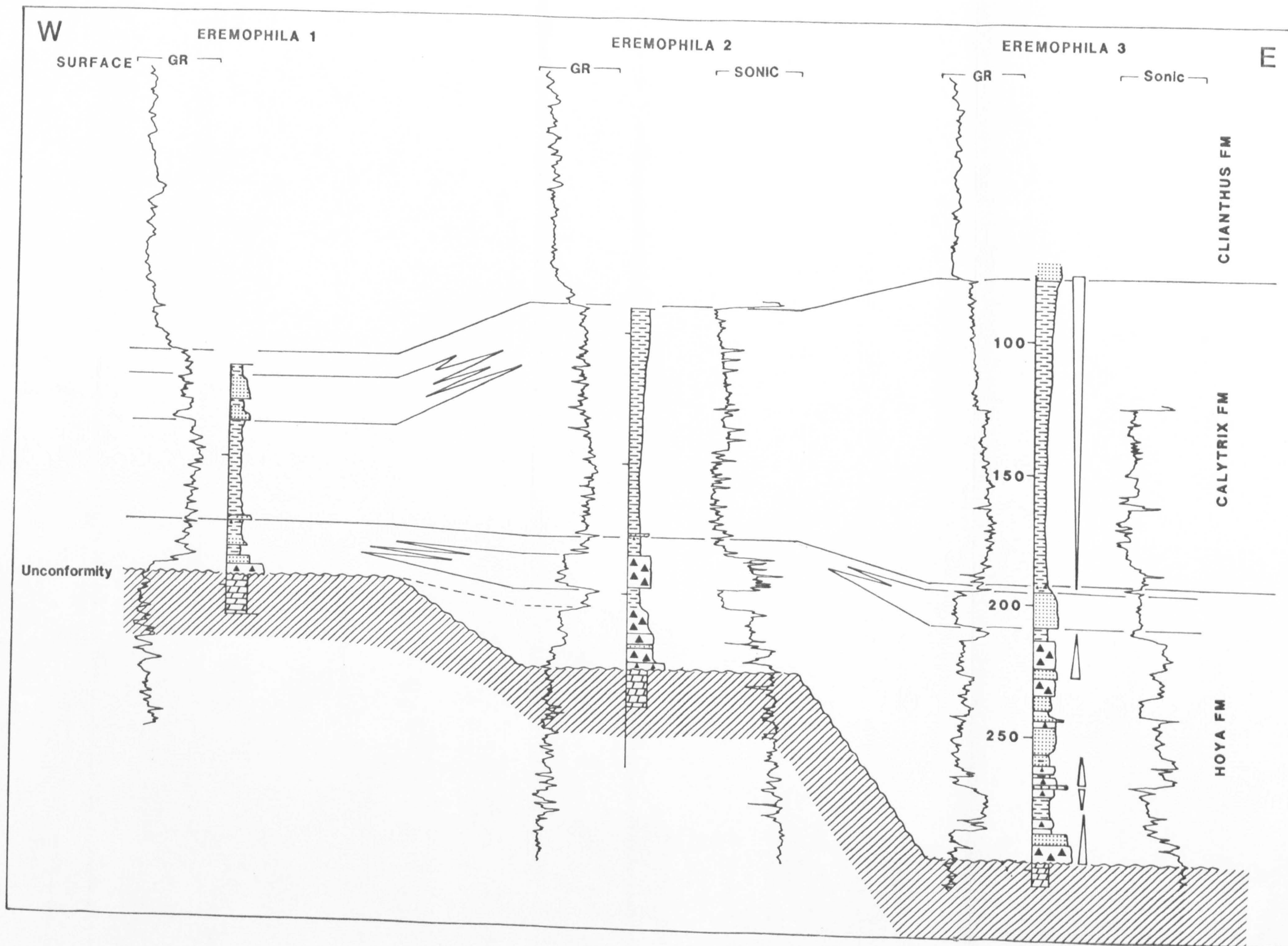


Figure 32. Detailed facies correlation of Eremophila 1, 2 and 3.

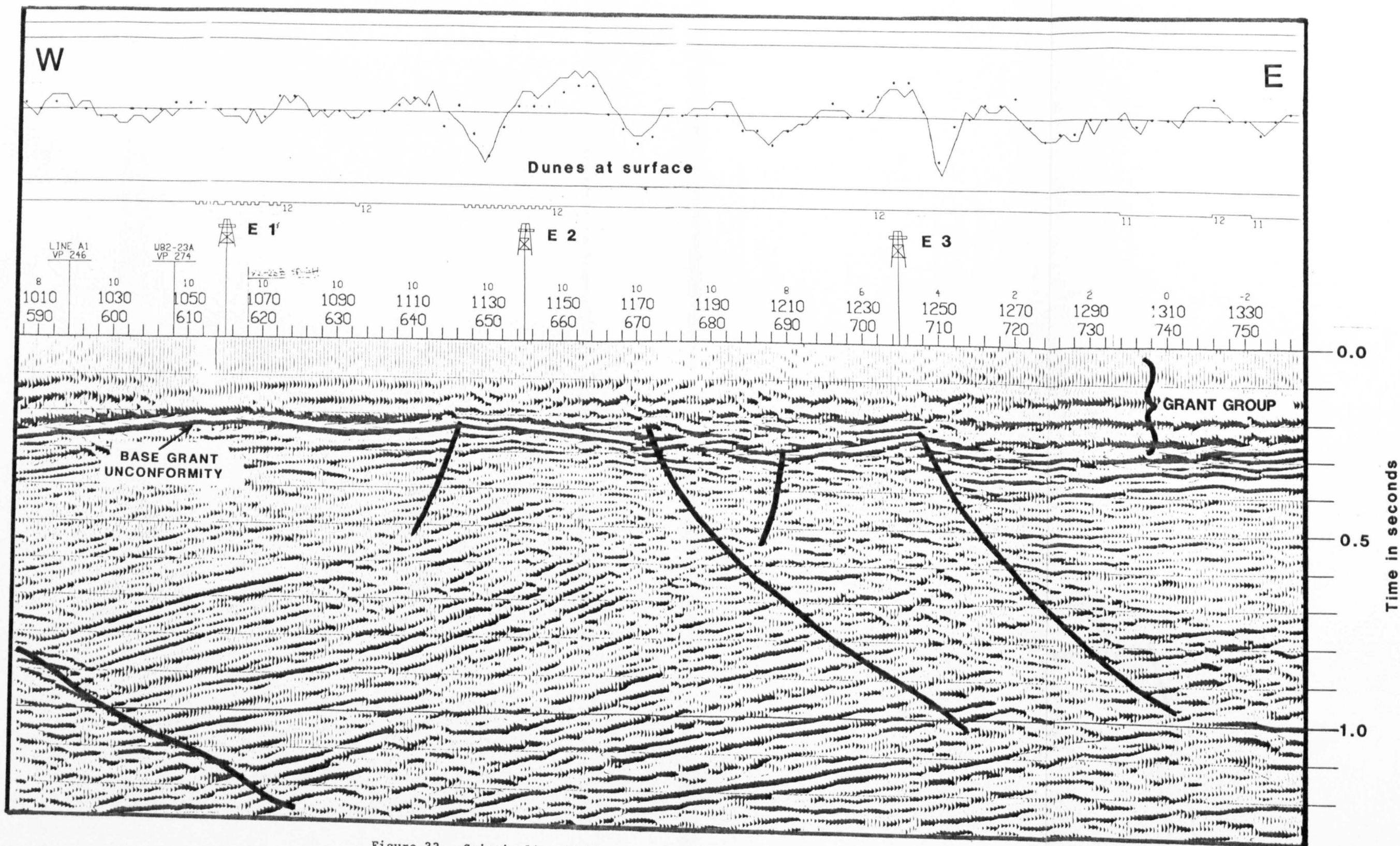


Figure 33. Seismic line 82-20A, running west to east, and controlled by Eremophila 1, 2 and 3. (for well correlation see Figure 32)

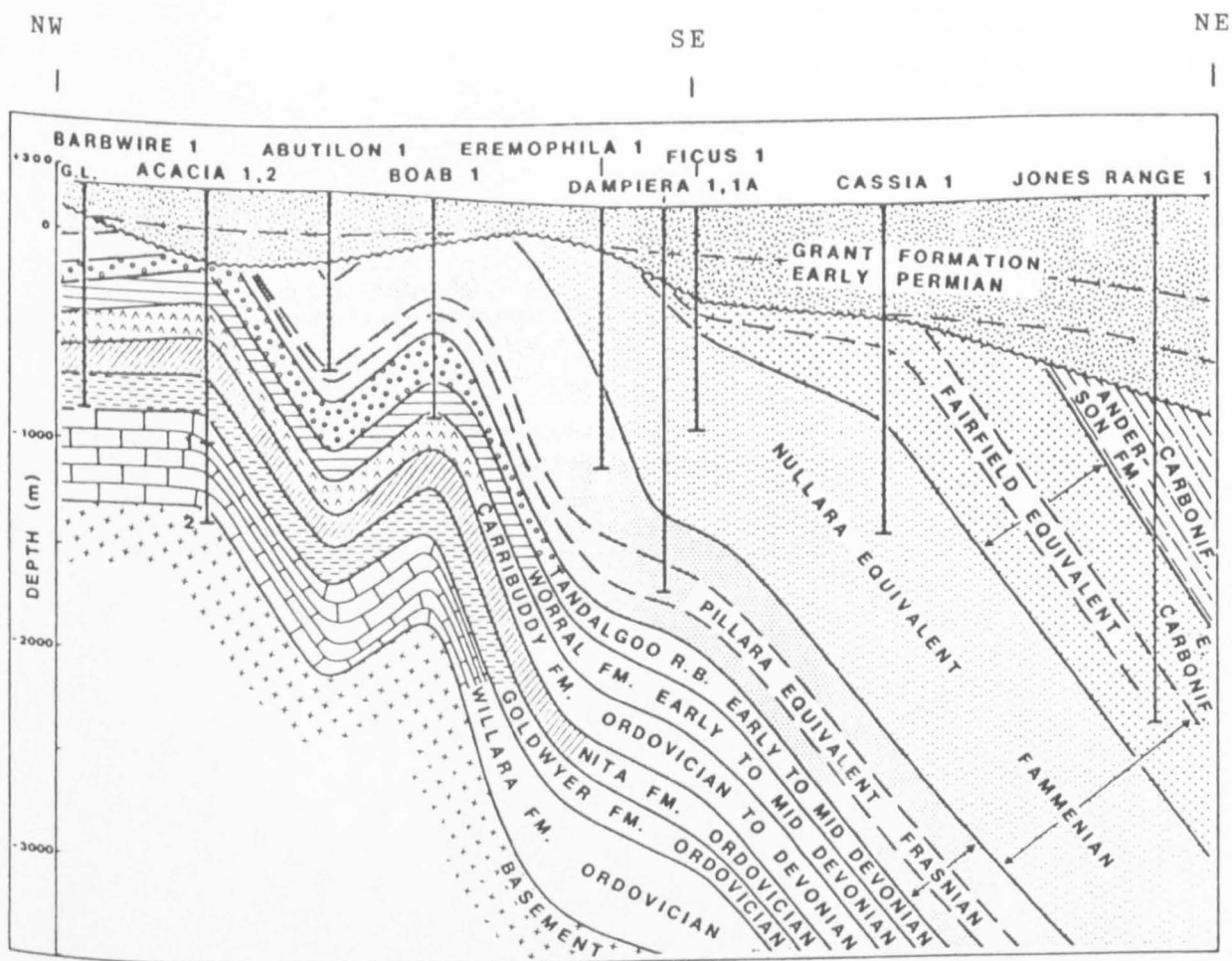


Figure 34. Diagrammatic cross section to illustrate the pre-Grant structure and the variability of subcropping formations on the Barbwire Terrace and Fitzroy Graben (From Ashton 1984).

(For well location see Figure 5)

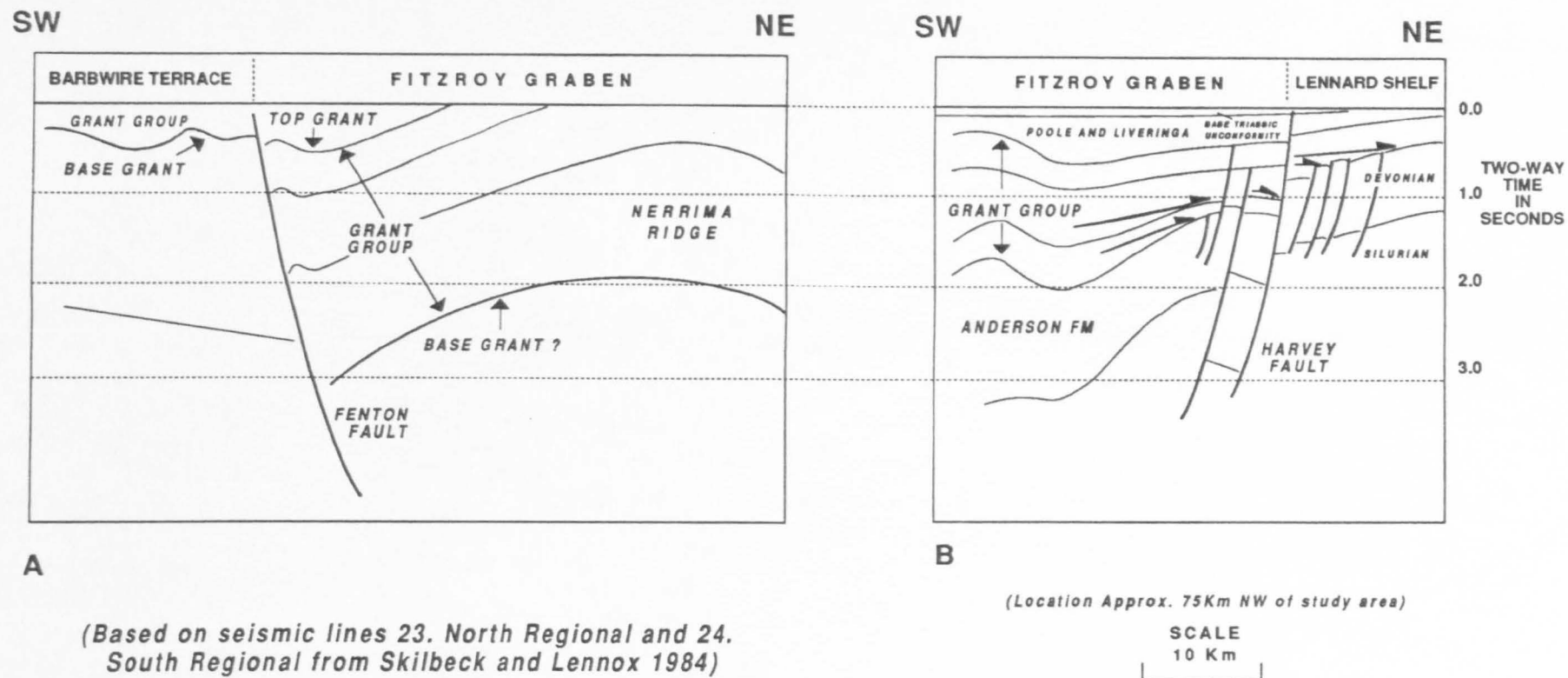


Figure 35. Interpretation of two regional seismic lines running SW to NE across the Fitzroy Graben. This illustrates a large anticline, interpreted to be analogous to the structure which results in exposure of the Grant Group in the St George Range.

BARBWIRE TERRACE SECTION

LAKE BETTY 1

ST GEORGE RANGE 1

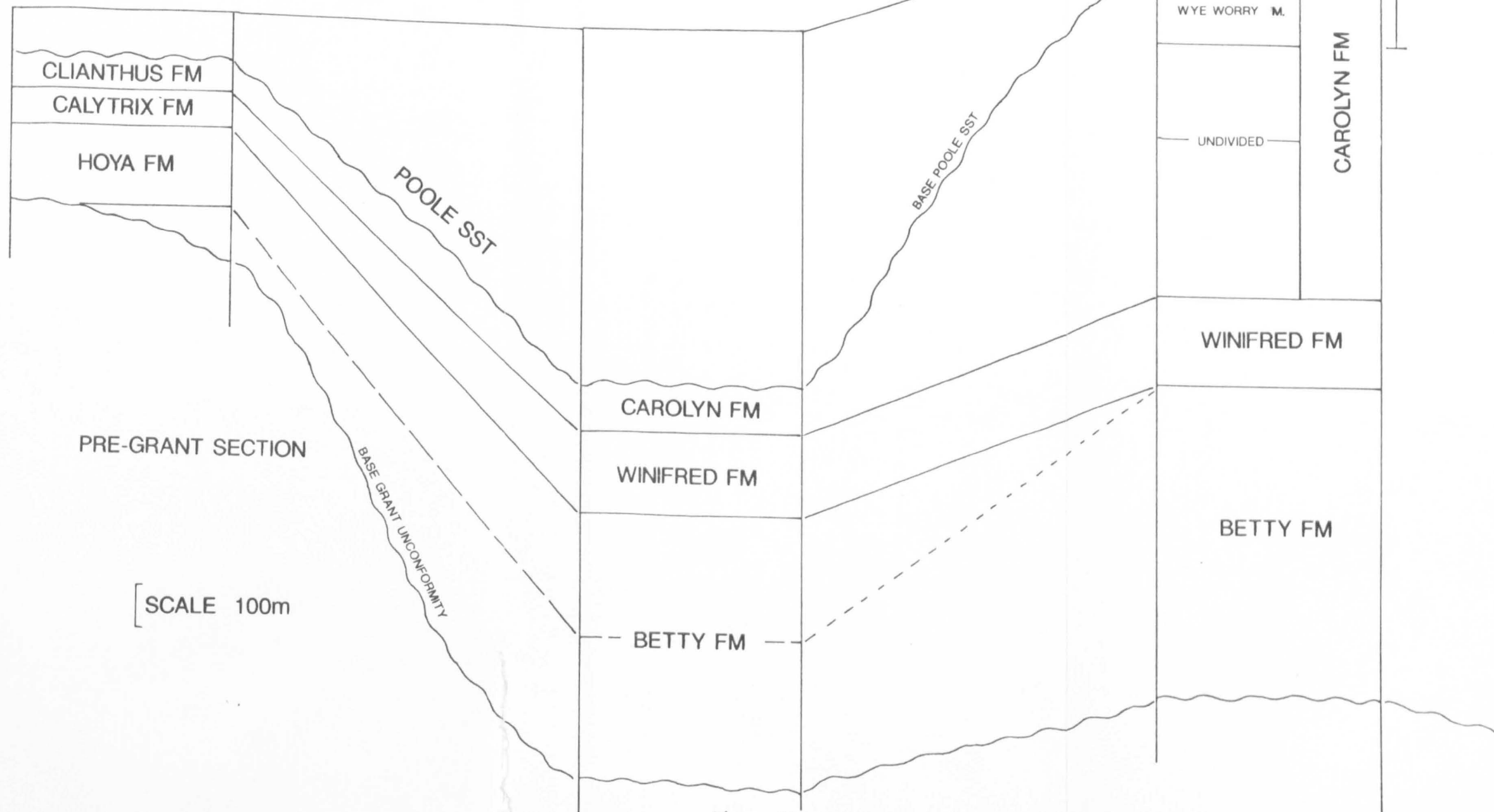
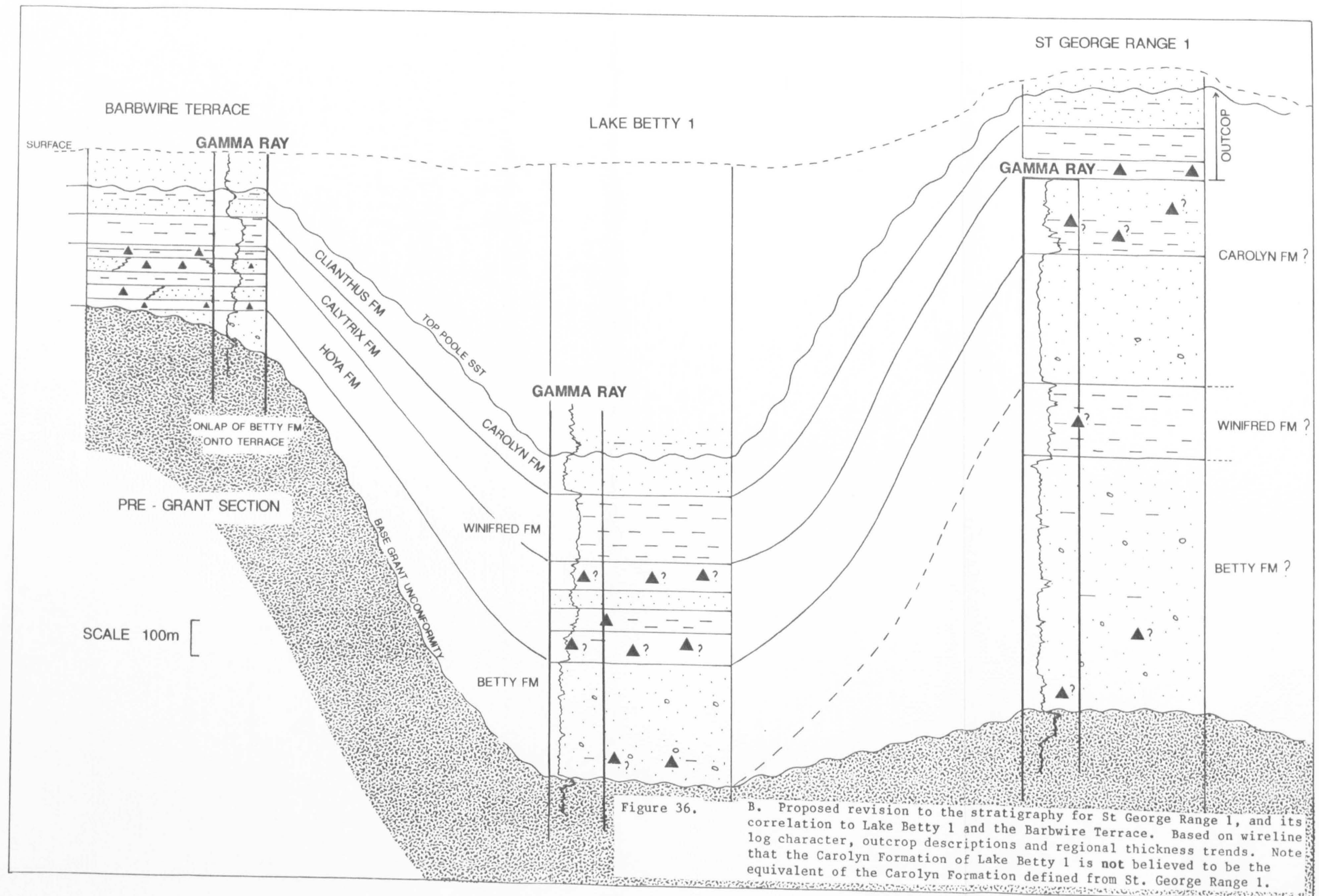


Figure 36. Summary correlations between the Barbwire Terrace stratigraphy (defined in this thesis), Lake Betty 1 (modified from Crowe *et al.* 1978) and St. George Range 1 (Crowe *et al.* 1978).
A. Correlation of the Barbwire Terrace stratigraphy with the previously defined stratigraphy for Lake Betty 1, extended to St George Range 1.



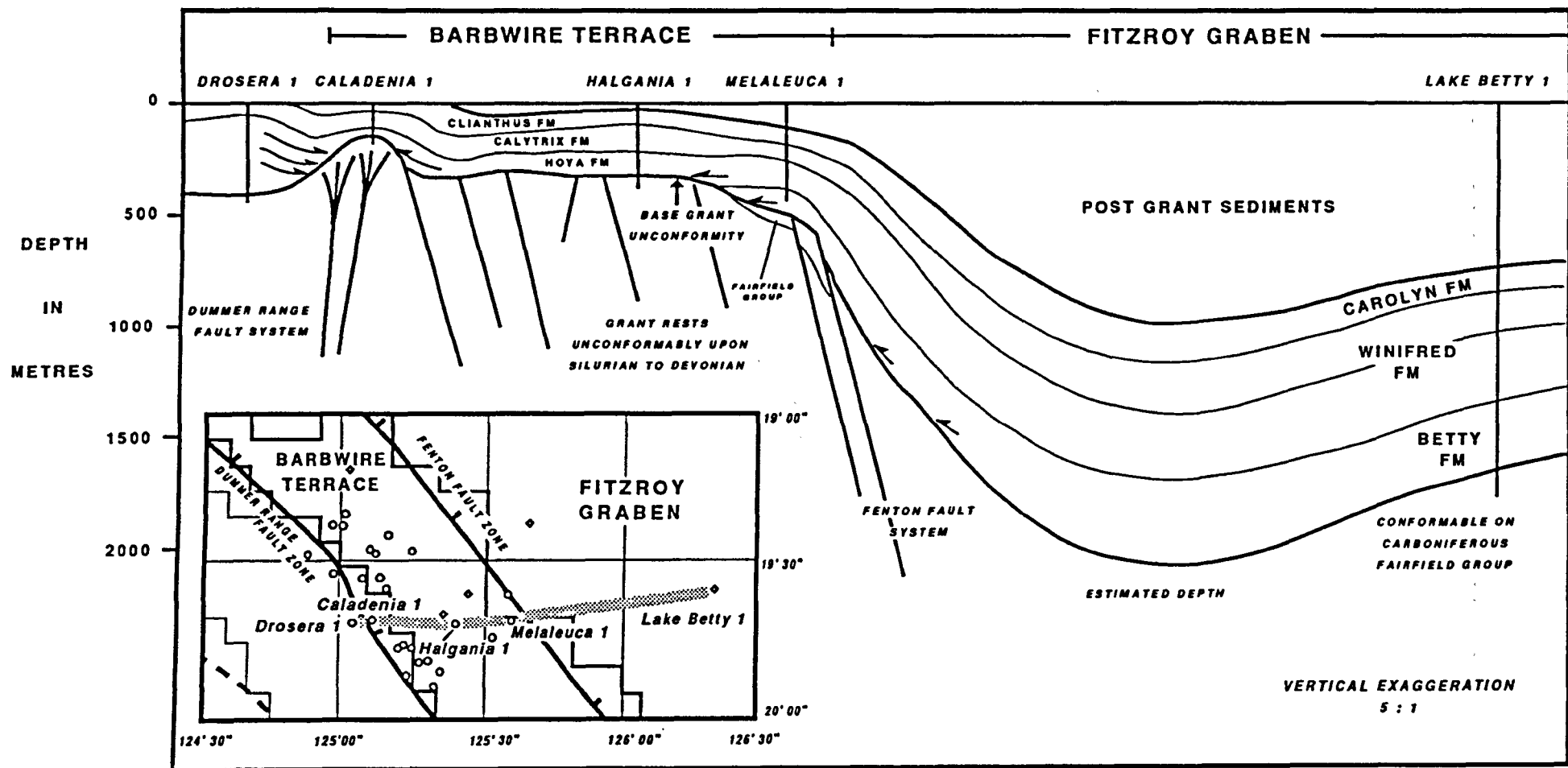


Figure 37. Correlation between the Barbwire Terrace Grant Group stratigraphy defined in this thesis and the published stratigraphy for Lake Betty 1. (Lake Betty 1 stratigraphy modified from Crowe et al. 1978)

SEQUENCE STRATIGRAPHY DEPOSITIONAL MODEL SHOWING SURFACES AND SYSTEMS TRACTS

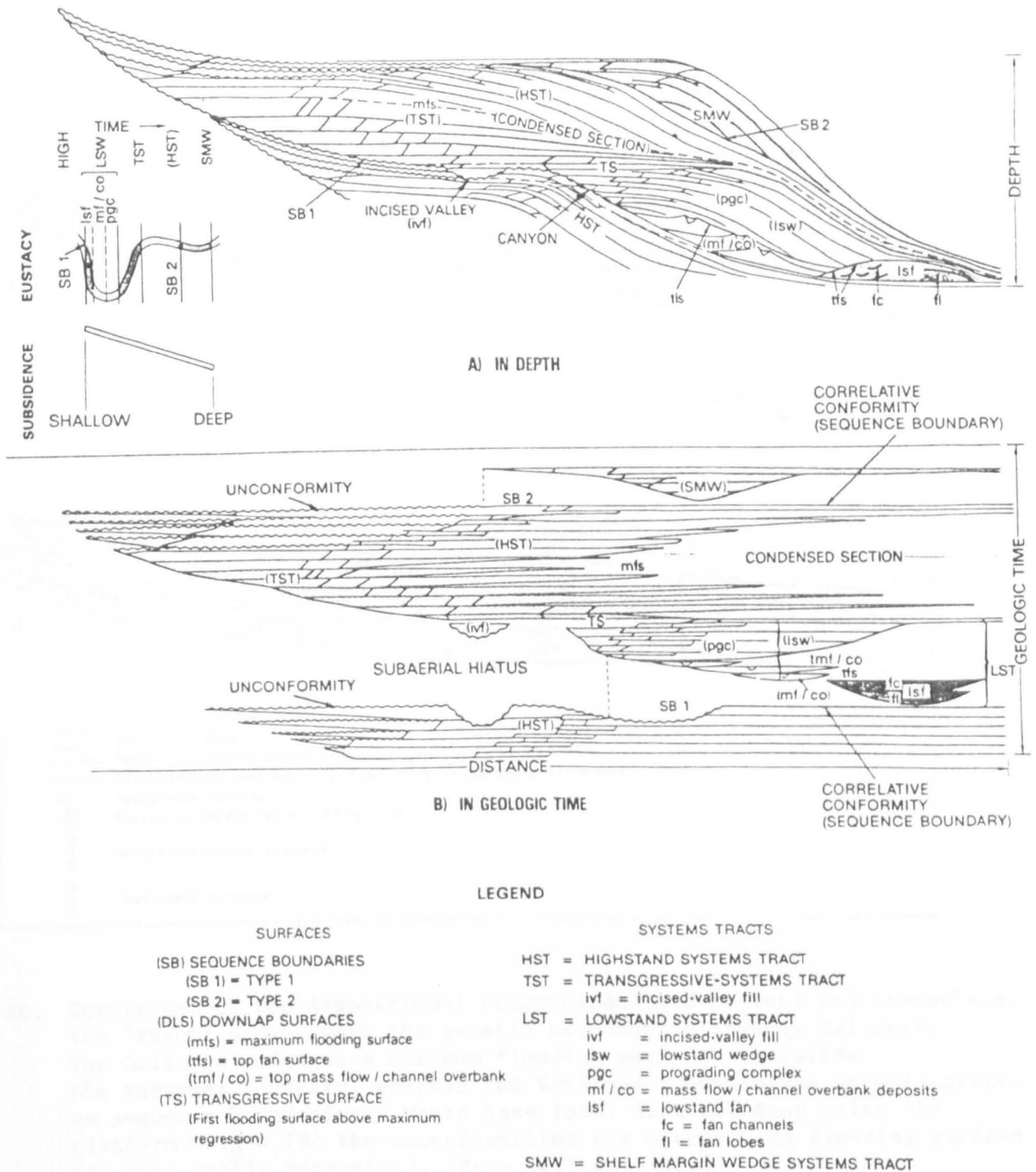


Figure 39. The main elements of the sequence stratigraphic depositional model as proposed by Vail and co-workers. (from Baum and Vail 1988)

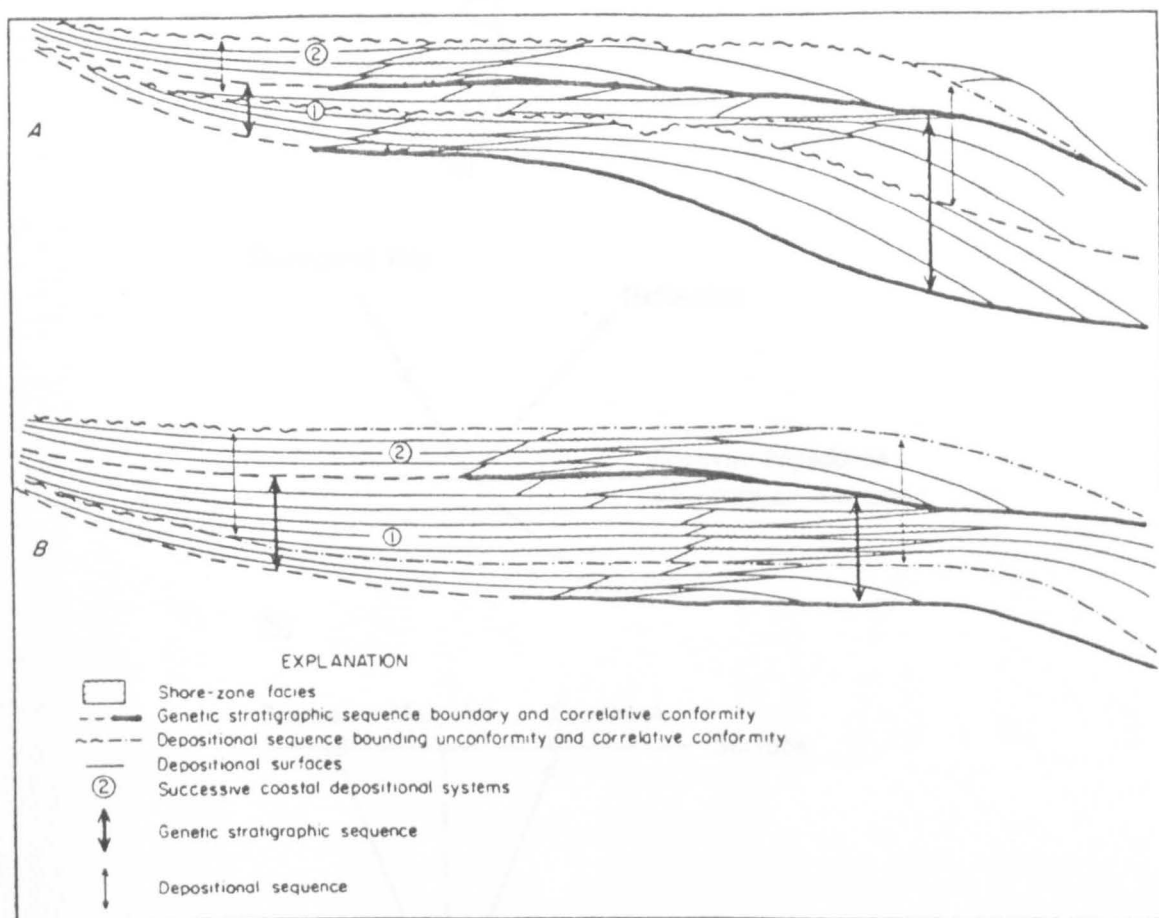


Figure 40. Comparison of the depositional sequence defined by Vail and co-workers, the 'Exxon' model, with the genetic sequence defined by Galloway. The Galloway model uses maximum flooding surfaces to define the sequence boundary, whereas the Vail model emphasises unconformities as sequence boundaries. Where base level does not drop below the platform margin (B) the unconformities are obscure and flooding surface are more easily recognised. (From Galloway 1989)

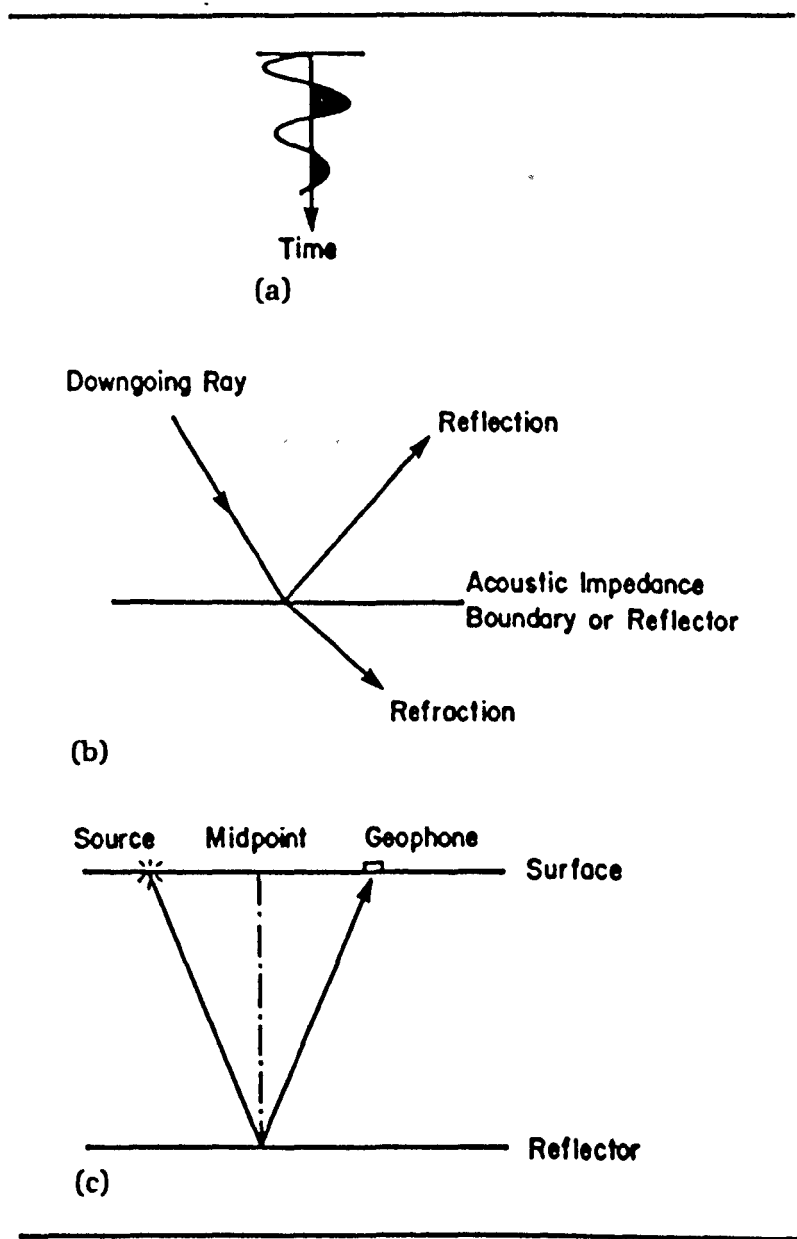
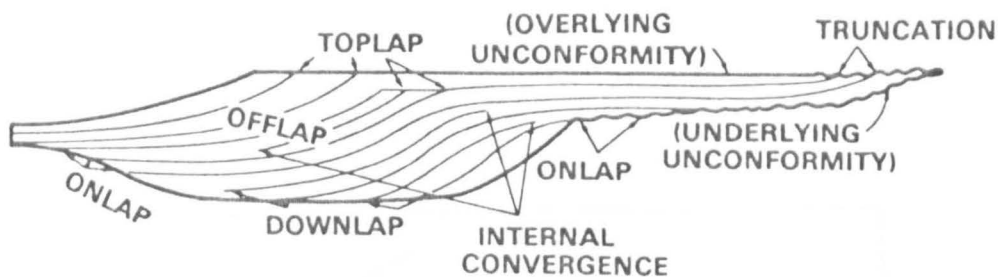


Figure 41. The main elements of seismic acquisition. (a) Diagrammatic representation of the source wavelet. (b) Reflection and refraction at an acoustic-impedance boundary (eg. lithological boundary, diagenetic change, fluid change or fault surface). (c) Reflection geometry for a horizontal reflector. (from Badley 1985)



A. Reflection relationships within an idealised seismic sequence.

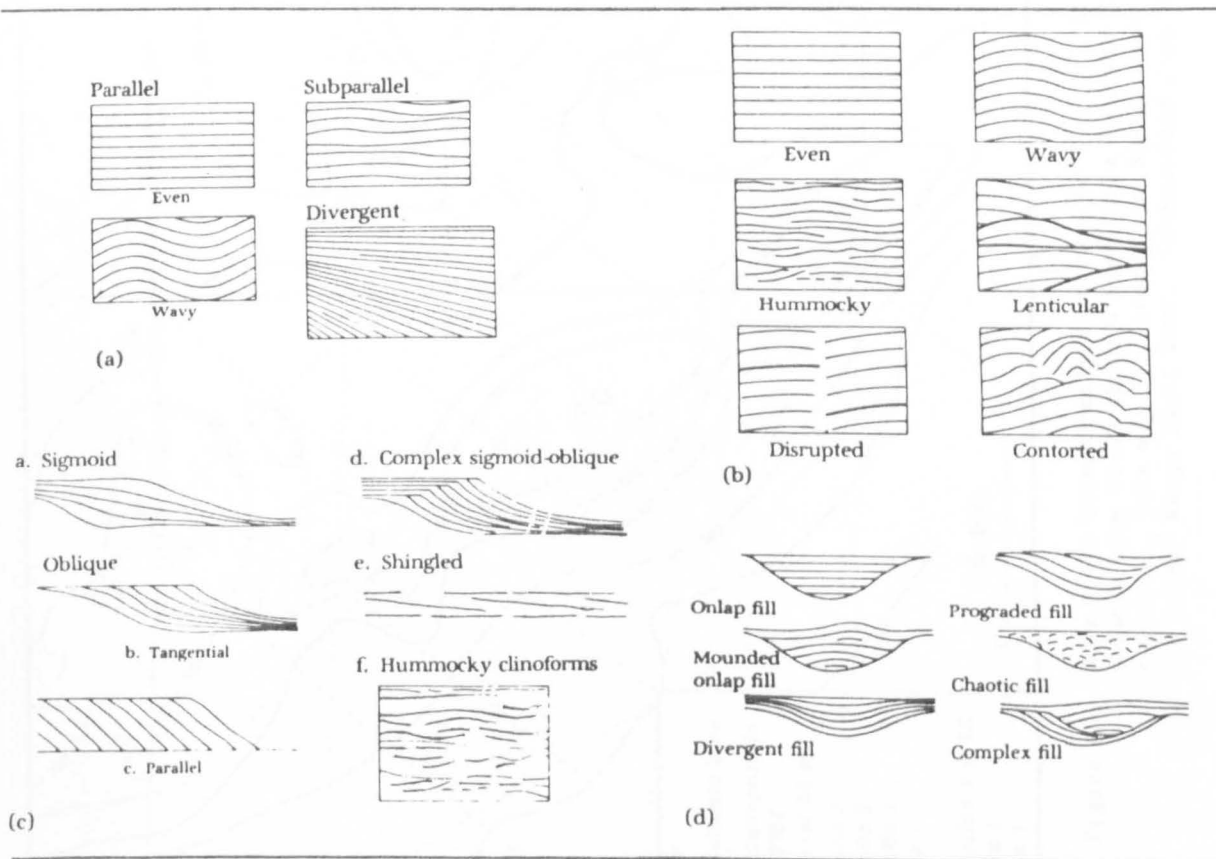


Figure 42. B. Examples of diagnostic reflection configurations.

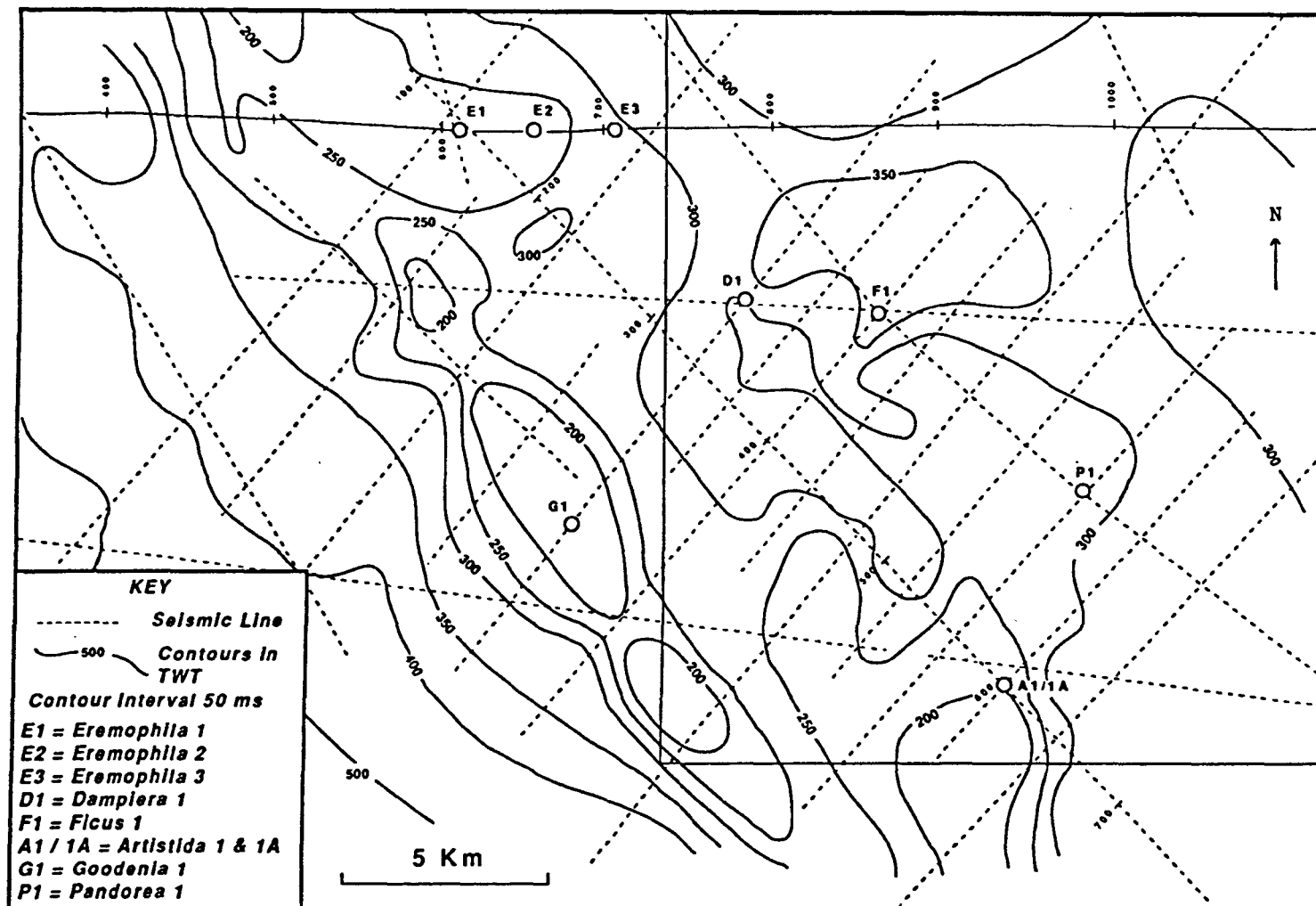


Figure 43. Base Grant Unconformity Structure in Time Map for the Eremophila area. Seismic line 82-20 through Eremophila 1, 2 and 3 is displayed on Figure 33. This map illustrates the NW-SE trending high located along the Dummer Range Fault Zone. (Summarised from WMC regional mapping)

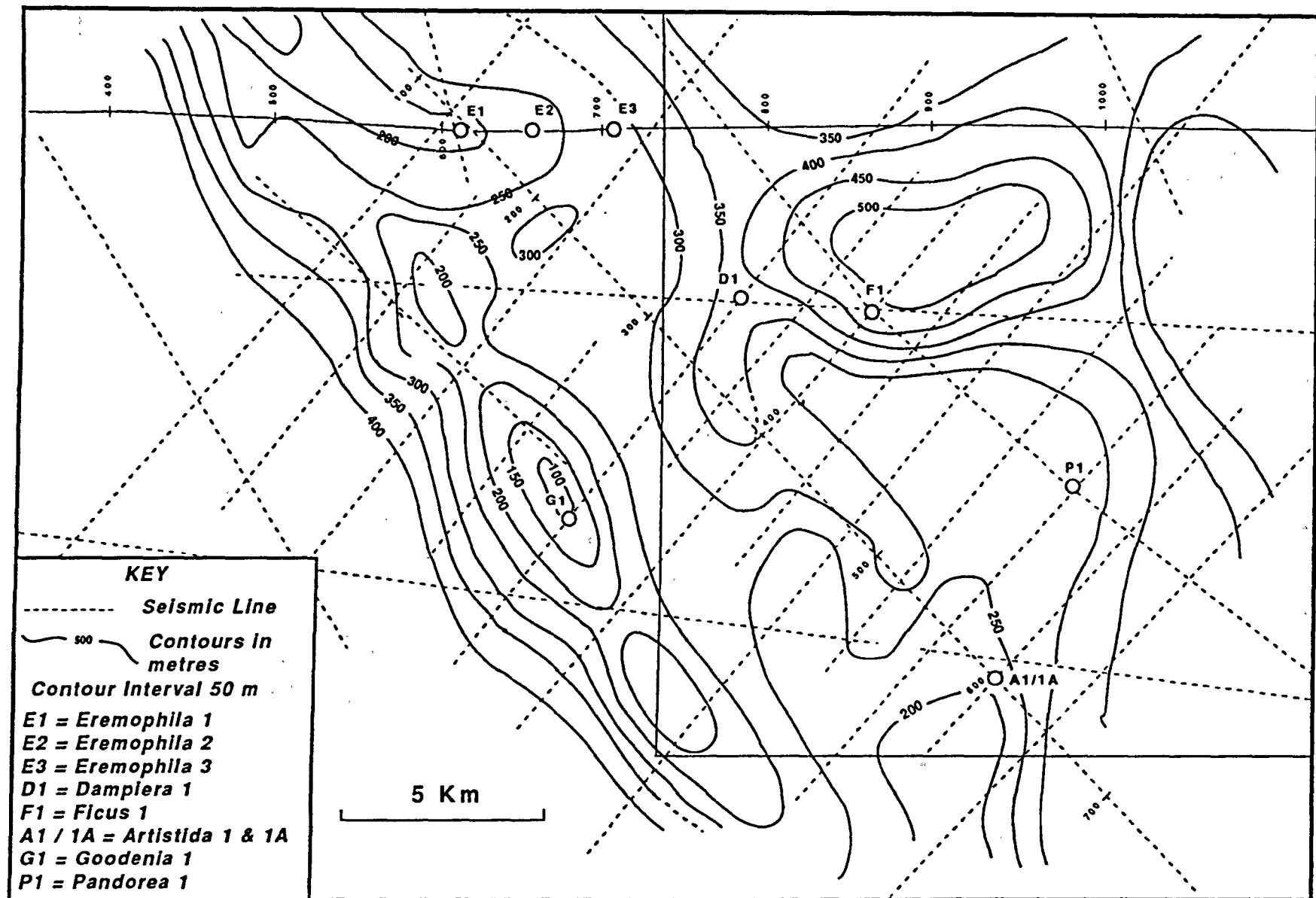


Figure 44. Depth to Base Grant Unconformity. (Interpreted from the structure in time map and well control). The Grant Group thins onto the highs and thickens into the lows, suggesting a structural control on deposition.

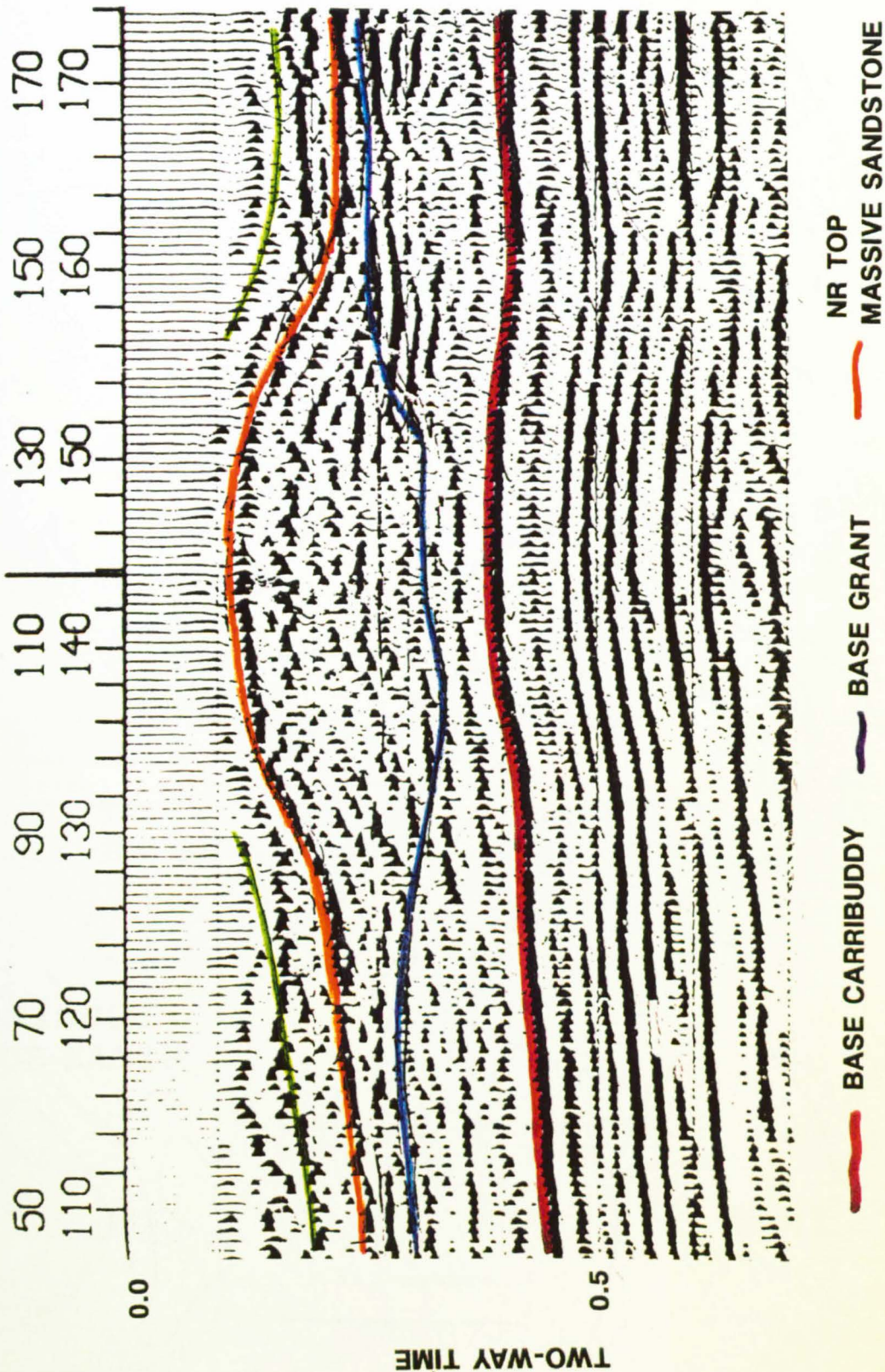


Figure 45. Detail of seismic line 82-24 (see Enclosure 2). The large rounded feature was cored by Drosera 1, which encountered a thick sequence of Grant Group sandstones resting on a sharp unconformity with the Carribuddy Formation.

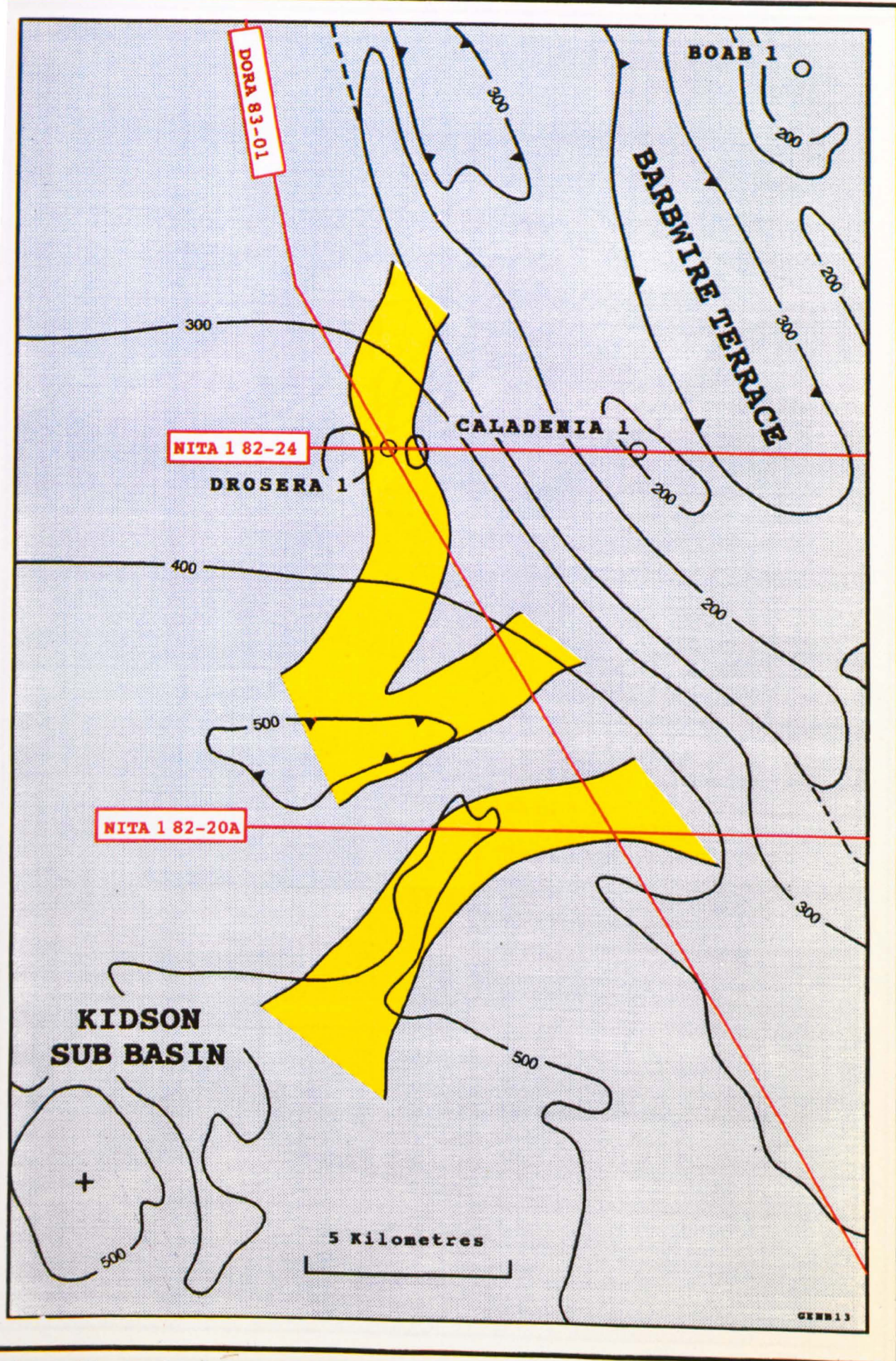
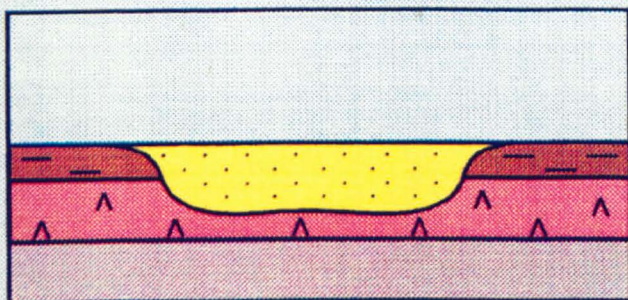
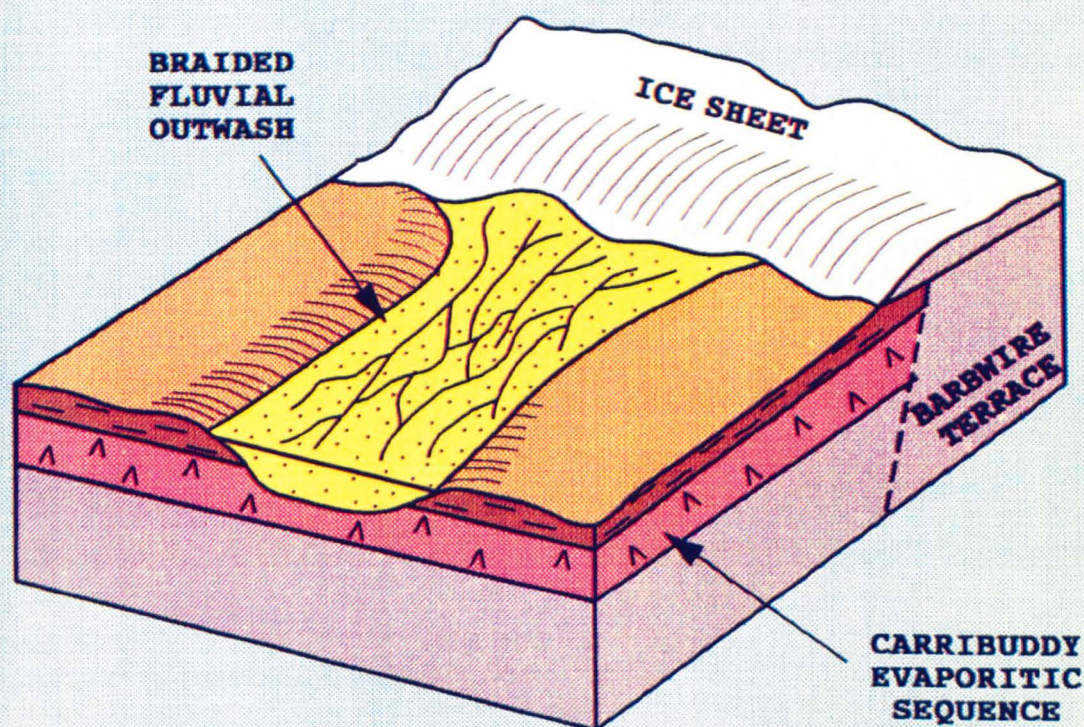
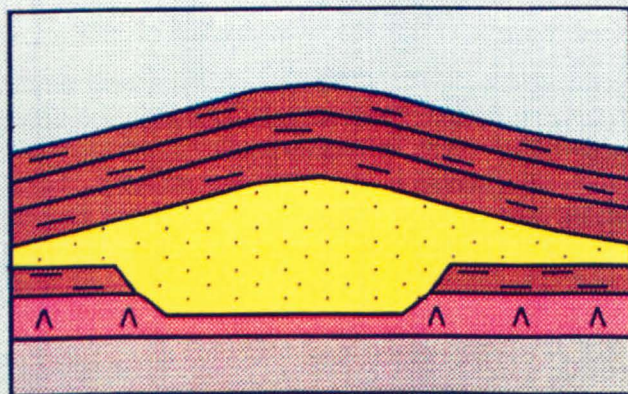


Figure 46. Regional interpretation of the 'mounded seismic facies', with apparent linear features trending away from the Barbwire Terrace. Displayed on Base Grant Unconformity structure in time map. (Line 82-24 is shown on Figure 45 and Enclosure 1, line 82-20a on Figure 48)



STAGE 1

RAPID EROSION
OF EVAPORITIC SEQUENCE.
DEPOSITION OF THICK
BRAIDED FLUVIAL
SANDSTONE PACKAGE.



STAGE 2

WITHDRAWAL / DISSOLUTION
OF REMAINING EVAPORITES
TOGETHER WITH
COMPACTION PRODUCES
"MOUNDED" FEATURES.

GENB15

Figure 47. Proposed depositional environment for the sandstones encountered in Drosera 1 and Kunzea 1, within a schematic palaeogeographic setting, and a model for the formation of the mounded features.

WEST

NITA 1 82-20A

EAST

CROSSLAND PLATFORM

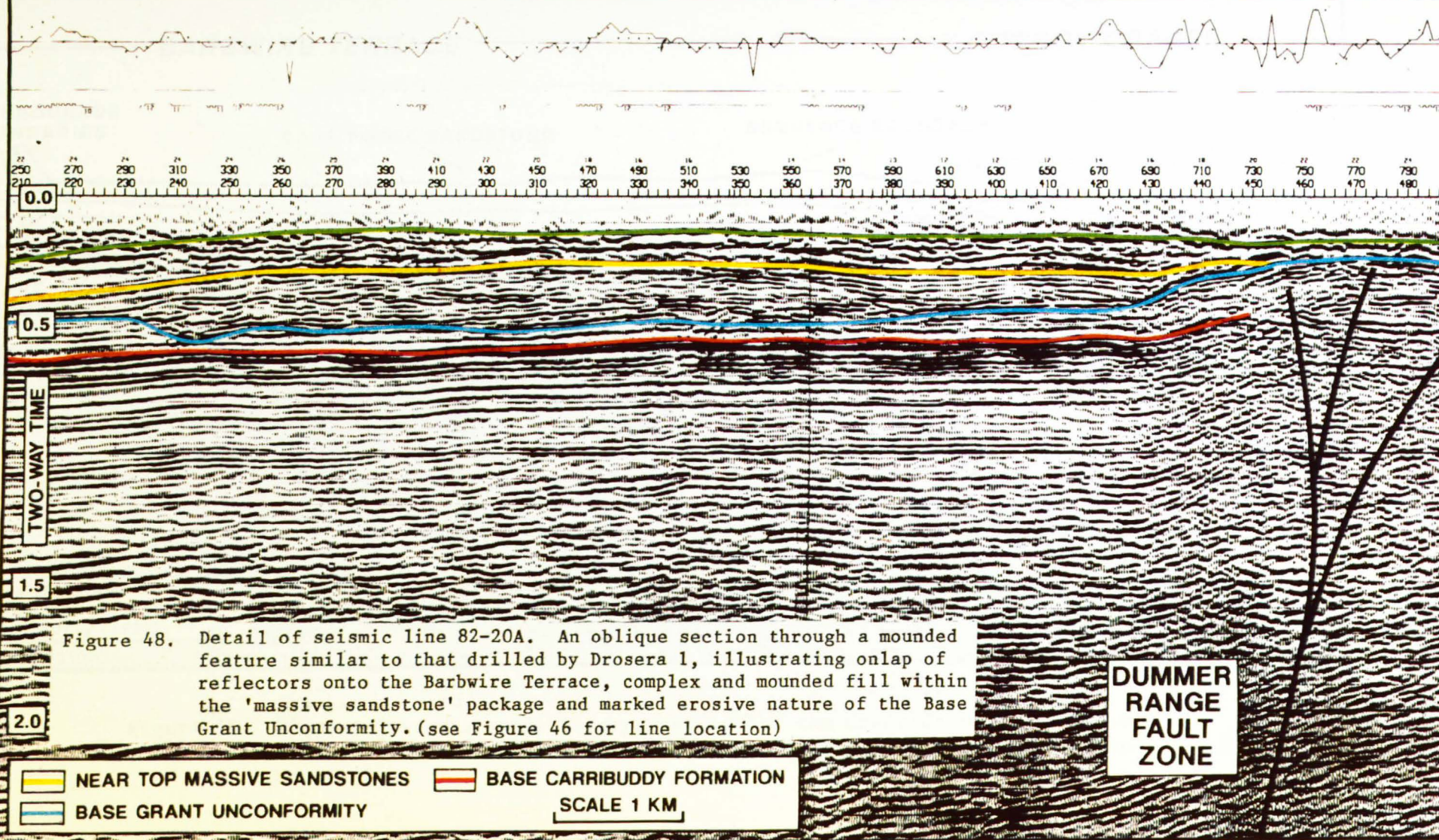
BARBWIRE
TERRACE

Figure 48. Detail of seismic line 82-20A. An oblique section through a mounded feature similar to that drilled by Drosera 1, illustrating onlap of reflectors onto the Barbwire Terrace, complex and mounded fill within the 'massive sandstone' package and marked erosive nature of the Base Grant Unconformity. (see Figure 46 for line location)

NEAR TOP MASSIVE SANDSTONES
BASE CARRIBUDDY FORMATION
BASE GRANT UNCONFORMITY

SCALE 1 KM

DUMMER
RANGE
FAULT
ZONE

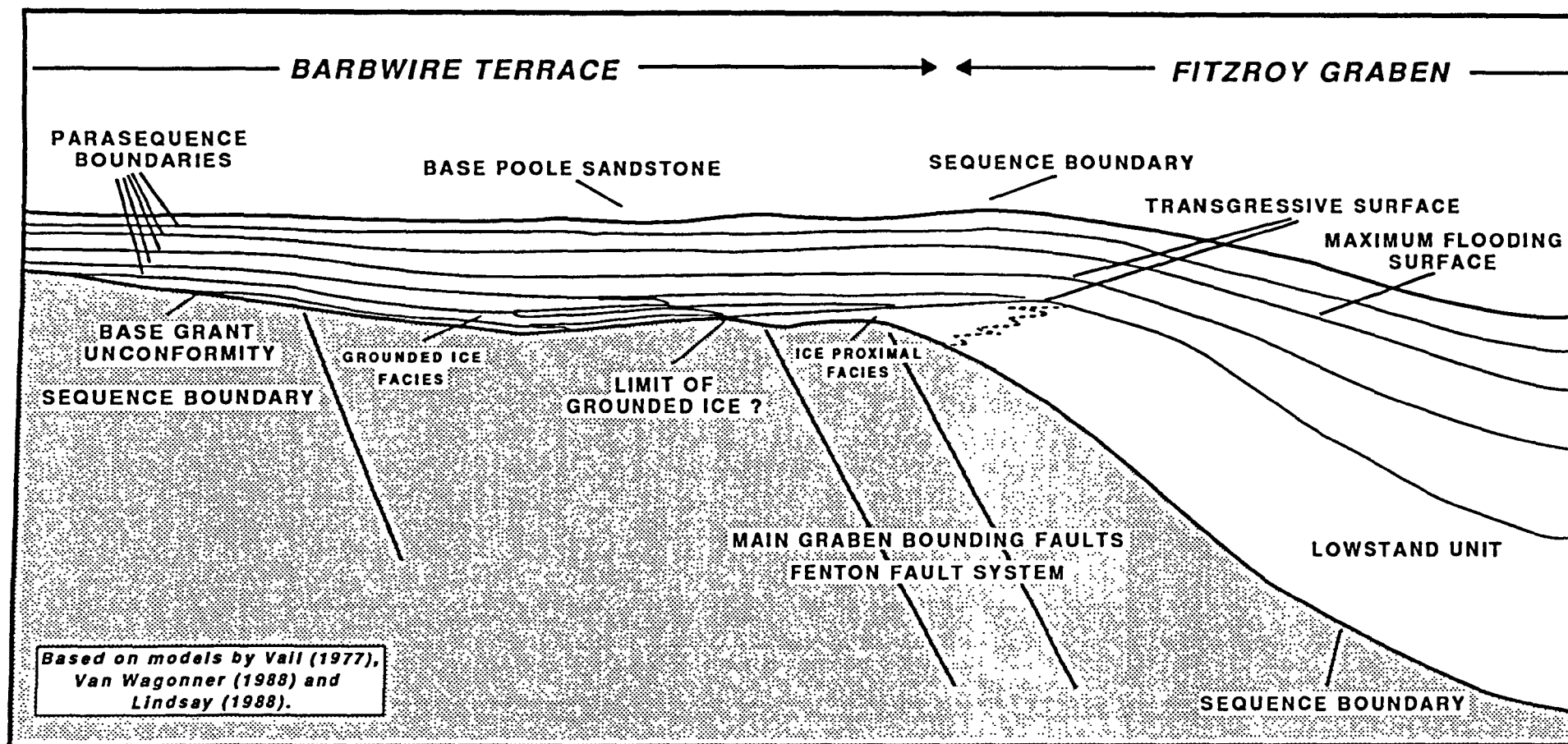


Figure 49. Sequence stratigraphic interpretation for the Grant Group deposited on the Barbwire Terrace and Fitzroy Graben, displaying the main sequence boundaries.

GLACIAL DEBRIS IN TRANSPORT		GLACIAL FACIES		
		POSITION OF DEPOSITION	PROCESS OF DEPOSITION TERRESTRIAL TILLITE	ICE-RAFTED SEDIMENTS
GLACIER ICE	SUPRAGLACIAL DEBRIS	PROGLACIAL	FLOW TILLITE	
	ENGLACIAL DEBRIS	SUPRAGLACIAL	FLOW TILLITE MELT-OUT TILLITE SUBLIMATION TILLITE	
	BASAL DEBRIS	SUBGLACIAL	FLOW TILLITE MELT-OUT TILLITE DEFORMATION TILLITE LODGE MENT TILLITE	
UNDIFFERENTIATED		DISTAL		ICE-RAFTED TILLITE
DEFORMED BEDROCK OR SEDIMENTS / GLACIALLY ERODED SURFACE				MARINE / LACUSTRINE SEDIMENTS

Figure 50. Classification of glacial deposits, illustrating the relationship between the transport of glacial debris and the process of deposition. (after Hambrey and Harland 1981)

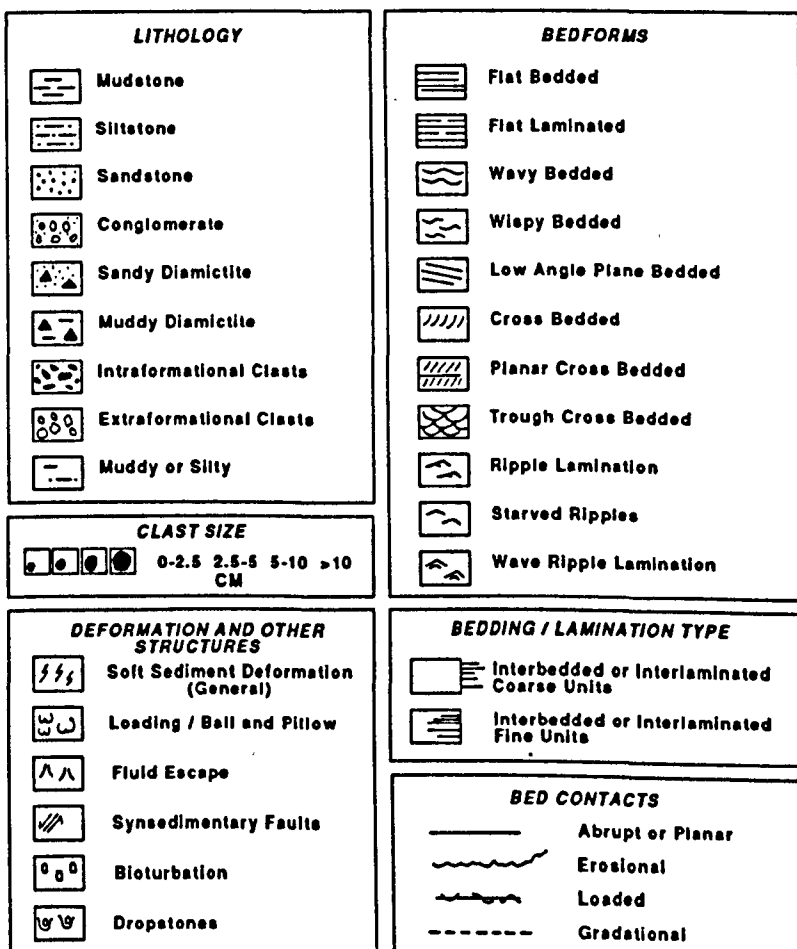
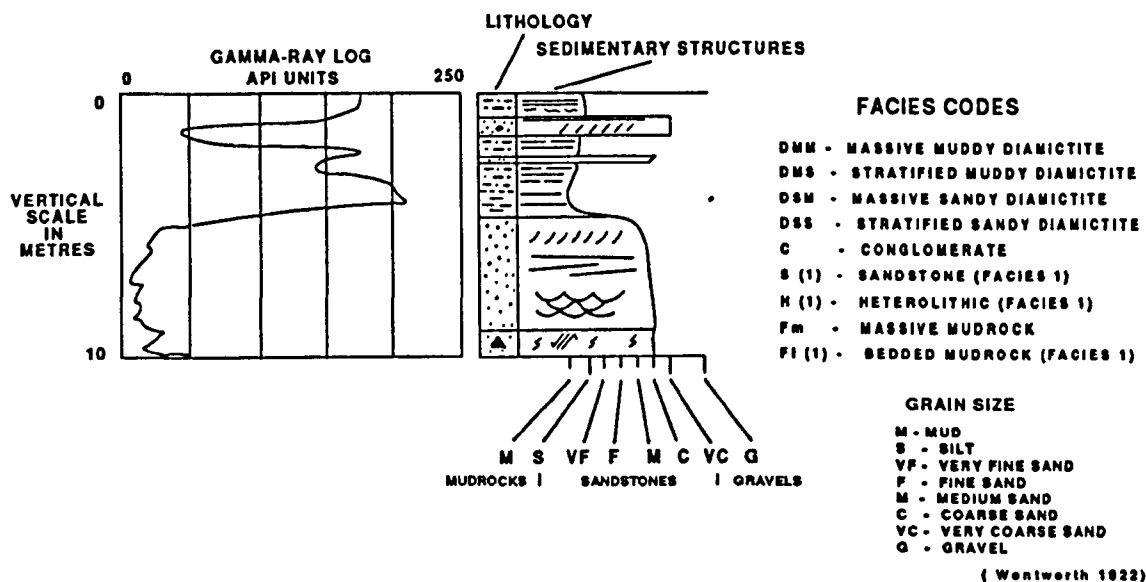


Figure 51. Key to facies log annotation (this is duplicated in Appendix 1

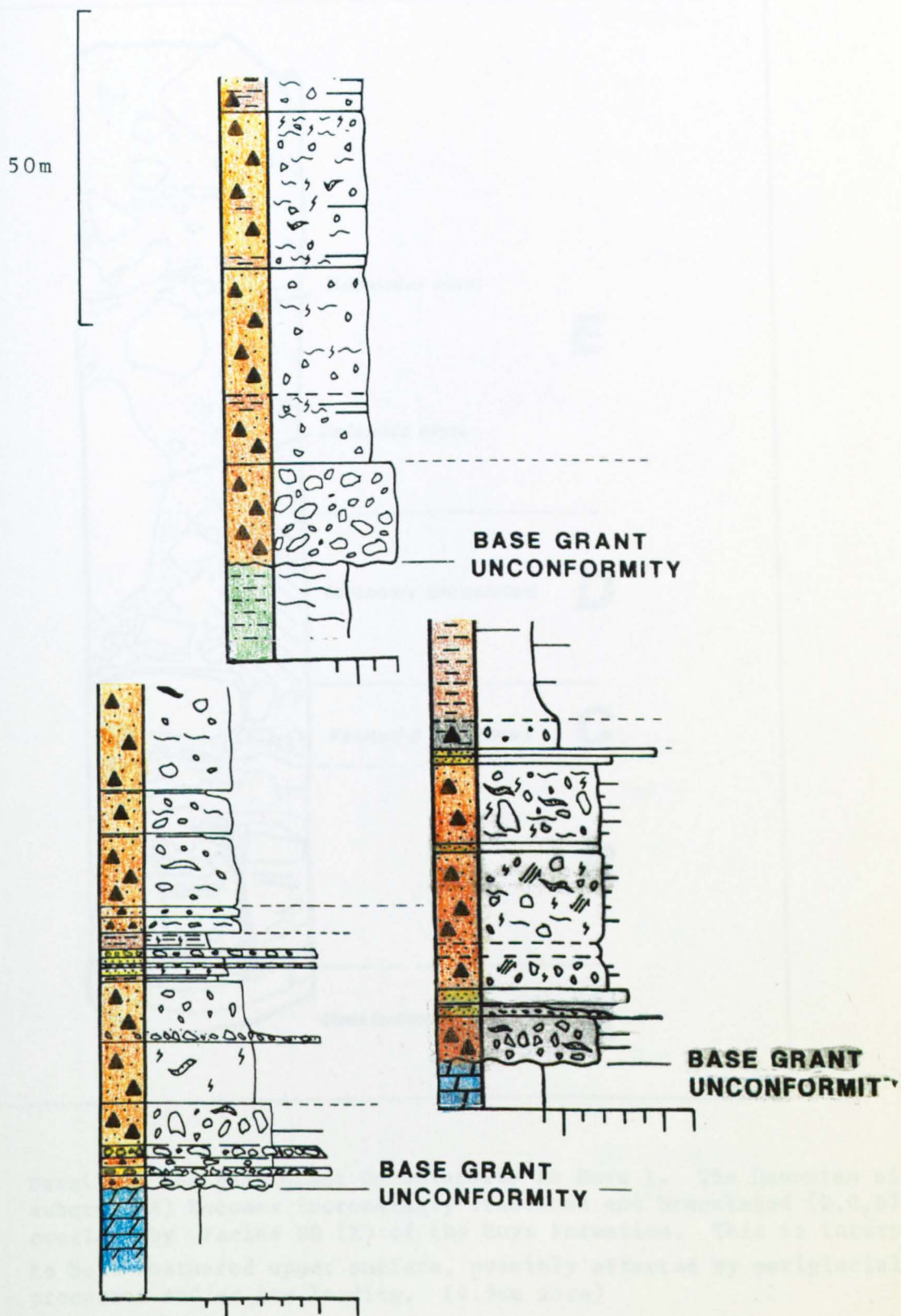


Figure 52. Typical facies logs for the Basal Diamictite Facies Association (BD).
 A. Hoya 1 B. Eremophila 2 C. Aristida 1

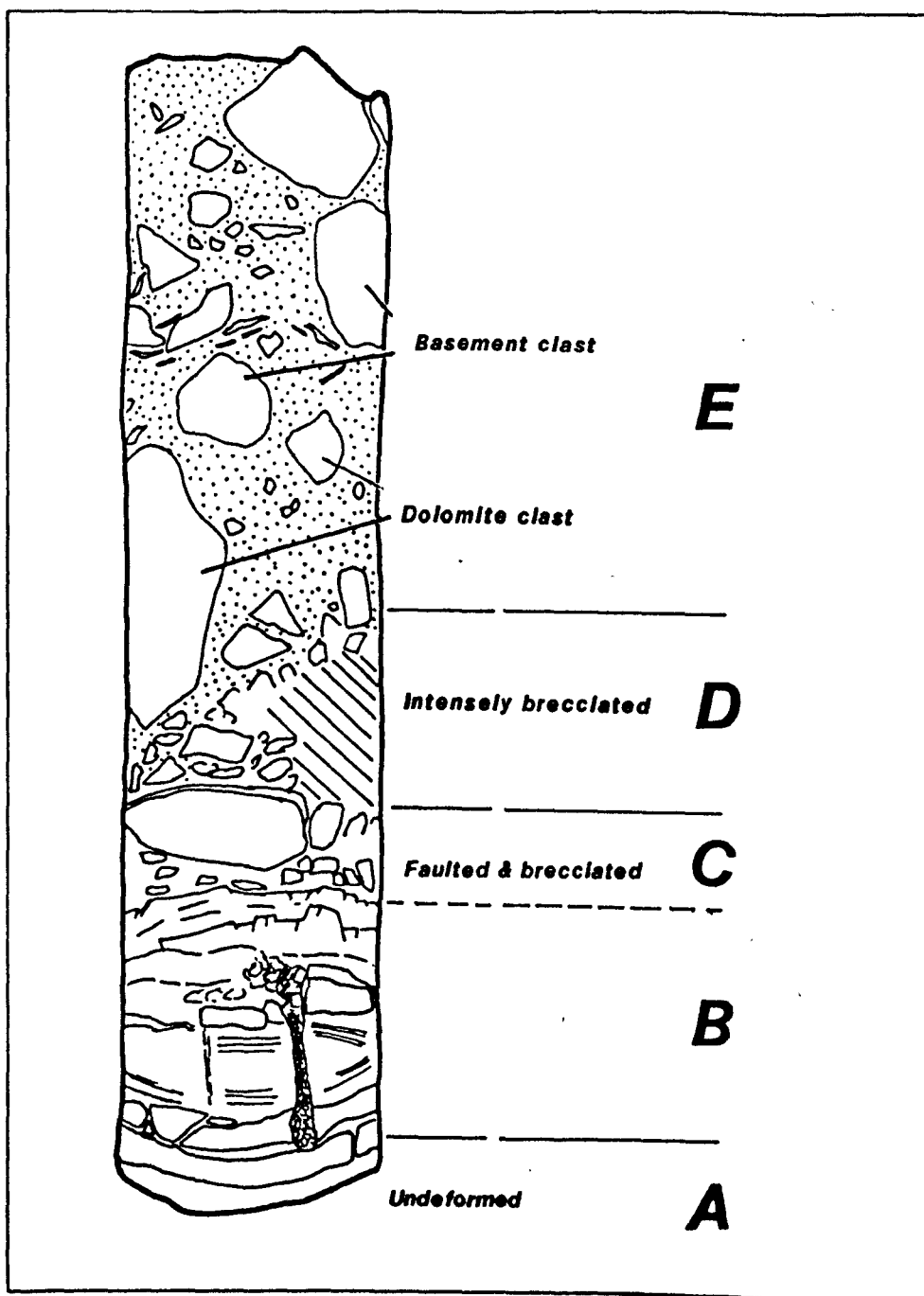


Figure 53. Detail of the Base Grant Unconformity in Hoya 1. The Devonian siltstone subcrop (A) becomes increasingly fractured and brecciated (B,C,D) and is overlain by Facies BD (E) of the Hoya Formation. This is interpreted to be a weathered upper surface, possibly affected by periglacial processes and/or ice loading. (4.5cm core)

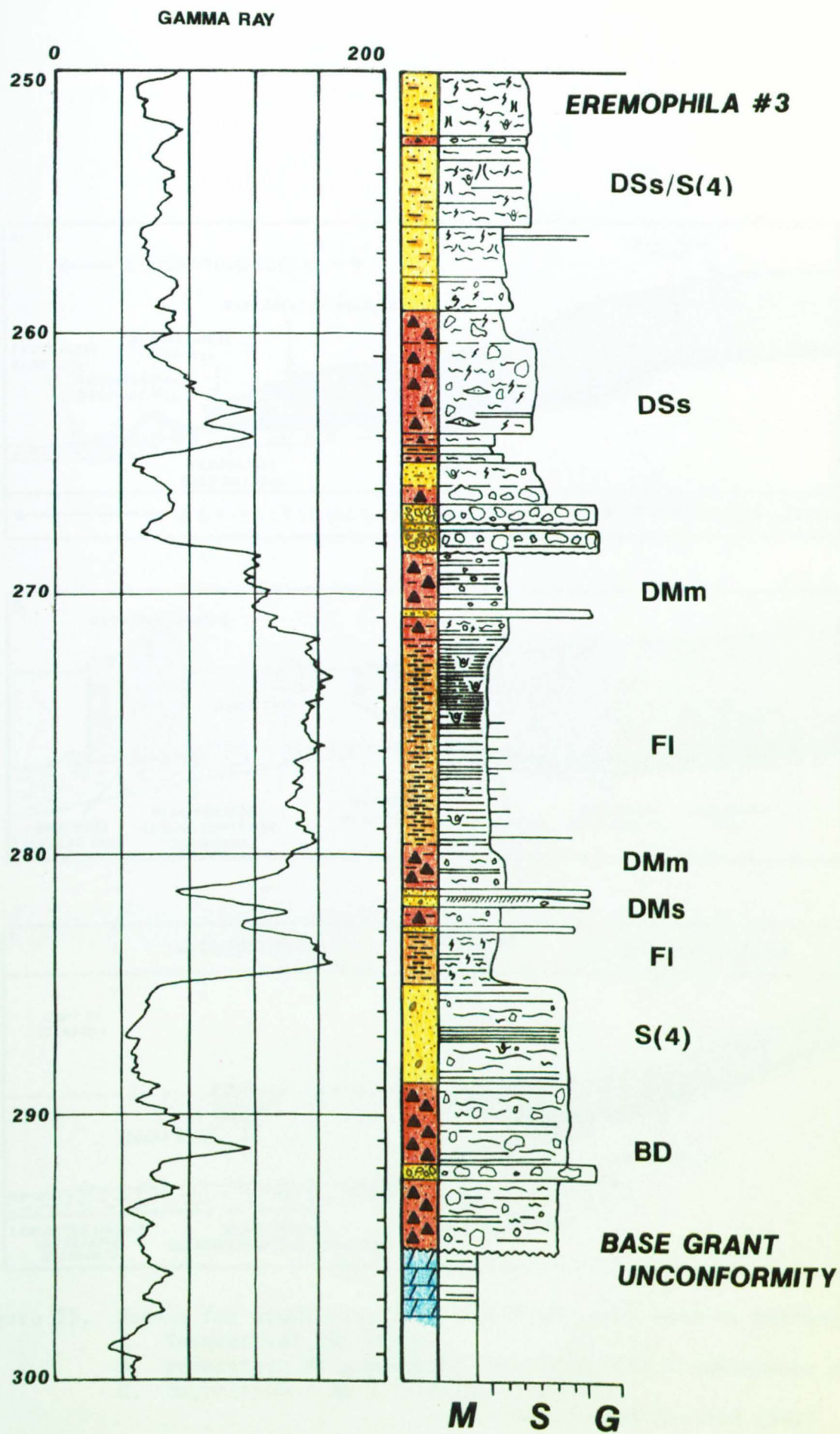


Figure 54. A section of the Hoya Formation from Eremophila 3, which displays the relationship between the facies.

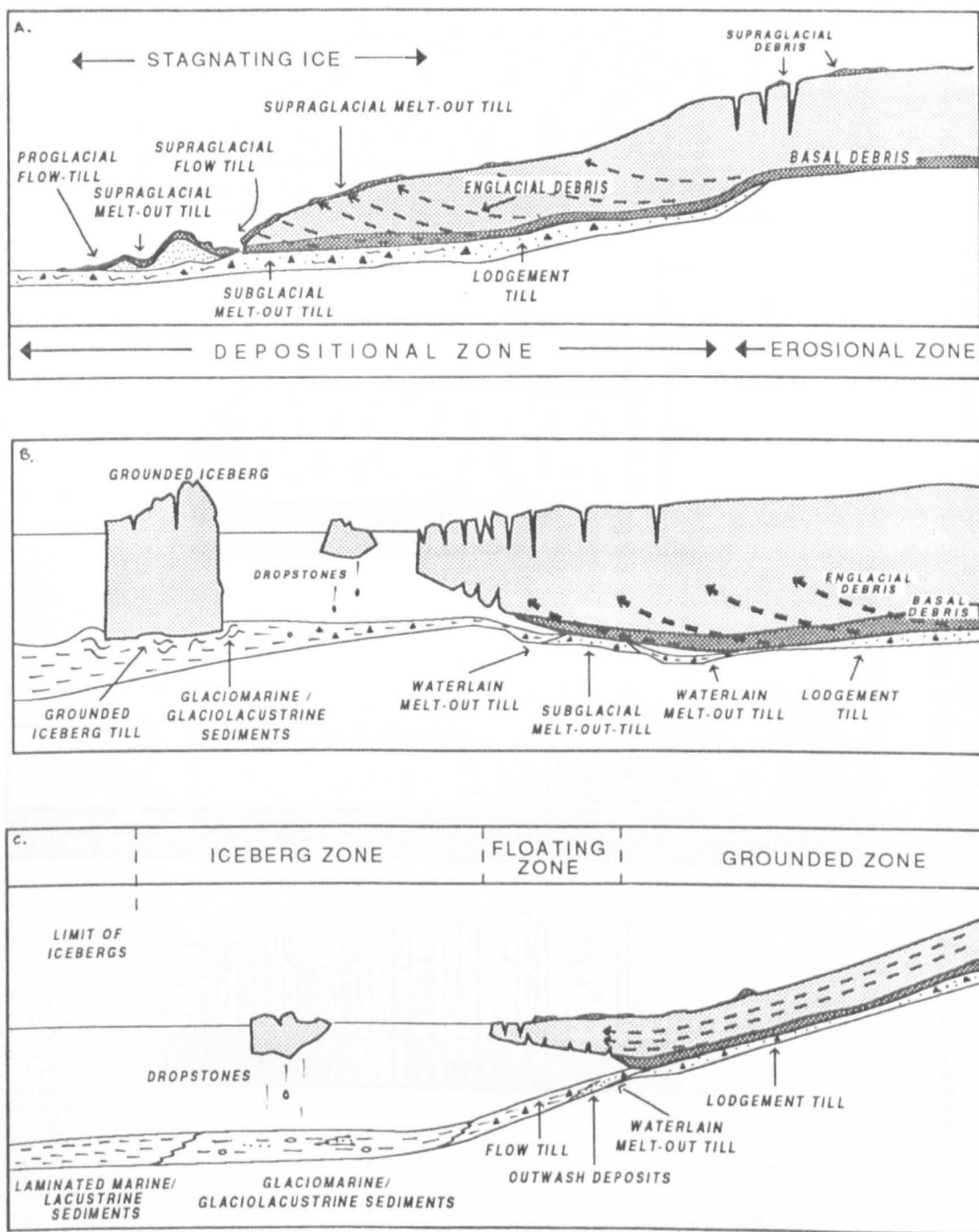


Figure 55. Models for deposition from ice sheets with base at melting point
 A. Terrestrial deposition.
 B. Deposition from grounded ice sheet into a subaqueous setting
 C. Deposition from a floating ice sheet.
 (from Hambrey and Harland 1981)

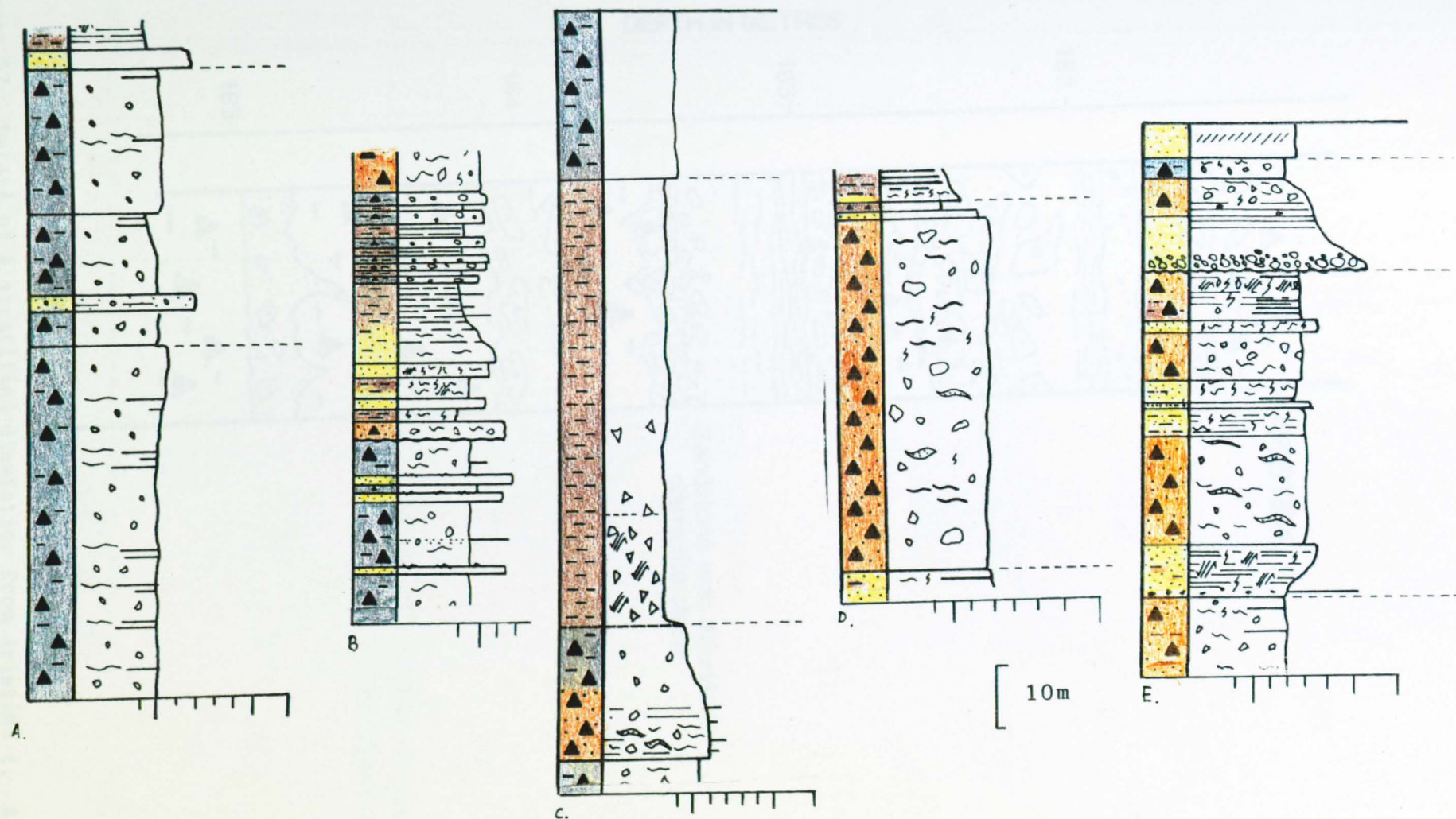


Figure 56. Typical facies logs for:

- A. Massive muddy diamictite facies (DMm). (Hoya 1)
- B. Stratified muddy diamictite facies (DMs). (Calytrix 1)
- C. An upper gradational contact and lower sharp contact between facies DMm and facies Fm. (Hoya 1)
- D. Massive sandy diamictite facies (DSm). (Eremophila 3)
- E. Stratified sandy diamictite facies (DSs). (Hoya 1)

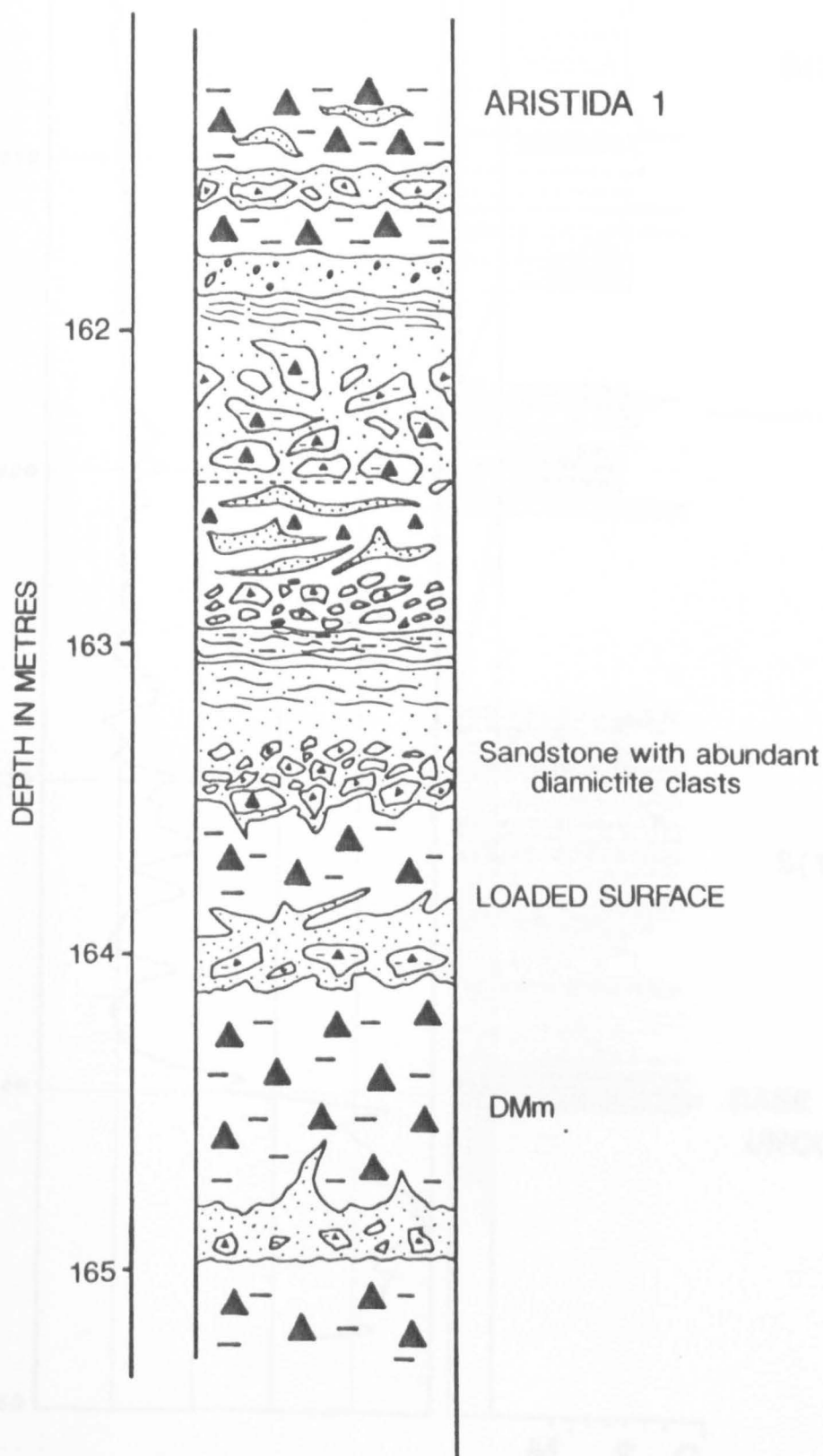


Figure 57. Detail of a stratified diamictite from Aristida 1. A medium-grey muddy diamictite (DMm) is interbedded with fine-grained sandstones, containing abundant diamictite rip-up clasts. The muddy diamictite is interpreted to be a basal rain-out deposit. The interbedded sandstones indicate intermittent high-energy mass flows.

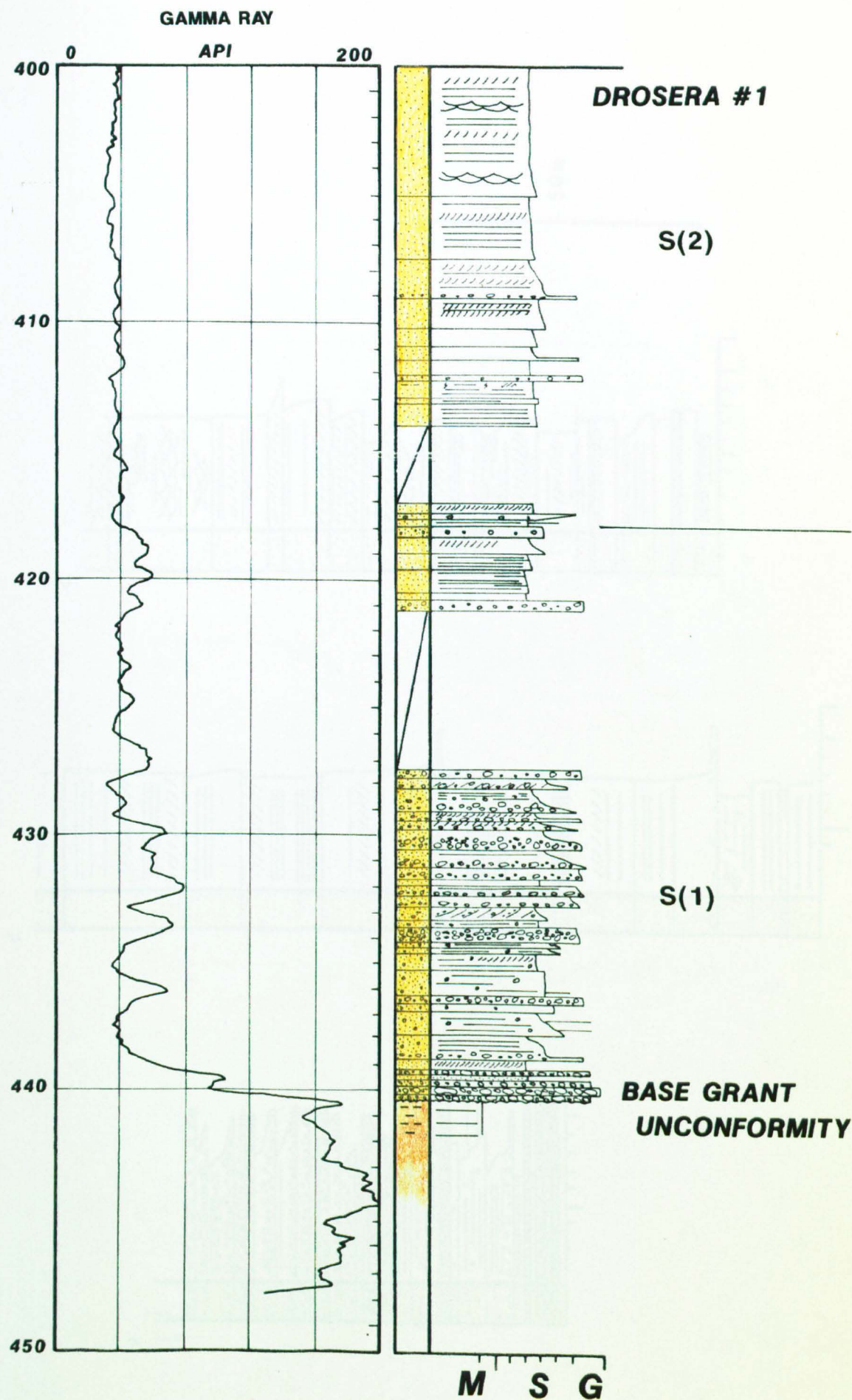


Figure 58. The relationship and gamma-ray log character of Sandstone Facies 1 and Sandstone Facies 2 from Drosera 1.

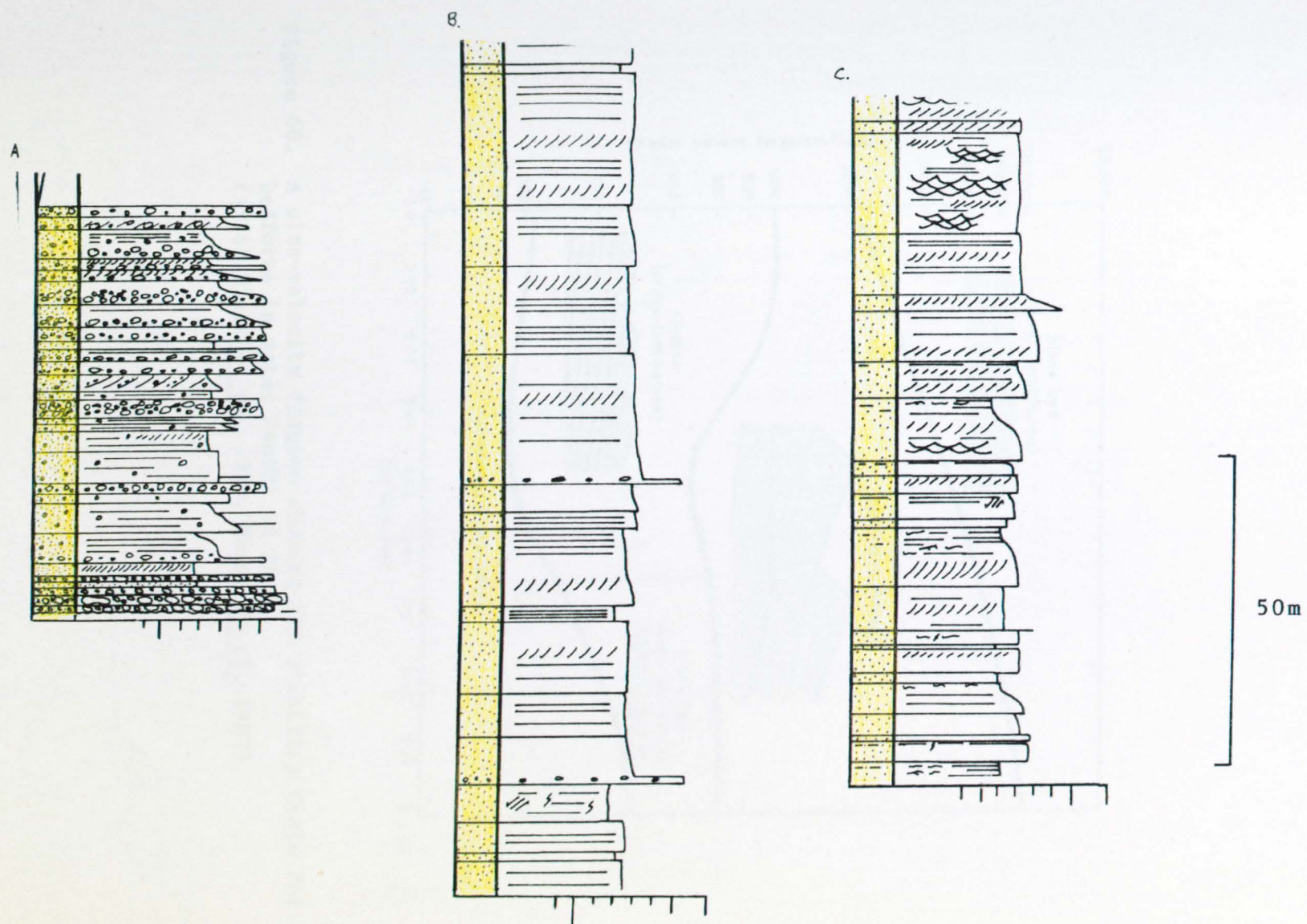


Figure 59. Typical facies logs for:
 A. Sandstone Facies 1 (Drosera 1)
 B. Sandstone Facies 2 (Drosera 1)
 C. Sandstone Facies 3 (Drosera 1)

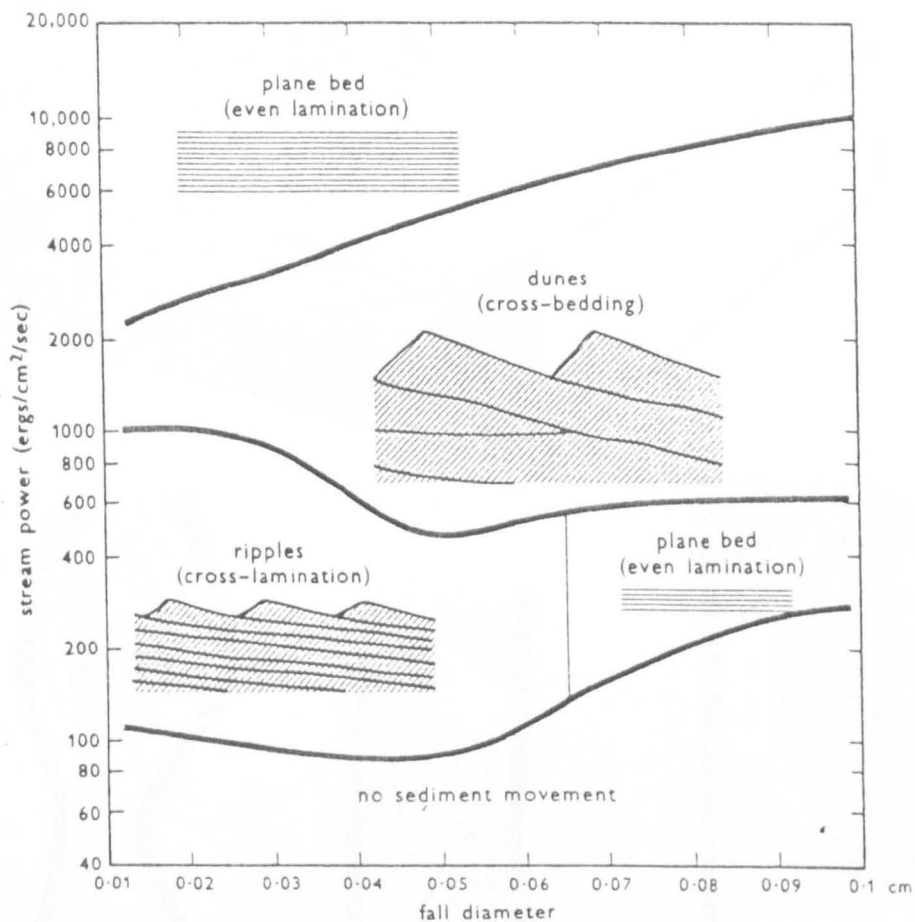


Figure 60. A size-velocity diagram showing the stability field for different bedforms in water depths of 20cm. (after Blatt et al. 1980, Harms et al. 1982).

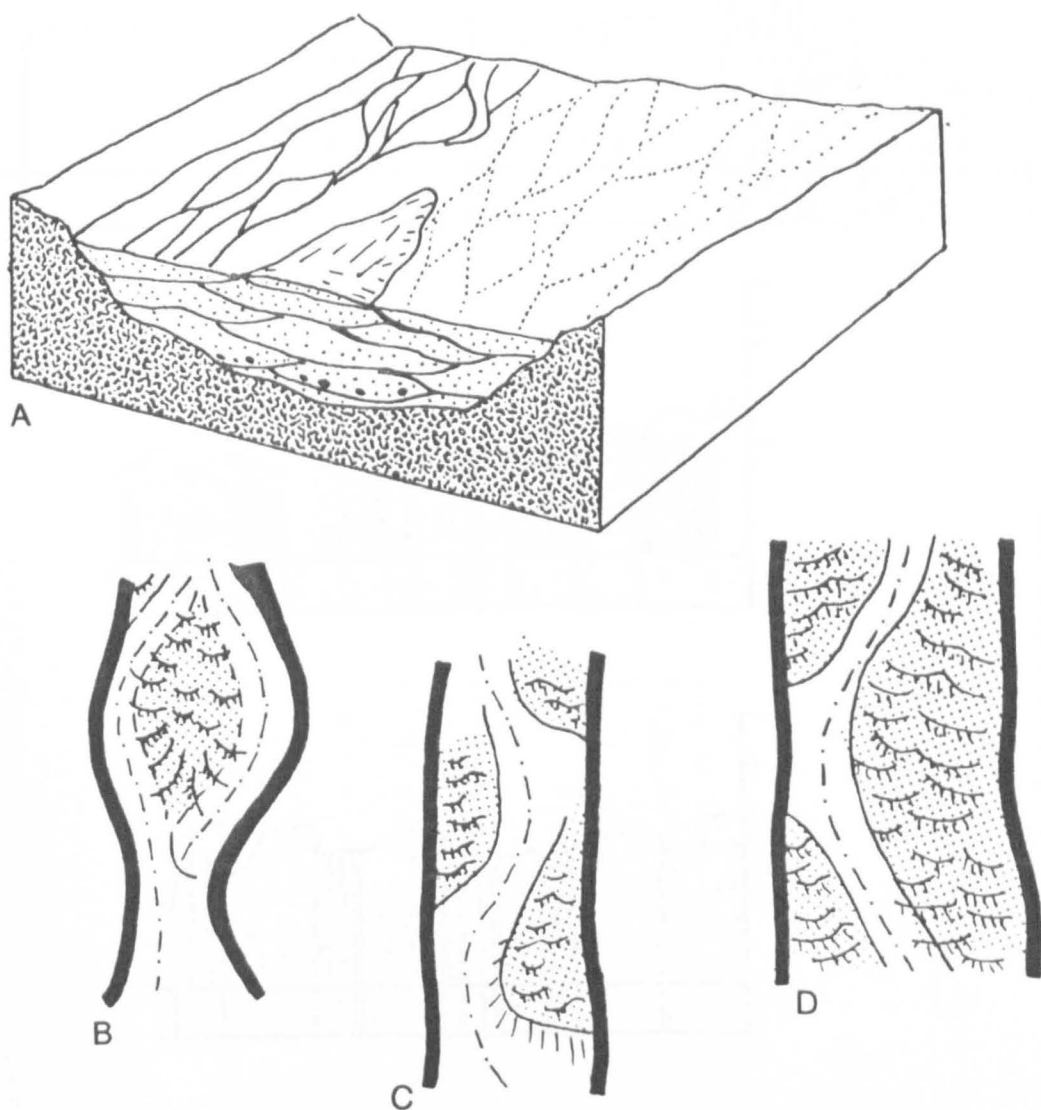


Figure 61. A. Block diagram illustrating the deposition of sheet sandstones within a braided river system, restricted laterally by topographic features. In detail the sandstones will contain abundant stratification types relating to the migration of bars and in-channel dunes.

Definition diagram for different bar types on a sandy river bed.
 B. Mid-channel or longitudinal bar C. Alternate or transverse bars with large scale slip faces D. Side bars.

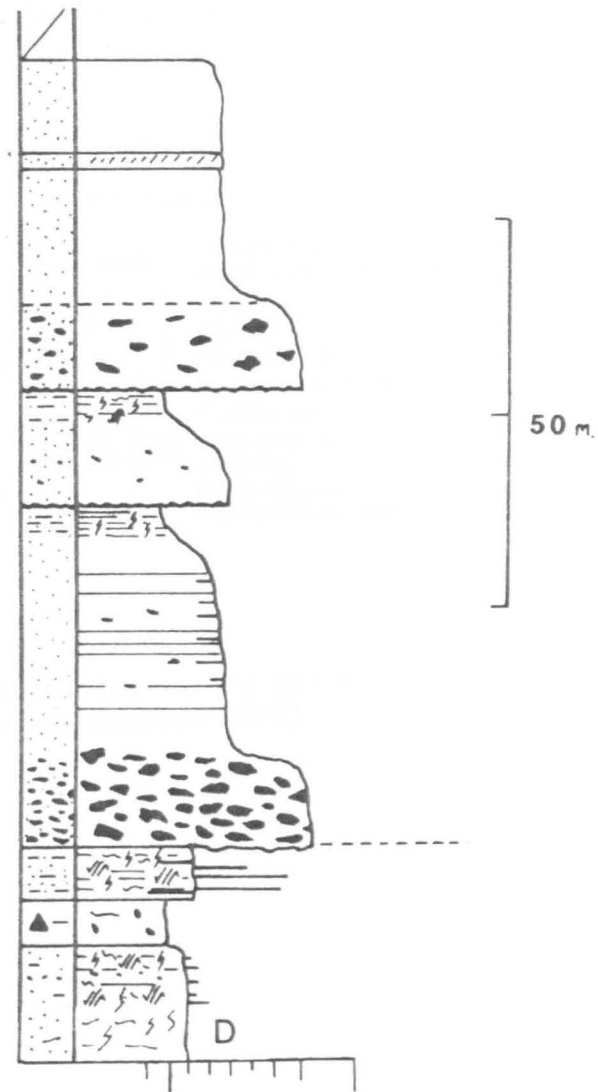
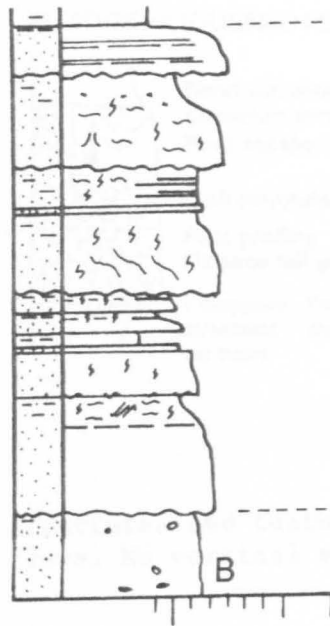
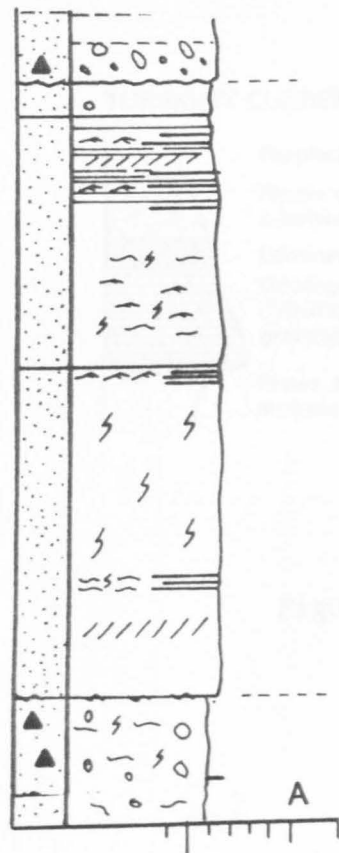
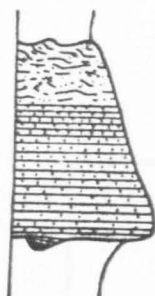


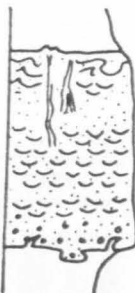
Figure 62. Typical facies logs for:
 A. Sandstone Facies 4 (Ficus 1)
 B. Sandstone Facies 5 (Ficus 1)
 C. Sandstone Facies 6 (Melaleuca 1)
 D. Sandstone Facies 7 (Hoya 1)

TURBIDITY CURRENT



Rippled or flat top
Ripple drift micro-
x-lamination
Laminated
Good grading
("distribution
grading")
Flutes, tool marks
on base

FLUIDIZED/LIQUEFIED FLOW

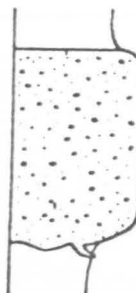


Sand volcanoes or flat top
Convolute lamination
Fluid escape 'pipes'

Dish structure?
Poor grading
("coarse tail grading")

? Grooves, Flame and load
striations structures
on base

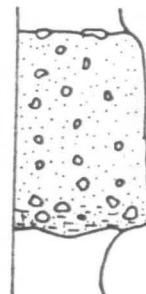
GRAIN FLOW



Flat top
No grading ?
Massive,
Grain orientation
parallel to flow

Reverse grading
near base?
Scours, injection
structures

DEBRIS FLOW



Irregular top
(large grains projecting)
Massive,
Poor sorting
Random fabric
Poor grading, if any
("coarse tail")
Basal zone of
'shearing'
Broad 'scours'.
? Striations at base

Figure 63. Structures and textures of deposits from single mechanism mass-gravity flows. No vertical scale implied. (from Middleton and Hampton 1976)

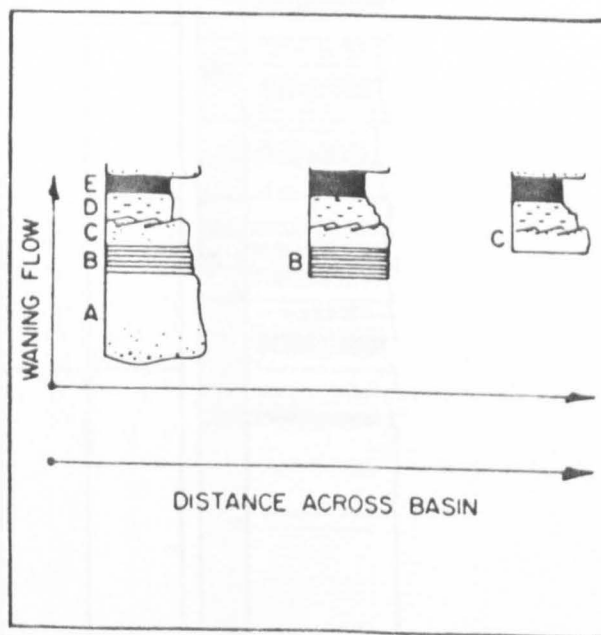
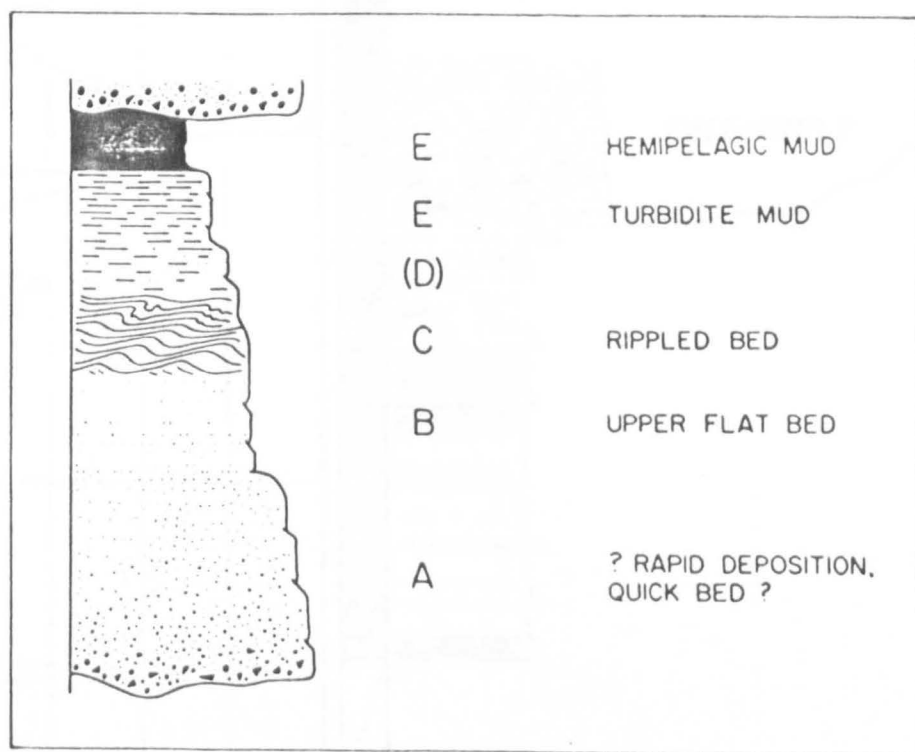


Figure 64. A. The divisions of the idealised 'Bouma' sequence.

B. Idealised change in turbidite character due to waning flow for proximal and distal locations.

FROM WALKER 1984

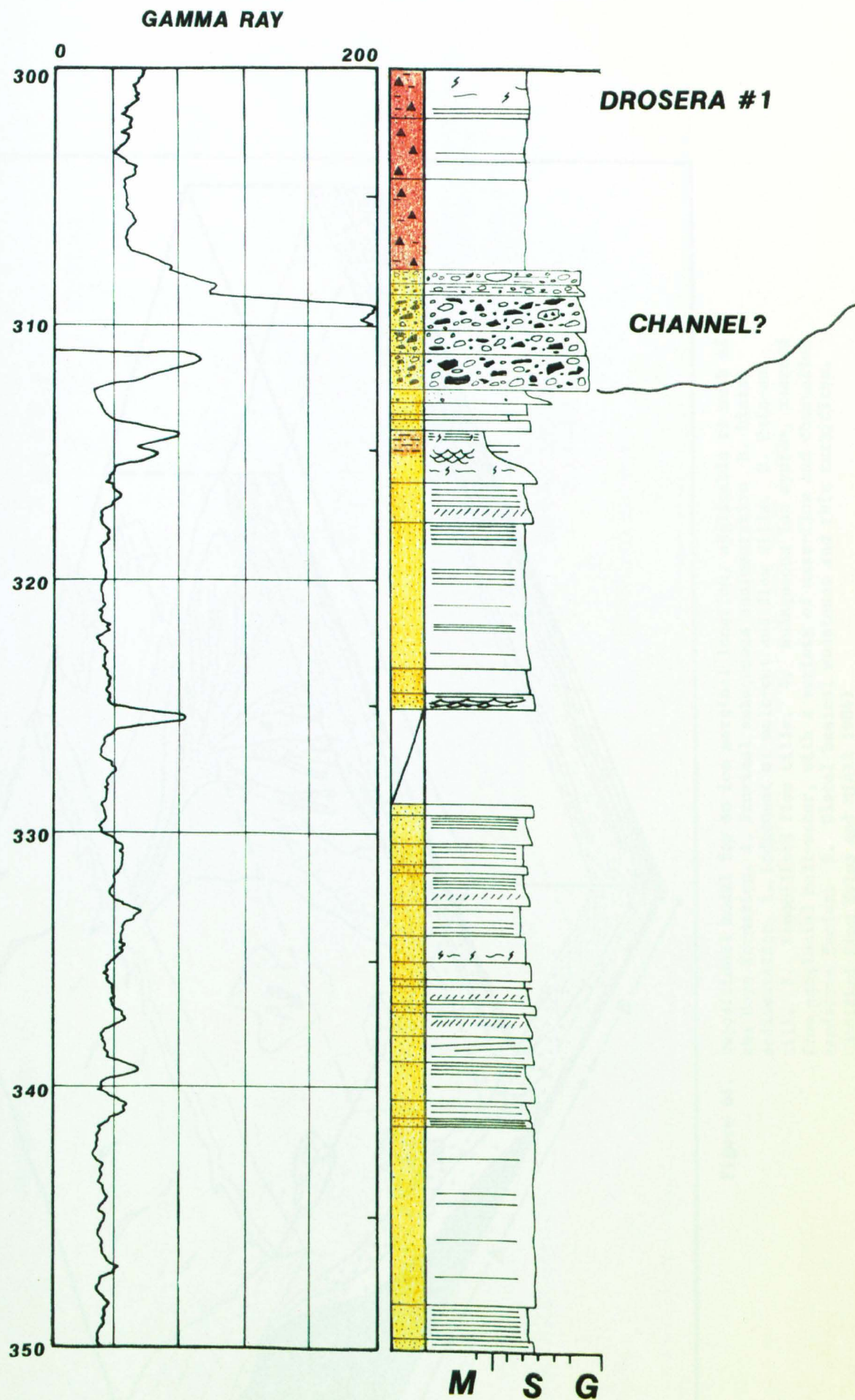


Figure 65. Detail of Drosera 1, displaying the upper section of Sandstone Facies cut by a stacked series of intraclast conglomerates (Sandstone Facies 7) interpreted to be a possible subaqueous channel.
(from Walker 1984)

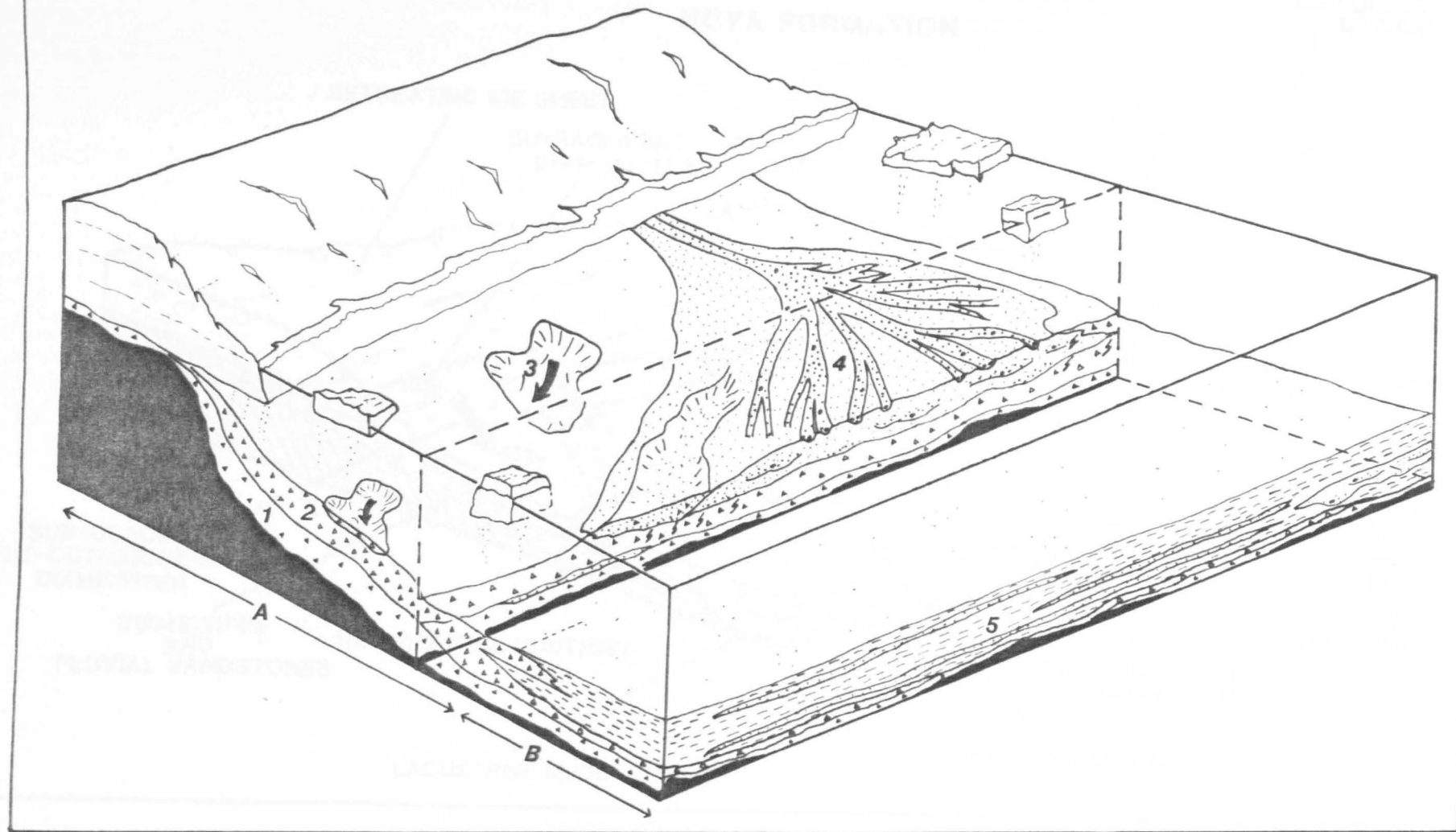


Figure 66. Depositional model for an ice marginal location, applicable to much of the Hoya Formation. A. Proximal subaqueous sedimentation B. Distal sedimentation 1. Lodgement or melt-out and flow tills. 2. Rain-out till. 3. Remobilised flow tills. 4. Subaqueous fan system, sourced from subglacial melt-water, with a variety of mass-flow and channelled sandstone facies. 5. Distal basinal mudstones and thin turbidites. (Modified from Eyles and Miall 1984)

SUMMARY DEPOSITIONAL MODEL HOYA FORMATION

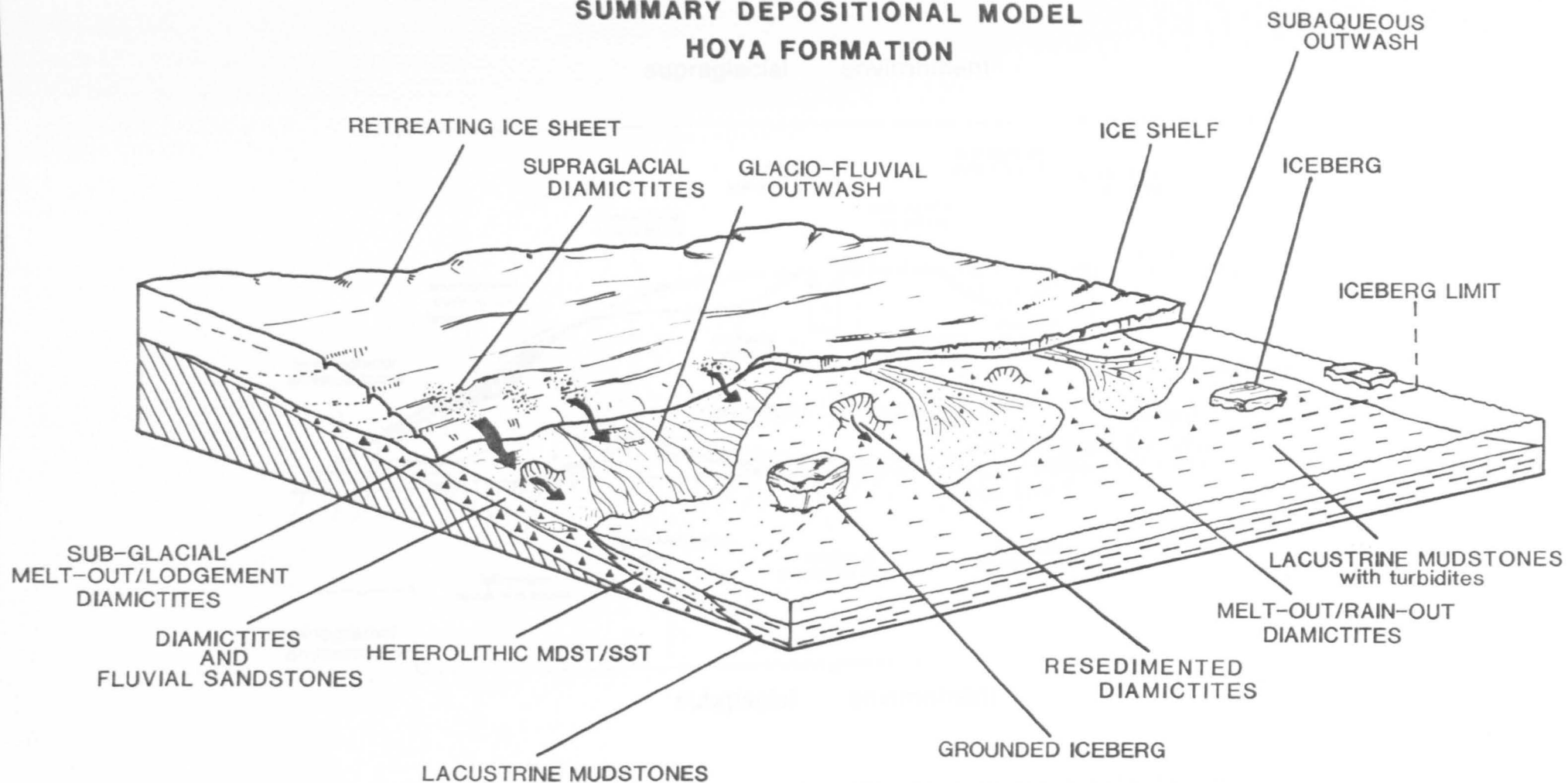


Figure 67. Summary depositional model for the Hoya Formation.

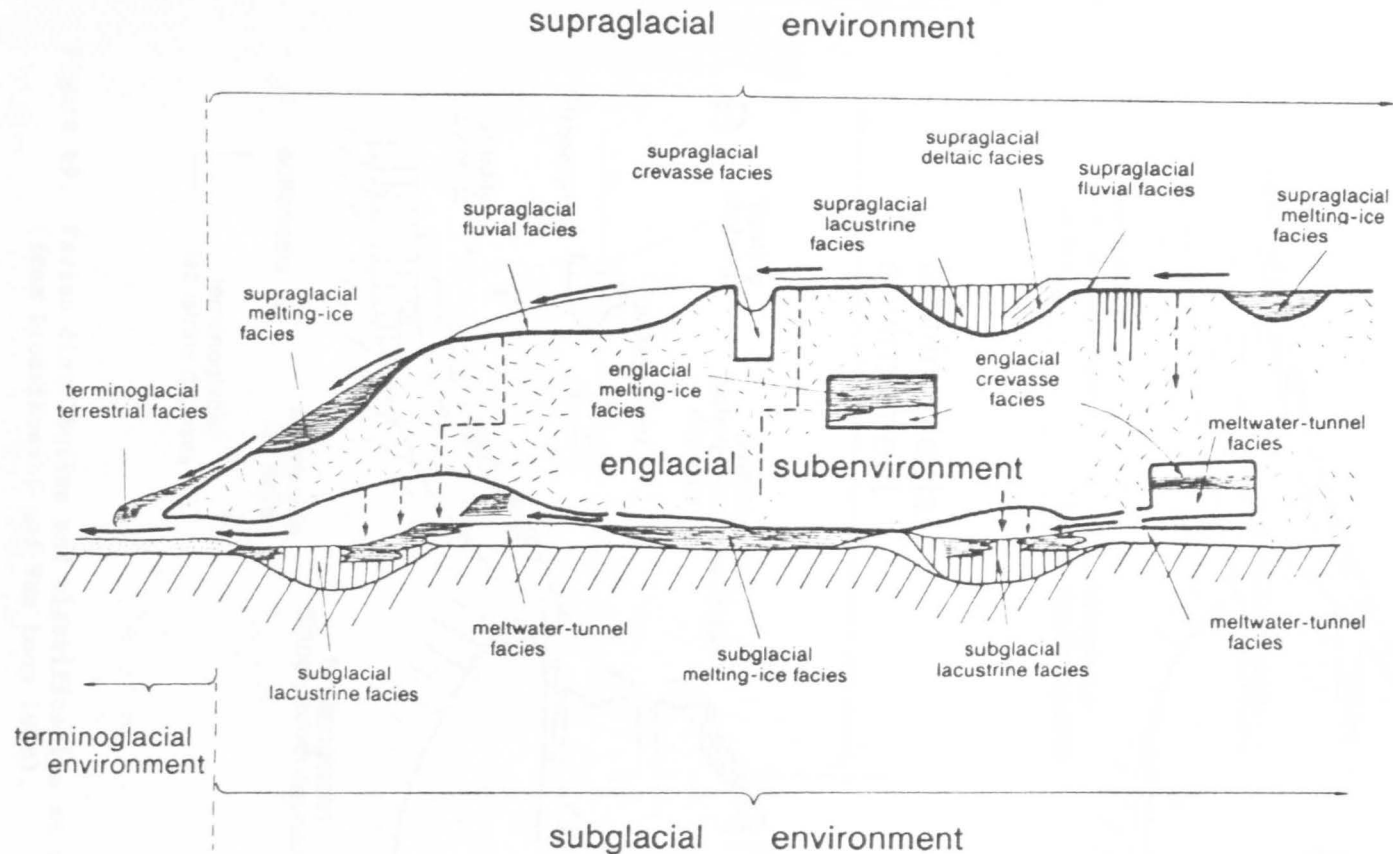


Figure 68. Facies distribution and classification in the subglacial and supraglacial environment.
(modified from Brodsikowski and Van Loon 1988)

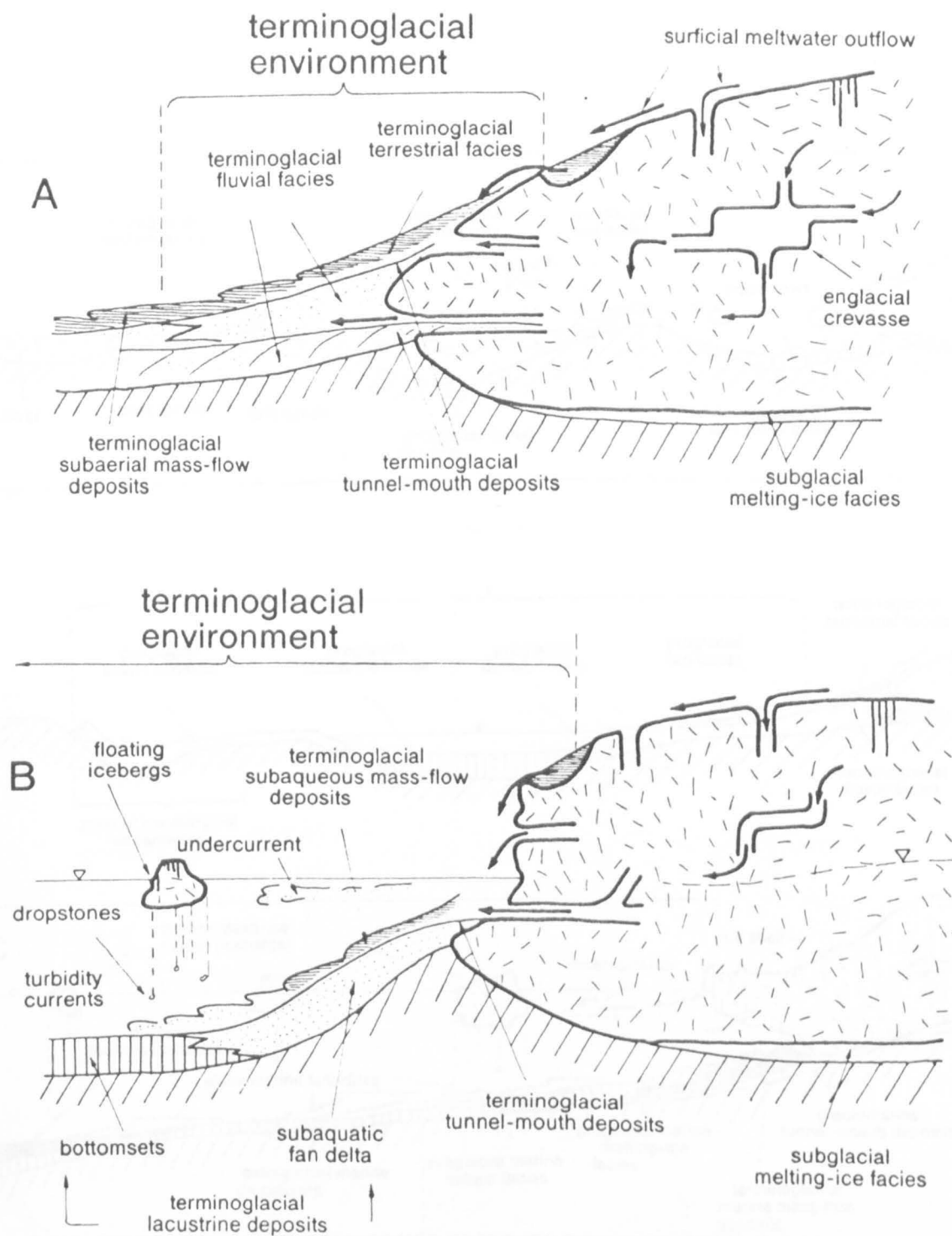


Figure 69. Facies distribution and classification at the margins of an ice sheet. (from Brodskowski and Van Loon 1988).

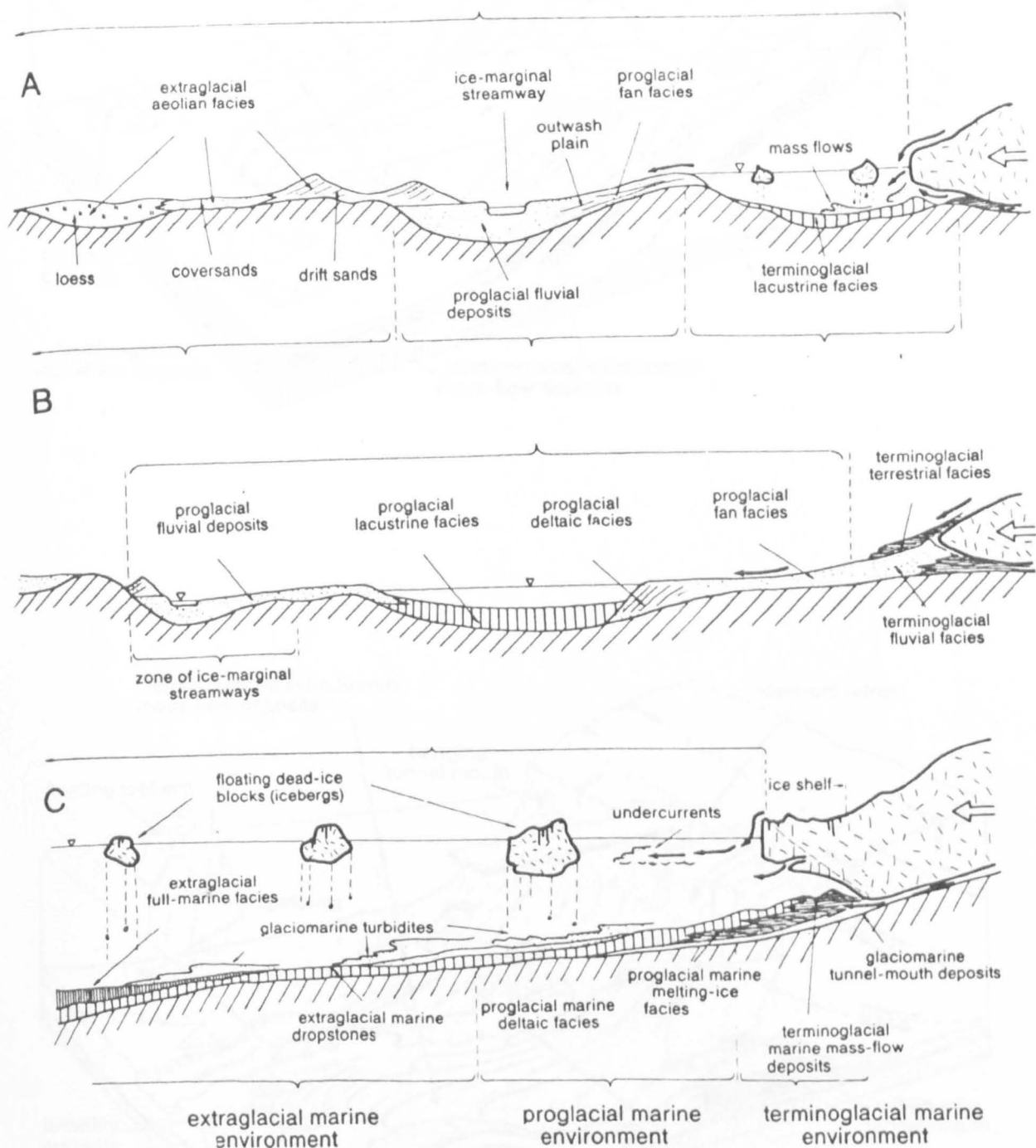


Figure 70. A schematic representation of the wide variety of facies deposited proximal to an ice sheet.

A. Terrestrial environment with ice contact lakes.

B. Terrestrial environment without ice contact lakes.

C. Subaqueous environment, with the ice sheet in contact with the basin, either under marine or lacustrine conditions.

(modified from Brodskowski and Van Loon 1988)

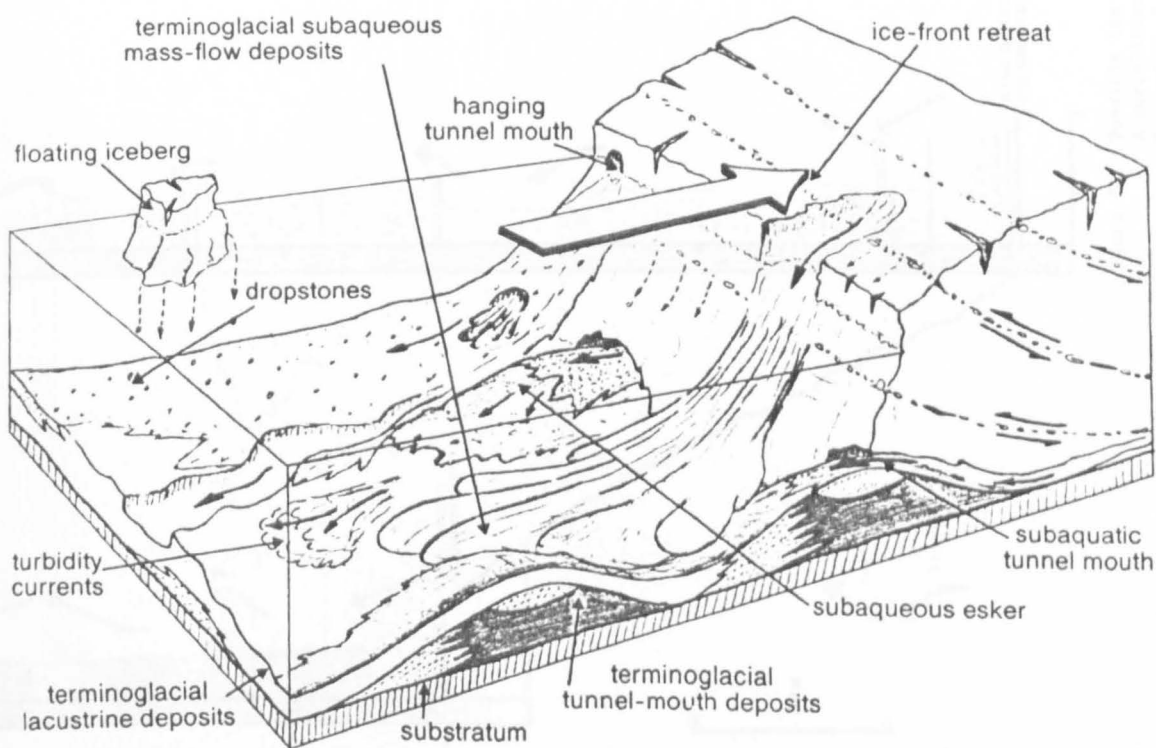
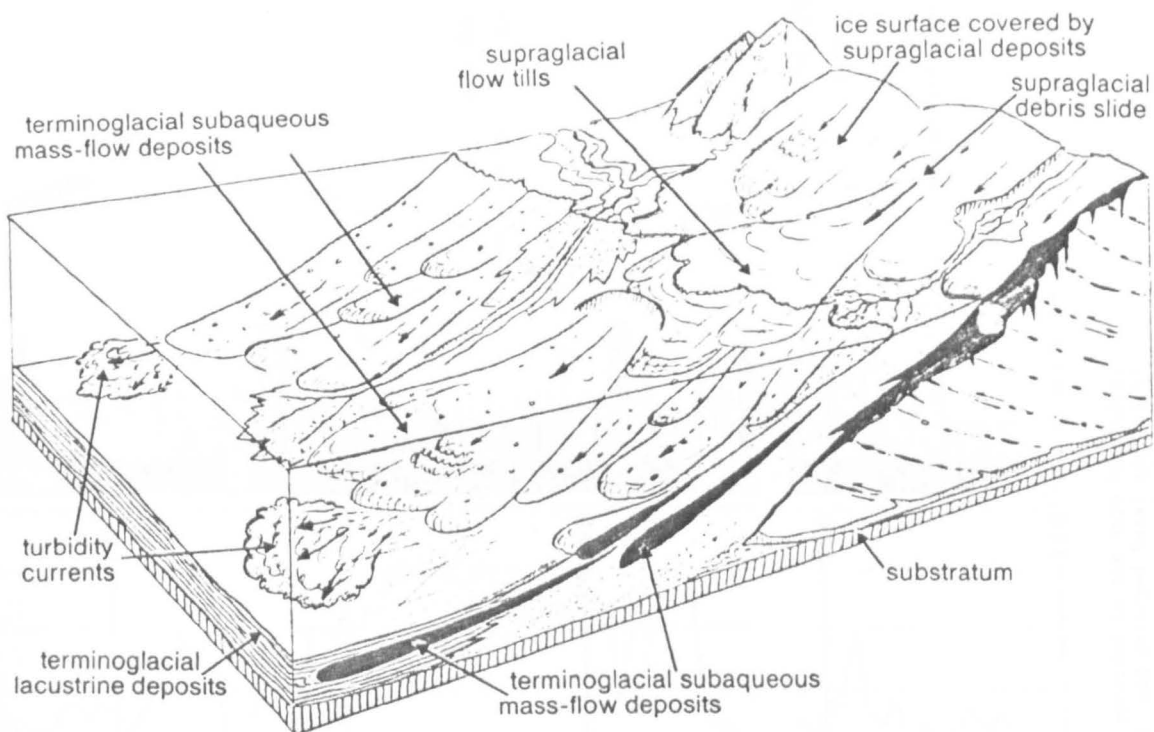


Figure 71. Two models for ice marginal sedimentation.
 A. A downwasting ice front.
 B. Rapidly retreating ice sheet in contact with marine/lacustrine conditions.
 Note in both cases the proposed rapid lateral and distal facies changes and the complex distribution of facies.
 (from Brodskowski and Van Loon 1988)

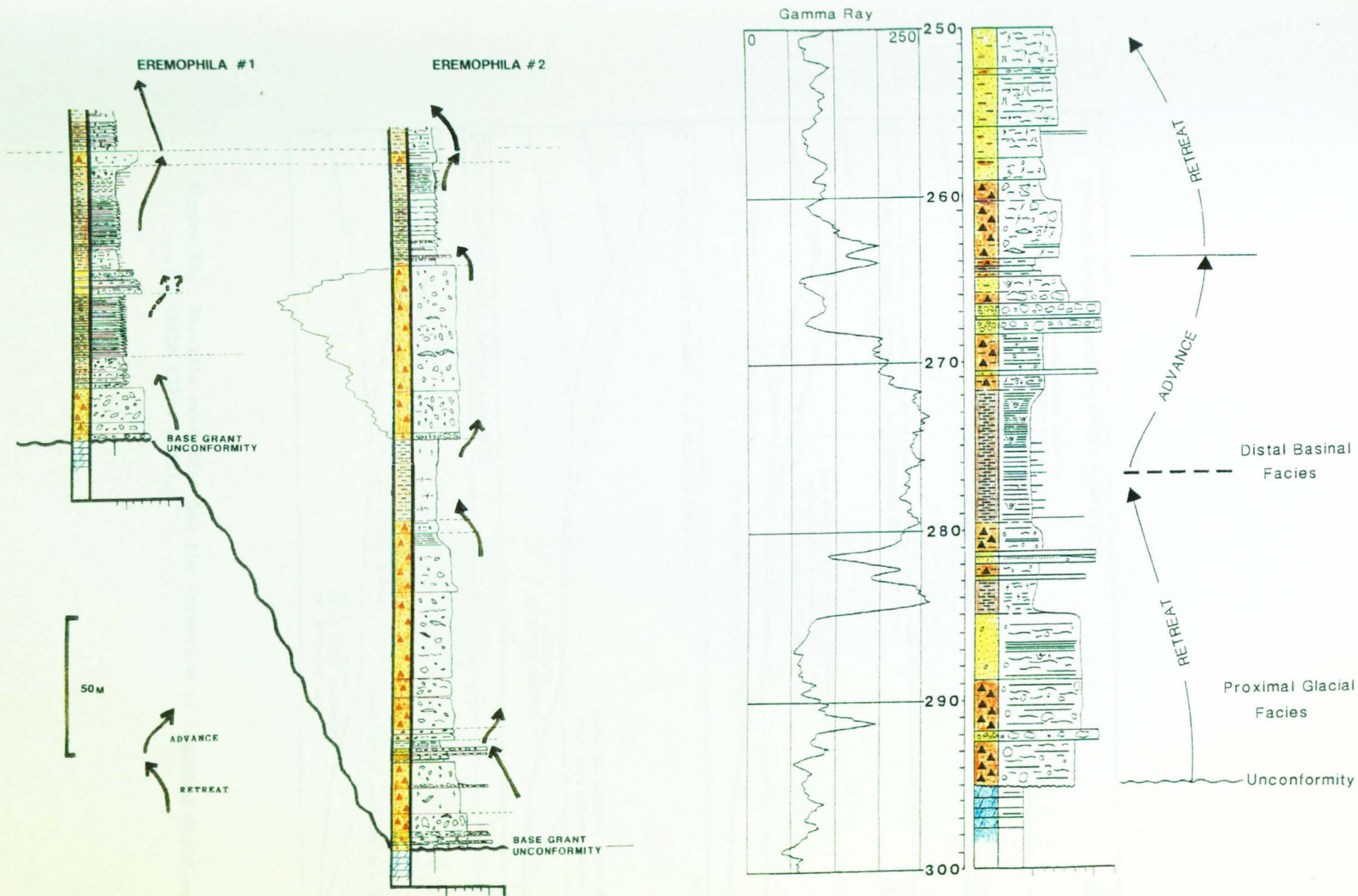


Figure 72. Possible ice advance and retreat cycles recorded in the Hoya Formation. A correlation between Eremophila 1 and 2, and enlarged basal section of Eremophila 3. (For key to lithologies and facies see Appendix 1)

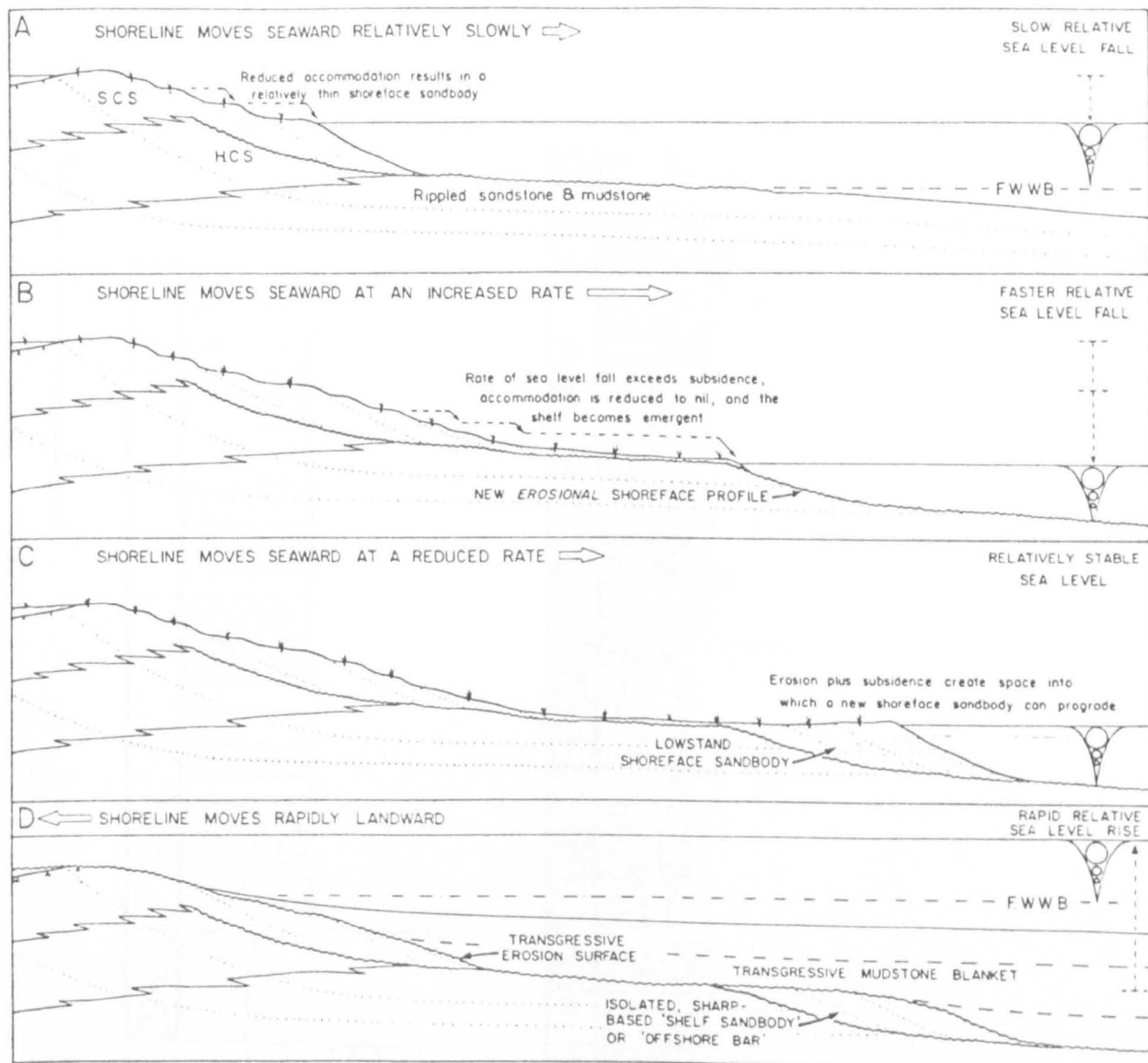


Figure 73. Possible mechanism for the formation of isolated shelf sandbodies. (from Plint 1988).

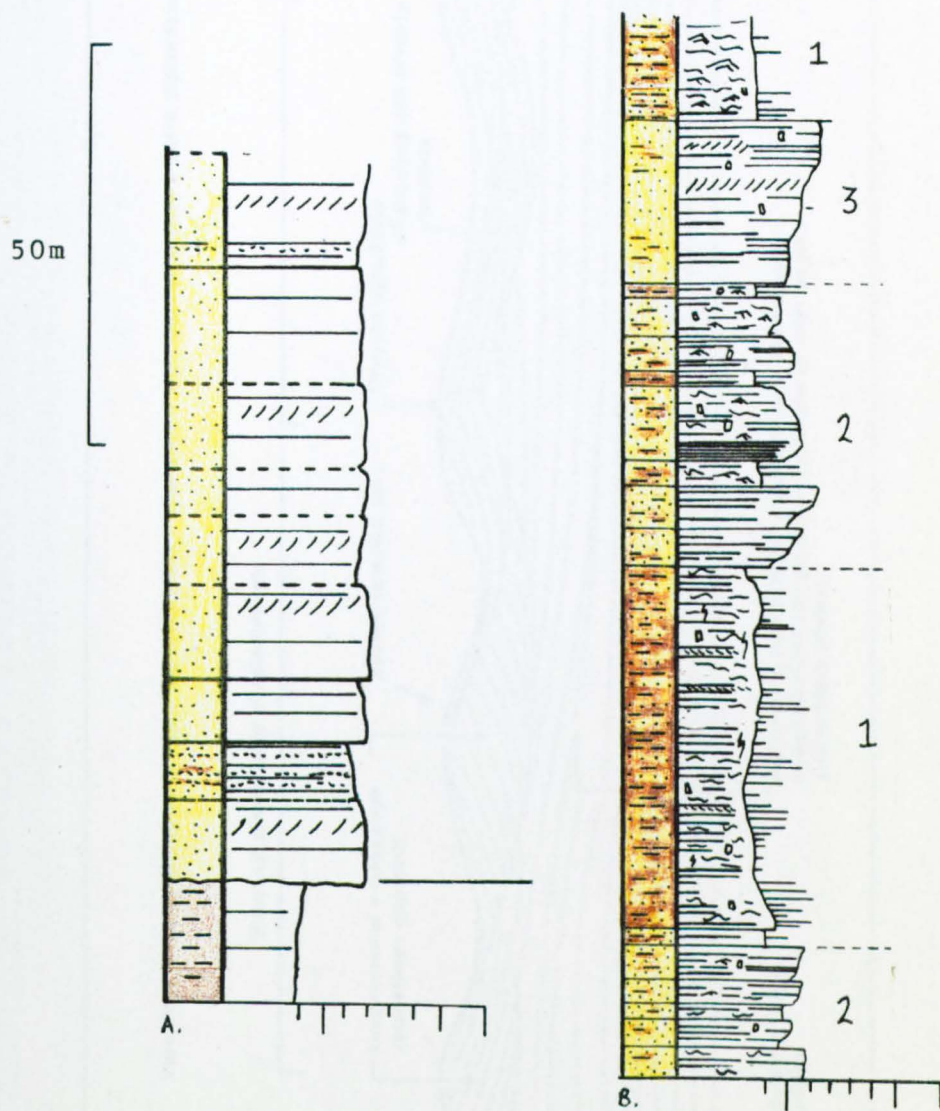


Figure 74. Typical facies logs for the Cliaanthus Formation.
 A. Sandstone facies
 B. Heterolithic facies.

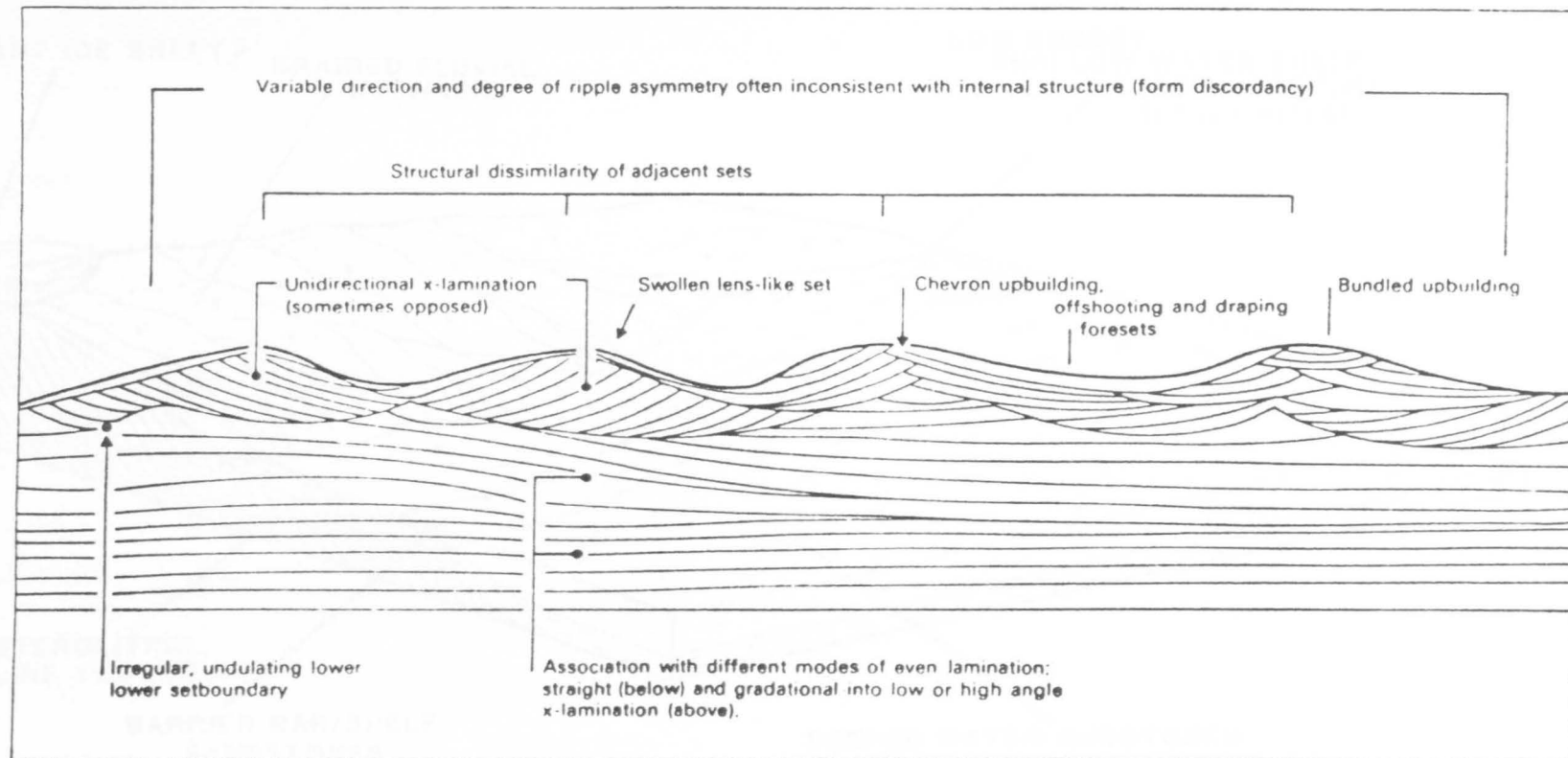


Figure 75. Characteristics of wave-generated ripples.
(from Reading 1981, after De Raaf et al. 1977.)

**SUMMARY DEPOSITIONAL MODEL
CALYTRIX/CLIANTHUS FORMATIONS**

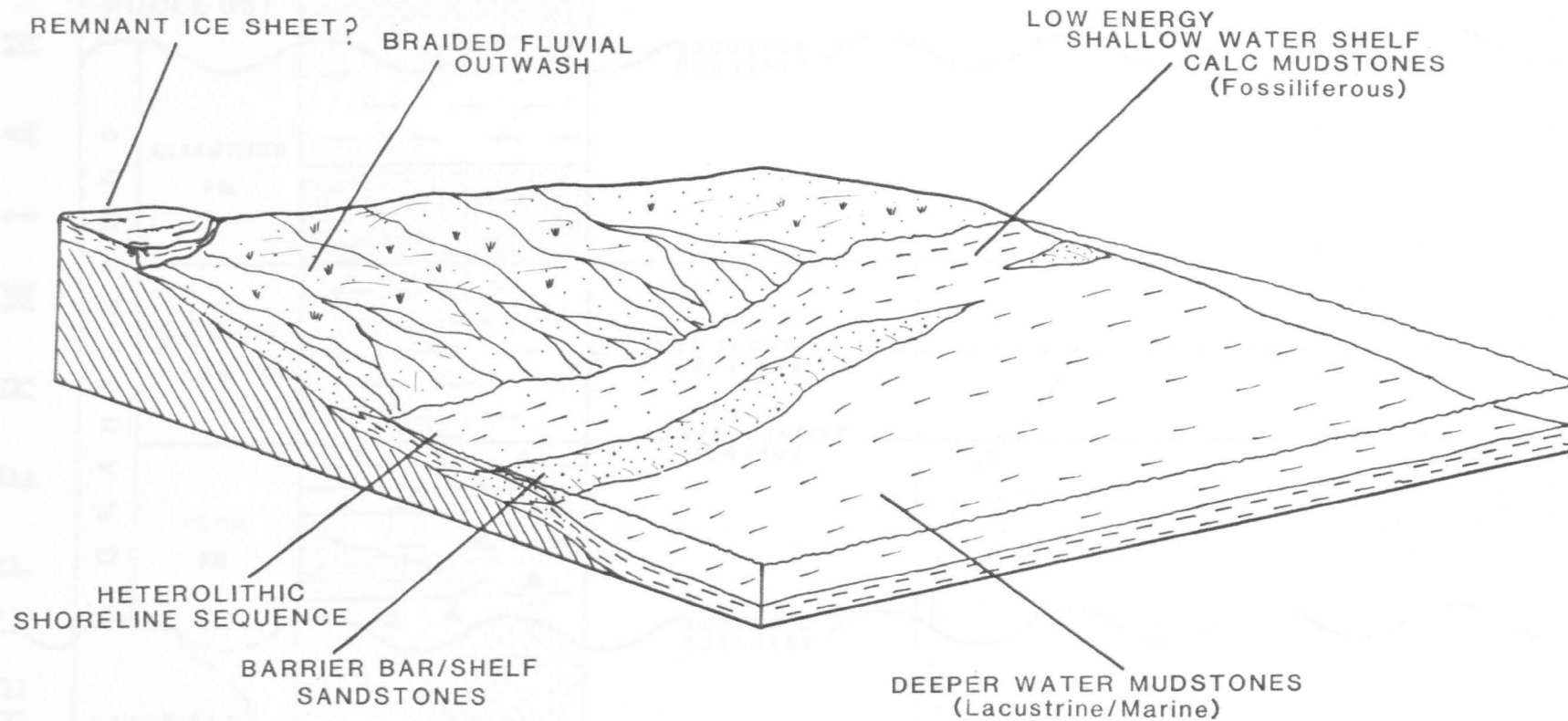


Figure 76. Combined summary depositional model for the Calytrix and Clianthus Formations.

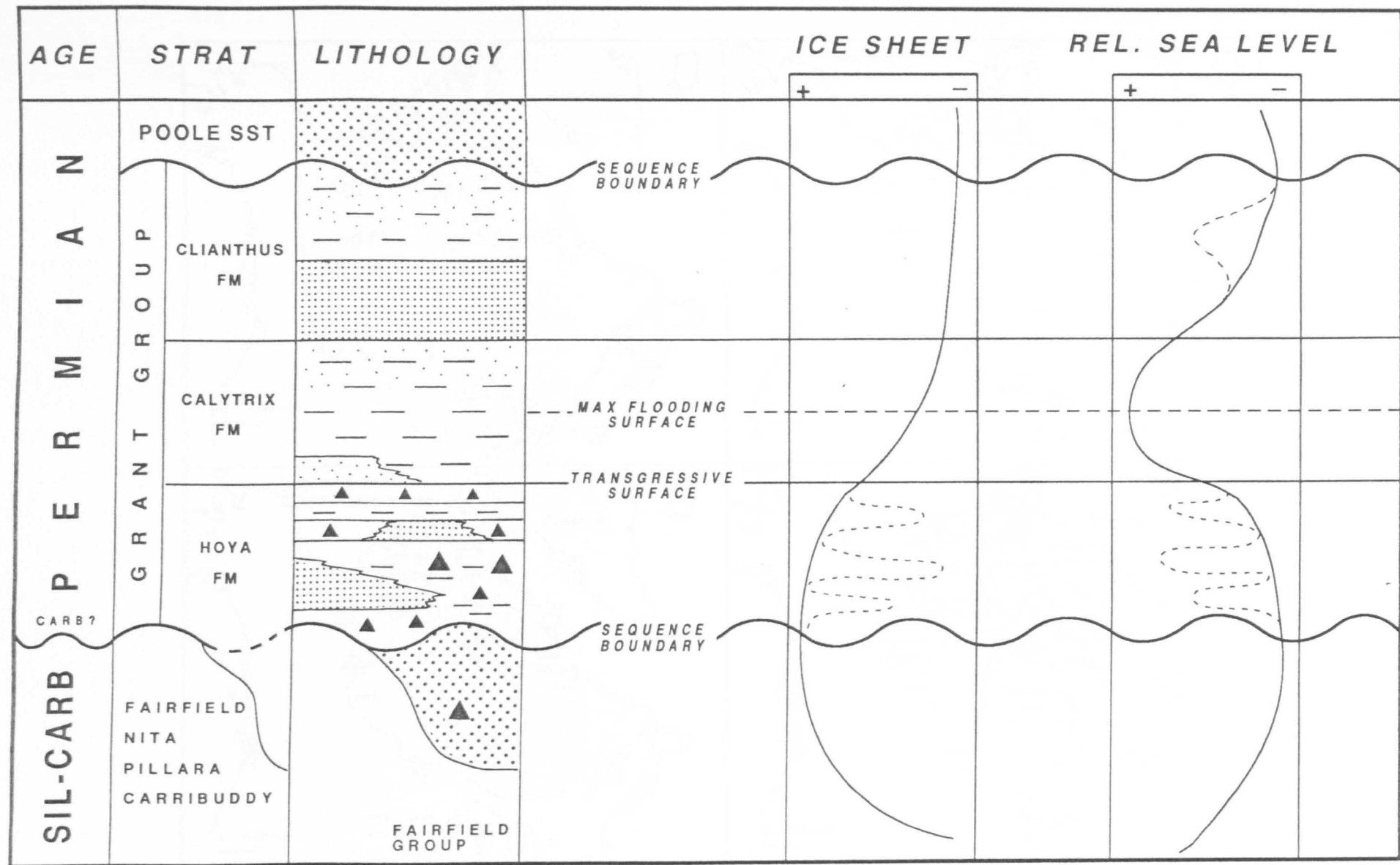


Figure 77. A model for the evolution of the Grant Group sedimentary package in relation to the ice sheet dynamics and changes in relative sea level.

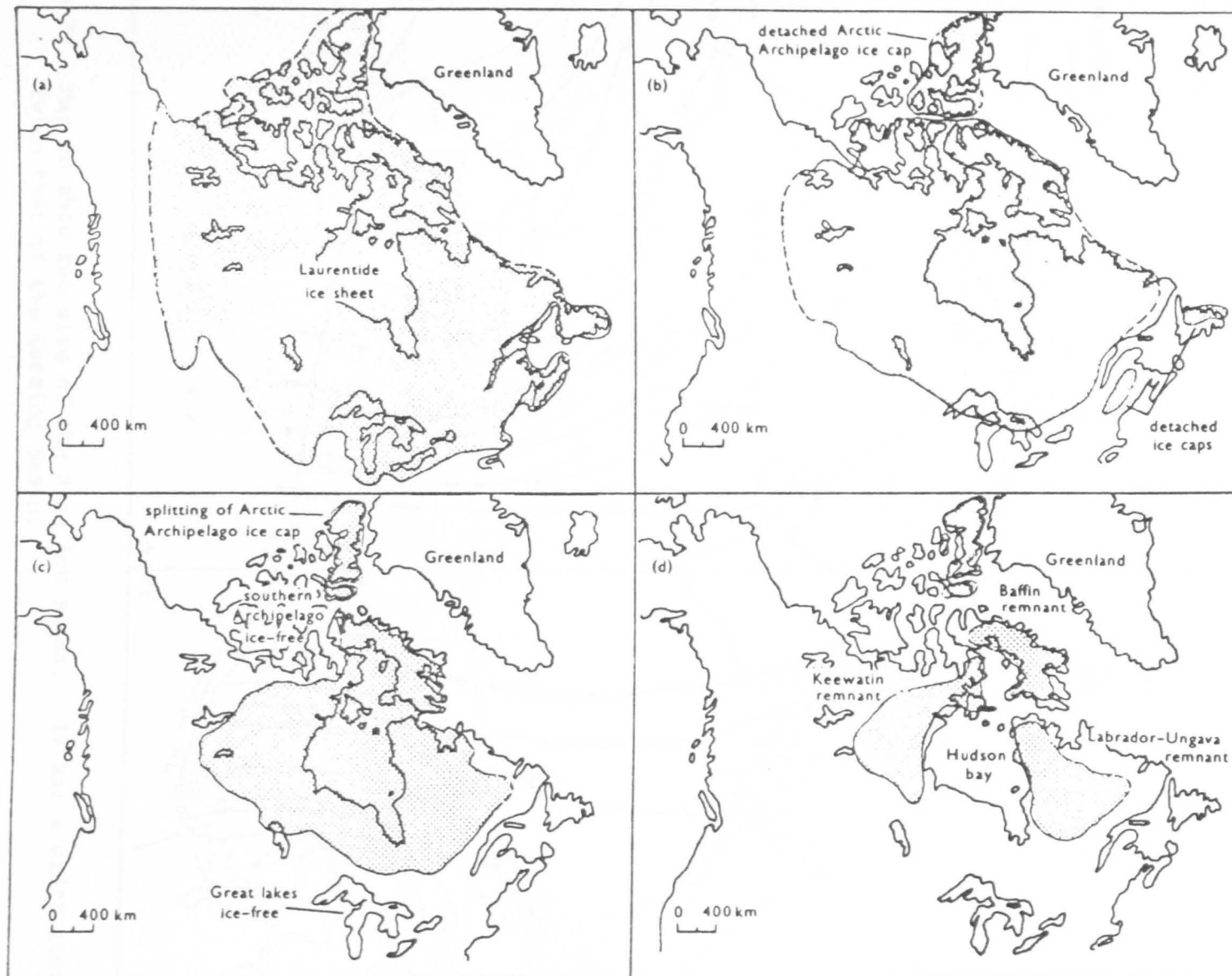


Figure 78. Map showing the various stages in the retreat of the Laurentide ice sheet. (a) 13,000yrs BP (b) 10,000yrs BP (c) 8000yrs BP (d) 7000yrs BP (from Sugden and John 1985, after Bryson et al. 1969)

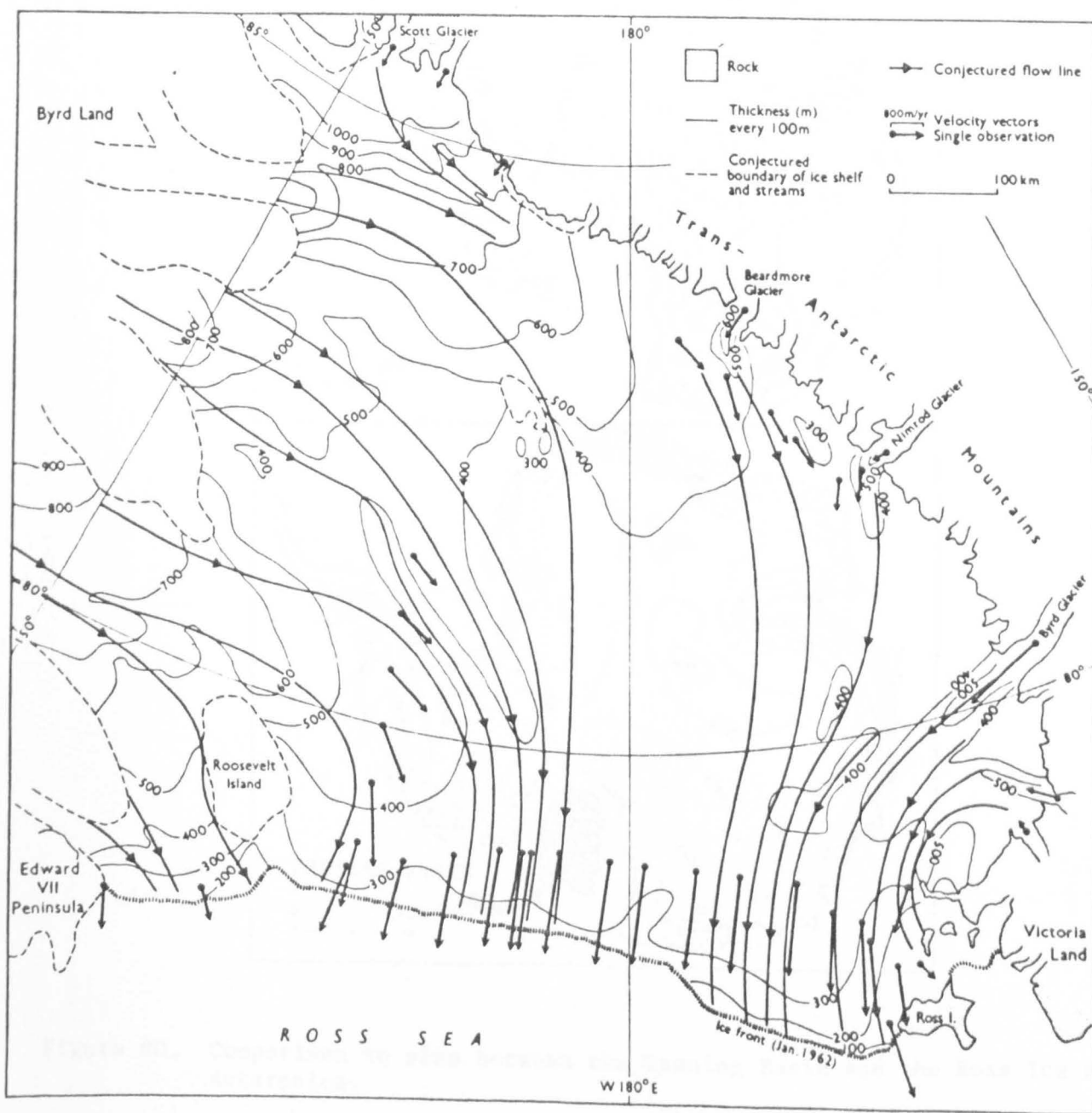


Figure 79. Map to show the size of the Ross ice sheet. It has a width almost twice that of the Canning Basin.

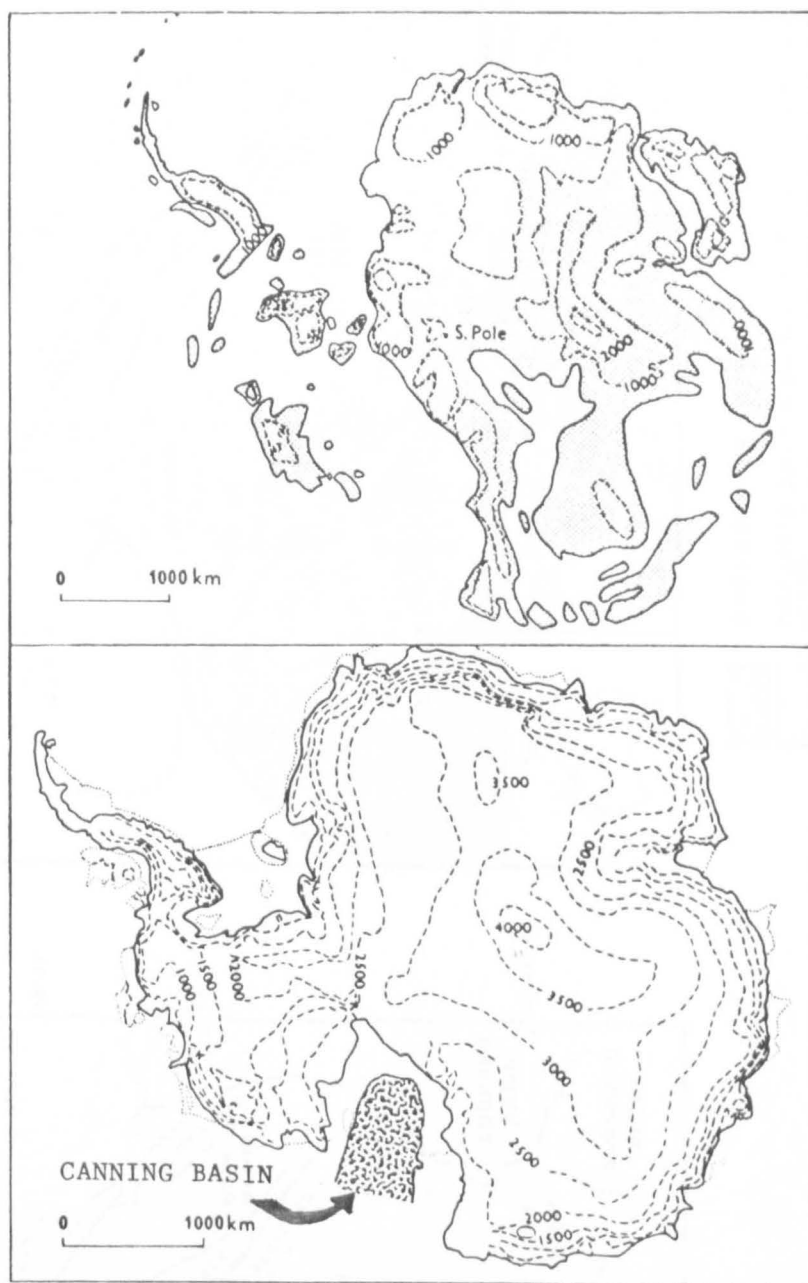
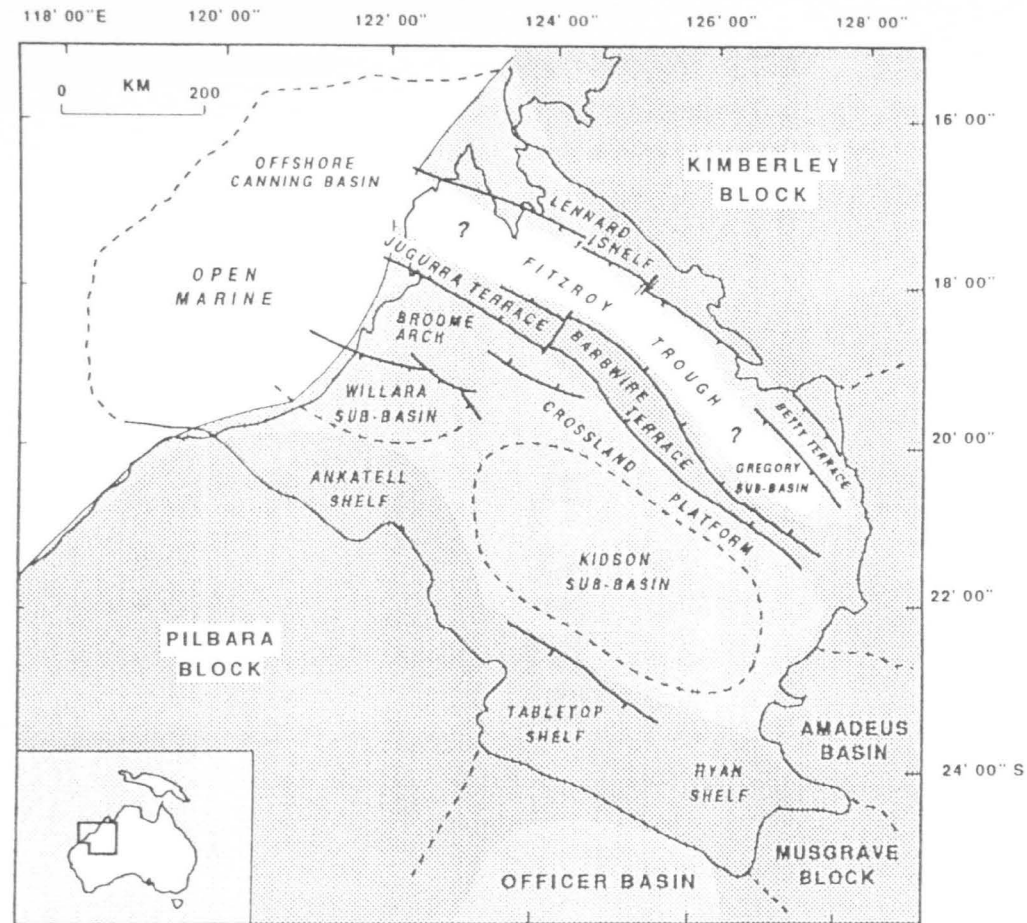
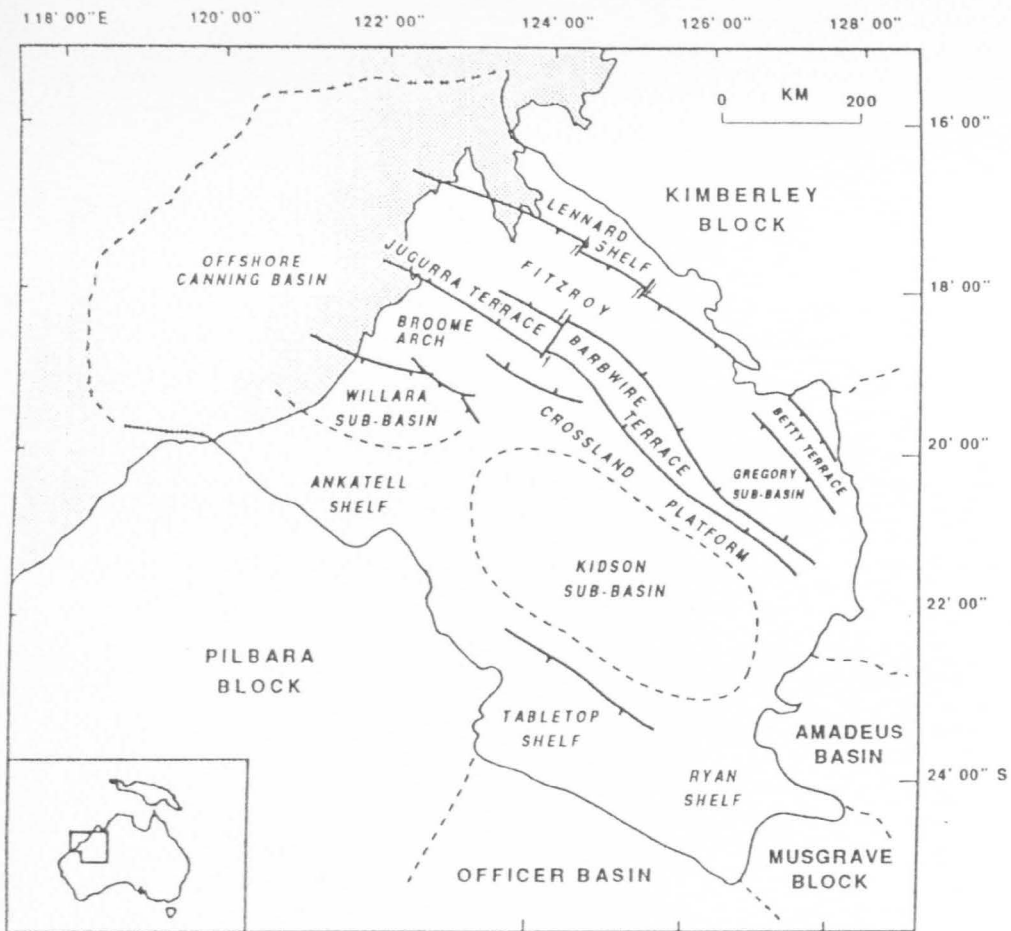


Figure 80. Comparison in size between the Canning Basin and the Ross Ice shelf of Antarctica.




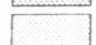

-  GROUNDING ICE SHEET
-  POSSIBLE GROUNDING ICE, FLOATING ICE SHEET, ICEBERGS.
-  POSSIBLE FLOATING ICE, ICEBERGS, EVIDENCE SUGGESTS CONTINUOUS DEPOSITION

Figure 81. Schematic model for the distribution of ice in the Canning Basin area during the Perm-Carboniferous

PLATES

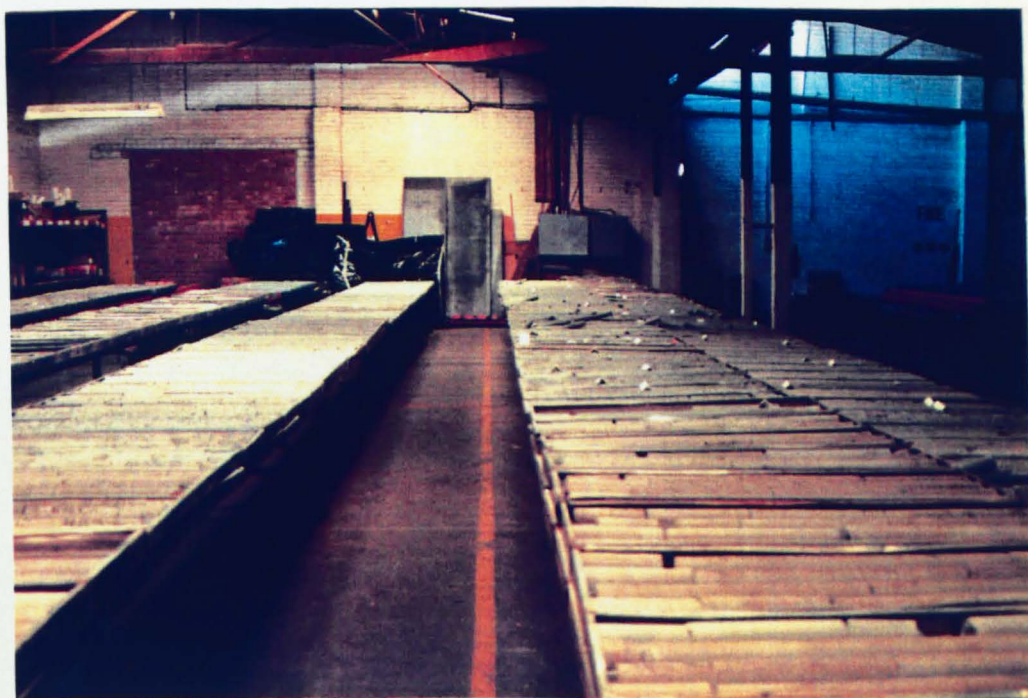
PLATE 1

A. Landsat composite image of Australia with computer enhanced colours; green-brown indicate wet vegetated areas, light brown to white indicate dry desert areas. The Great Sandy Desert covers most of NW Australia, overlying the Canning Basin.

B. The 'Challenger Geological Services' core store, where Western Mining's Canning Basin core was viewed. Each tray contains 5m of core, cut into 1m lengths.



A

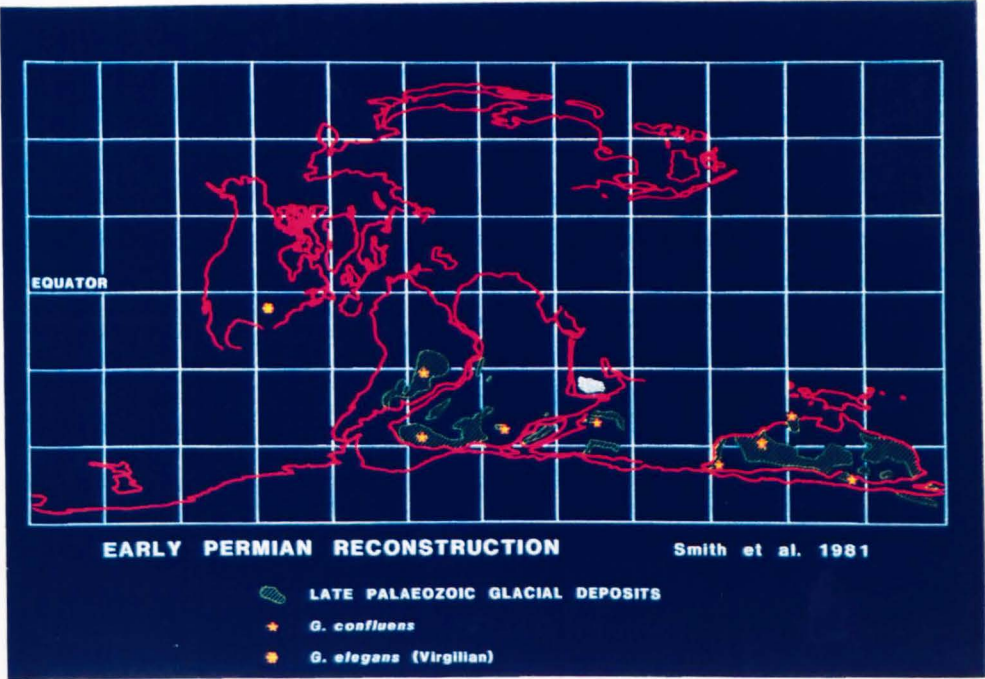


B

PLATE 2

A. Early Permian palaeogeographic reconstruction of Gondwana and Eurasia, highlighting areas of known glacial deposits, and the occurrence of the G.confluens assemblage. (Courtesy of C. Foster, Western Mining Corporation Ltd.)

B. Alternative projection of the Gondwanan continent during the Early Permian. The G.confluens assemblage has been recognised in glacial sediments from Brazil, South Africa, India and numerous basins in Australia, confirming the age equivalence of these deposits. (Courtesy of C. Foster, Western Mining Corporation Ltd.)



A



B

PLATE 3

Fence diagram showing the BMR correlation between the older wells surrounding the study area. The Barbwire Terrace is bounded by the Fenton and Dummer Range Faults, and the study area lies between the well Crossland 3 to the south and Barbwire 1 to the north. Note the interpreted anticline on which St George Range 1 is located. (from BMR Noonkanbah Sheet SE51-16 1977)

Subsurface Correlation

Scale: $\frac{V}{H} = 5$

Symbols as in reference except:

J Undivided Jurassic

T Undivided Triassic

Fault plane

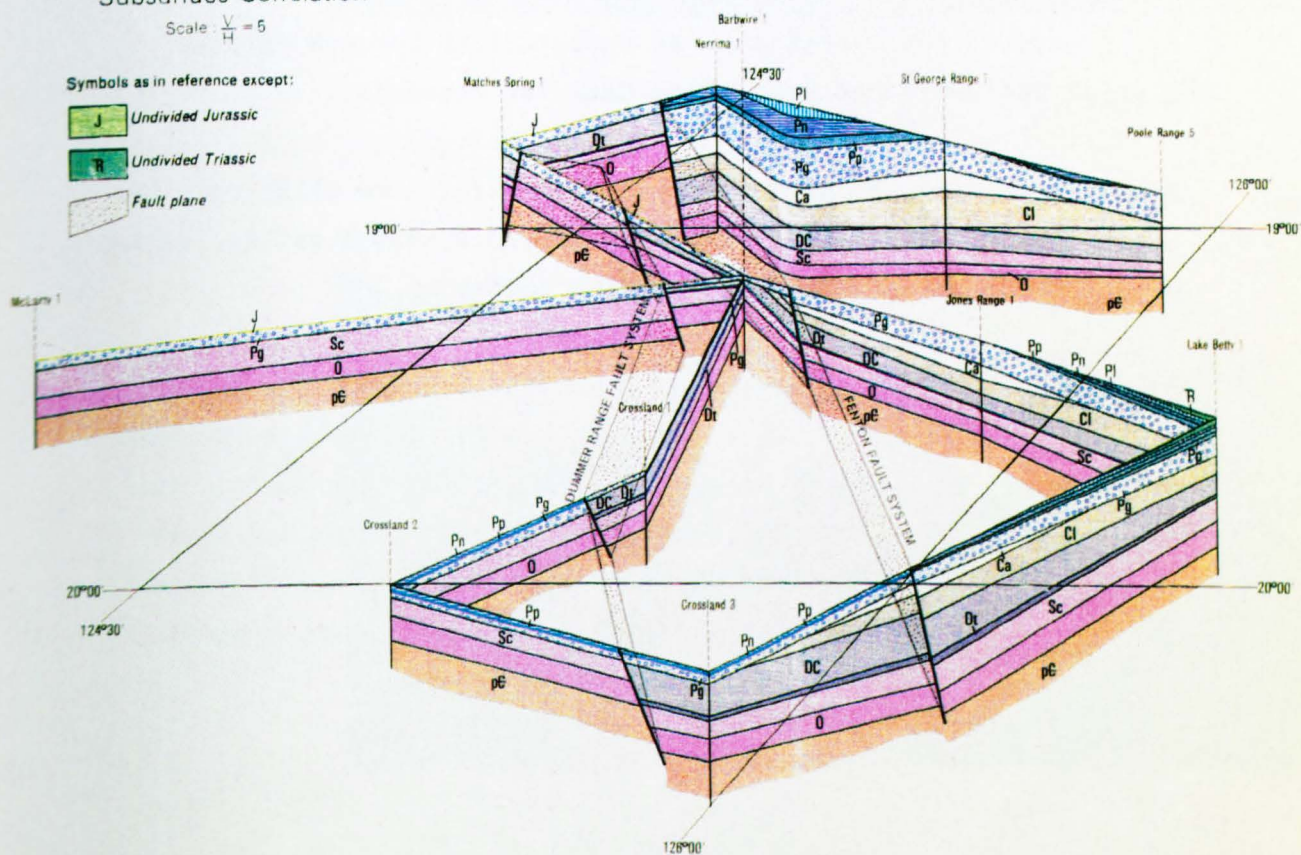


PLATE 4

HALLETT COVE, SOUTH AUSTRALIA

A. A view of the marked angular unconformity between Permian glacial sediments and the folded Cambrian sequence.

B. Another view of the unconformity surface. The cliff face in the background contains a glacially eroded U-shaped valley, filled with lighter coloured Permian glacial sediments.

C. Glacial striations on the unconformity surface. The deep linear grooves were cut into the Cambrian surface by a hard clast embedded in the base of the over-riding grounded ice sheet. The grooves vary in orientation suggesting changes in the ice sheet flow direction and multiple phases of grounding. Less distinct chatter-marks, partially filled with loose beach sand, suggest a transport direct towards the right of the picture.

A



B



C

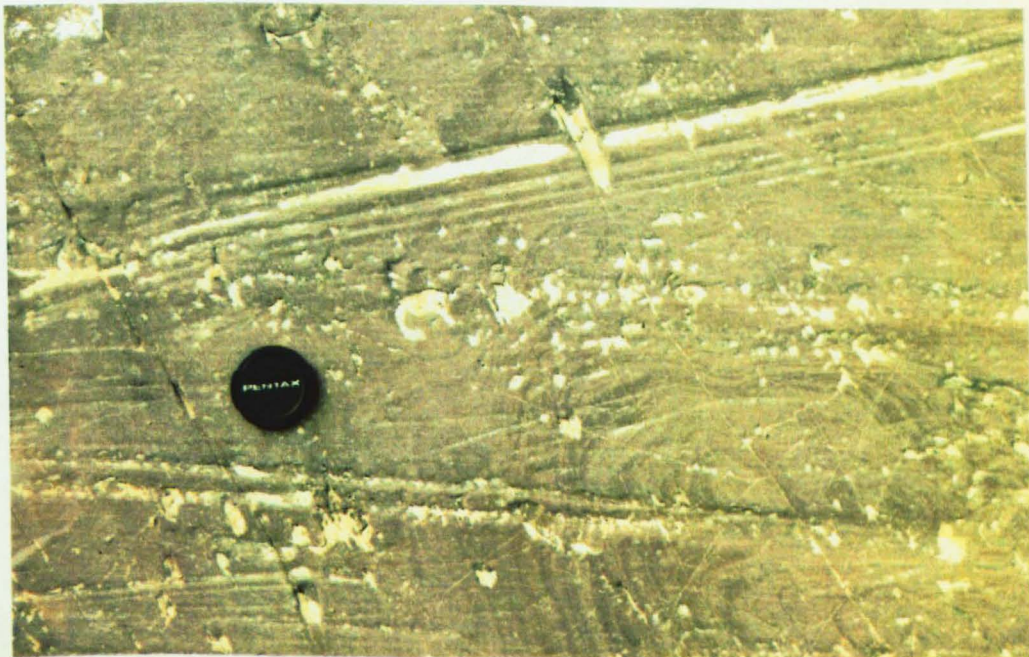


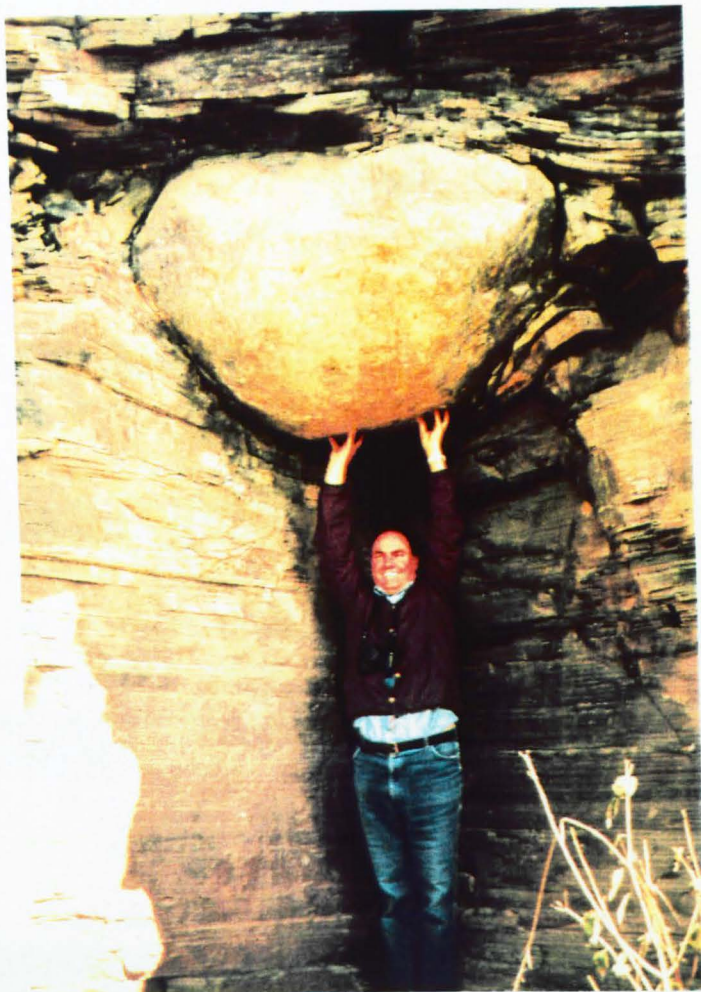
PLATE 5

PARANA BASIN, SOUTHERN BRAZIL

A. A large dropstone within a suite of laminated mudstones, from the Itarare Group, the Parana Basin, Brazil. The underlying sediments have been deformed by the sudden impact of the dropstone, with folding of the laminations. Continued deposition of the mudstones drape the large clast.

B. Close up of folding and soft-sediment deformation associated with the sudden impact. The clast is interpreted to have been released from a floating iceberg within the basin.

In core, the deformation commonly apparent in the Grant Group sediments may in part be due to impacts of this kind. Large clasts were cored from diamictite and mudstones lithologies, although the limitation of the core size prevents clear identification of loading features such as seen here.



A



B

PLATE 6

A. Hoya 1 433.80m (Hoya Formation)

The basal unconformity between the Grant Group and underlying Devonian siltstones. The upper 5cm of the Devonian section is brecciated indicating possible loading and shearing by the grounded ice sheet, or weathering, prior to the deposition of the Basal Diamictite of the Grant Group. Facies BD comprises a sandy diamictite containing abundant large angular dolomitic limestone clasts (similar to the Devonian subcrop of the area) and less common basement clasts.

B. Eremophila 2 228.05m (Hoya Formation)

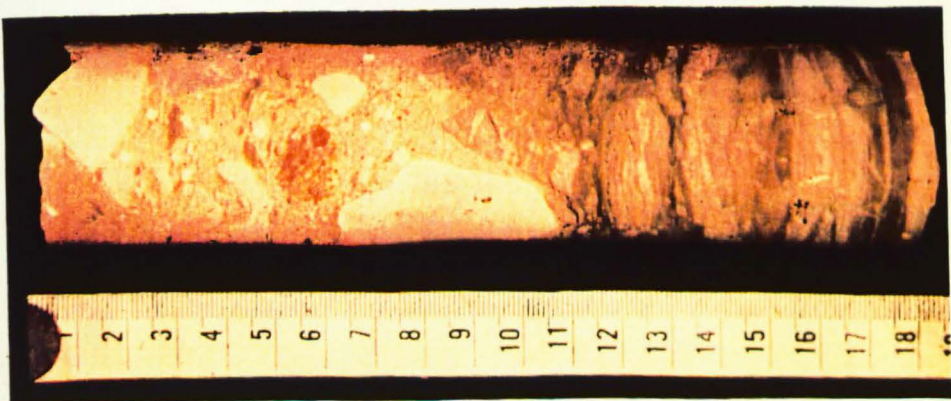
A clast-rich sandy diamictite of facies BD. Large dolomitic limestone clasts float in a light-brown sandy matrix. The clasts are angular, and often appear to be faceted. (4.5cm core)

C. Eremophila 3 292.10m (Hoya Formation)

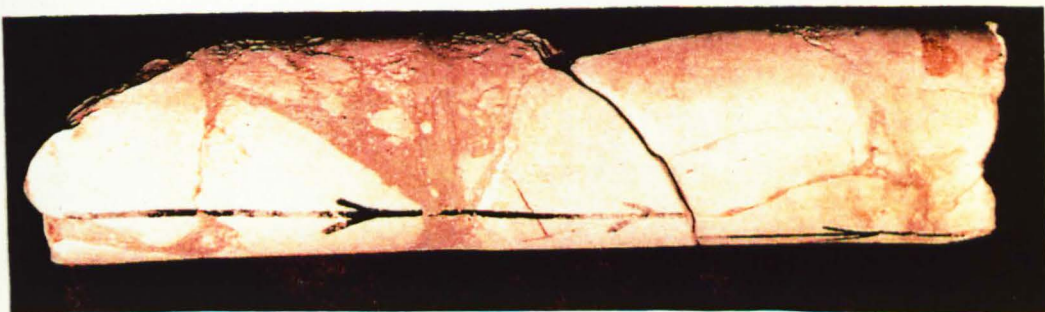
Another example of the basal diamictite, this time containing more abundant basement clasts, often rounded to subrounded. The diamictite is sandy and clast-rich. (6.5cm core)

D. Eremophila 1 195.50m (Hoya Formation)

Located above a clast-rich diamictite similar to (A), this sandy diamictite contains contorted bedding in the lower section, picked out by darker, slightly more argillaceous streaks and wisps. This suggest a primary bedding, distorted by subsequent soft-sediment deformation and slumping. The diamictite is interpreted to be a melt-out till, which has undergone some remobilisation. (6.5cm core)



A



B



C



D

PLATE 7

A. Halgania 1 304.10m (Hoya Formation)

A clast-rich sandy diamictite from the Basal Diamictite Association. Note the abundant angular clasts of locally derived dolomitic limestone. (4.5cm core)

B. Eremophila 1 191.50m (Hoya Formation)

The abrupt upper contact between a sandy diamictite of the Facies BD, and a heterolithic unit comprising laminated silts, muds and very fine-grained sandstones. The heterolithic unit contains complex lensoid and wispy bedding, which suggests subaqueous deposition and subsequent intense soft-sediment deformation. A small basement clast, denoted by the arrow, is possibly a dropstone. (6.5cm core)

C. Eremophila 3 223.10m (Hoya Formation)

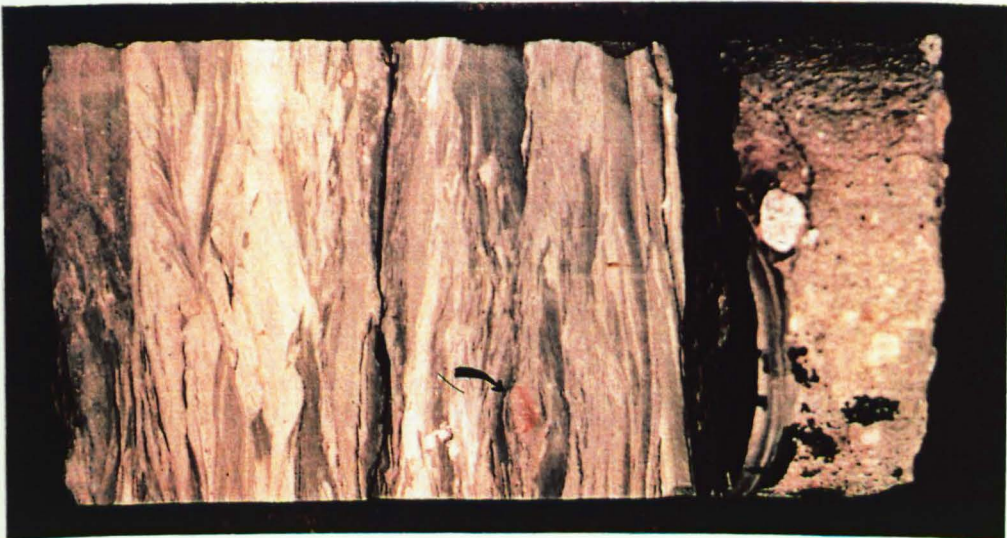
A massive sandy diamictite of Facies DSm. Scattered clasts of dolomitic limestone in a light brown sandy matrix. Basement clasts are rare. This resembles the diamictites of Facies BD, and is interpreted to be a melt-out or possibly lodgement tillite. (6.5cm core)

D. Eremophila 2 185.96m (Hoya Formation)

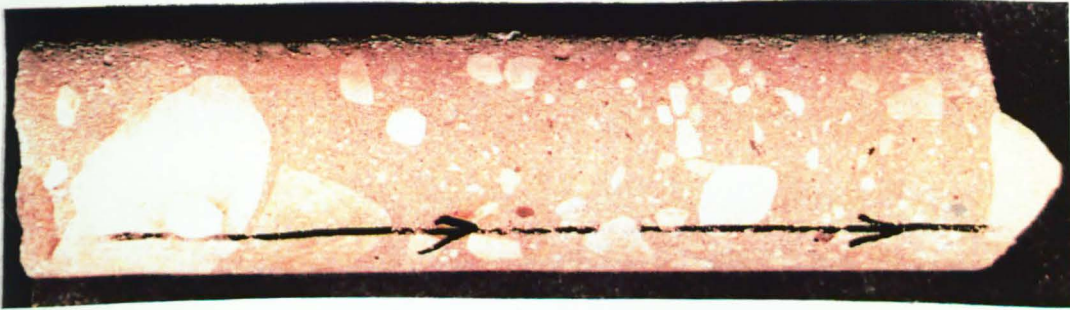
The sharp upper contact between a sandy diamictite (Facies DSm) and overlying mudstones of Facies Fl. The sharp contact indicates either a rapid change in the depositional environment, or that the diamictite has moved by mass-flow processes into the basinal environment, and is thus a flow till. (6.5cm core)



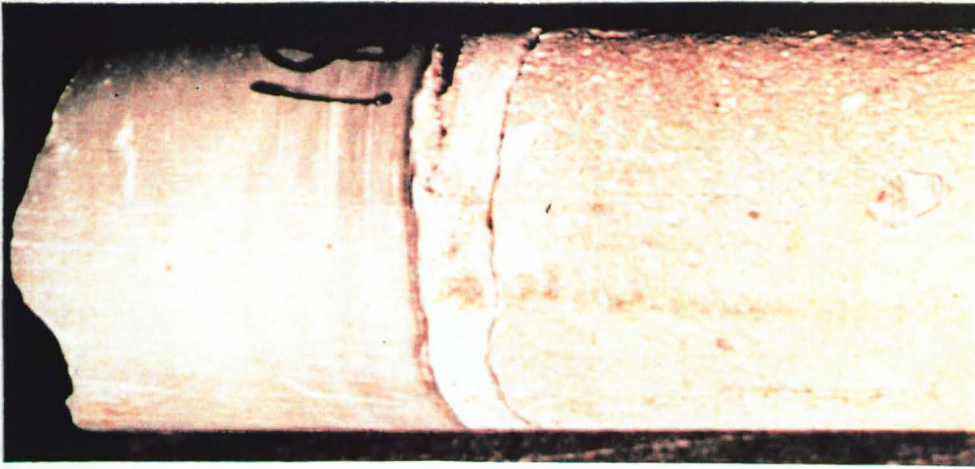
A



B



C



D

PLATE 8

A. Eremophila 2 205.60m (Hoya Formation)

The transition from a massive muddy diamictite (DMm) to a laminated mudstone (Fl). Layers become evident within the 'massive' diamictite that contain a lower percentage of coarse material, and this continues up section. The 'diamictite' layers both reduce in thickness and becoming more argillaceous, until the sequence grades into a mudstone. This is clear evidence that this diamictite was deposited under subaqueous 'basinal' conditions.

B. Eremophila 3 258.70m (Hoya Formation)

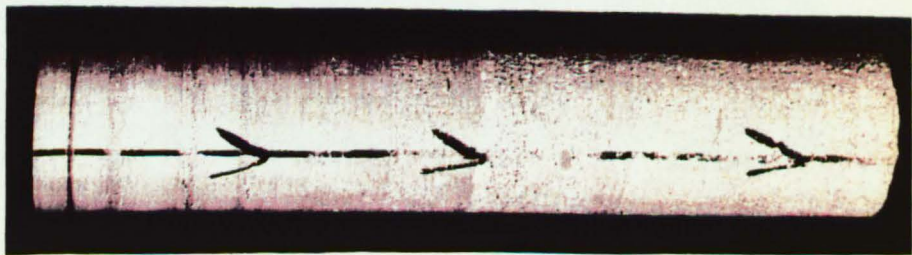
The upper section of a sandy diamictite (Facies DSs), displaying intense soft-sediment deformation, with folded and contorted bedding. The lighter coloured sandstone streaks comprise are similar to thinly bedded sandstones overlying this diamictite. The deformed character of this diamictite indicates remobilisation.

C. Eremophila 3 220.95 (Hoya Formation)

A lens of fine-grained sandstone within a sandy diamictite. The lens displays high-angle contacts, and is possibly a small channel. It incorporates clasts of the diamictite, and basement and dolomitic limestone clasts derived from the diamictite. The feature appears to be deformed and loaded.

D. Calytrix 1 263.60m (Hoya Formation)

Part of a complex sequence of interbedded sandy diamictites and sandstones (Facies DSs). The lower 5cm is the top of a sandy diamictite, which is cut by an erosively based sandstone. The sandstone grades from a coarse conglomeratic base up to medium-grained sandstone. The conglomeratic clasts are of a similar composition to clasts from the diamictite. This is interpreted to be a melt-water channel deposit cutting and reworking the diamictite. This could form in either subaerial or subaqueous conditions



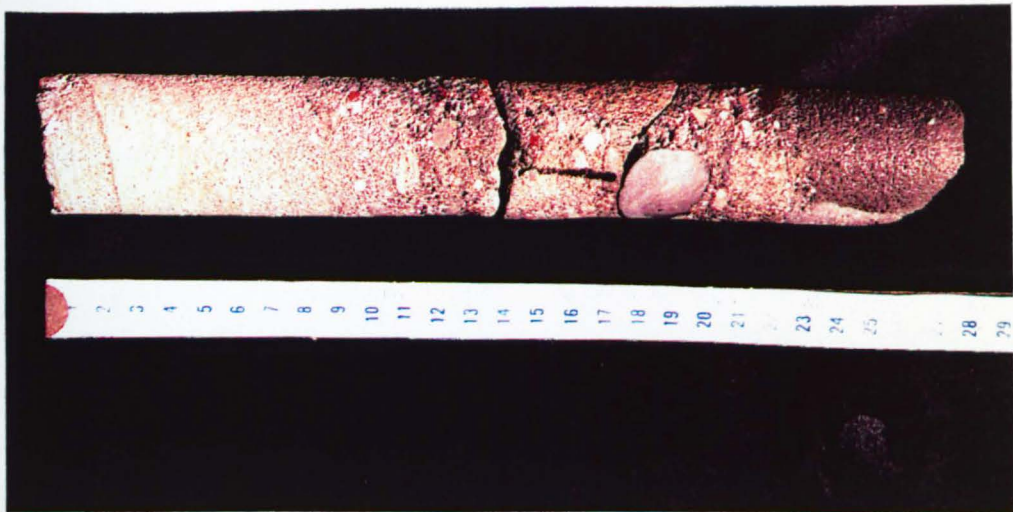
A



B



C



D

PLATE 9

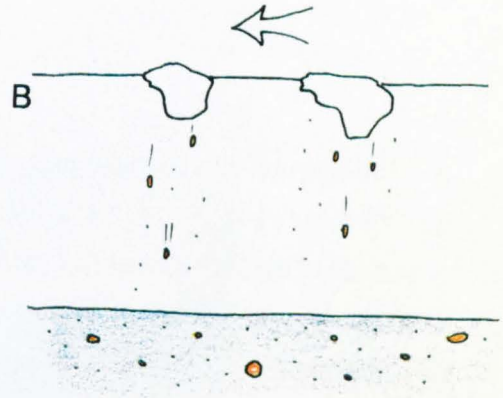
A. Calytrix 1 281.20m (Hoya Formation)

A typical massive muddy diamictite(DMm), containing scattered clasts, introduced as dropstones released from floating icebergs. The diamictite is interpreted to be a 'rain-out' deposit. (4.5cm core)

B. Diagrammatic representation of the 'rain out' depositional environment. Icebergs, moved by basin currents or wind, slowly melt and release the trapped englacial debris. In addition, normal sedimentation of mud and silt from suspension provides the dominant muddy matrix.

C. Outcrop of similar muddy diamictite from the Itarare Group of the Parana Basin, Brazil. Evidence from outcrop suggests that these diamictites are commonly laterally extensive and grade into normal basinal mudrocks, supporting a subaqueous 'rain-out' origin.

A



C

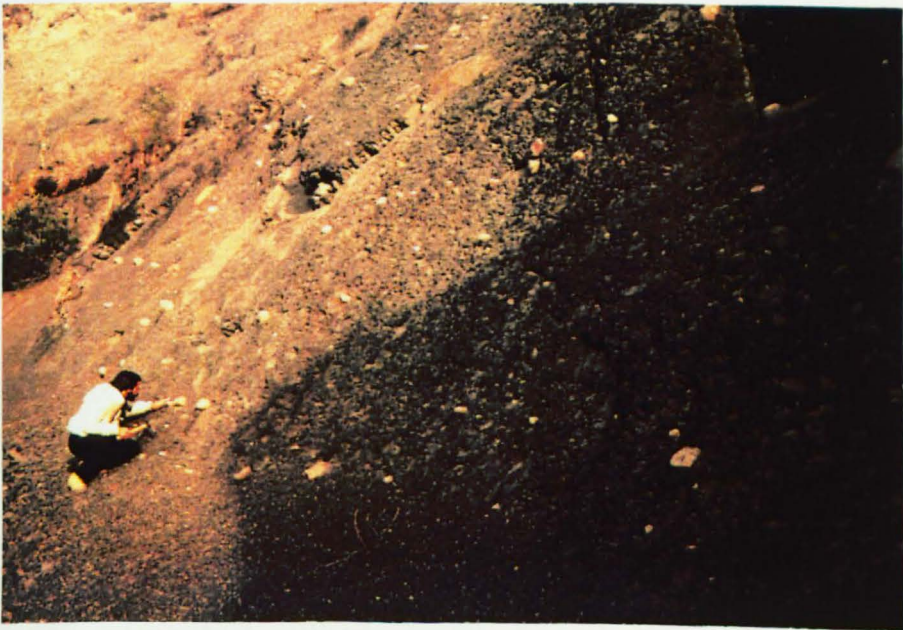


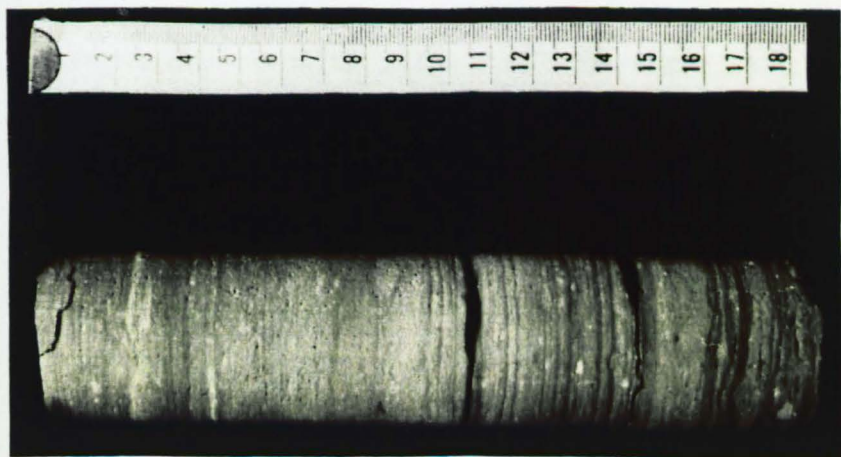
PLATE 10

A. Halgania 1 229.85m (Hoya Formation)

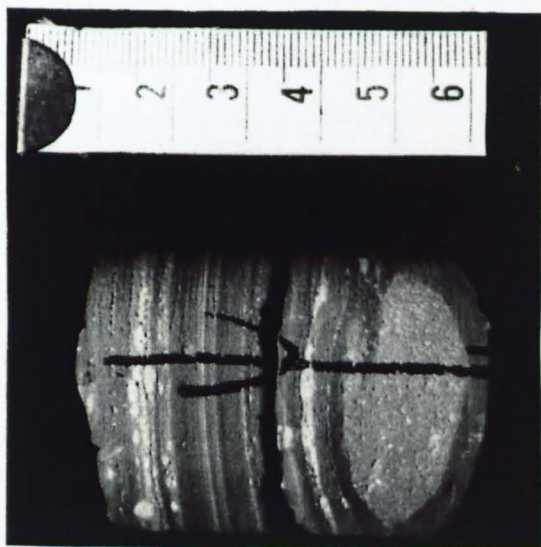
The gradual upward transition from a laminated mudrock (F1) to a massive muddy diamictite (DMm). Thin layers rich in small diamictite clasts grade into layers of diamictite composition, which become thicker and more frequent, until the bedded nature is lost and the diamictite appears to be massive. This suggests a subaqueous origin for the diamictite, and is taken to indicate an ice advance sequence.

B. Halgania 1 230.30m (Hoya Formation)

Close up of the base of the transitional unit, which contains clasts of diamictite composition within the laminated mudrock. The clasts are interpreted to be transported by floating ice into the basinal setting.



A



B

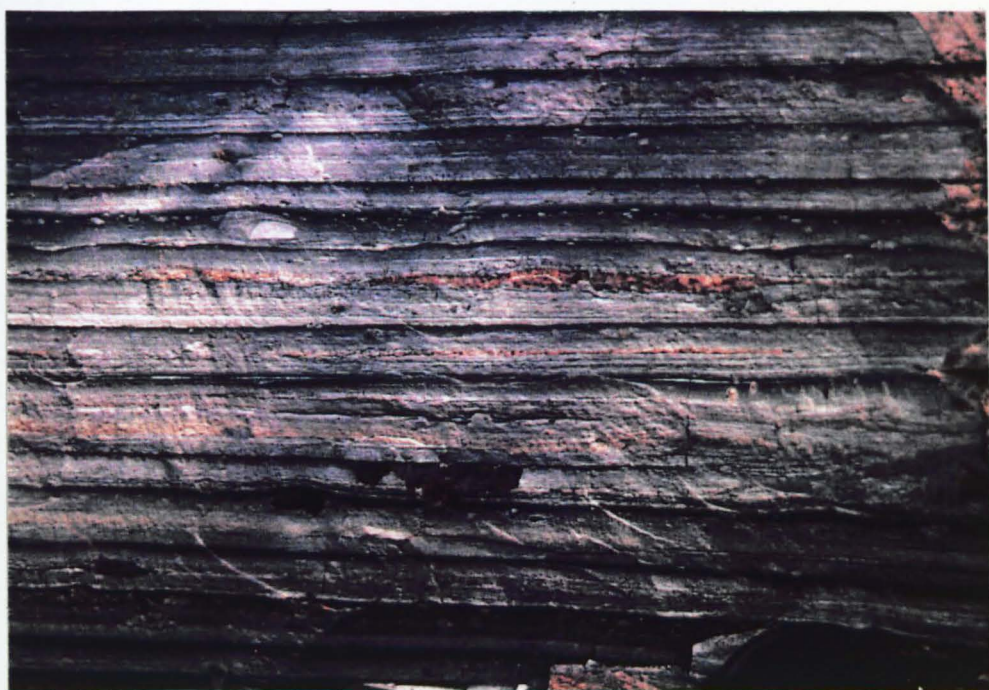
PLATE 11

A. The Itarare Group, Parana Basin, Brazil.

A thinly bedded mudrock containing abundant small clasts. Individual layers comprise a light grey multi-graded basal siltstone overlain by a thin dark mudstone. Clasts are angular and scattered throughout. (Width of photograph approx. 25cm)

B. Eremophila 1 175.85m (Hoya Formation)

Similar bedded mudrock from the Grant Group, with couplets comprising a thick lower siltstone layer and thin upper mudstone layer. The silt layer is multi-graded in parts, with very thin lighter silt layers interpreted to be underflow deposits. Small clasts are scattered throughout, and interpreted to be ice-rafted debris. The folding of laminae around the clasts is a differential compaction and drape effect. The bedding is interpreted to have a seasonal element, with silts deposited during the spring melt, and associated increased clastic input to the basin. The mudstone layer represents deposition of clay grade particles from suspension during the winter. This could also represent non-seasonal periodic fluctuations in clastic input to the basin, and it is notable that the layers are not of equal thickness. (6cm core)



A



B

PLATE 12

A. Eremophila 1 186.0m (Hoya Formation)

Type 1 bedded mudrocks (FL), each bed displaying a smooth gradation from light-grey siltstone to a dark-grey mudstone. There are hints of laminations within the silt unit, but these are not well developed. (6cm core)

This is interpreted to be a lacustrine mudstone, deposited from combined underflow, interflow and overflow currents, the overall grading resulting from periodic reduction in clastic supply to the basin, possibly seasonal.

B. Eremophila 1 178.40m (Hoya Formation)

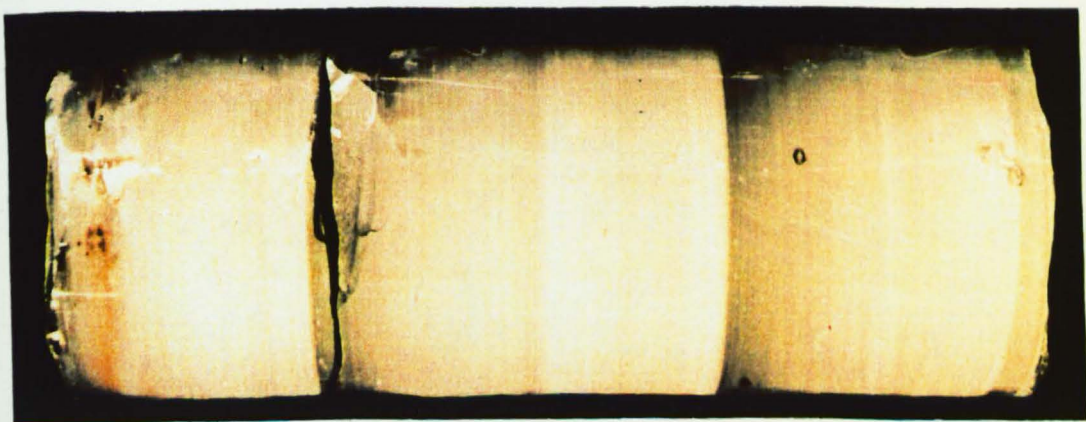
Type 2 bedded mudrocks (Fl) each bed grading from light-grey siltstone to very dark grey mudstone. The siltstone layer is multi-layered, with numerous thin laminae of silt and occasional very fine-grained sandstone. The mudstone layer is thicker than type 1.

Similar to type 1, but with increased input from underflow current producing the multi-layered siltstone layer.

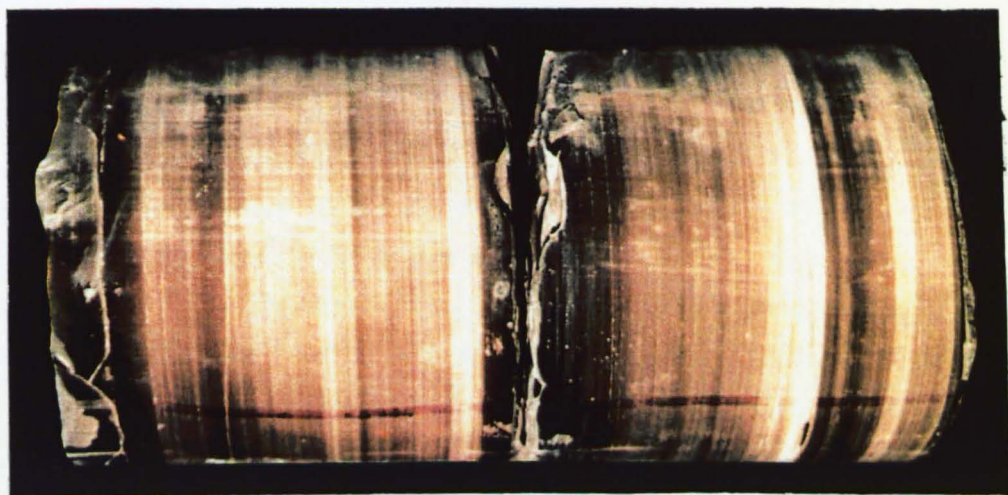
C. Eremophila 1 176.80m (Hoya Formation)

Type 3 bedded mudrocks (Fl) comprising thinly laminated light-coloured siltstones and very-fine sandstones, and darker mudstones. Many of the layers are internally graded and fine-upward into a mudstone. Lamination thickness is variable, but appears to be grouped into sets in places.

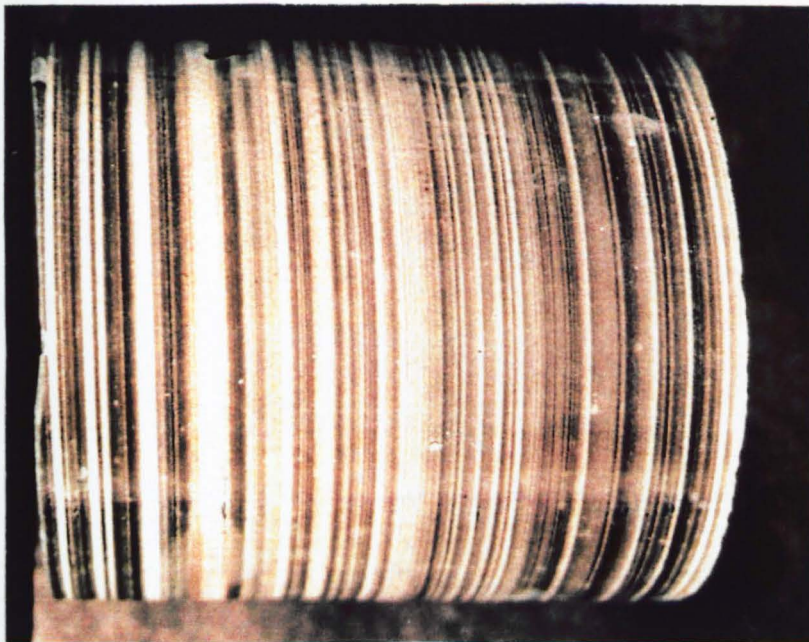
This suggests a highly variable input, dominated by underflows within a lacustrine setting. The gradation from Type 1 to Type 3 suggests the increasing proximity of the clastic source.



A



B



C

PLATE 13

A. Cliaanthus 1 423.57m (Hoya Formation)

A bedded mudrock (F1) comprising dark-grey mudstone and thin light grey-brown siltstone layers. Interbedded within this unit are a number of clasts of mixed lithologies (mainly basement material) randomly oriented and ill-sorted. The lower clasts appear to be embedded into the mudrock. Isolated clasts 'dropstones' are also recorded from this mudrock unit.

The mudrock is interpreted to be deposited within a low-energy basinal environment, with occasional input of silt-grade material from periodic underflows. The collection of clasts are interpreted to represent a 'dropstone cluster' deposited rapidly from a floating iceberg. During transport icebergs commonly concentrate debris on their upper surface due to melting (see Plate 17). Irregular melting of the submerged basal section during transport of the iceberg may result in an unstable configuration (B) and subsequent 'roll over' into a more stable orientation (C). This process allows for the rapid deposition of clasts to form a 'cluster' (C & D).

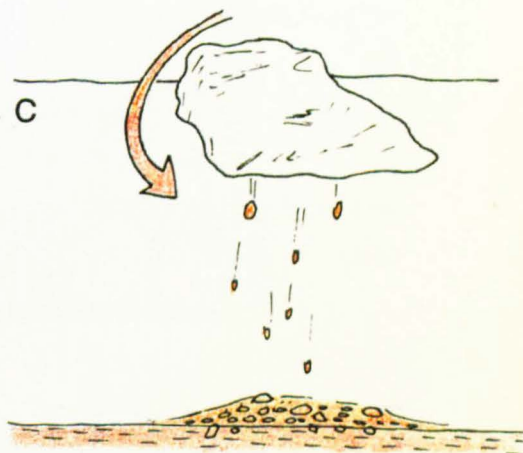
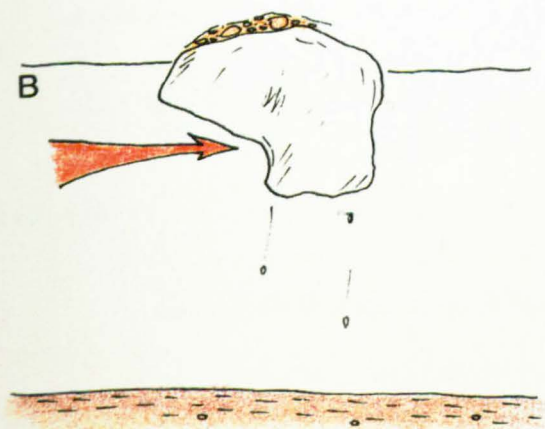
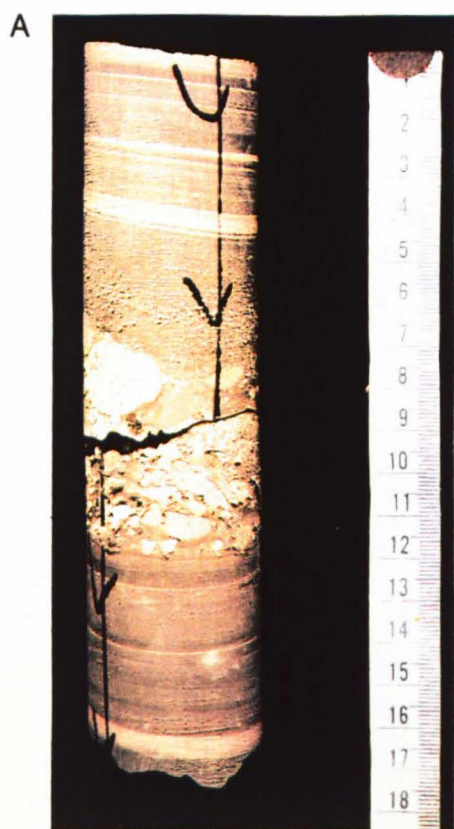


PLATE 14

A. Drosera 1 430m (Hoya Formation)

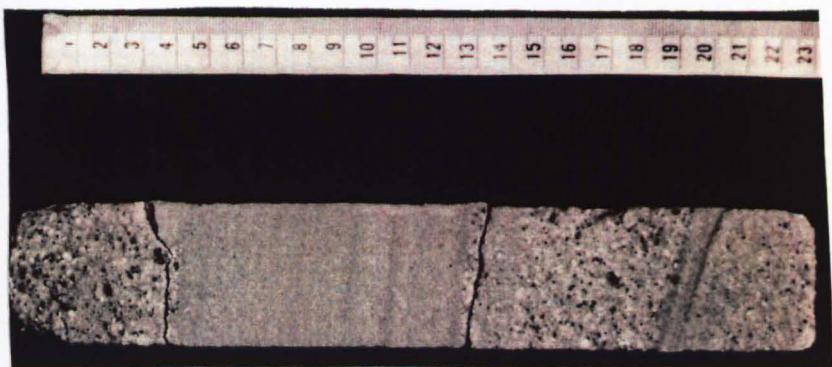
Close up of a conglomerate from Sandstone Facies 1, comprised of subrounded to subangular basement clasts and more locally derived dolomitic limestone clasts. (4.5cm core)

B. Drosera 1 420.81m (Hoya Formation)

The upper contact between a petromict conglomerate, possibly exhibiting low-angle plane-bed lamination (see core break), overlain abruptly by a medium-grained, flat-bedded sandstone.

C. Kunzea 1 192.95m (Hoya Formation)

Low-angle plane-bedded and cross-bedded medium to coarse-grained sandstones. Fining-upward is clearly observed within each bed.



C



B



A

PLATE 15

A. Ficus 361.30m (Hoya Formation)

The sharp basal contact of a fining-upward sandstone, sandstone facies 5, with abundant mudstone rip-up clasts. (4cm core)

B. Hoya 1 279m (Hoya Formation)

Intraclast conglomerate, comprising abundant mudstone and siltstone clasts in a fine to medium-grained sandstone matrix. The clasts display a bed parallel lineation. (4cm core)

C. Hoya 320.05m (Hoya Formation)

Intraclast conglomerate, with large mudstone clasts, which commonly appear to be slightly deformed suggesting only partial lithification prior to transport. (4cm core)

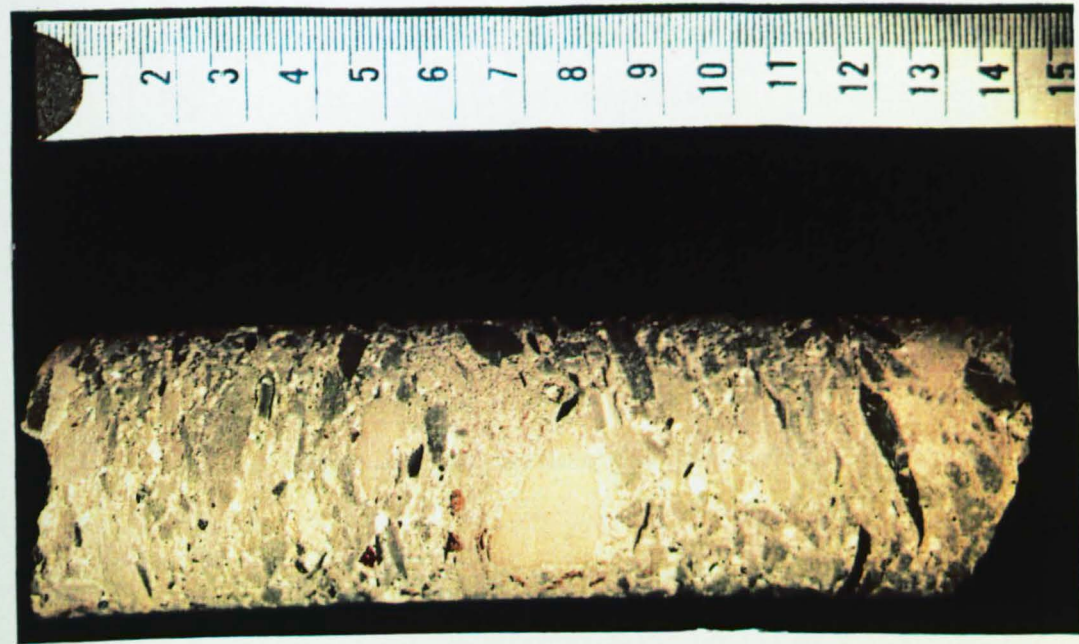
D. Drosera 1 311.80m (Hoya Formation)

Intraclast conglomerate, containing large clasts of massive and laminated mudstones. The large clast of laminated mudstone contains small dropstones, indicating it was derived from a glacial environment. (6cm core)

All these conglomerates are interpreted to contain rip-up clasts, and were probably deposited within channels.



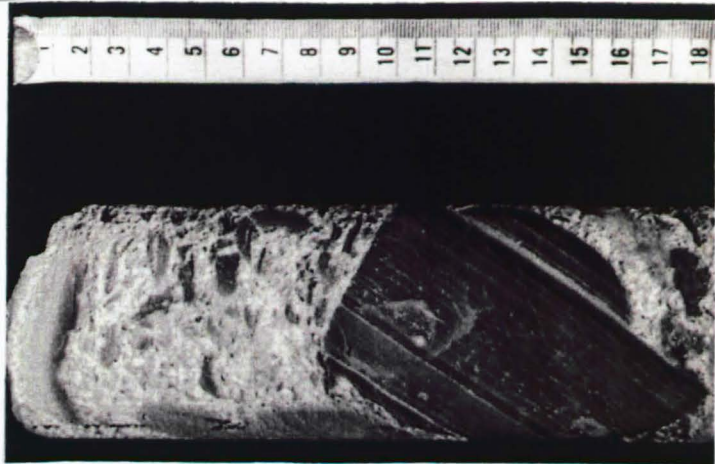
A



B



C



D

PLATE 17

Examples of present day glacial environments which bear some similarity to the depositional models proposed for the Hoya Formation.

A. Iceberg with concentration of debris on upper surface. This is evidence for the transport of clasts by ice, and can be viewed in conjunction with Plate 13. (Portage Lake, Alaska)

B. Fan complex fed by a glacier building out into a marine/lacustrine setting. This could also form entirely subaqueously. Note the plumes of suspended sediment and abundance of floating ice. (Glacier Bay, Alaska)

C. Braided fluvial outwash fed by a glacier/ice sheet, and controlled by topographic constraints. An analogue perhaps for the Drosera type fluvial sandstones. (Unknown location, source Bristol University Library)

A



B



C

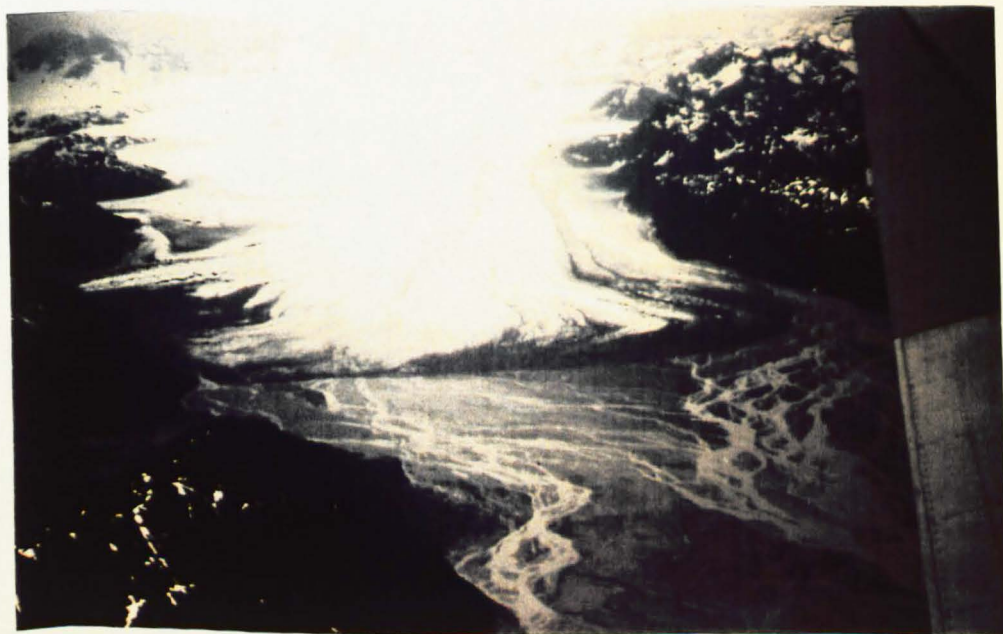


PLATE 18

A. Calytrix 1 218.61m (Calytrix Formation)

Sandstone facies Thinly bedded medium to fine-grained sandstone, coarser layers picked out by the mud filter-cake, due to their increased permeability. (4cm core)

B. Calytrix 1 (Calytrix Formation)

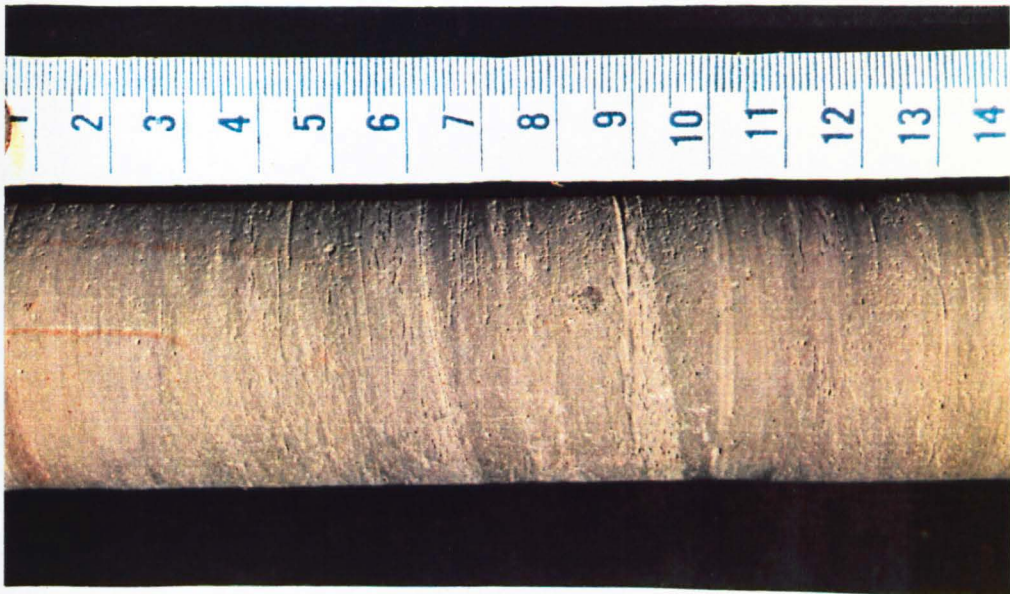
Sandstone facies Interbedded coarse sandstone containing large pebble size clasts and scattered shelly material (large bivalve shell towards the top of the core) and interbedded fine-grained argillaceous sandstone, with a mottled bioturbated appearance. Interpreted to be storm sands. (6cm core)

C. Calytrix 1 199.05m (Calytrix Formation)

Calcareous mudstone facies. Medium grey calcareous mudstone containing abundant delicately preserved bryozoa, and less common bivalves. Deposited in a low-energy marine basinal setting. (6cm core)

D. Calytrix 1 182.50m (Calytrix Formation)

Mudrock facies. Thinly bedded mudstones and silty mudstones. Fining-upward units from silty mudstone to mudstone, with abundant small lozenge shaped burrows (possibly Chondrites) in the lower silty horizons. Deposited under marine low-energy basinal conditions, with a periodic control on clastic input producing the grading. (6cm core)



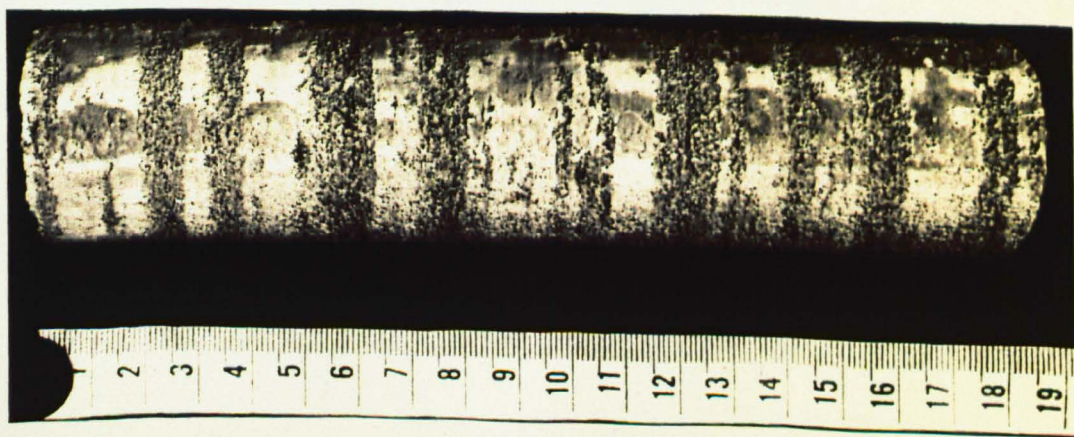
D



C



B



A

PLATE 19

A. Calytrix 1 141.40m (Clianthus Formation)

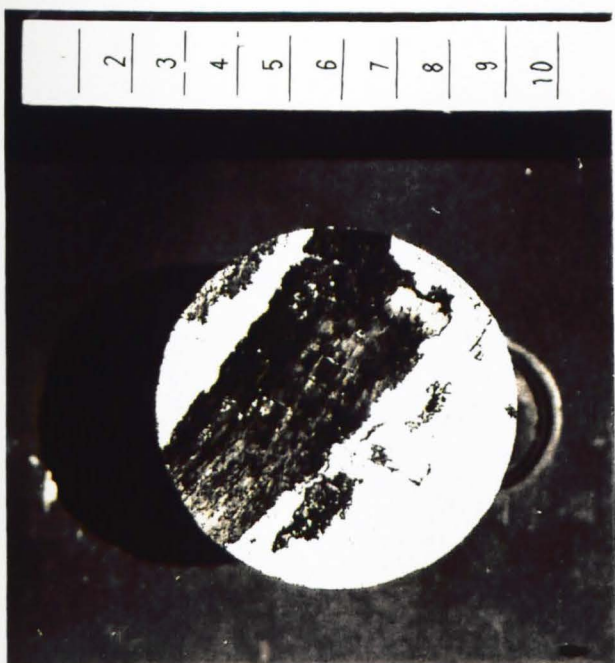
The top of an upward-fining sandstone, with thin carbonaceous laminations or 'hash'. The sandstone is abruptly overlain by a medium-grained sandstone containing large coaly clasts as lag. Interpreted to be deposited within a sandy bedload-dominant fluvial system. The upward-fining sequence indicates waning flow, with fine carbonaceous material finally coming out of suspension as draping lamination, possibly as a bar-top deposit. (6cm core)

B. Calytrix 1 136.59m (Clianthus Formation)

An example of a large fragment of coaly material, indicating the abundance of vegetated areas in the source area (6cm core).

C. Calytrix 1 136.59m (Clianthus Formation)

Similar to above, large coaly debris as lags within the medium-grained sandstone. (6cm core)



B



C



A

PLATE 20

A. Calytrix 1 108.28m (Cliaanthus Formation)

Heterolithic sandstone, siltstone and mudstone. The fine to very fine-grained sandstones contain abundant wave and current ripples. Also ptymatically folded syneresis cracks, or possibly water escape features. (6cm)

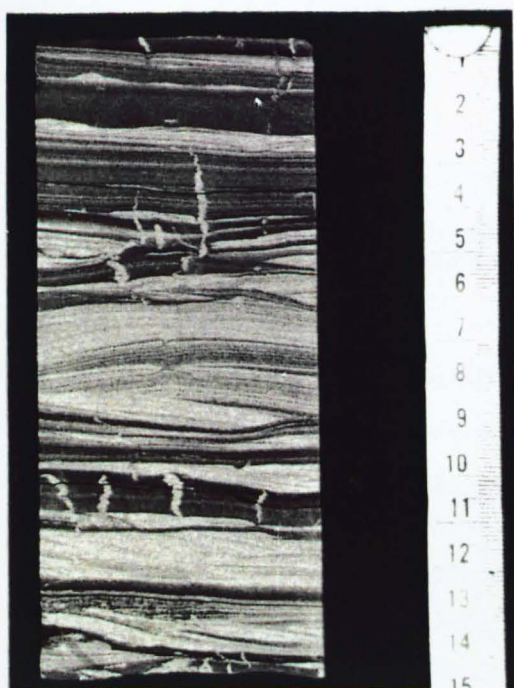
B. View of the bedding plane, clearly displaying the linear injection features, possibly syneresis cracks or water escape features. (6cm)

C. Calytrix 1 92.37m (Cliaanthus Formation)

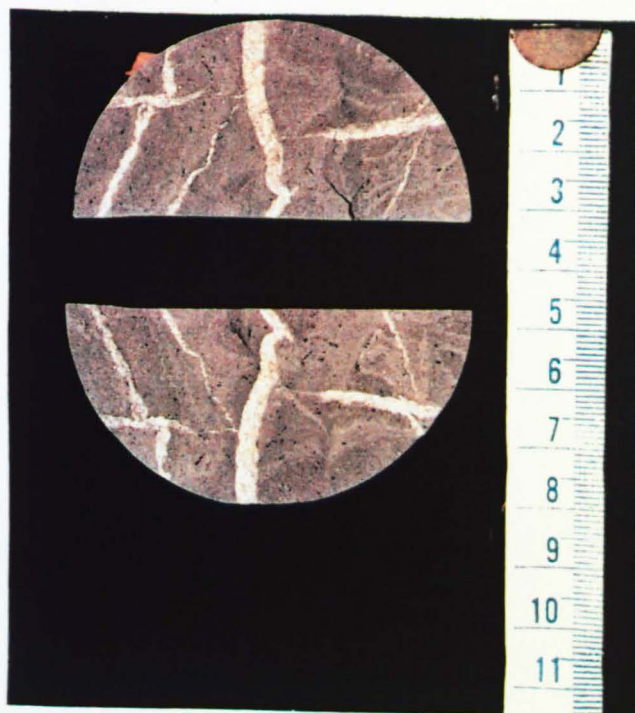
Laminated fine to very fine-grained sandstone and interbedded thin silty mudstones. Bioturbation is evident although not pervasive. Isolated zones display soft-sediment deformation, slumped and contorted bedding. The sandstones display low-angle bedding, perhaps representing hummocky cross-stratification. (6cm core)

D. Ficus 1 176.50m (Cliaanthus Formation)

Interbedded fine to very fine-grained laminated sandstones and mudstones. The sandstones are parallel laminated, occasionally rippled, with minor amounts of bioturbation. (6cm core)



A



B



C



D

PLATE 21

A. Eremophila 1 165.60m (Clanthus Formation)

A reactivation surface at the top of a bioturbated silty mudstone, overlain by laminated silty sandstones. This suggests periods of erosion on the shelf, reflecting periodic storm events. Note the trace fossil assemblages in this facies are larger than those in the silty sandstone, again reflecting a change in the energy of the environment of deposition. (6cm core)

B. Eremophila 1 169.55m (Clanthus Formation)

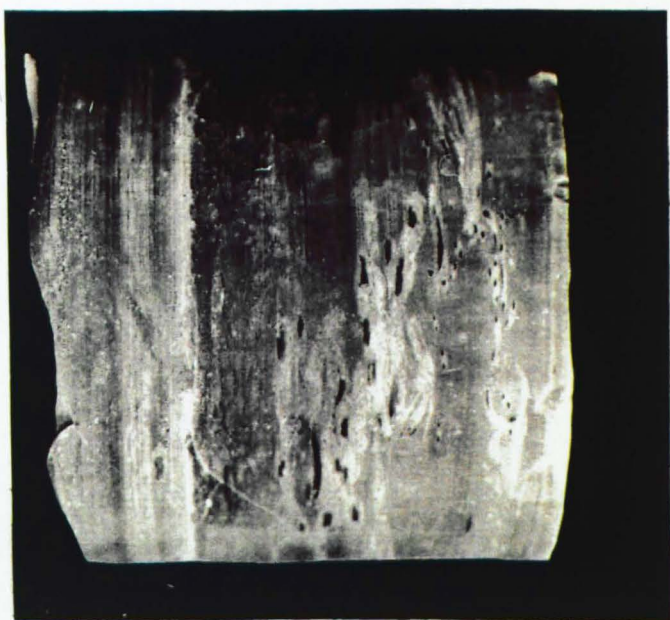
Example of small lozenge shaped burrows within a mudstone, possibly Chondrites. (6cm core)

C. Ficus 1 159.20m (Clanthus Formation)

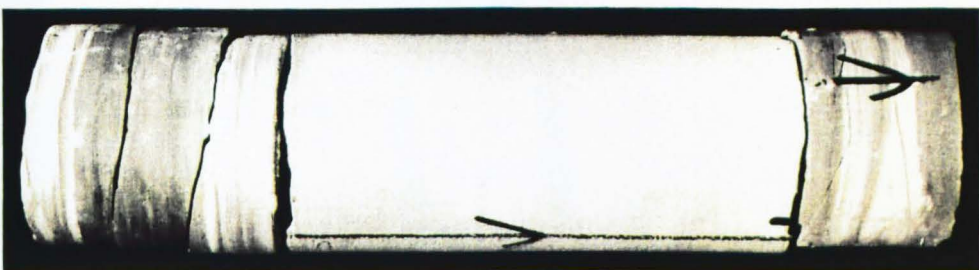
A sharp based fine to very fine-grained sandstone within a mudstone sequence. The sandstone is predominantly massive, the top 3cm fining upward to display fine laminations, before it is overlain by a medium grey mudstone. This is interpreted to be a rapidly deposited storm-induced mass flow. Thin sandstones in the underlying mudstones display ripple lamination, indicating periodic current activity. (6cm core)



A



B



C

PLATE 22

A. *Melaleuca* 1 133.76m (Clanthus Formation)

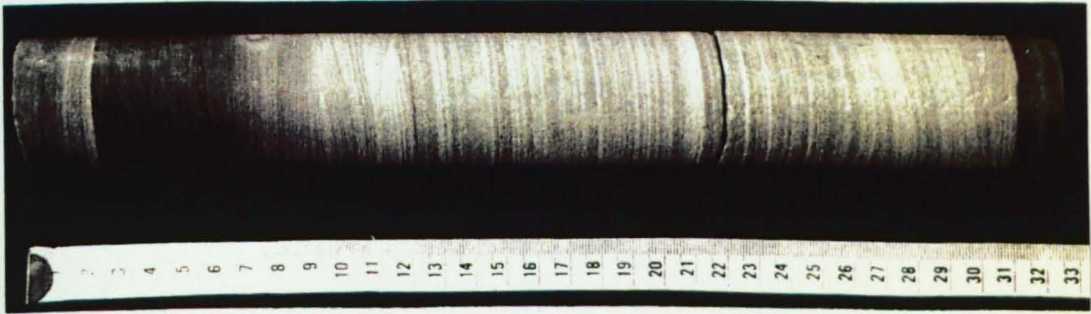
Large fining-upward unit, grading from a light grey, fine-grained sandstone to a dark-grey mudstone. The sandstone is sharp based and displays low angle cross-stratification, ripple lamination and fine parallel-lamination towards the top. The grading signifies a waning flow and cross stratification indicates current activity, suggesting emplacement by mass-flow processes. (4cm core)

B. *Calytrix* 1 86.95m (Clanthus Formation)

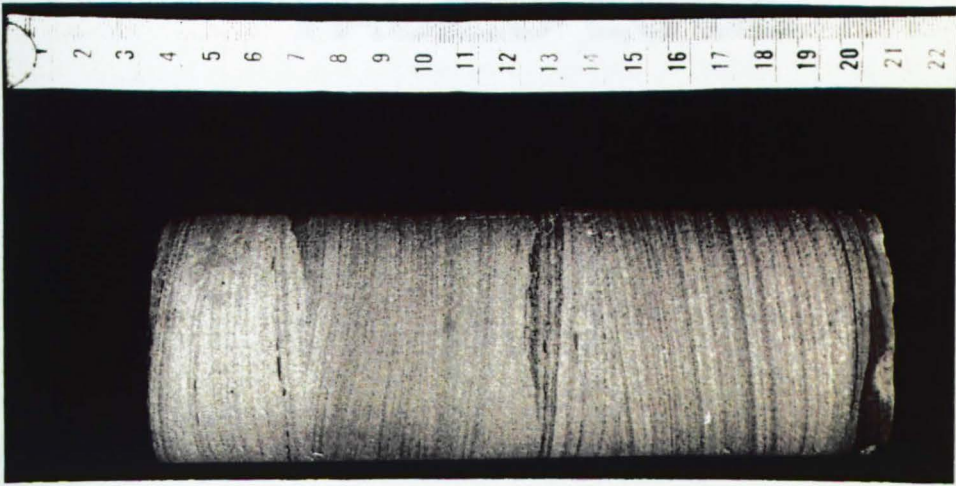
Laminated fine to very fine-grained sandstone displaying low angle cross-bedding, either trough sets or possibly hummocky cross stratification. (6cm core)

C. *Ficus* 1 108.0m (Clanthus Formation)

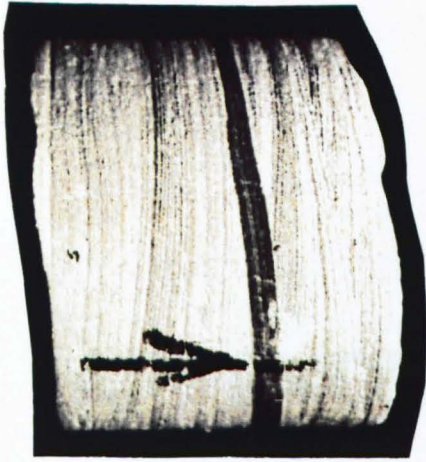
Cross-laminated sandstone with thin mudstone drape. (6cm core)



A



B



C

APPENDIX 1

FACIES LOGS

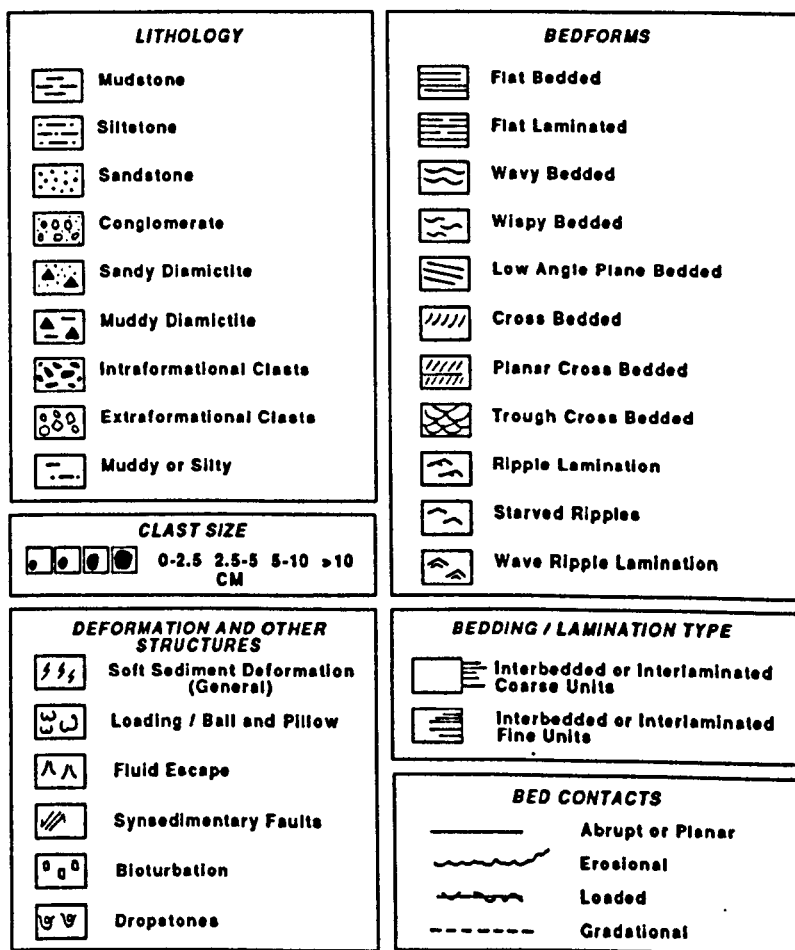
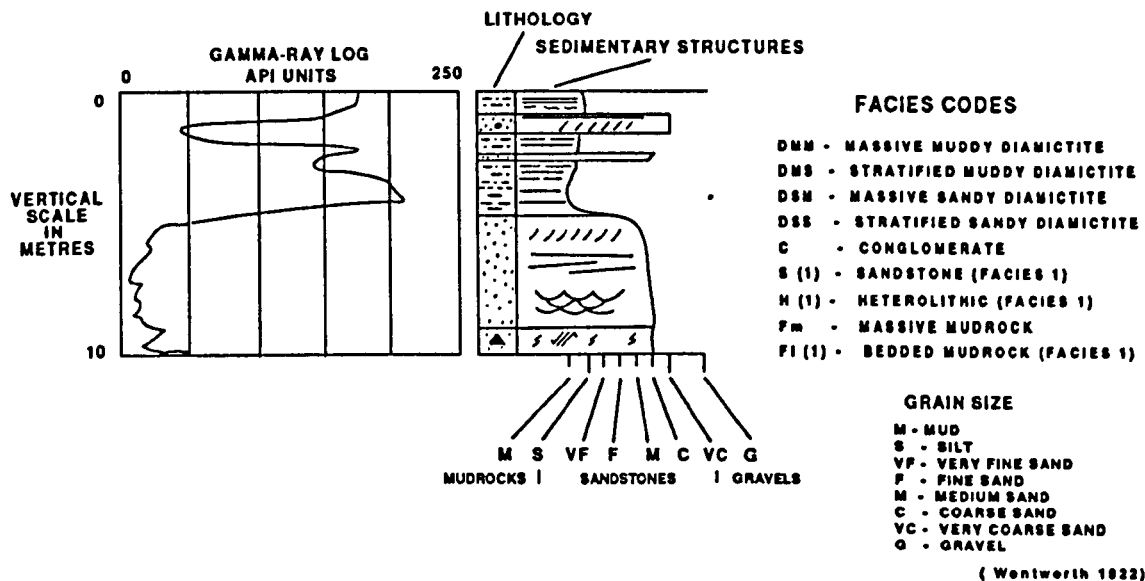
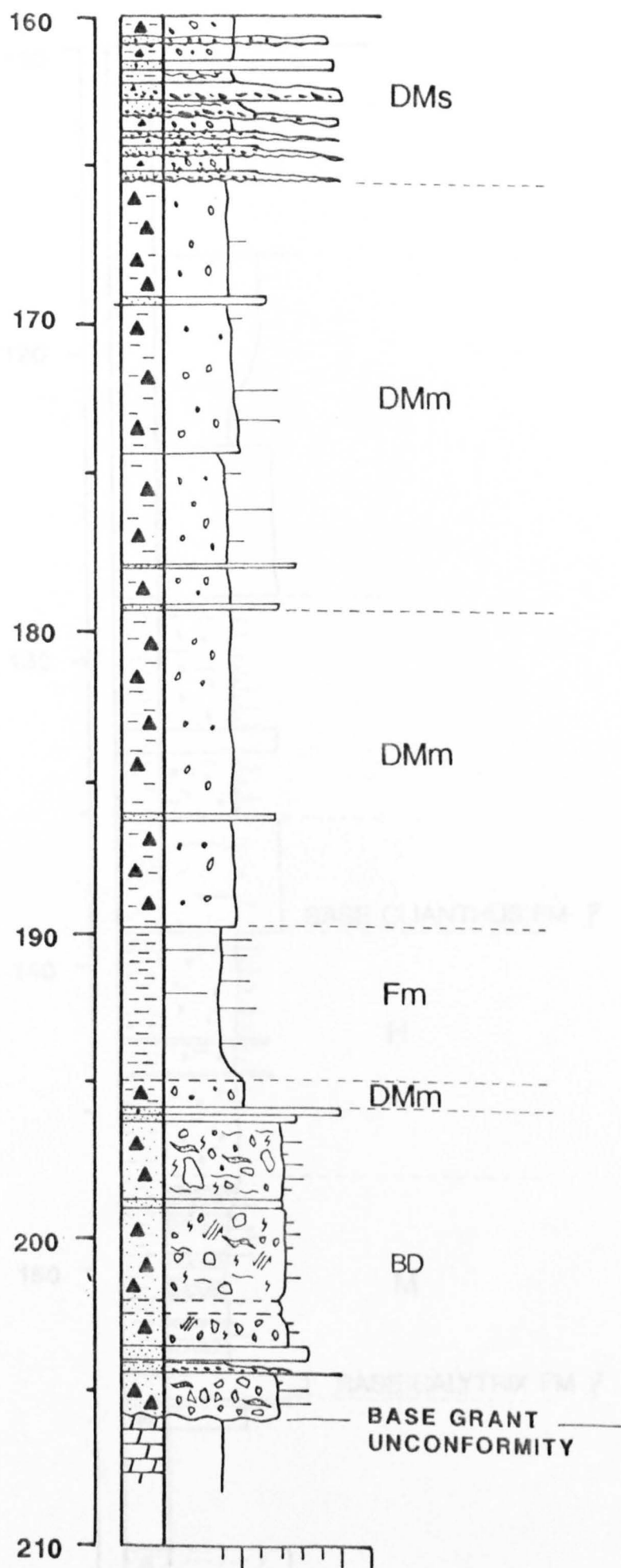
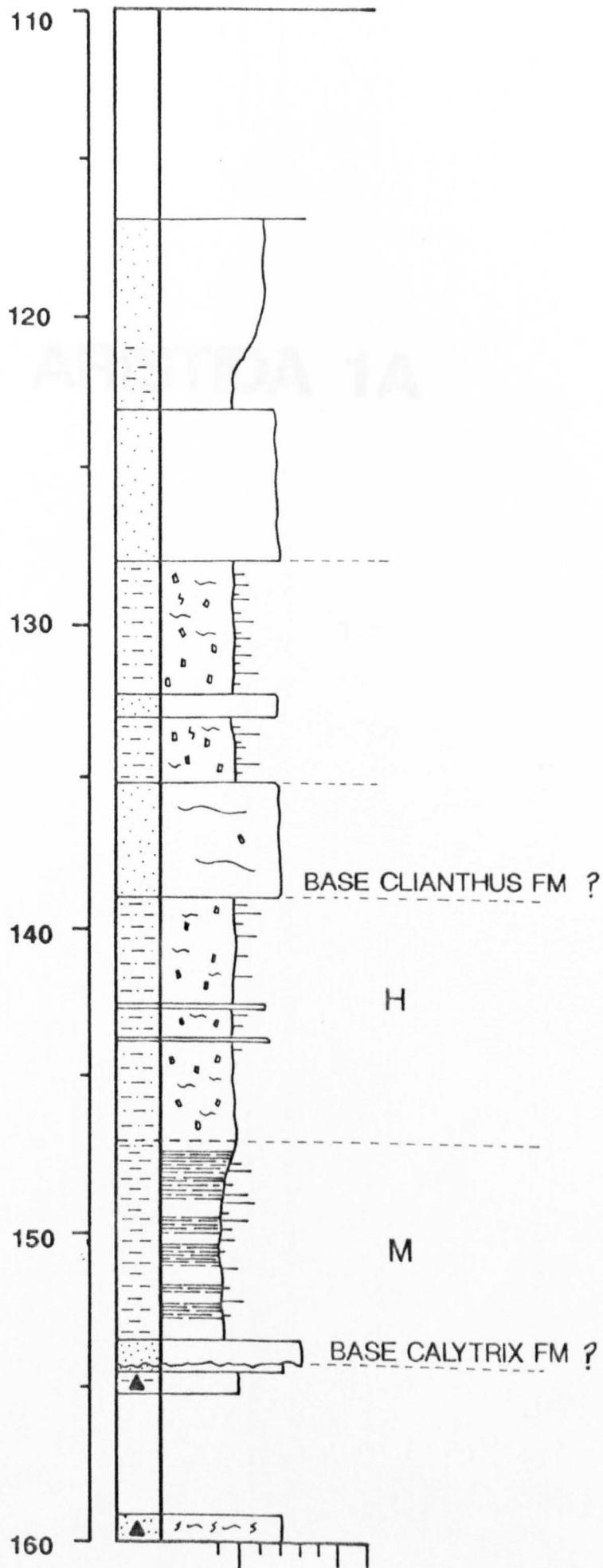


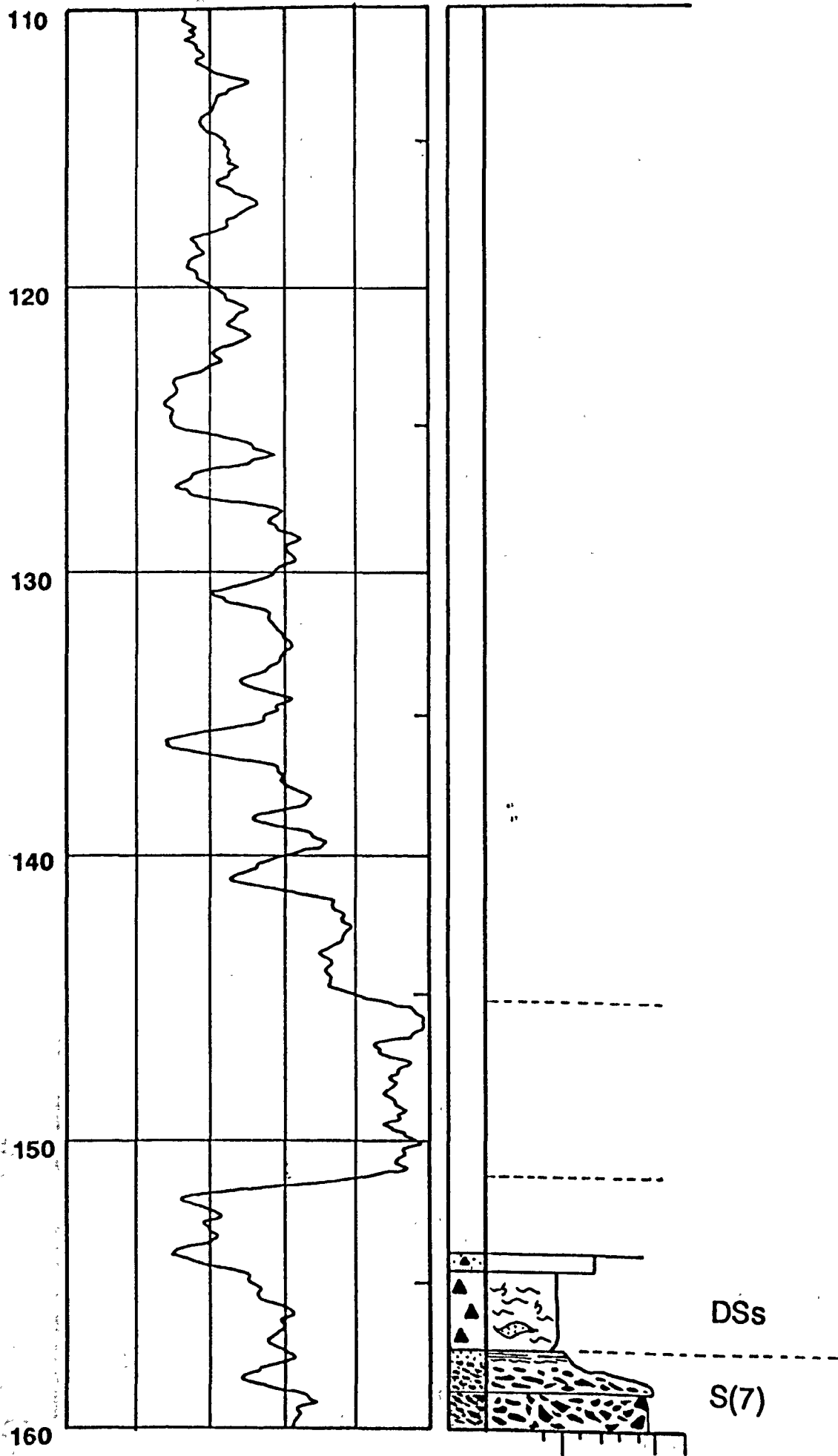
Figure 51. Key to facies log annotation

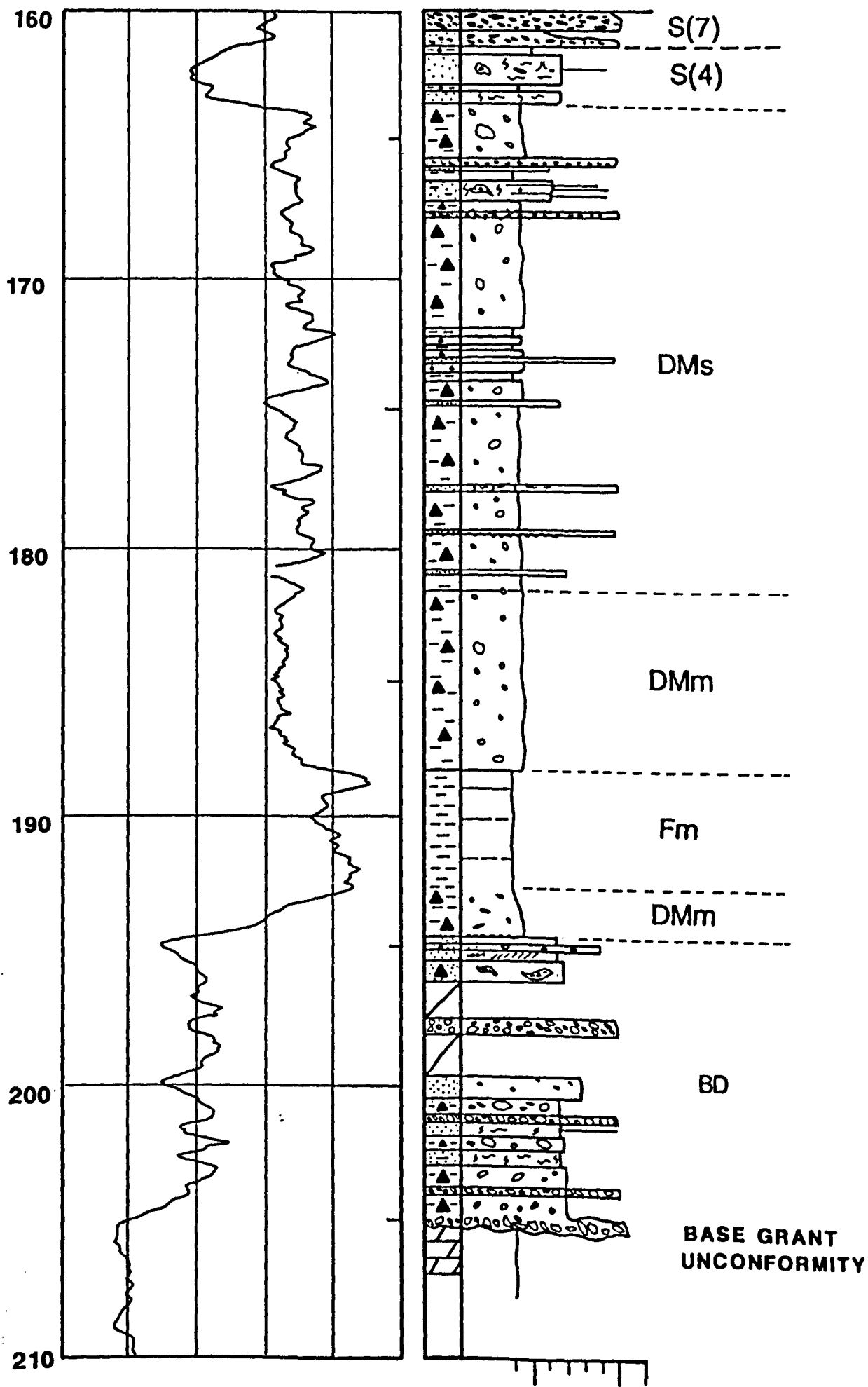
ARISTIDA 1





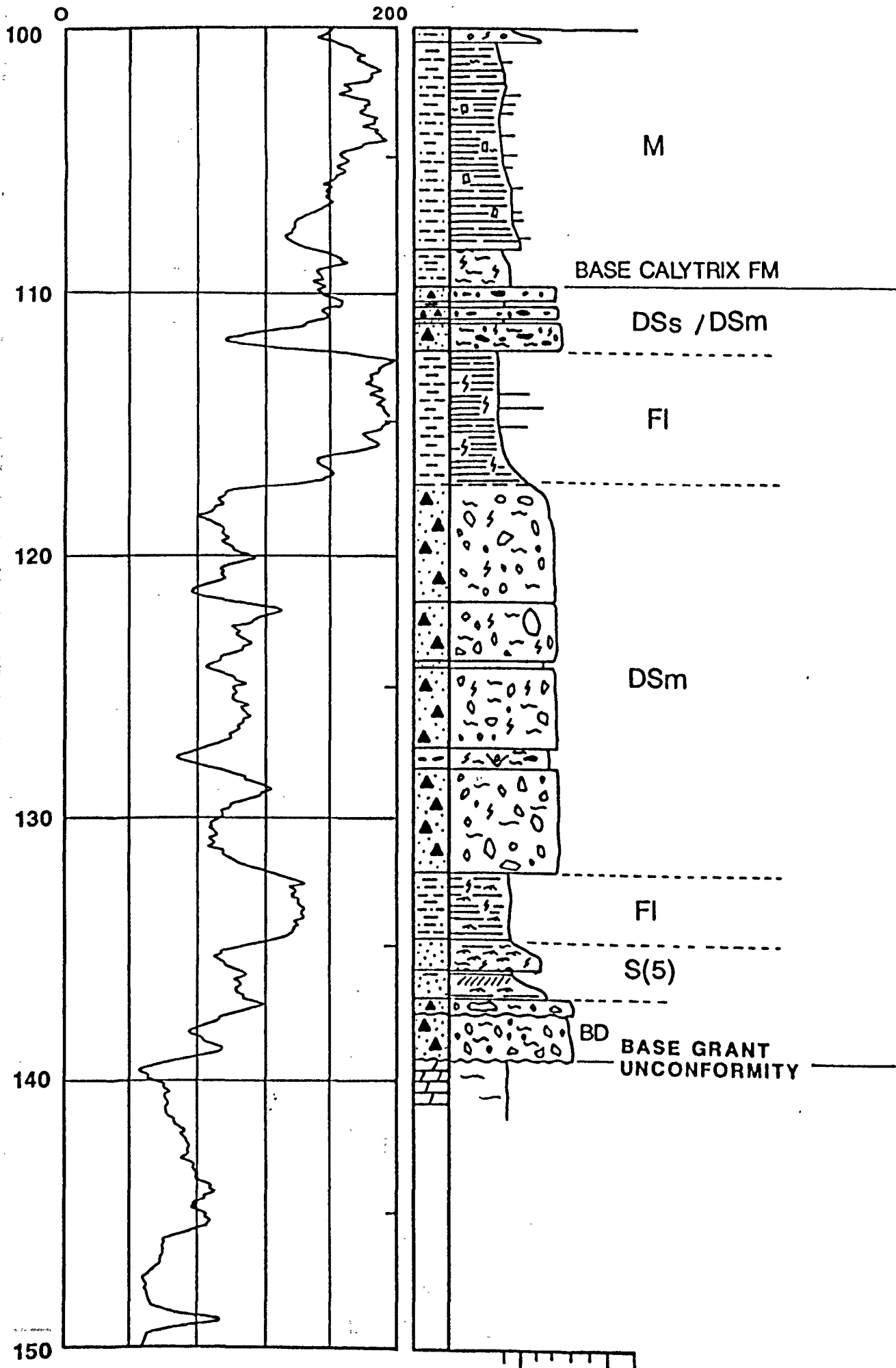
ARISTIDA 1A



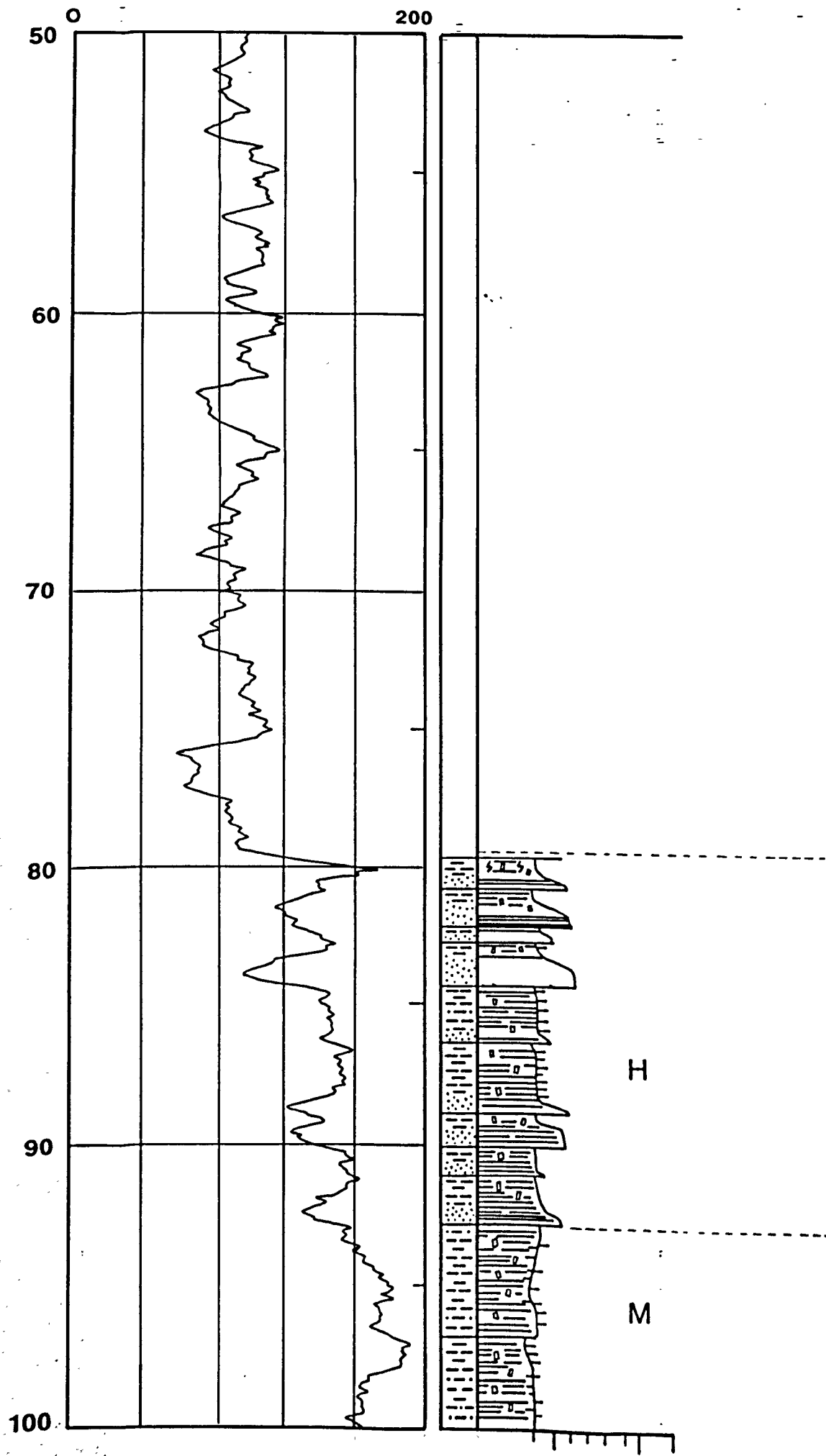


CALADENIA 1

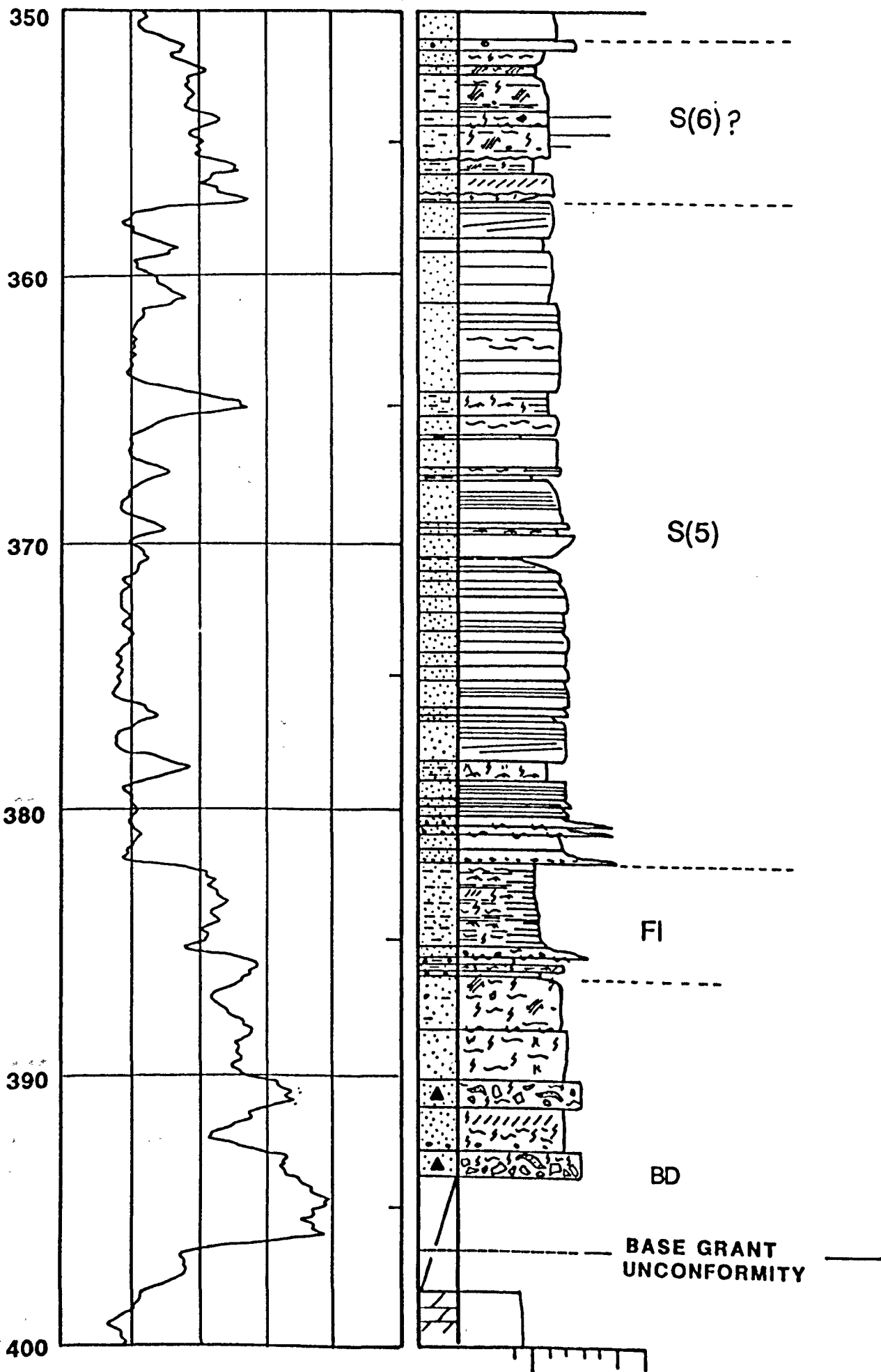
GAMMA RAY

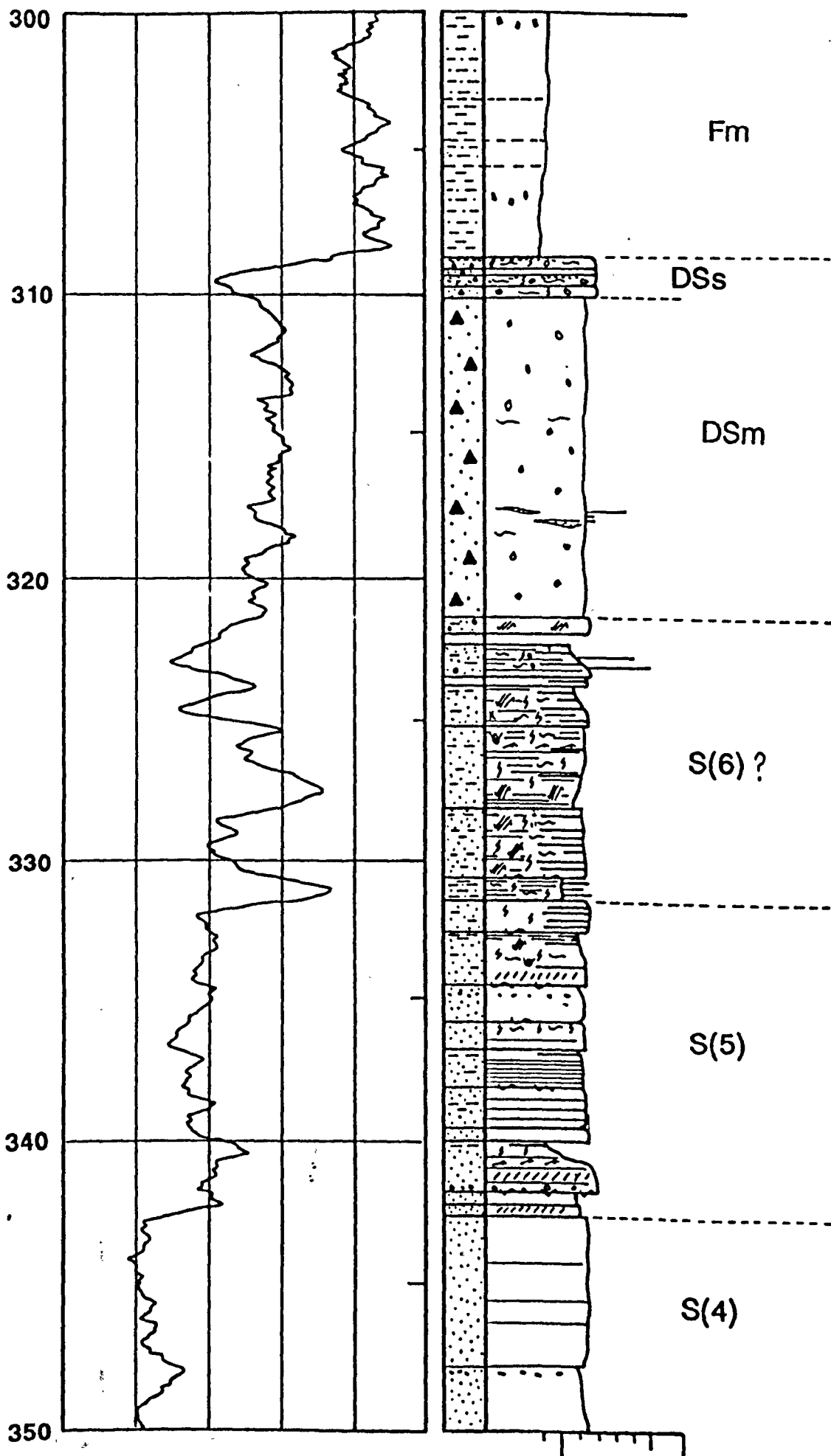


GAMMA RAY



CALYTRIX 1





250

260

270

280

290

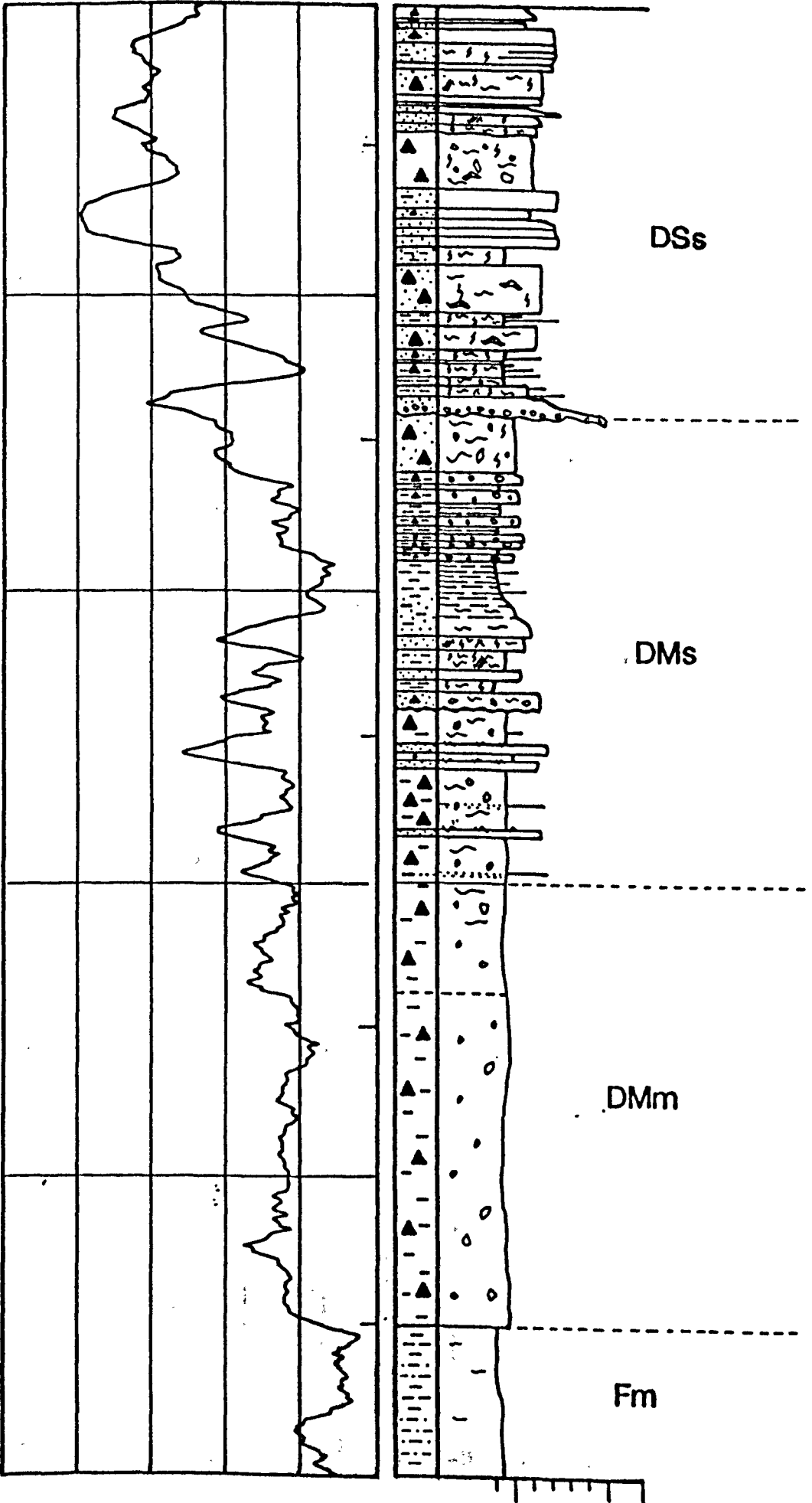
300

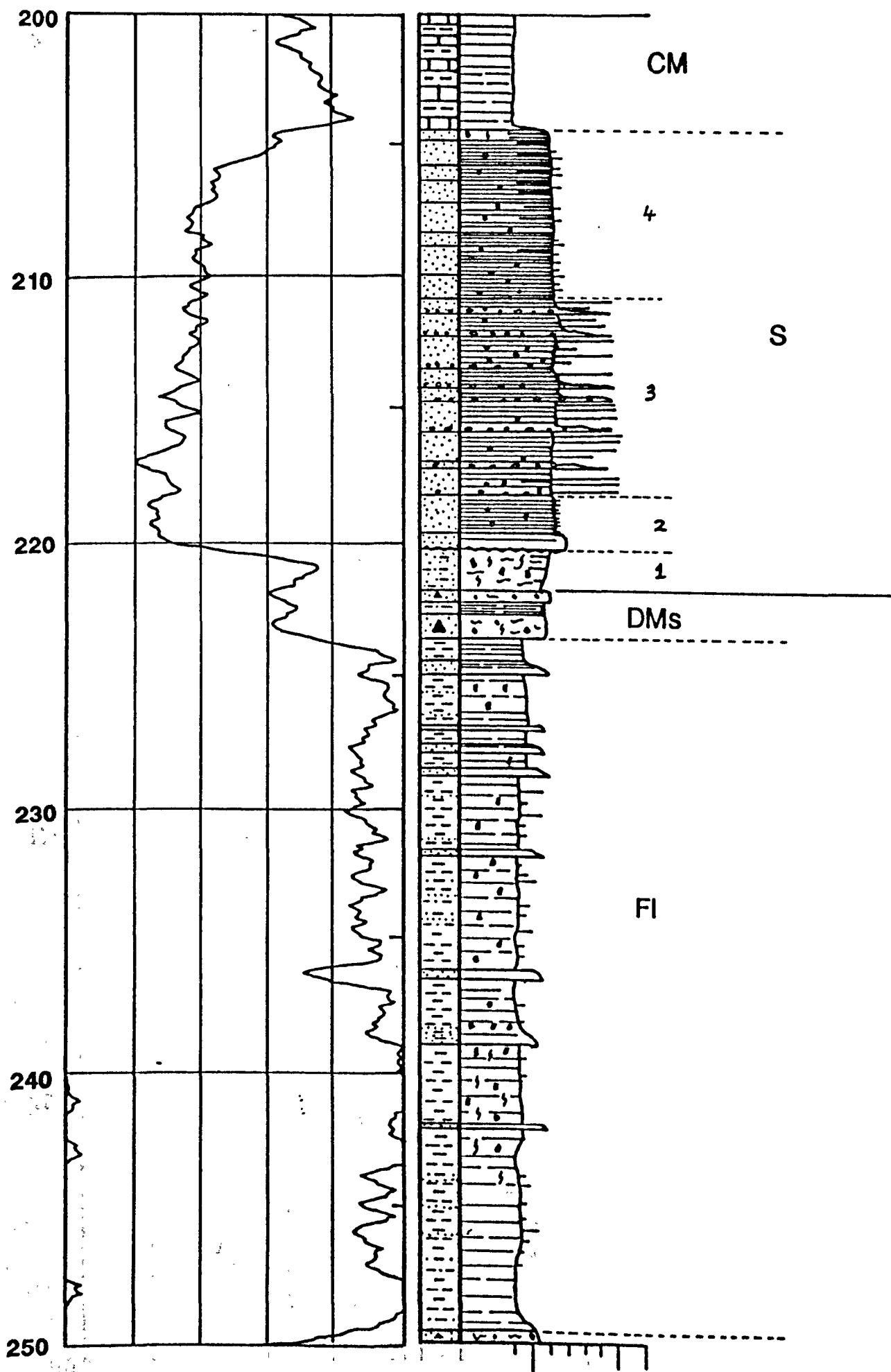
DSs

DMs

DMm

Fm





150

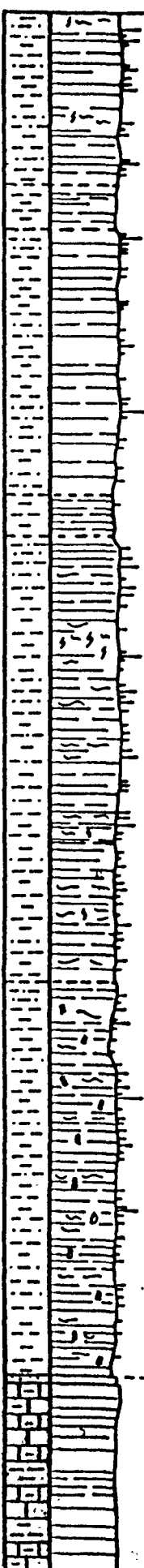
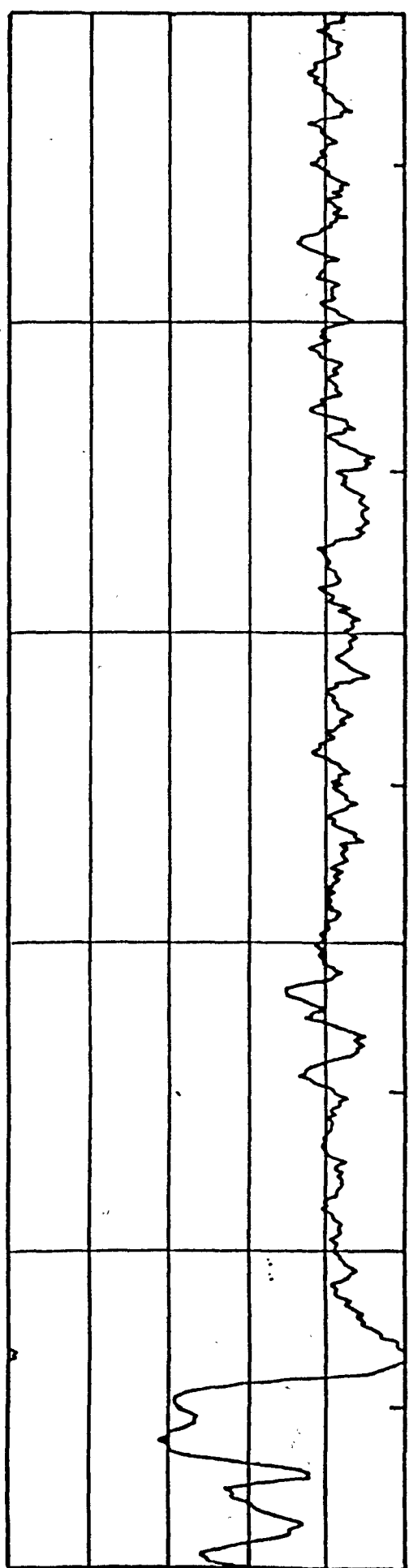
160

170

180

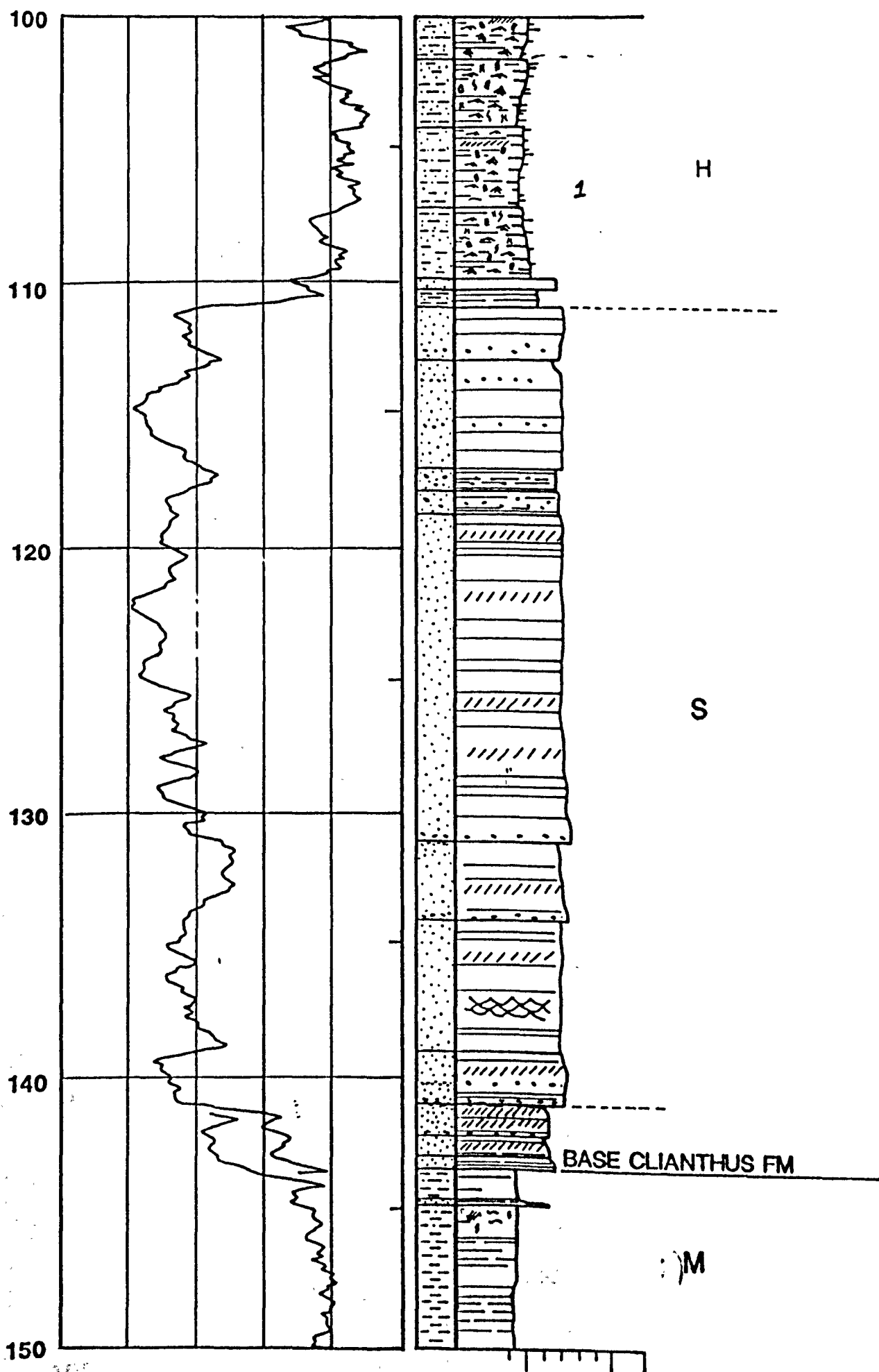
190

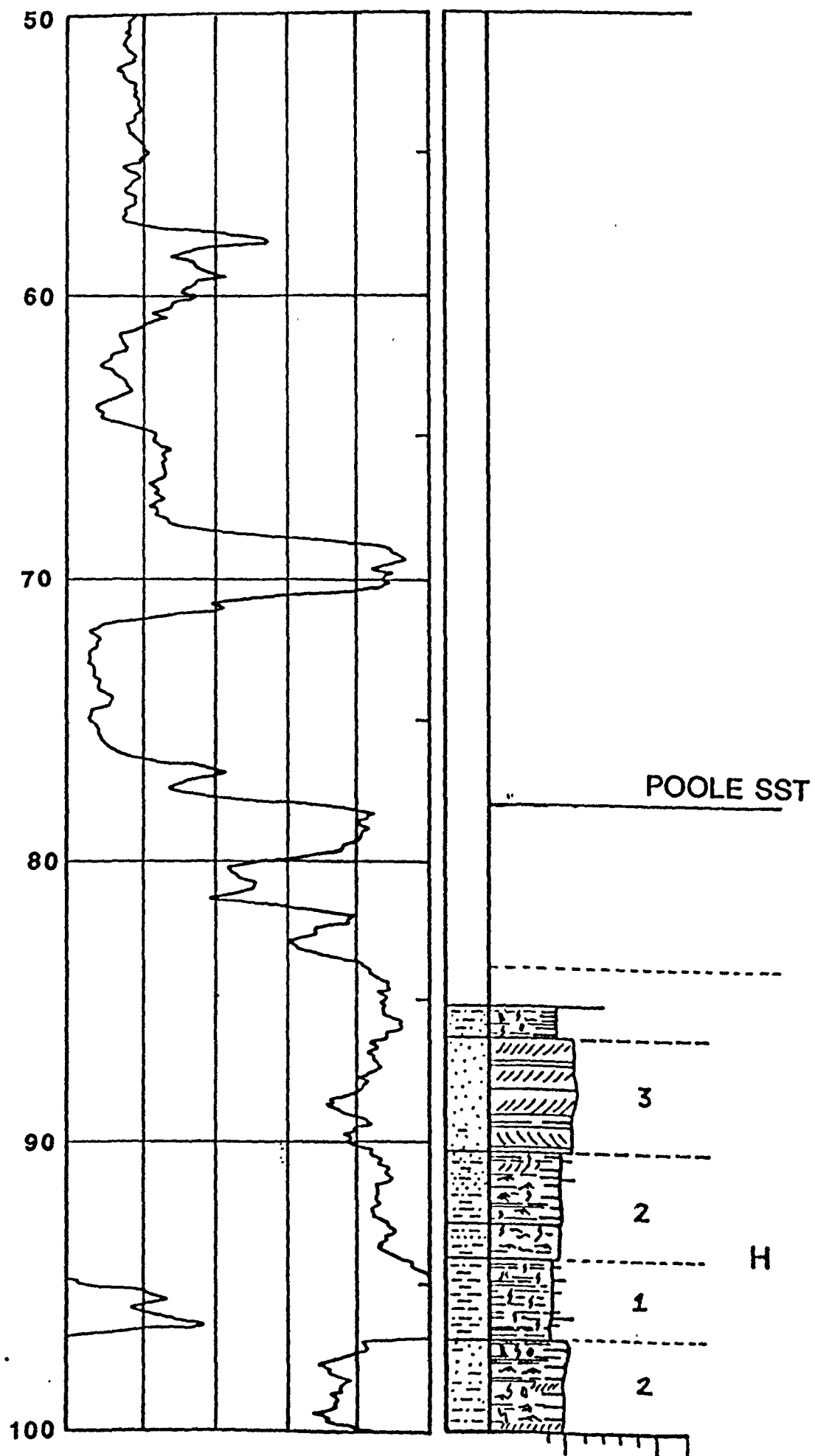
200



M

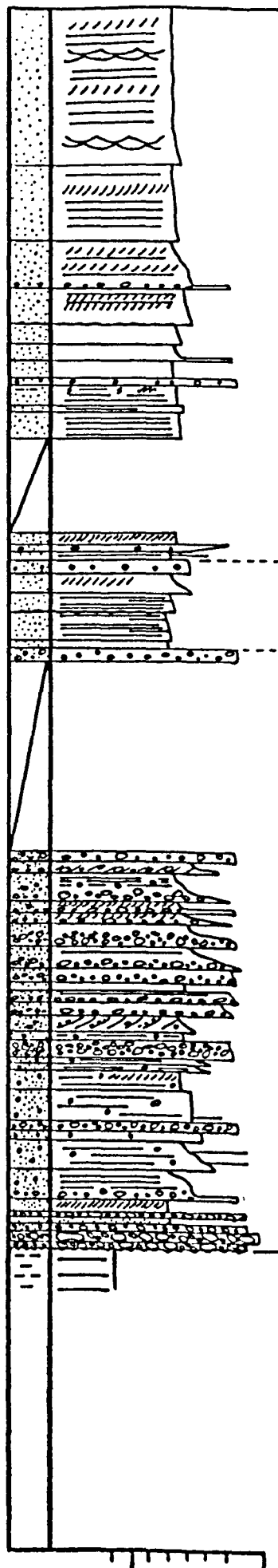
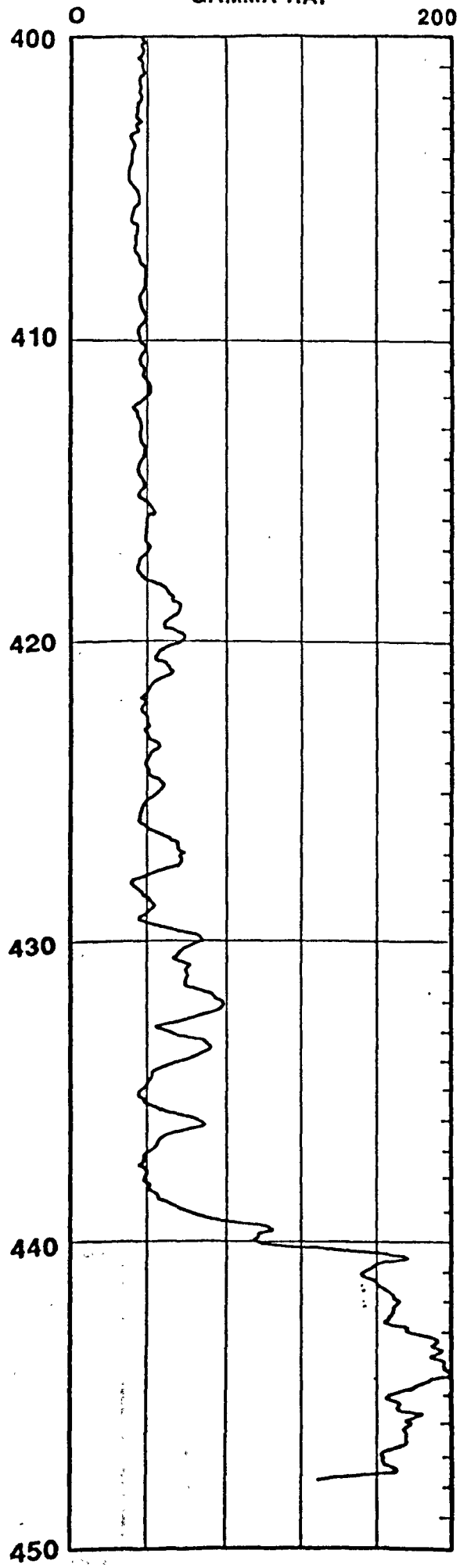
CM





DROSER 1

GAMMA RAY

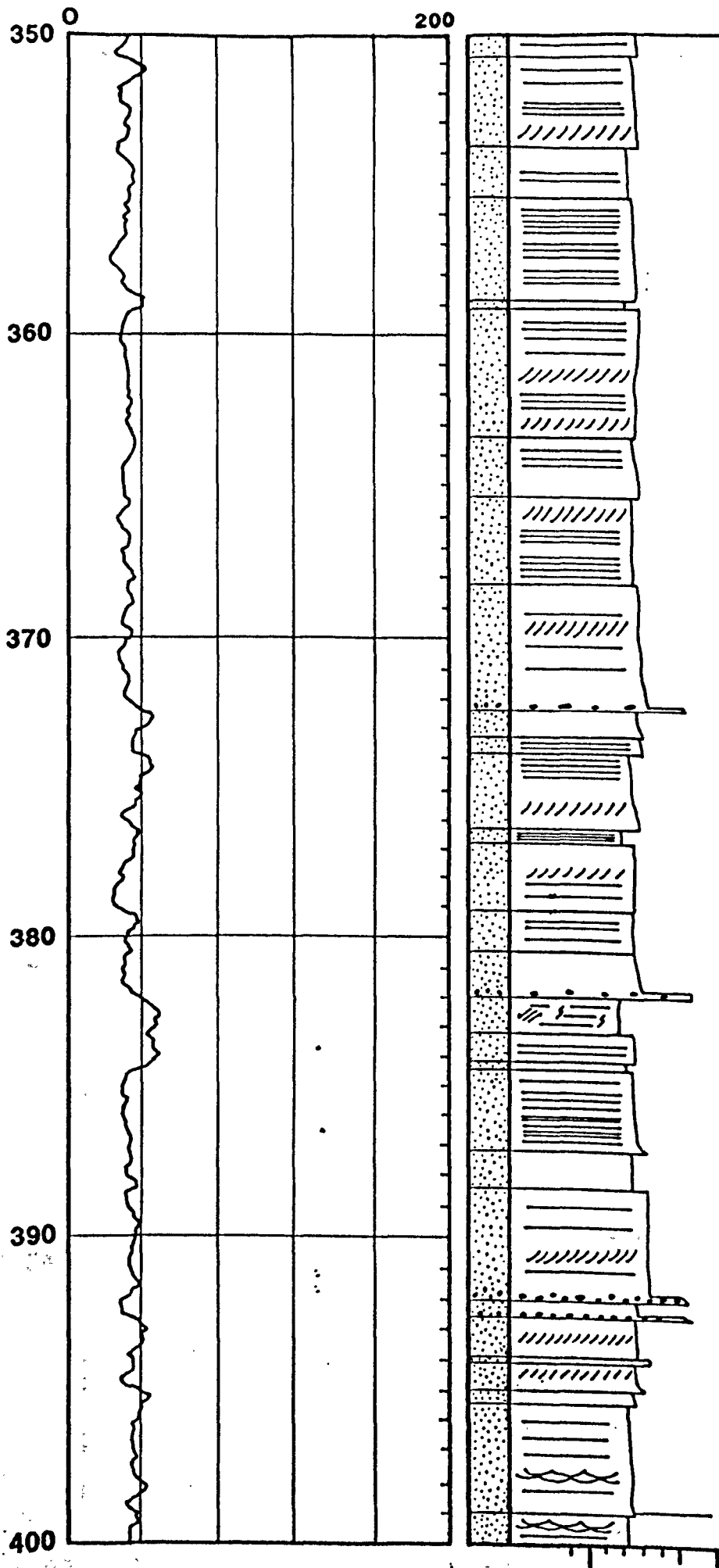


S(2)

S(1)

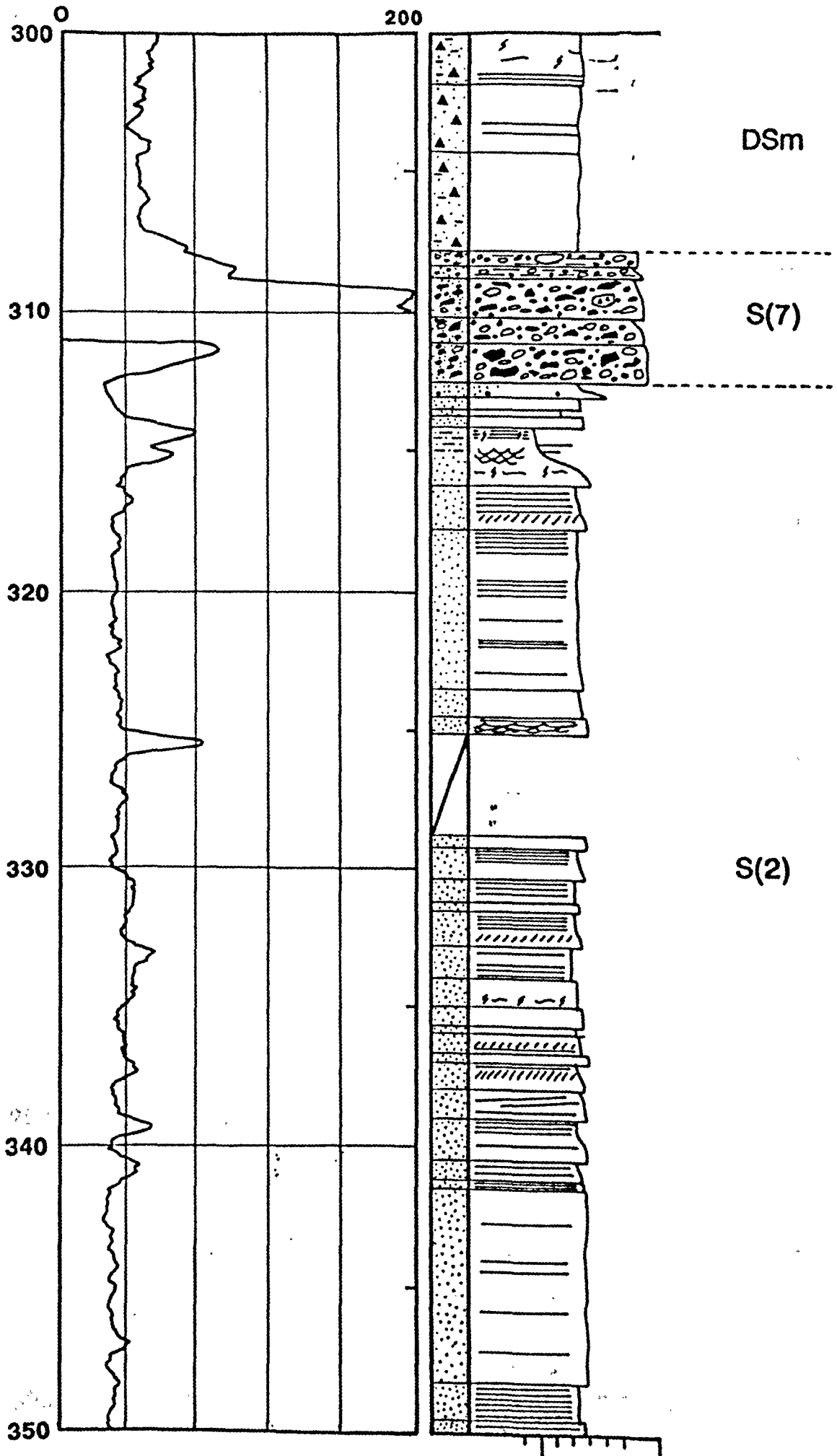
BASE GRANT
UNCONFORMITY

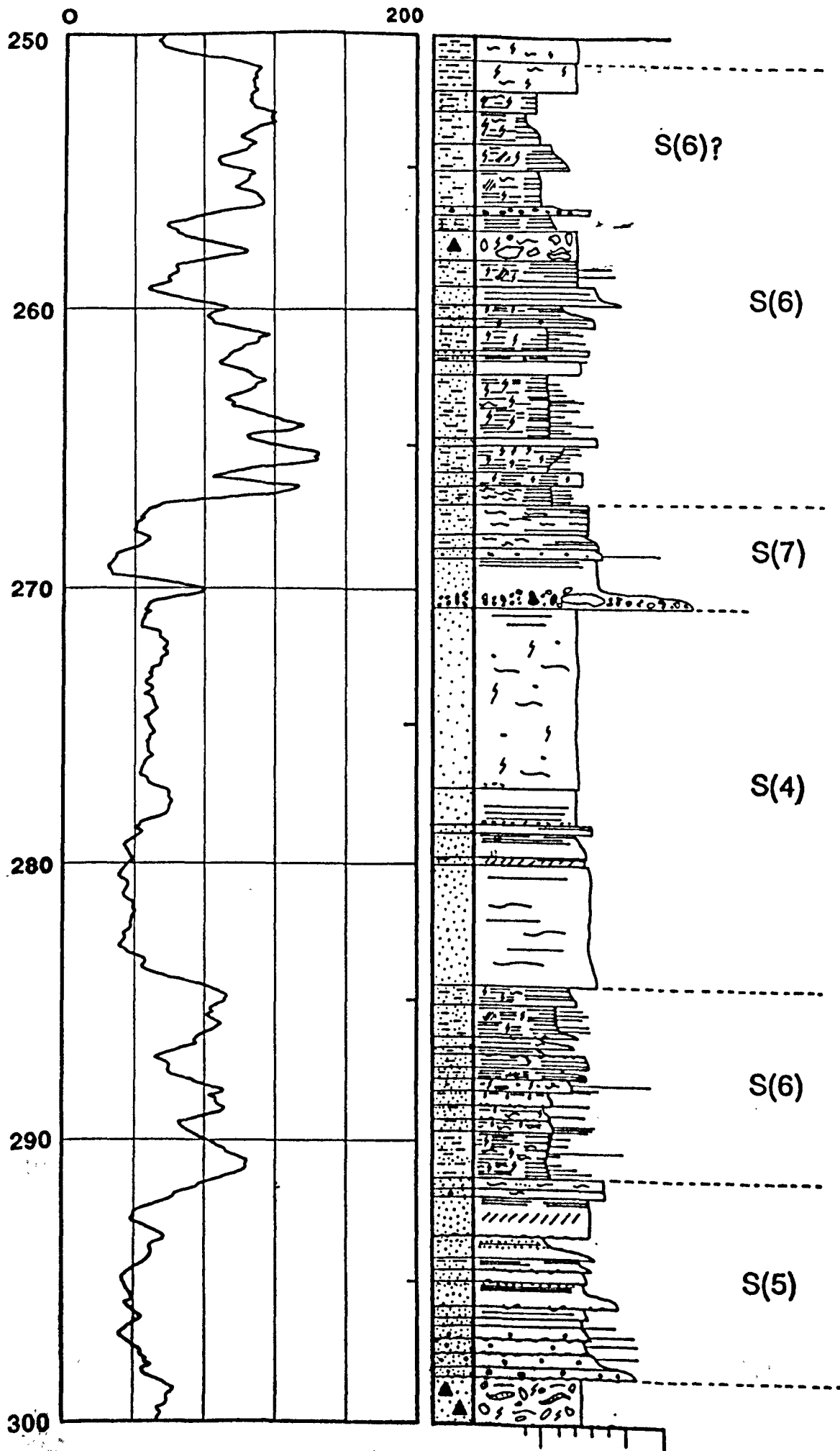
GAMMA RAY



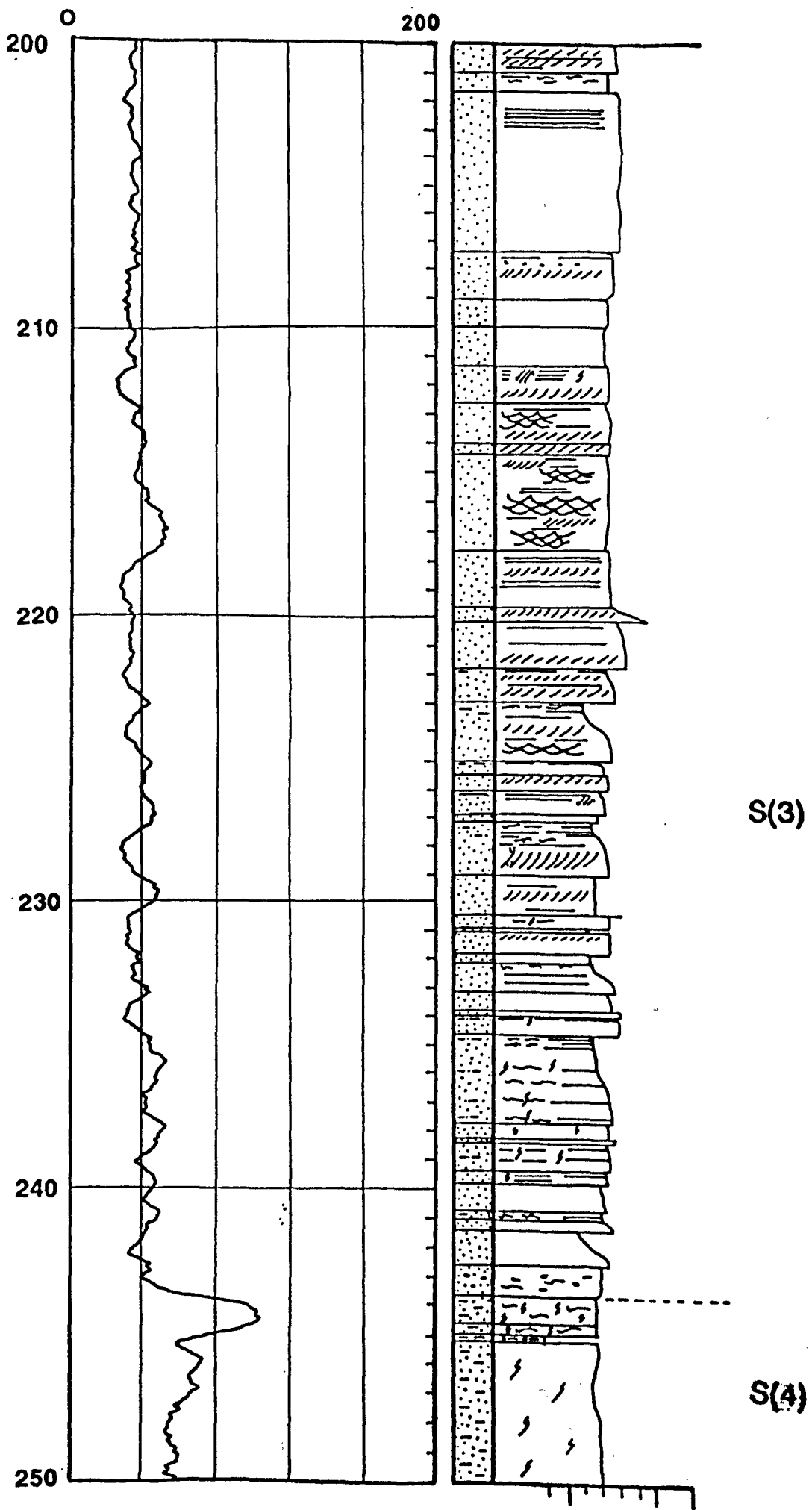
S(2)

GAMMA RAY

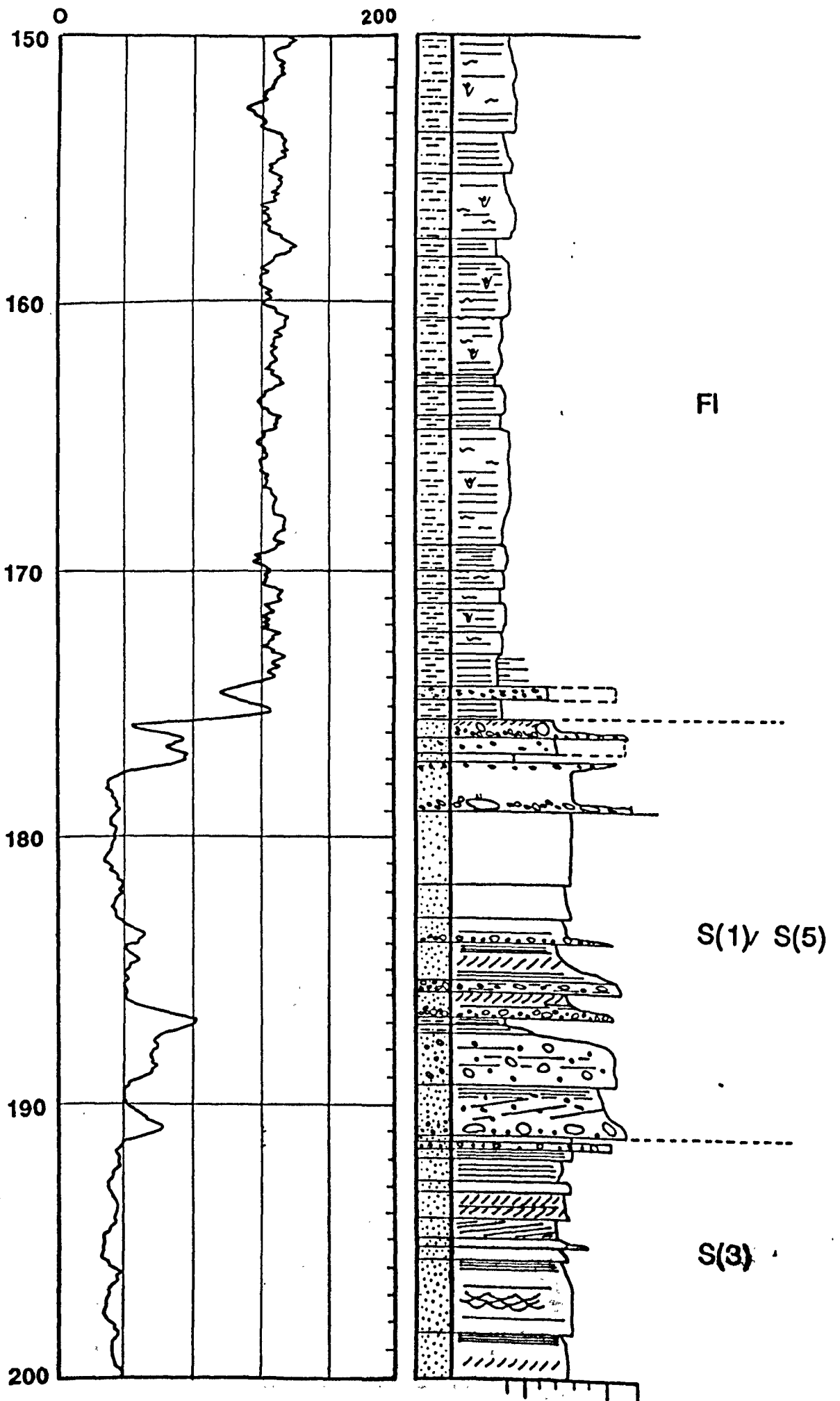




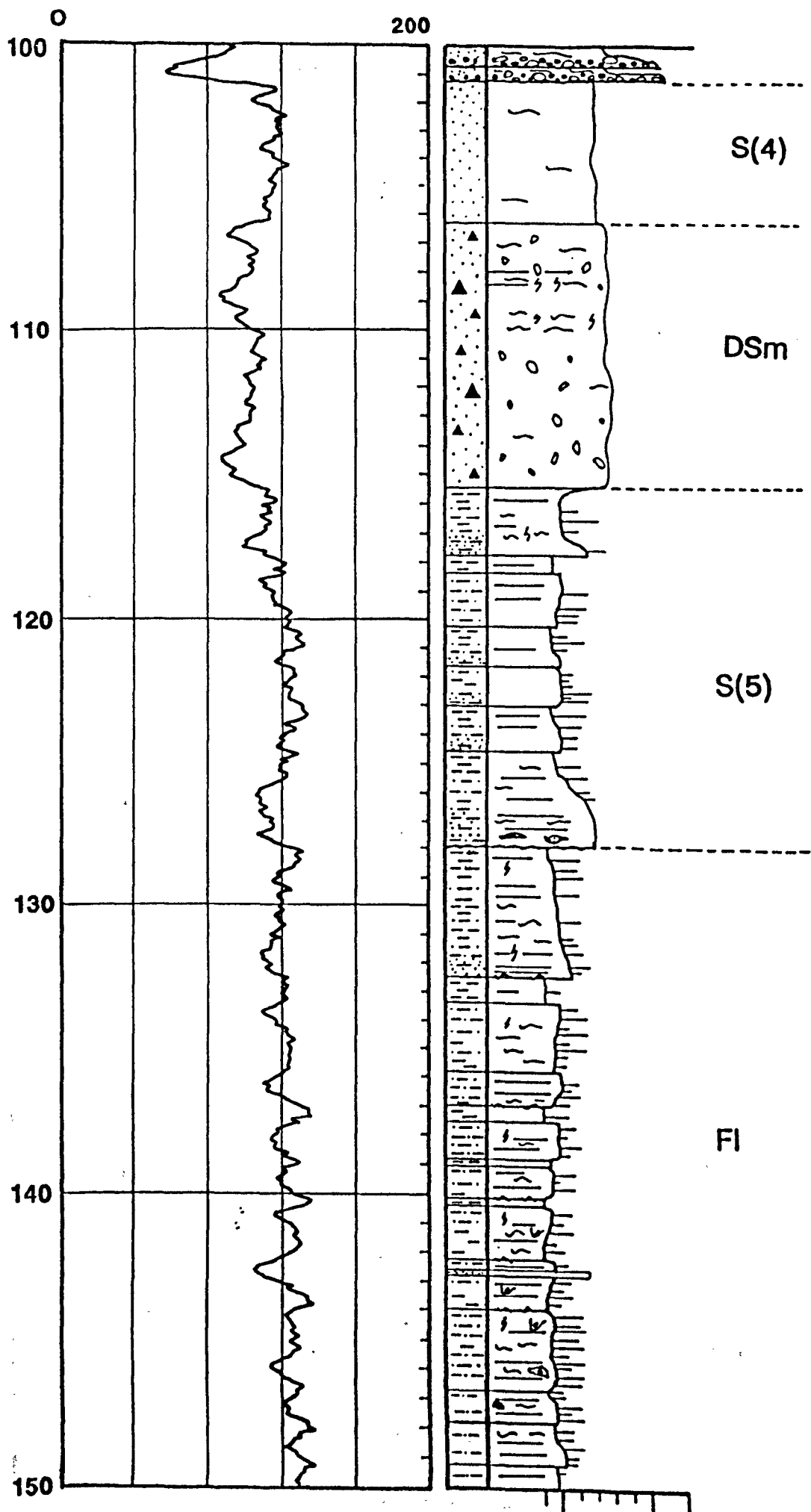
GAMMA RAY



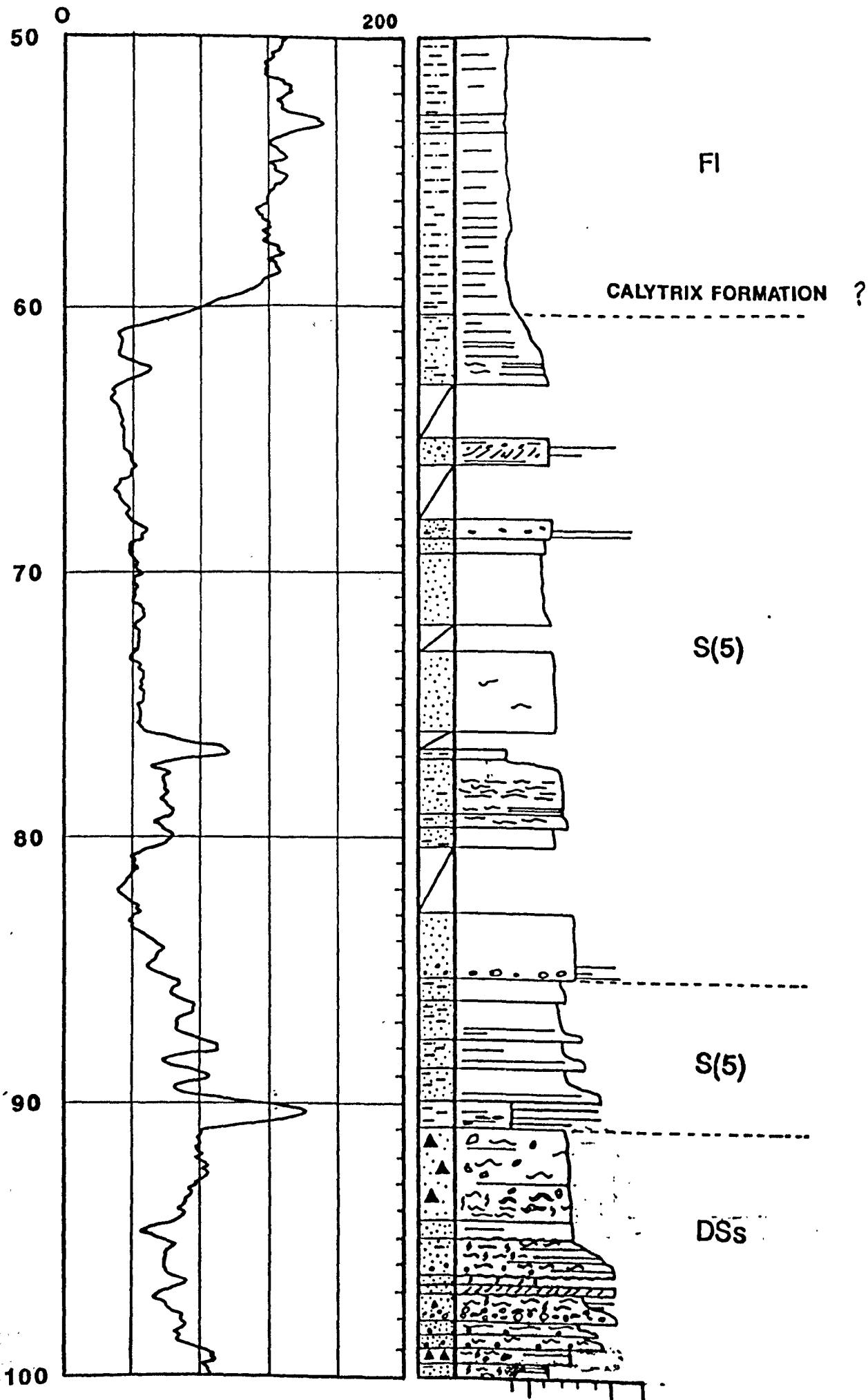
GAMMA RAY



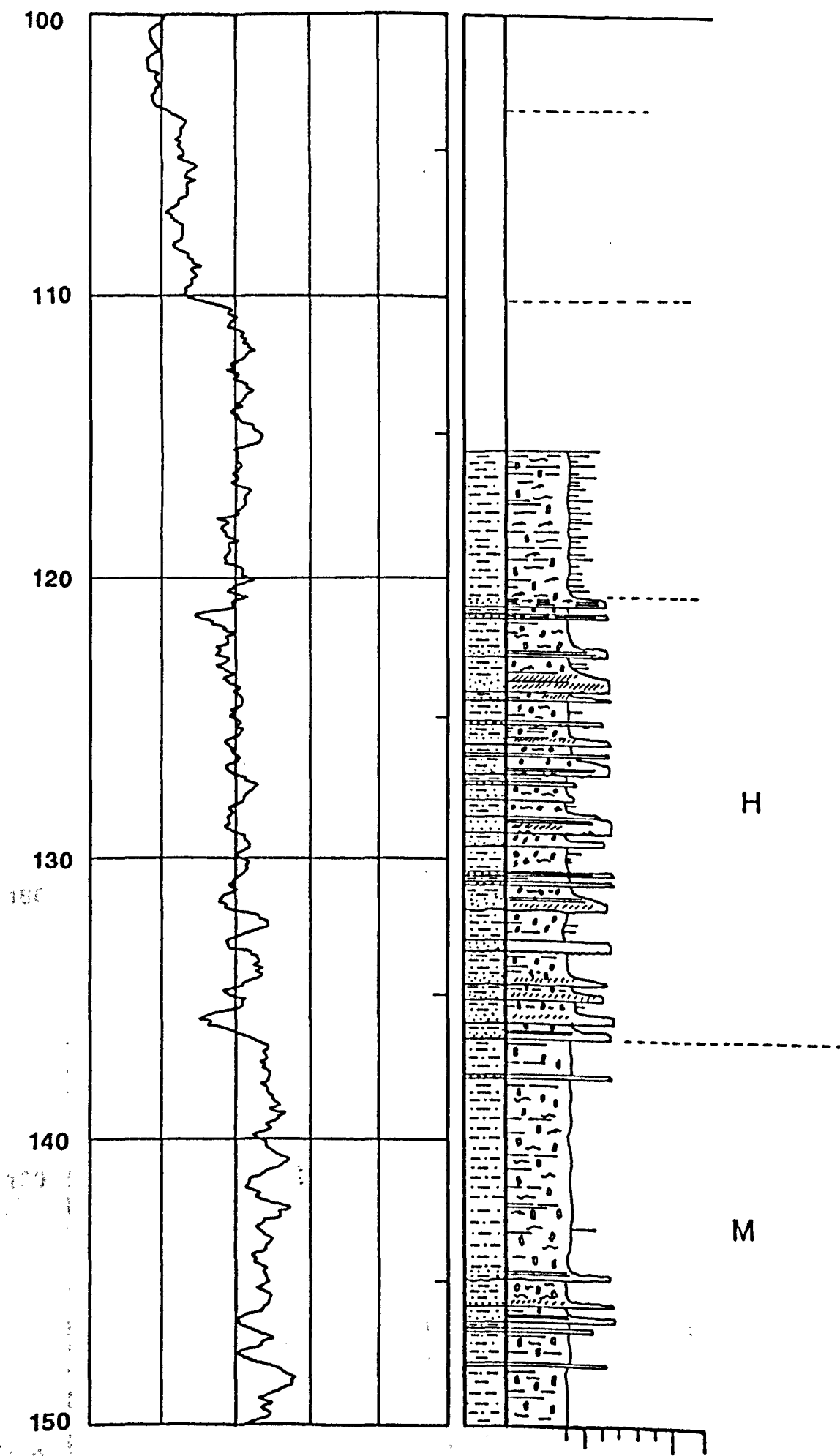
GAMMA RAY

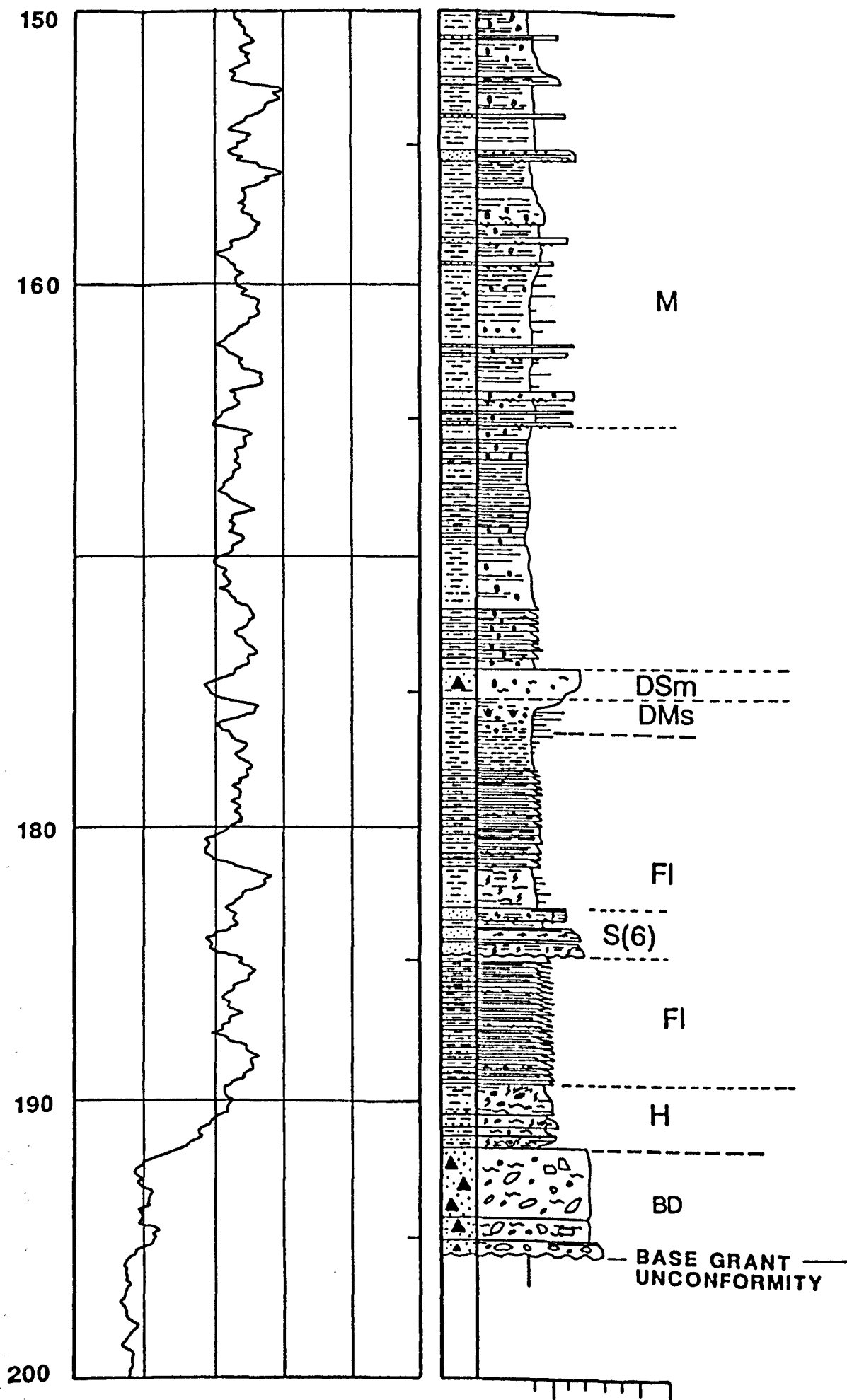


GAMMA RAY

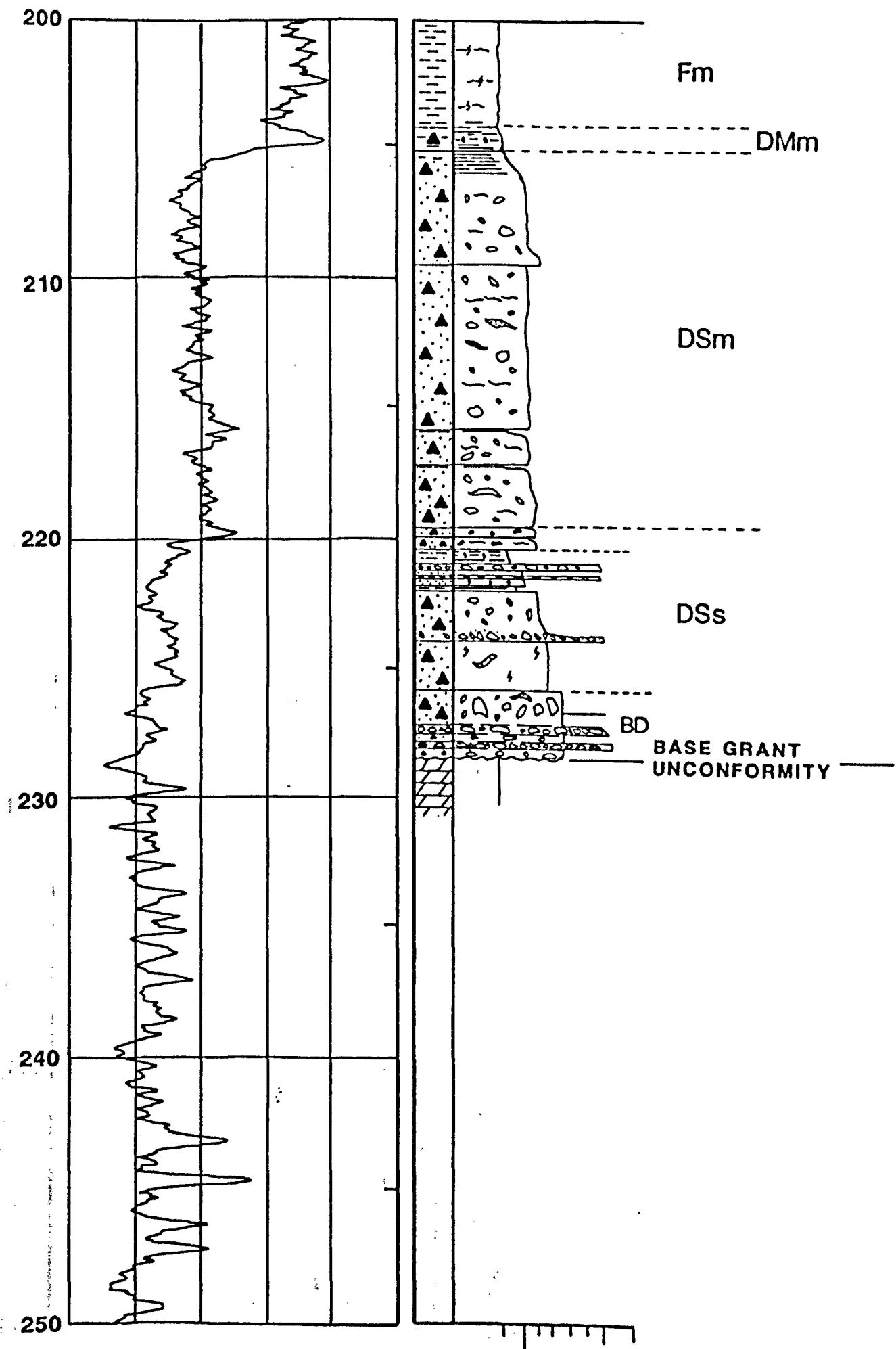


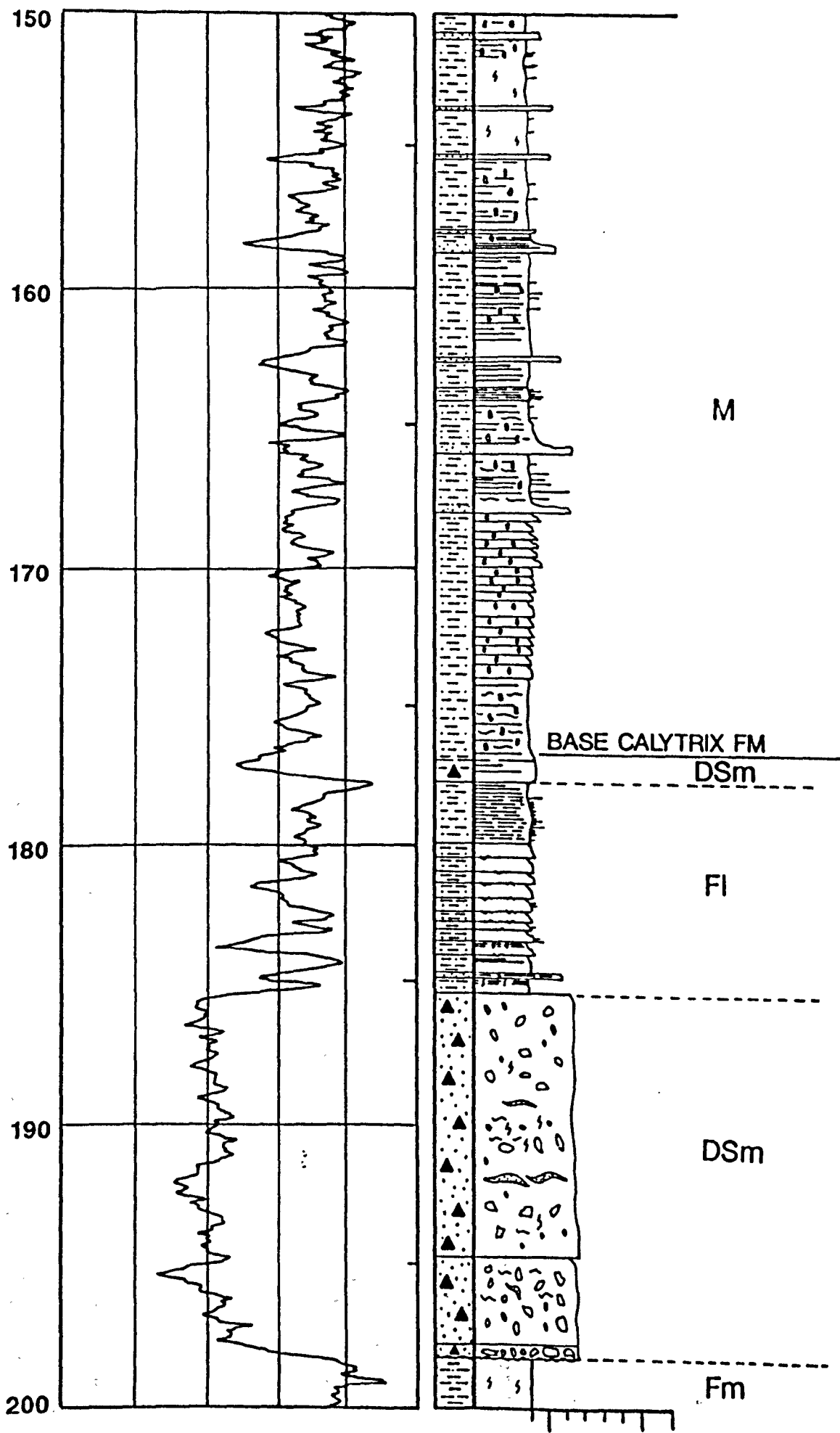
EREMOPHILA 1





EREMOPHILA 2





100

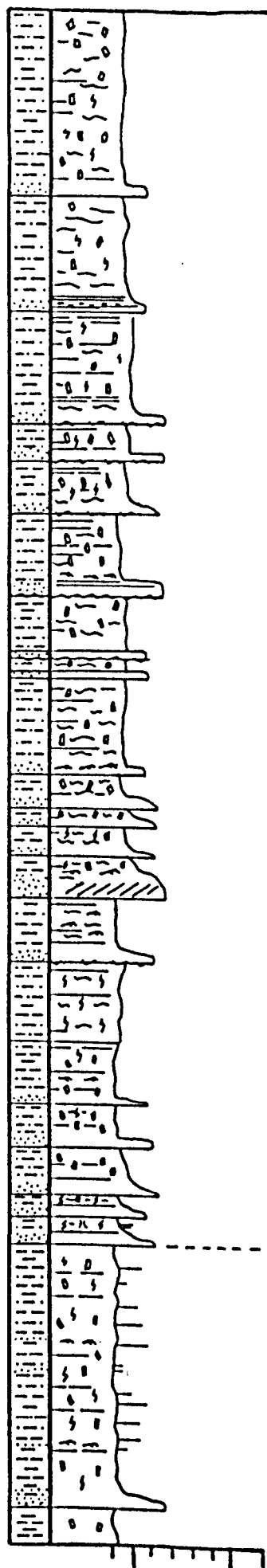
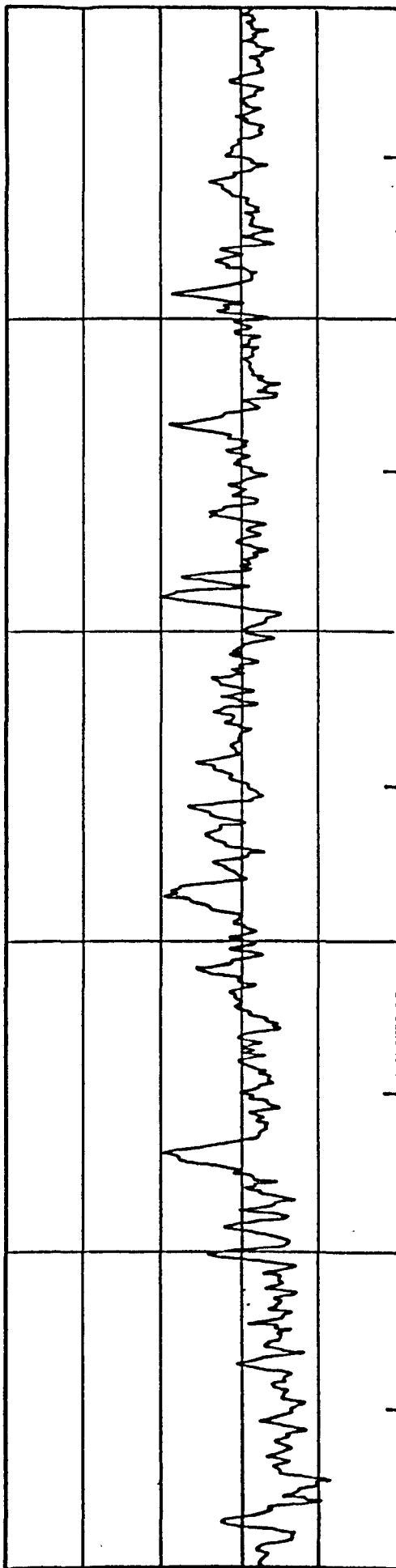
110

120

130

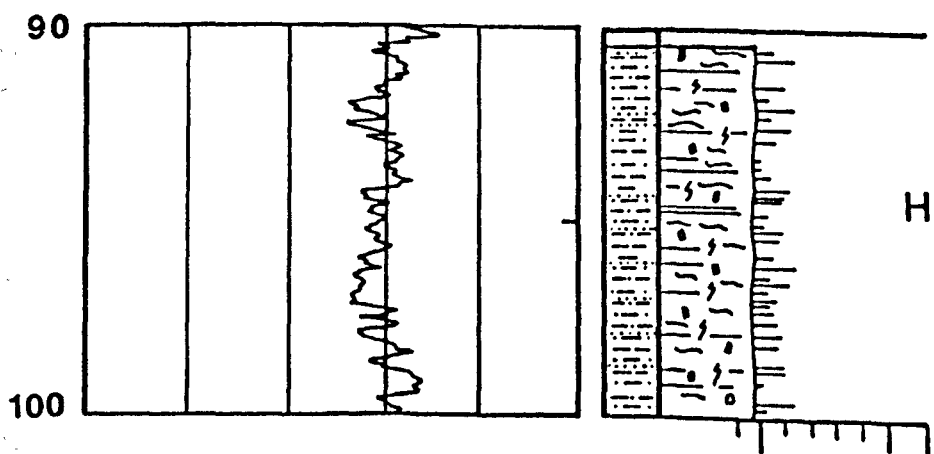
140

150



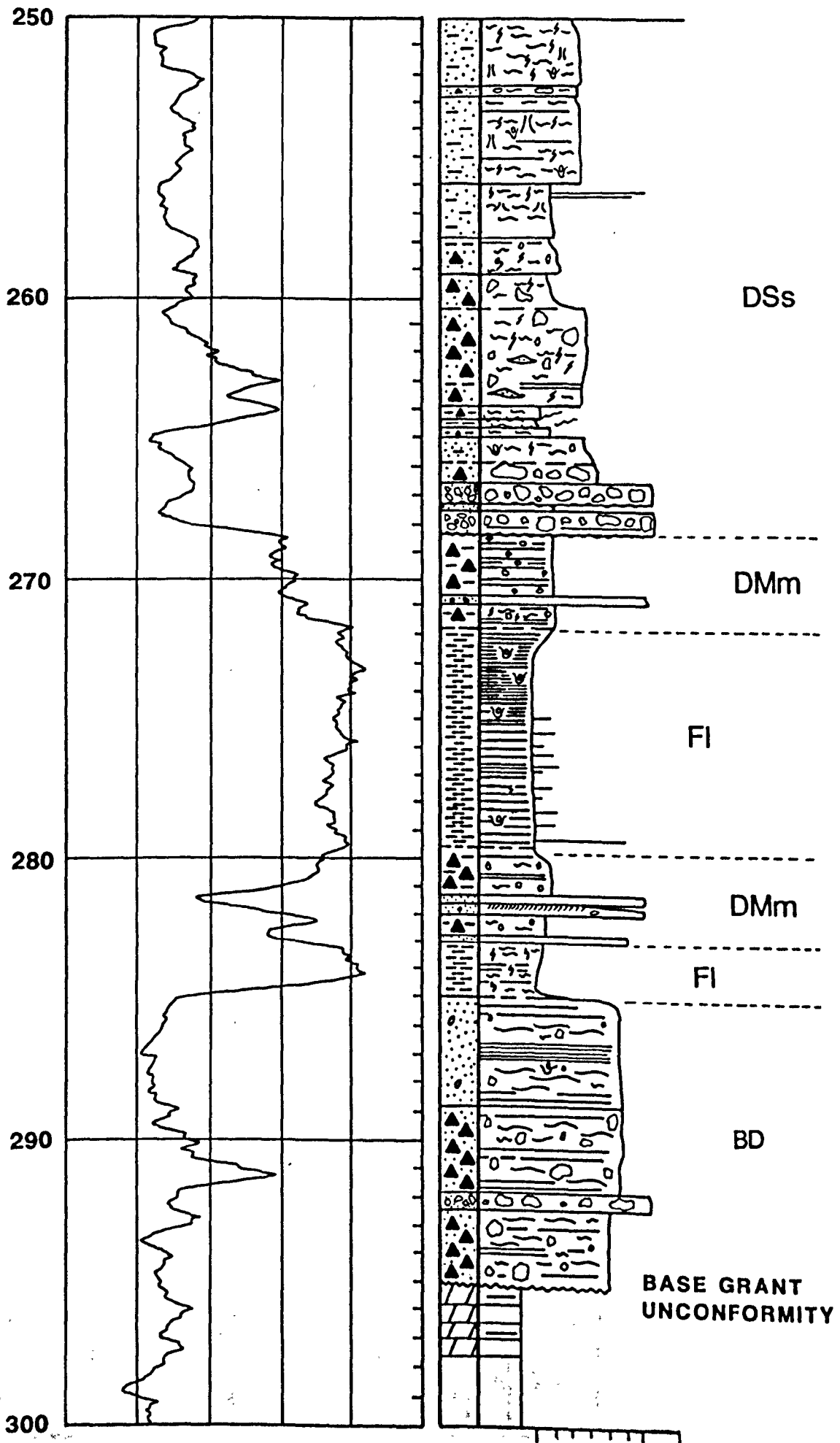
H

M

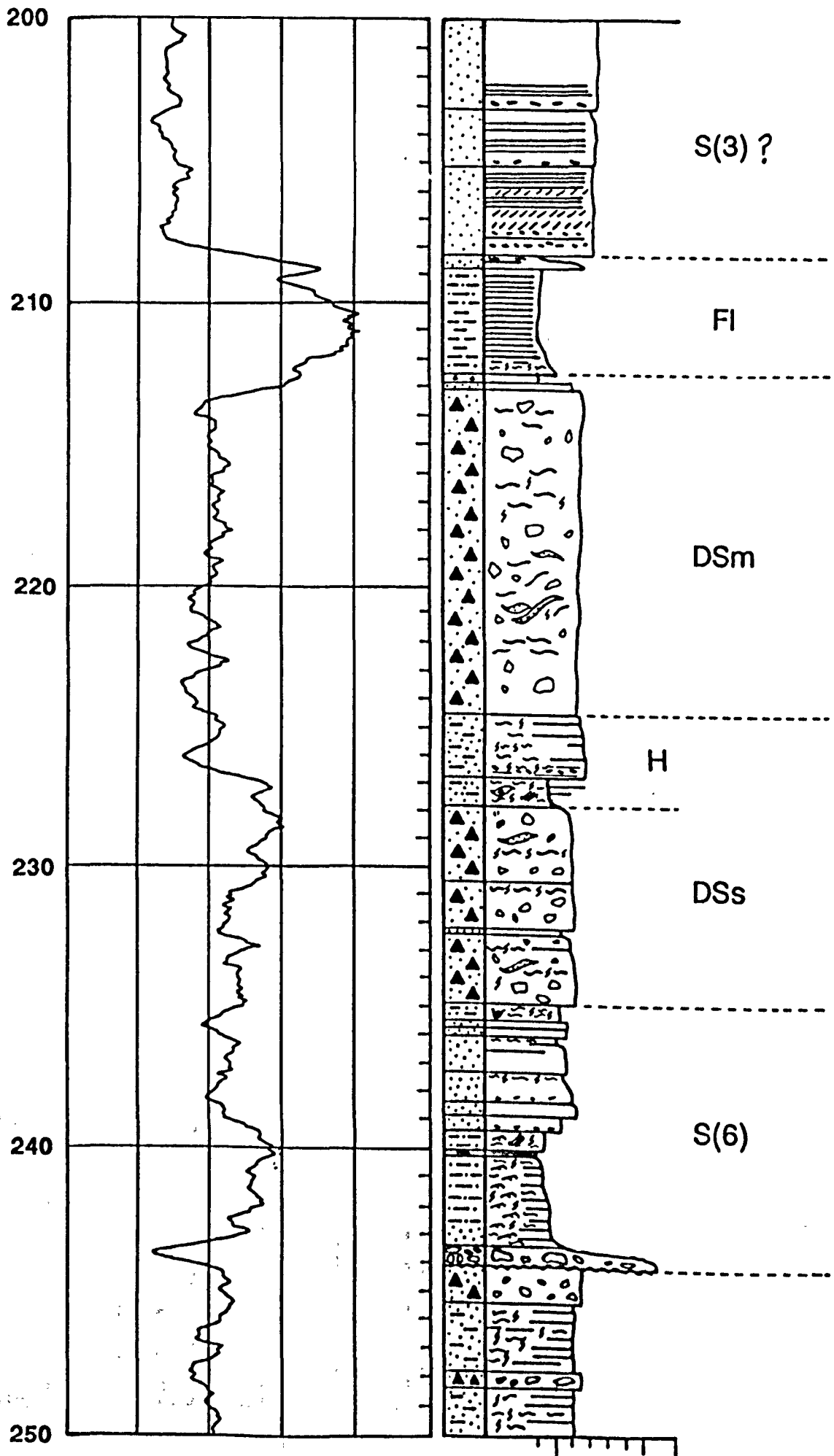


EREMOPHILA 3

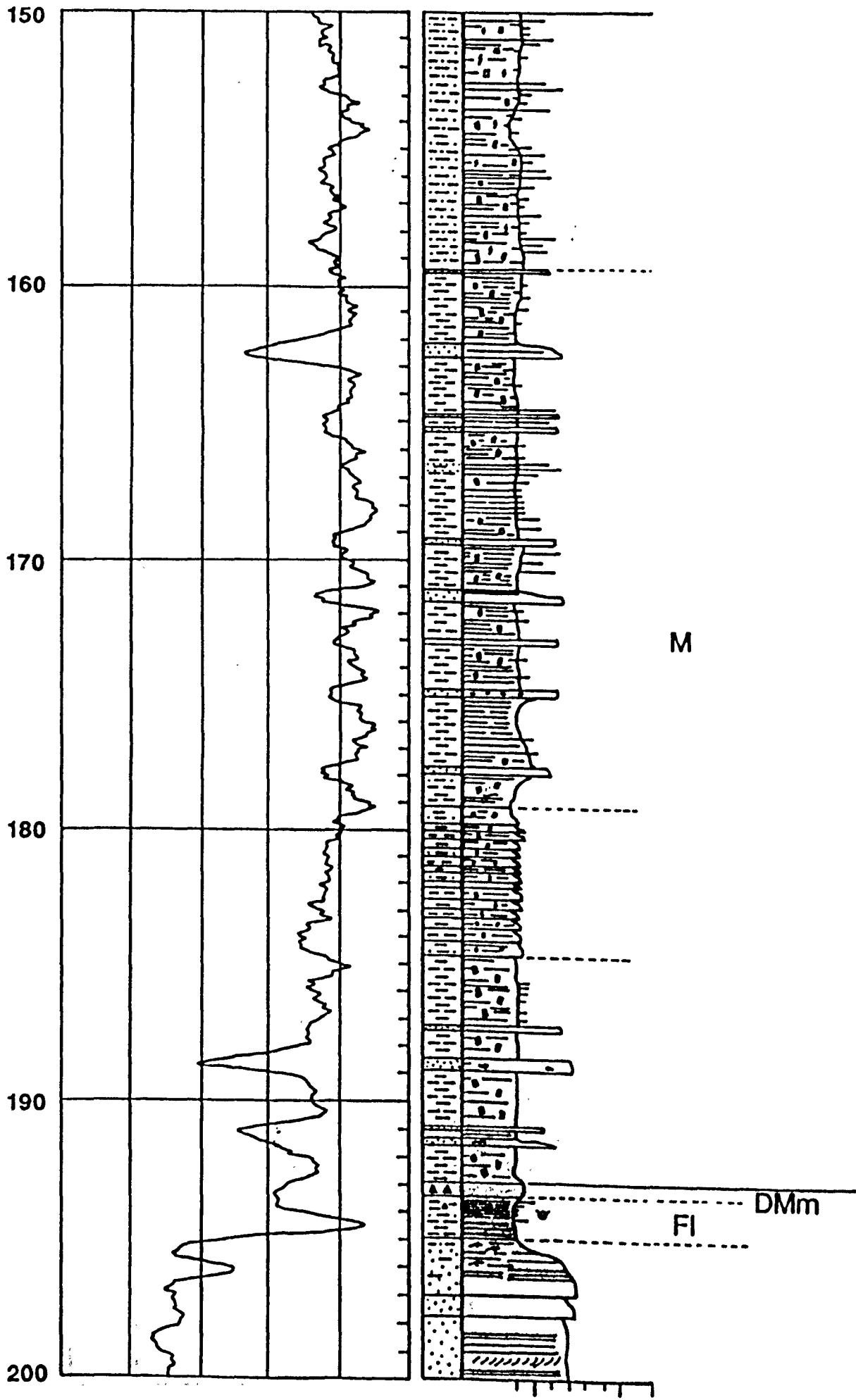
GAMMA RAY



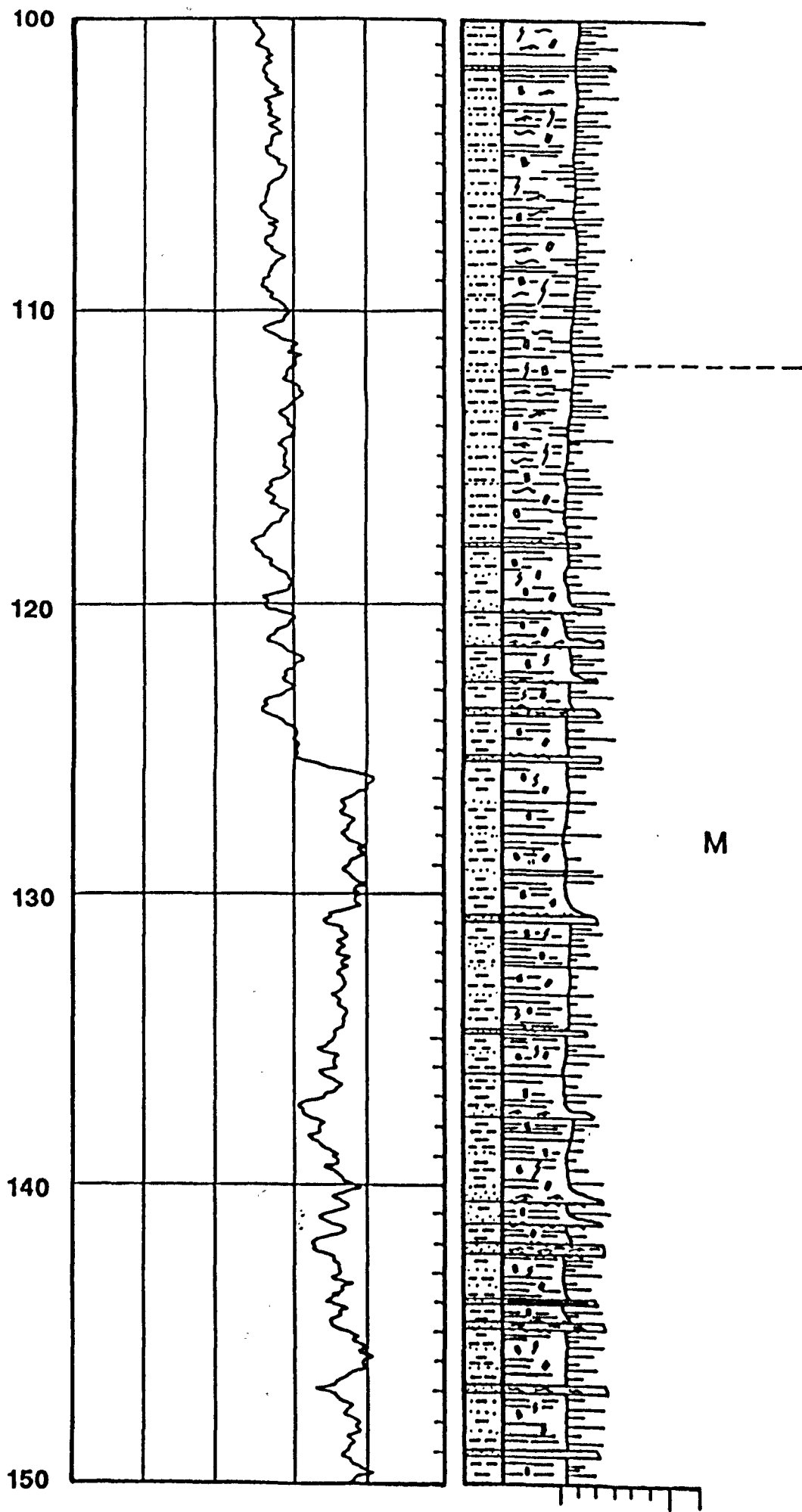
GAMMA RAY



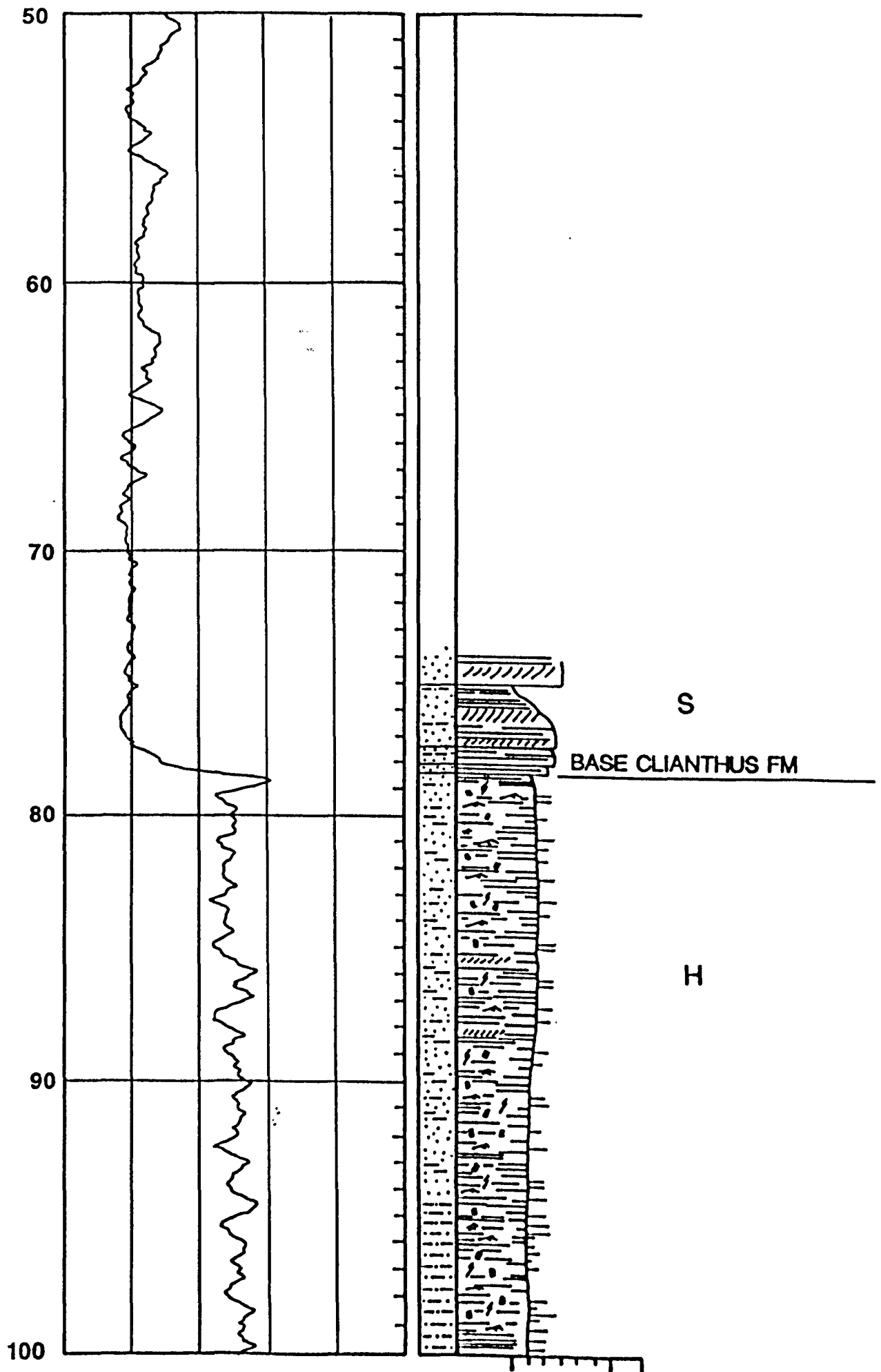
GAMMA RAY



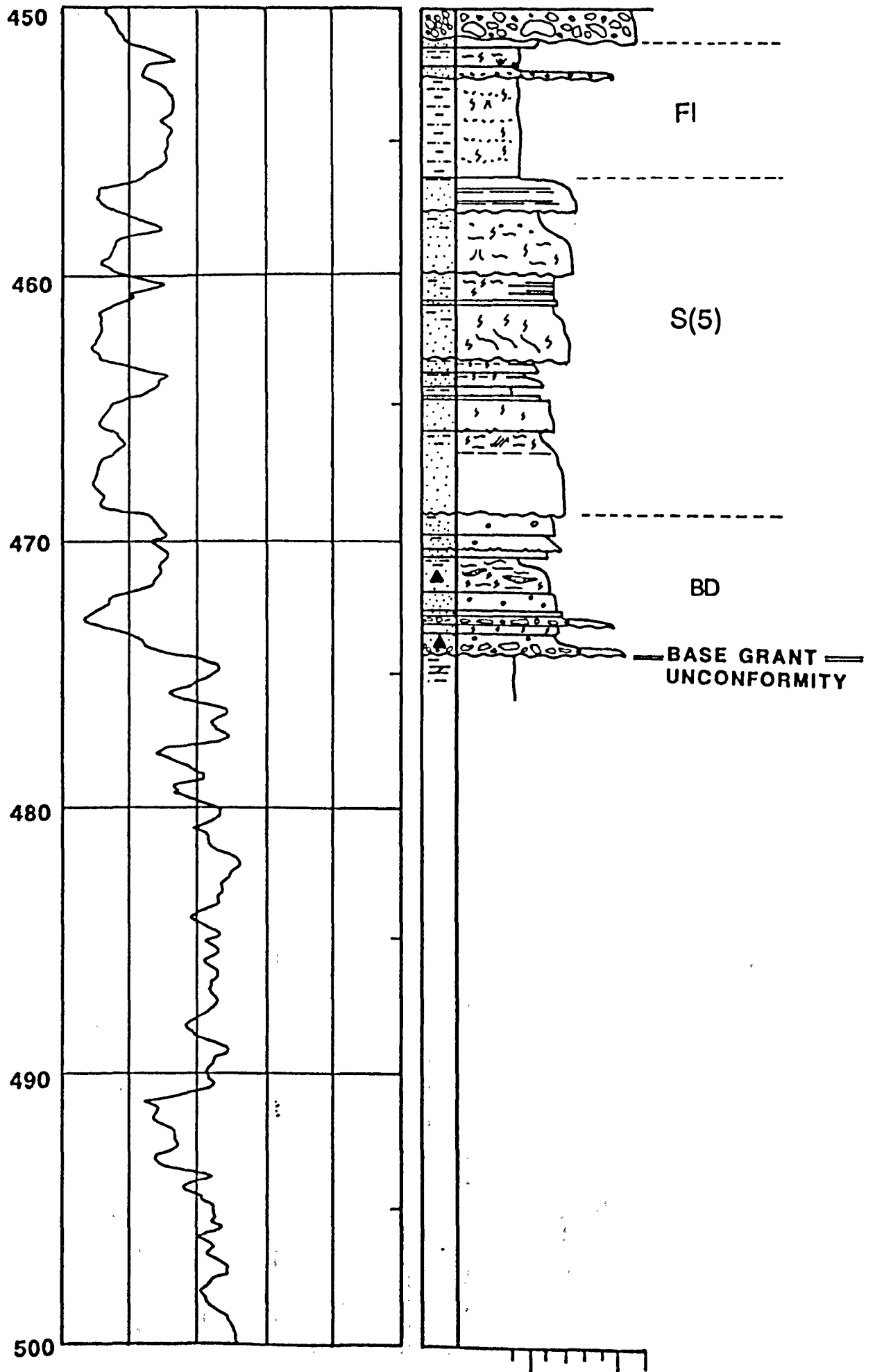
GAMMA RAY

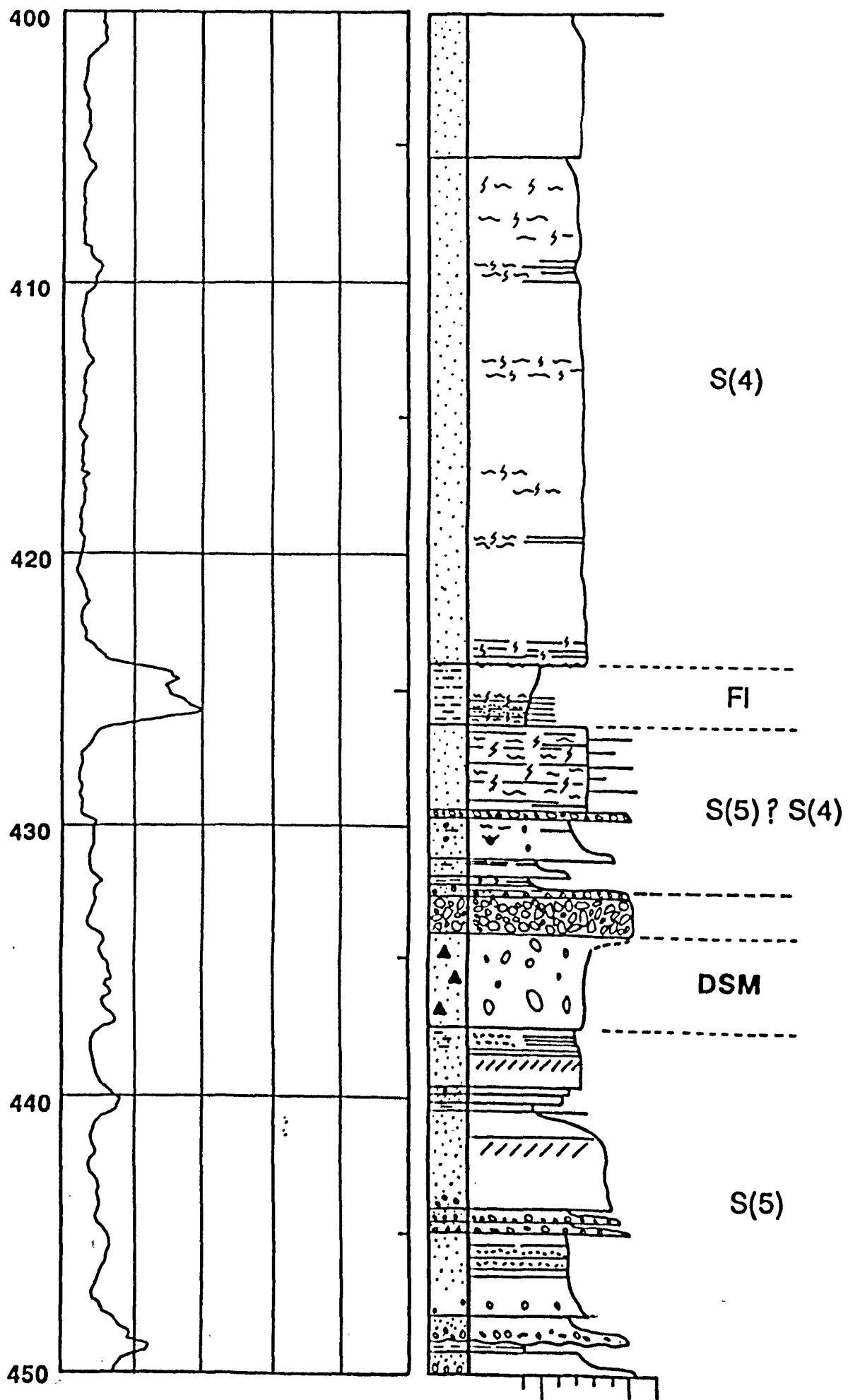


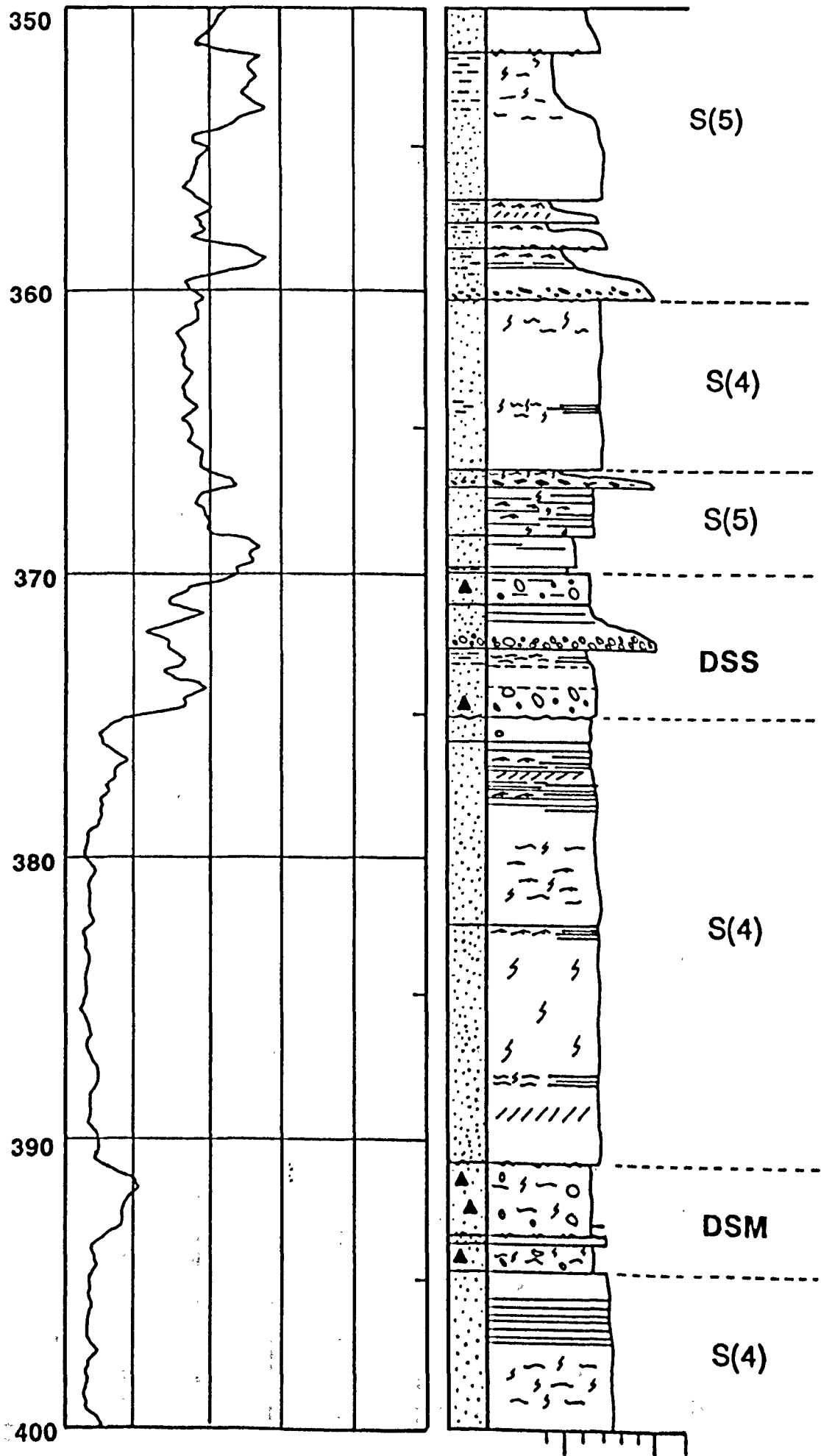
GAMMA RAY

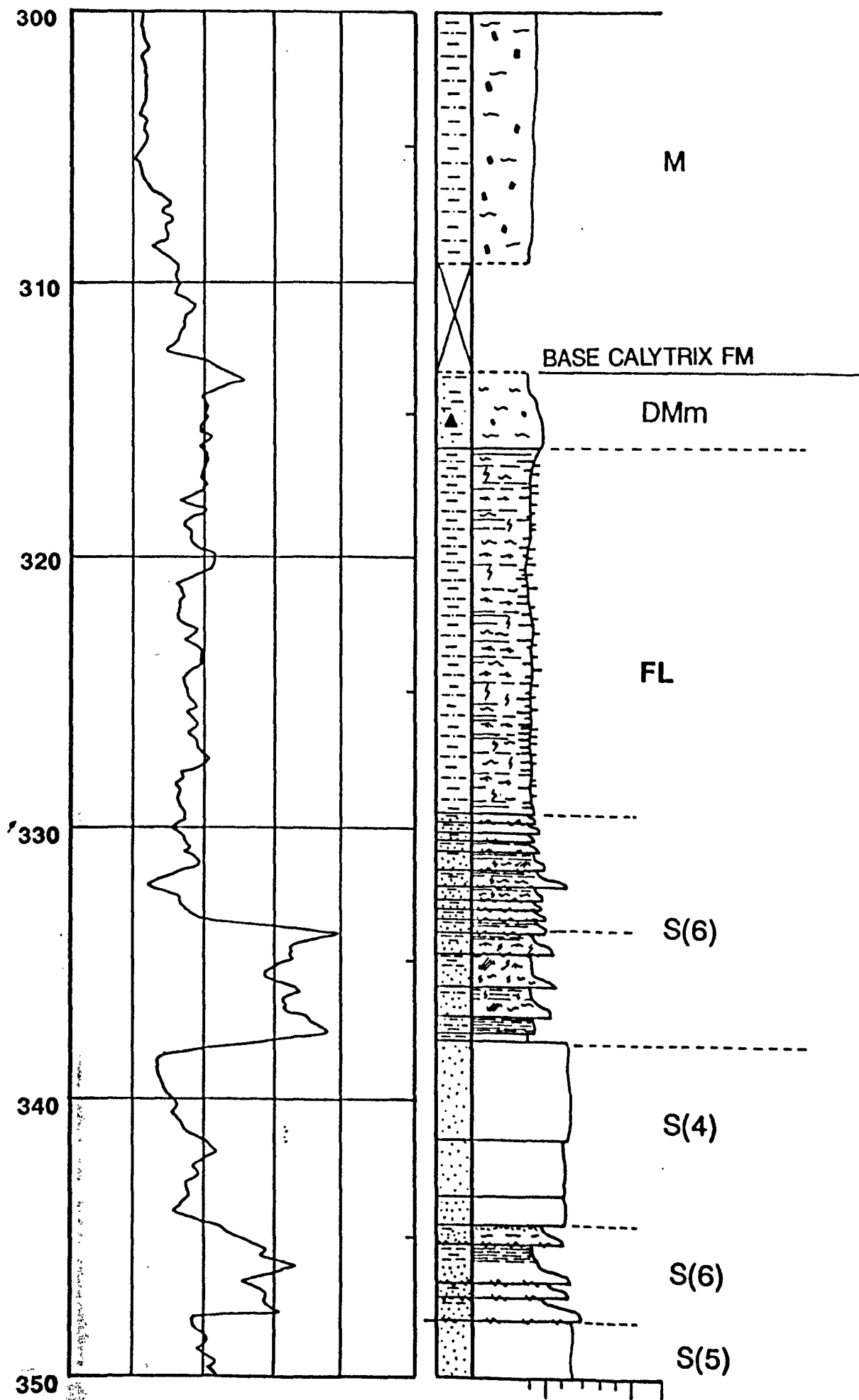


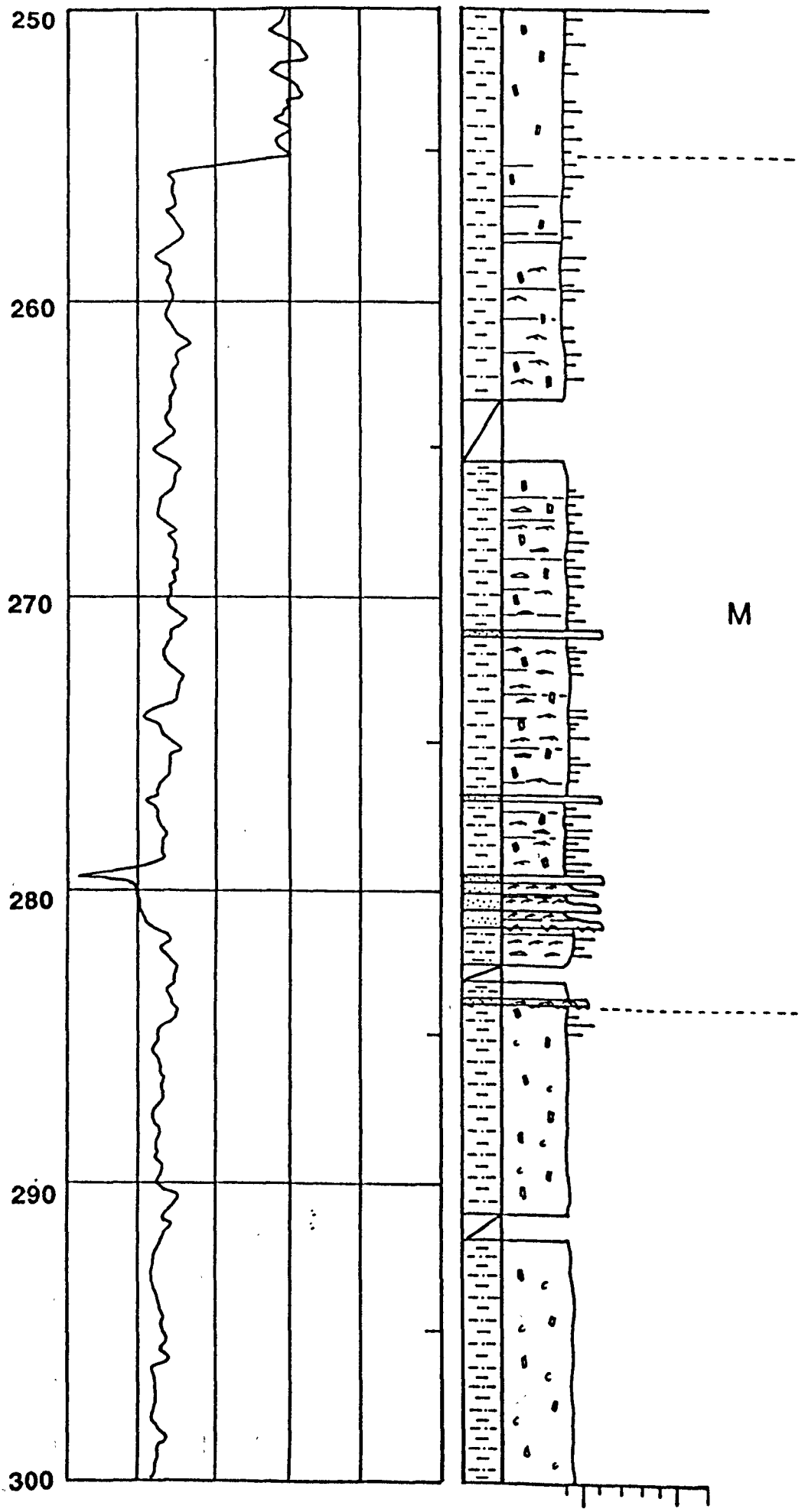
FICUS 1

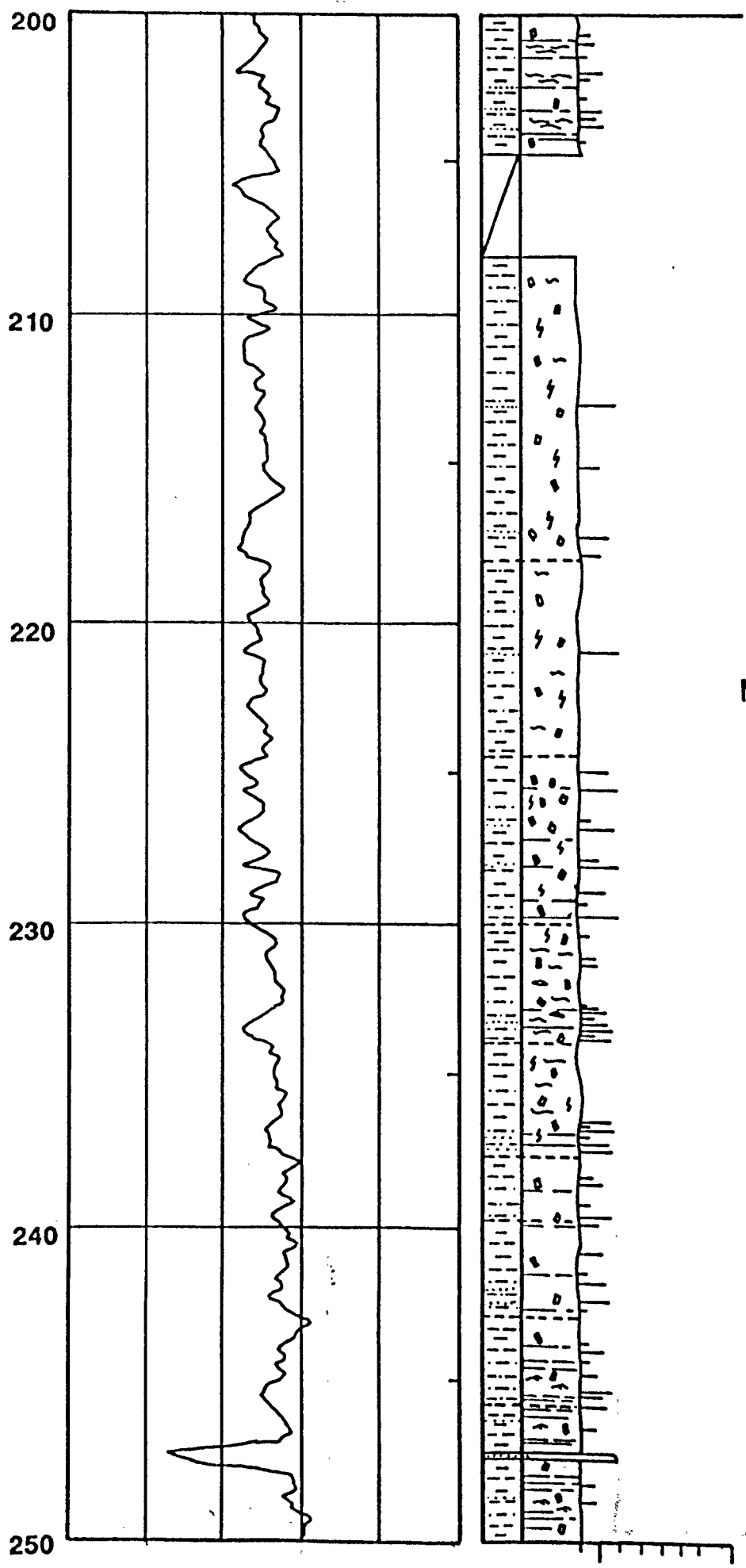




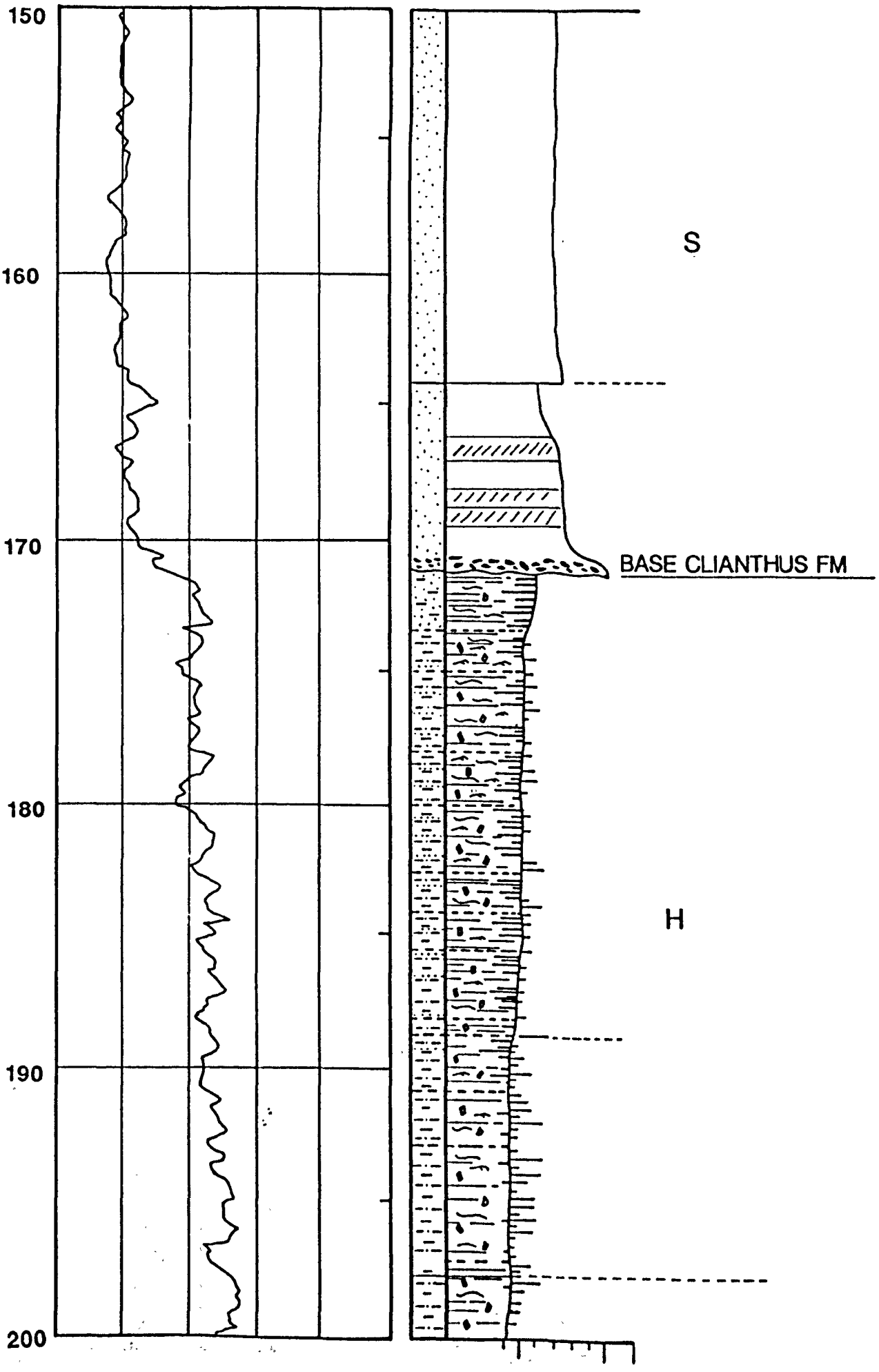


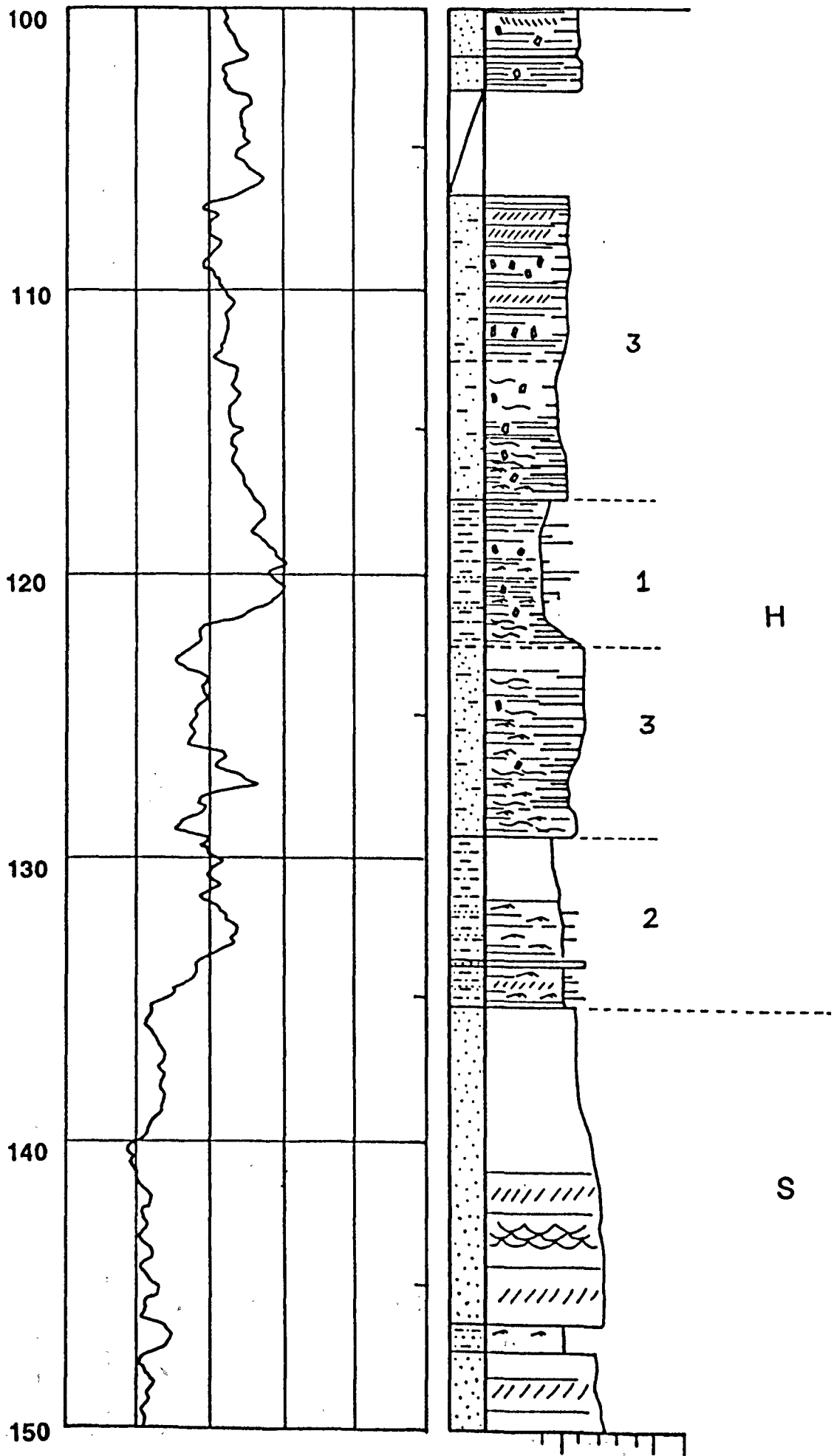




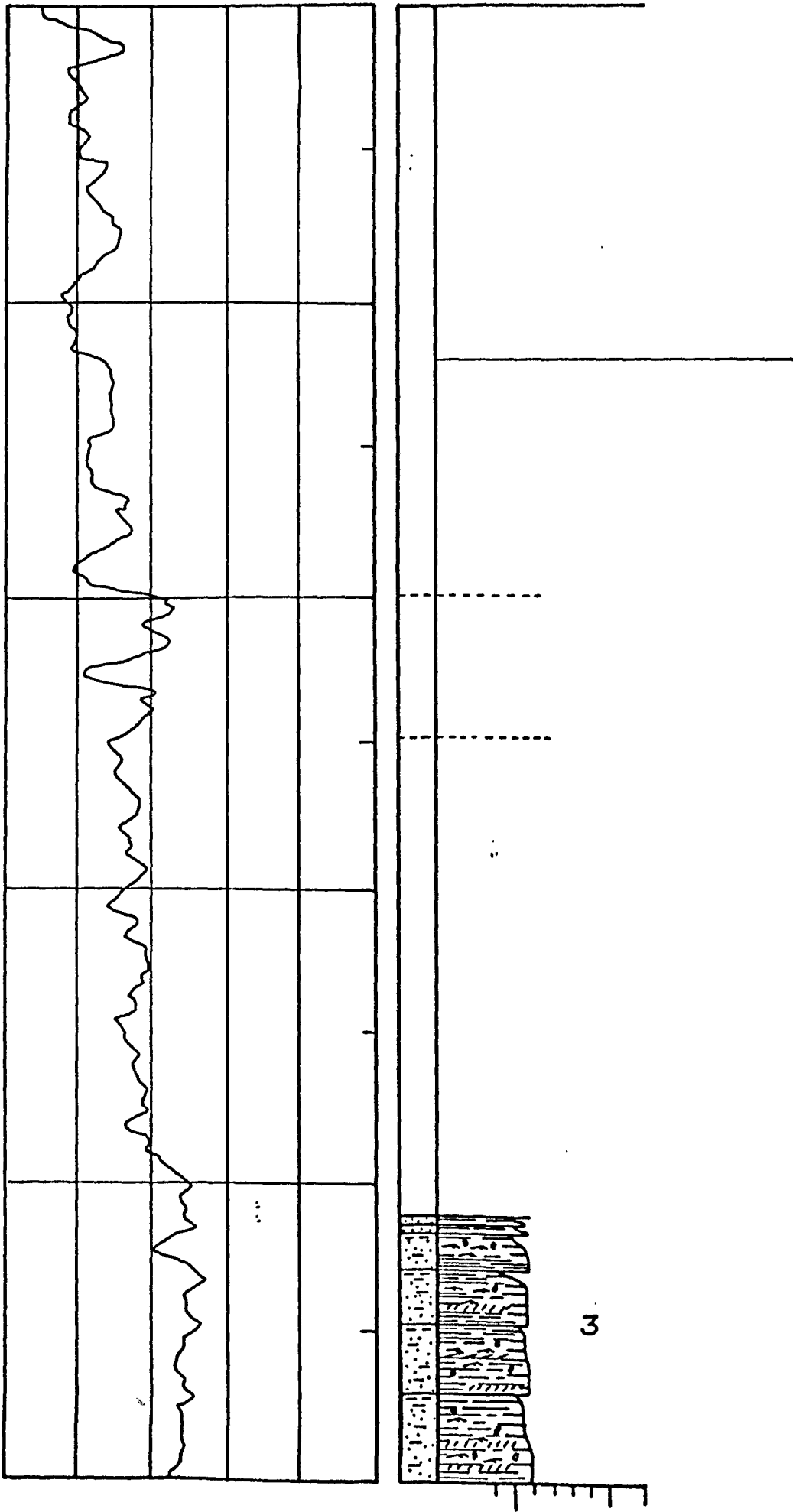


M



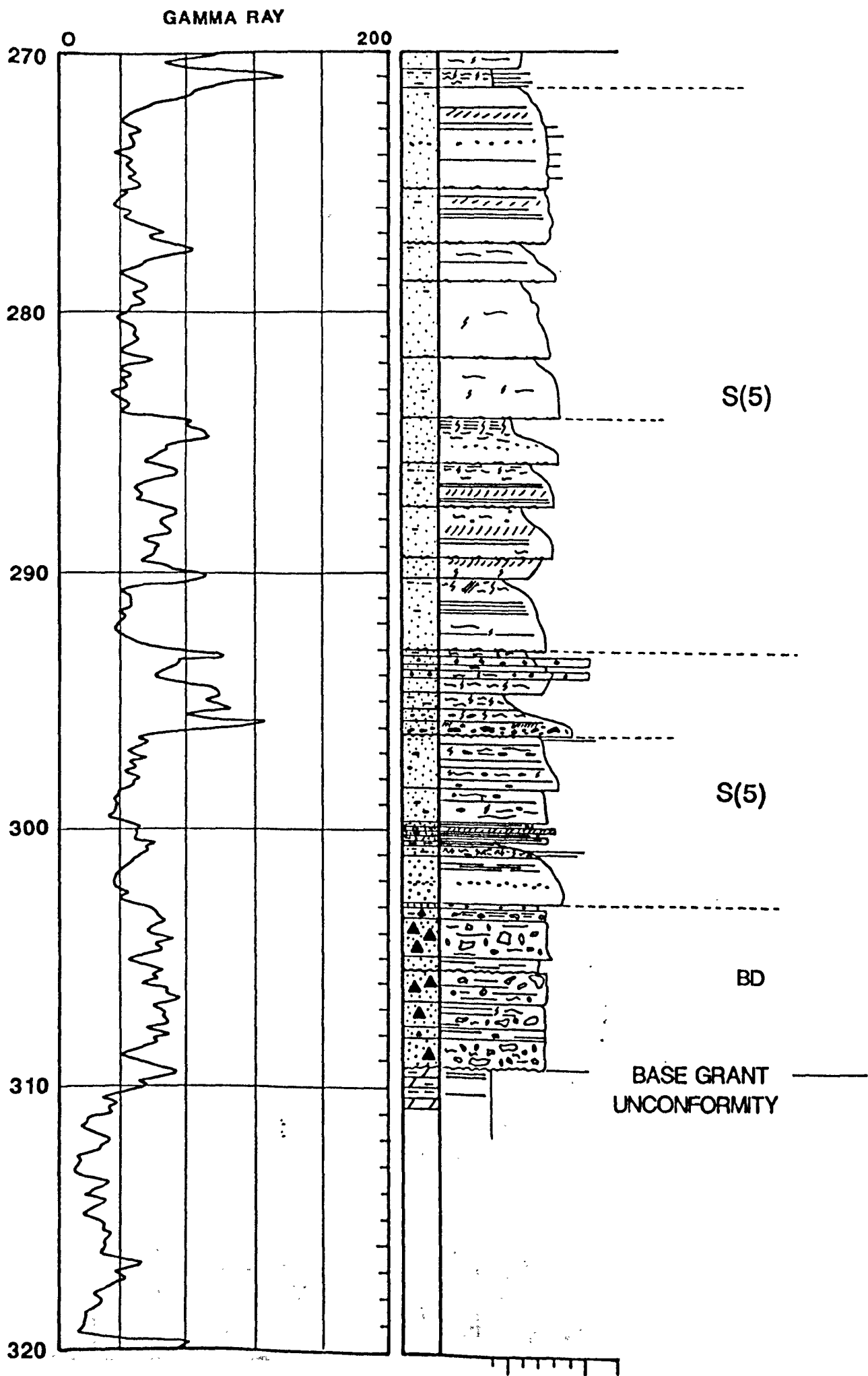


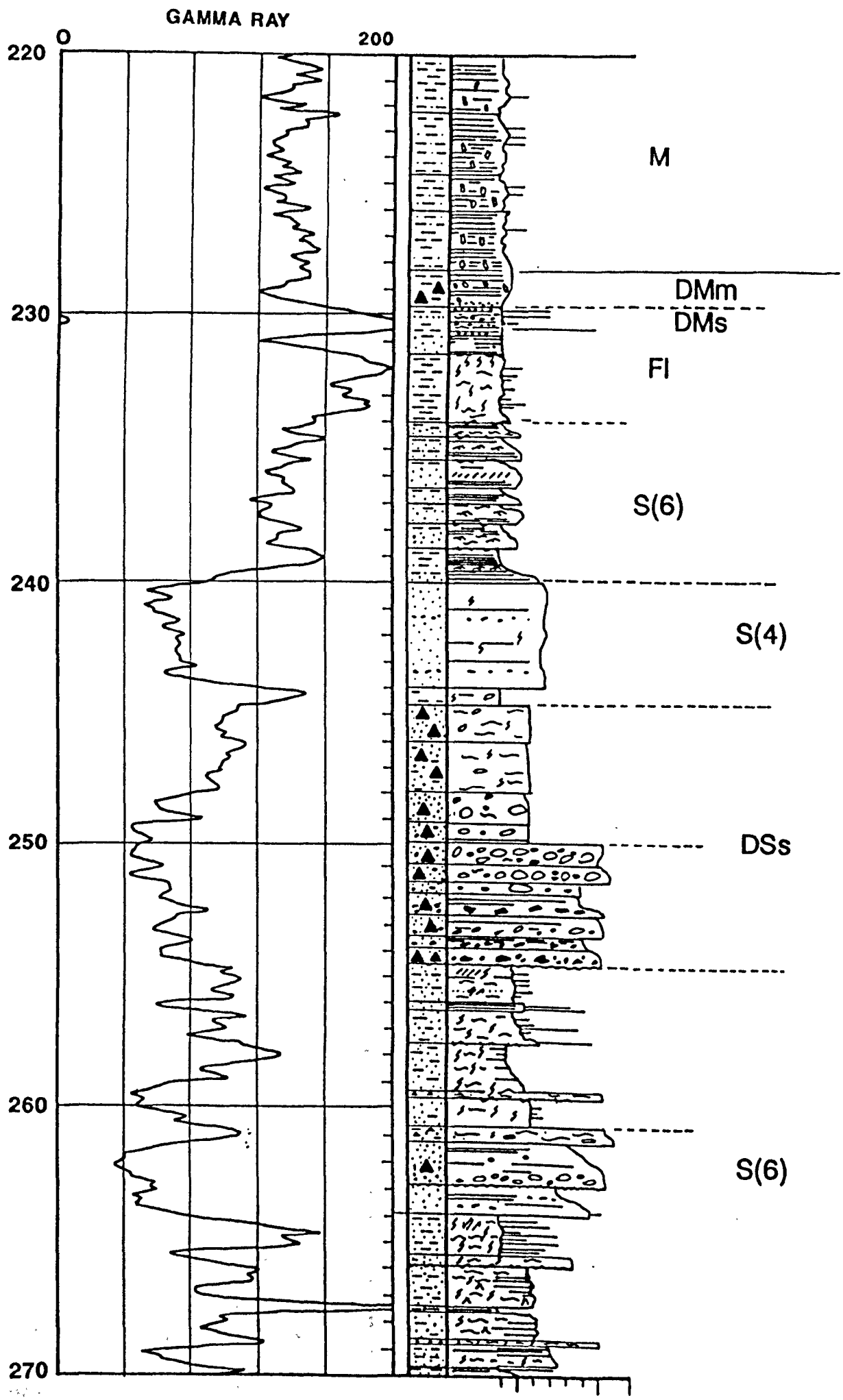
100



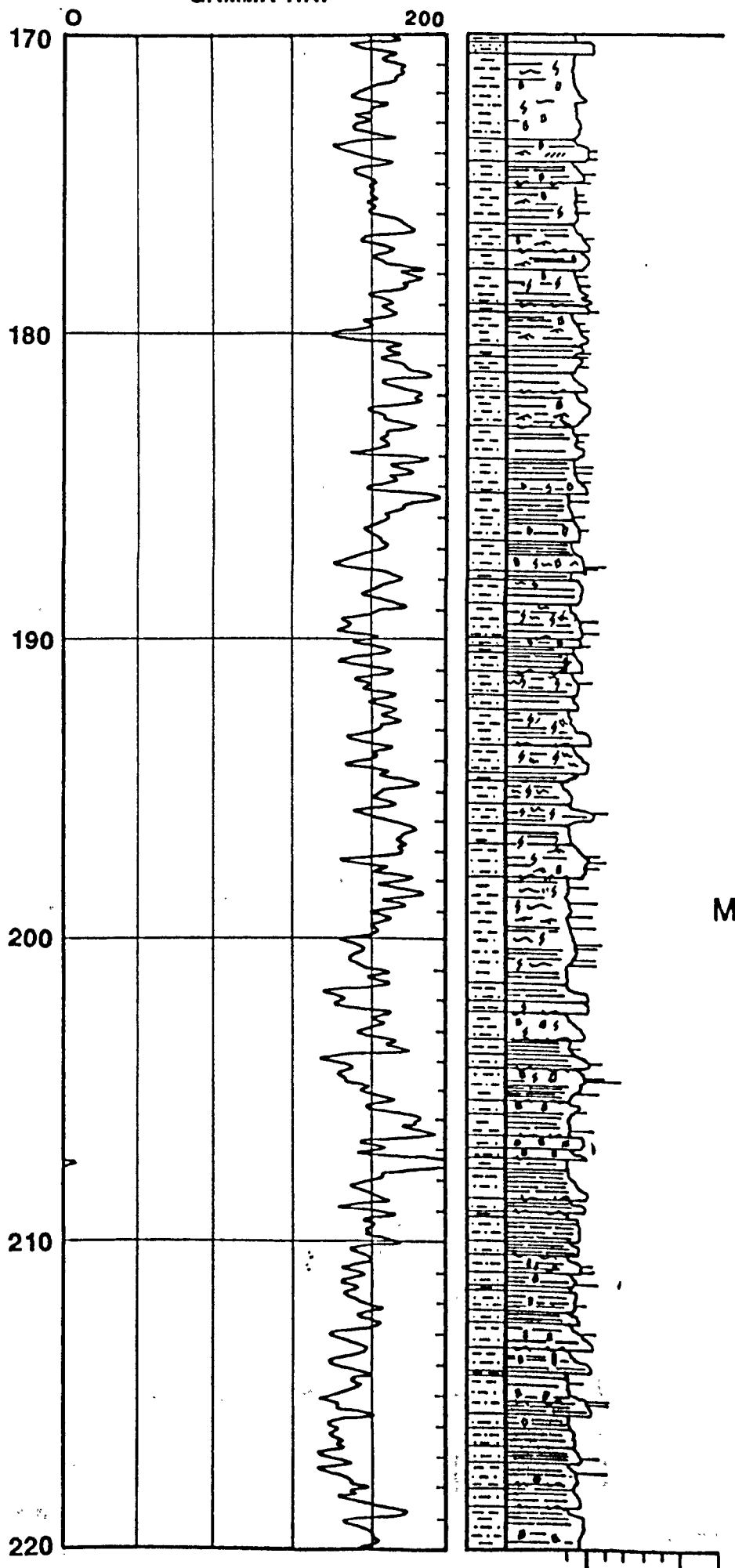
3

HALGANIA 1

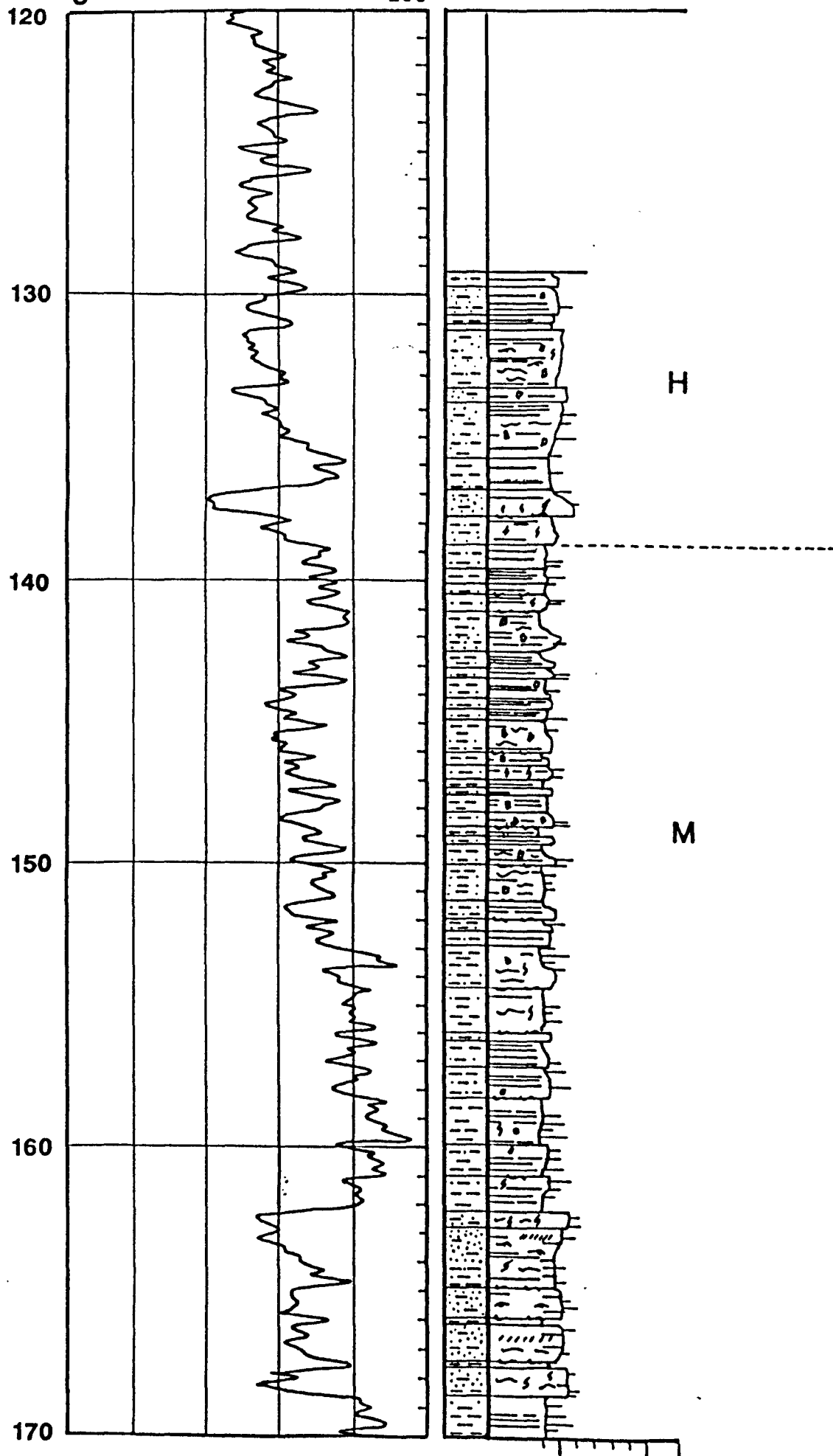




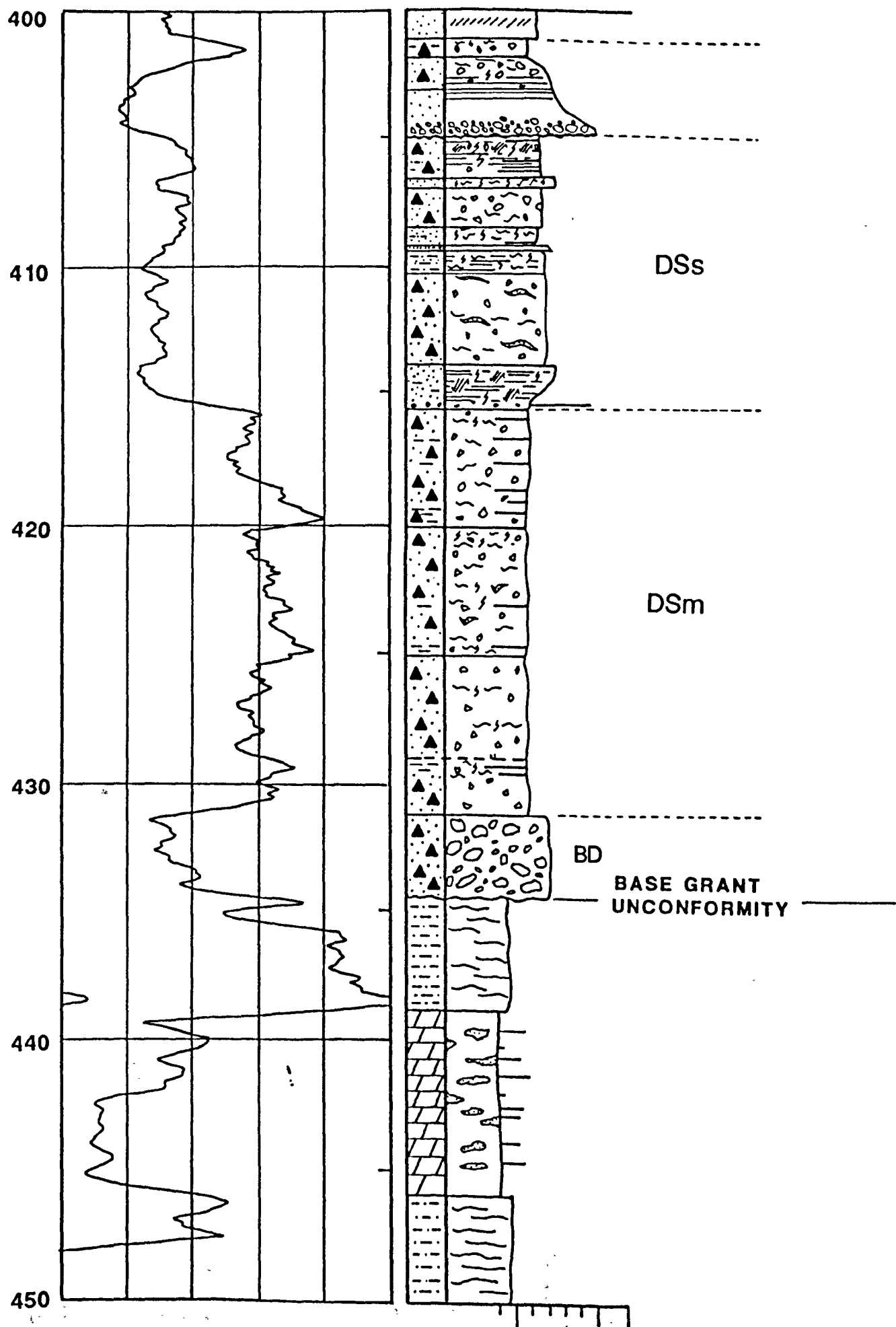
GAMMA RAY

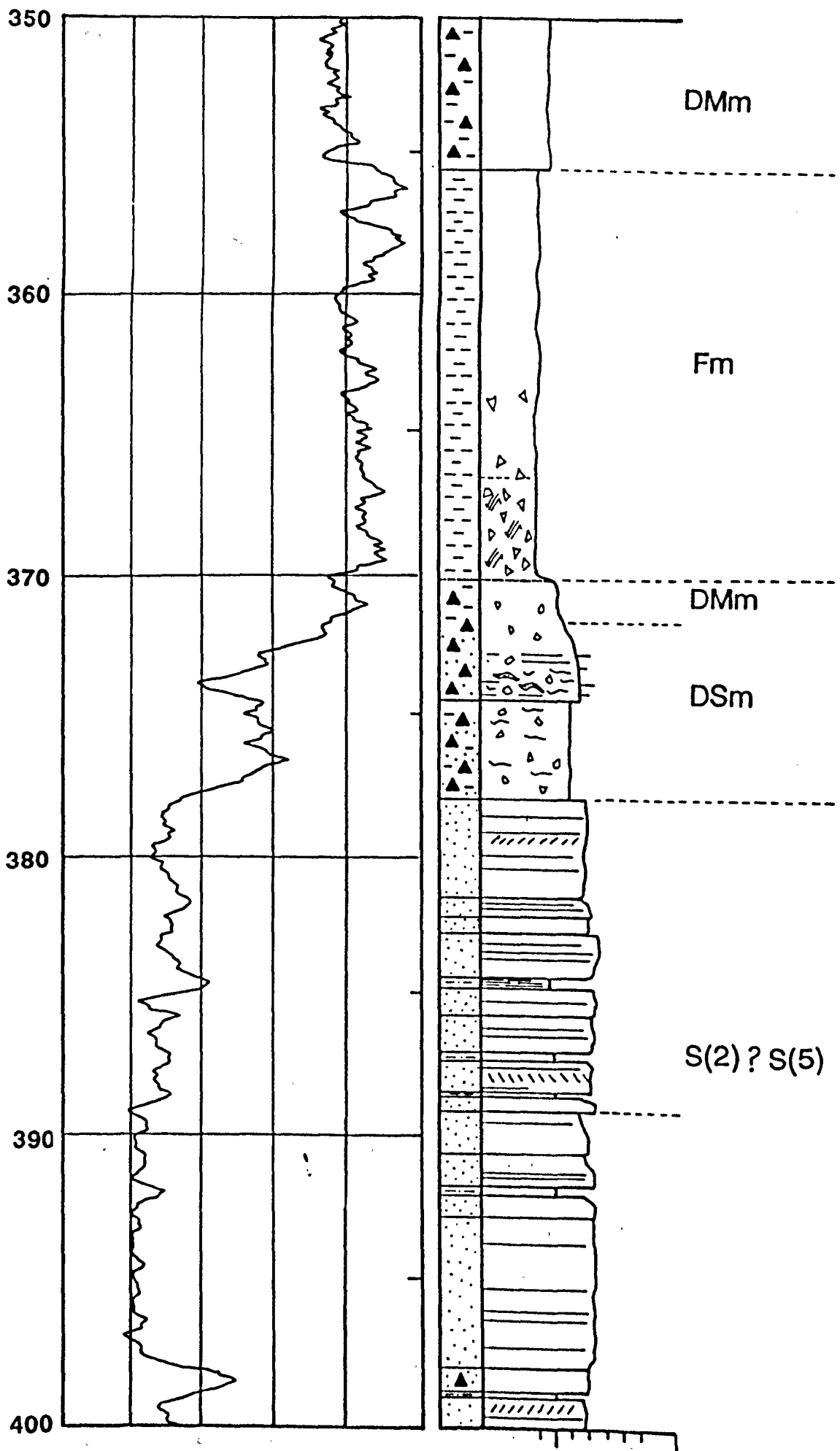


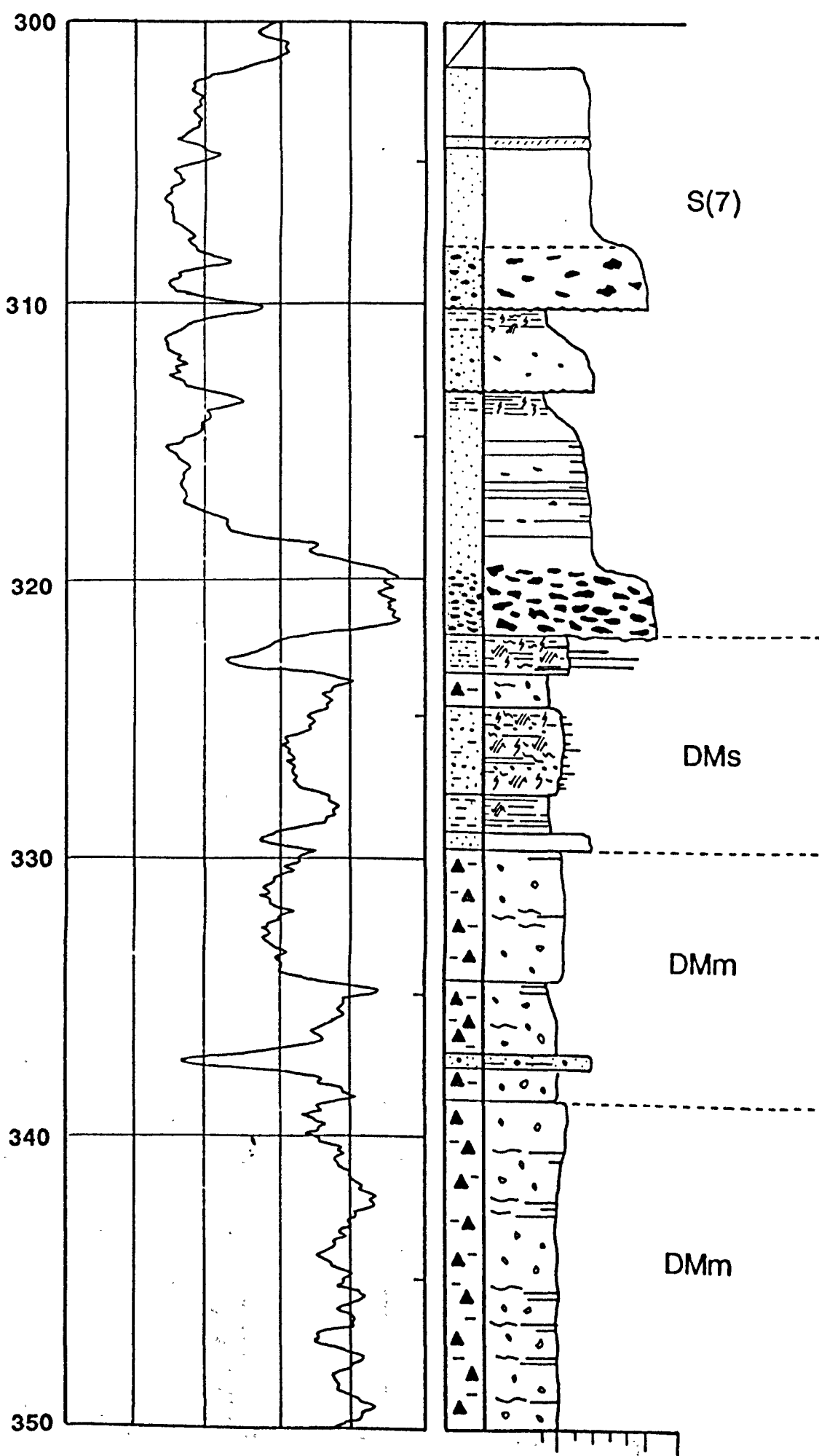
0 200



HOYA 1







250

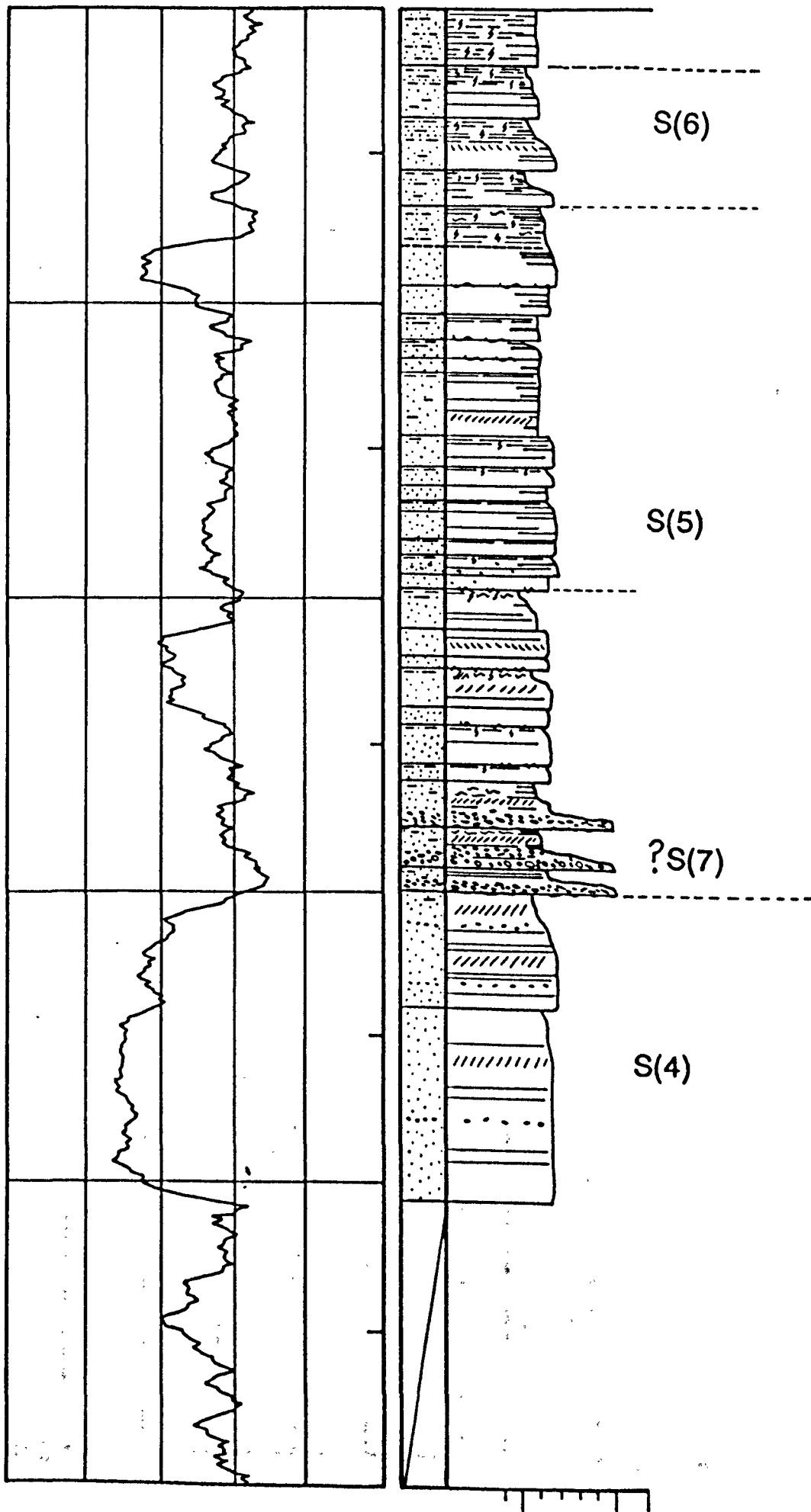
260

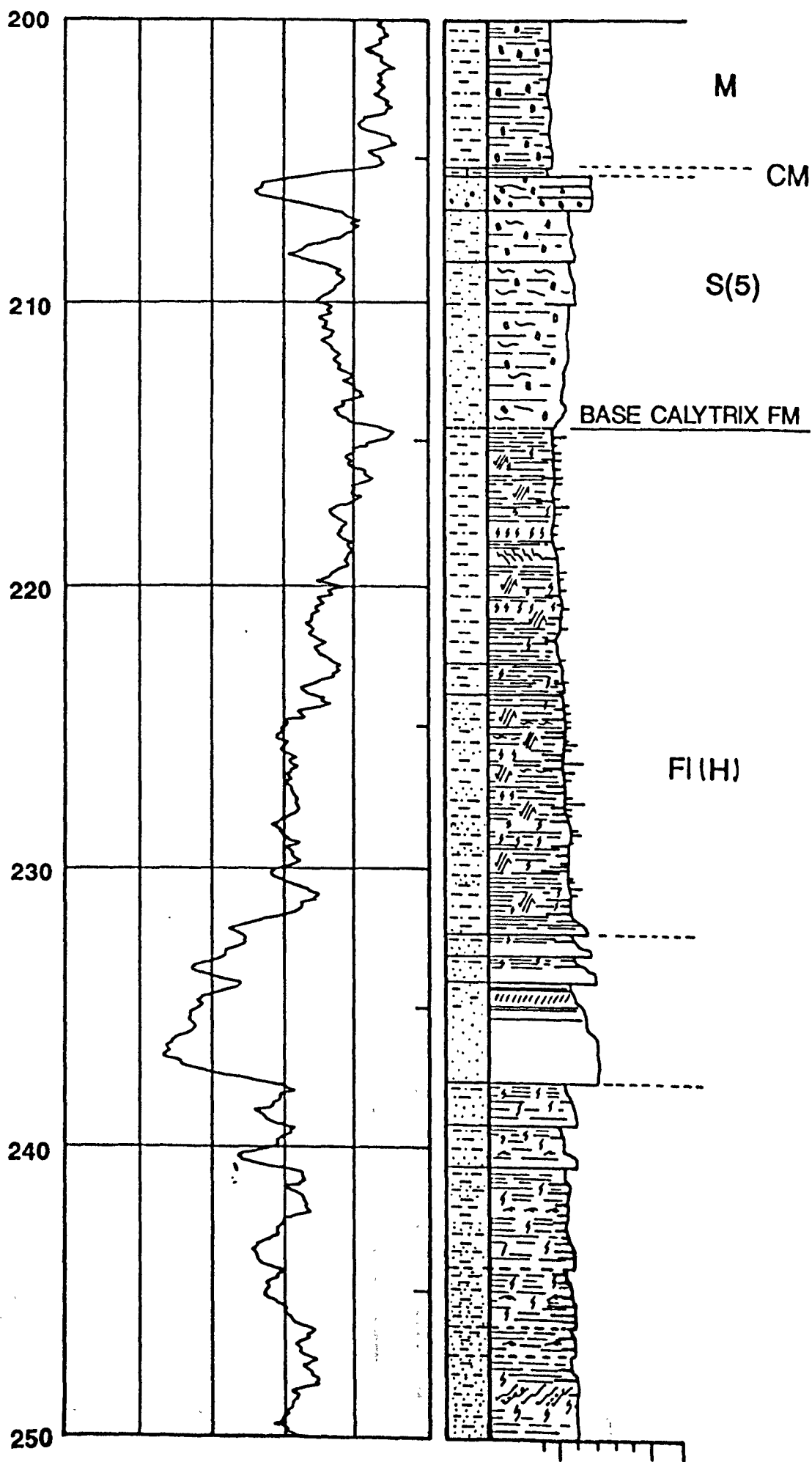
270

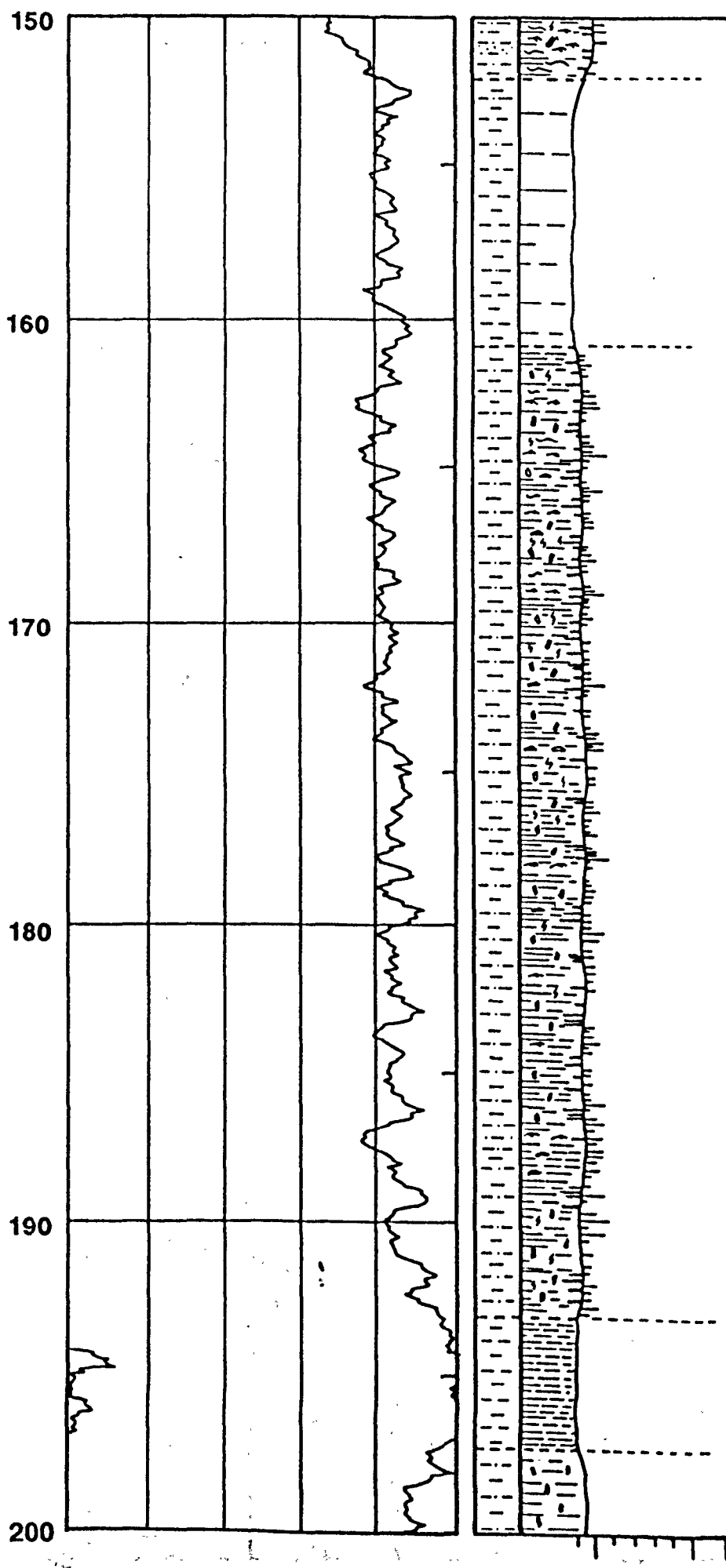
280

290

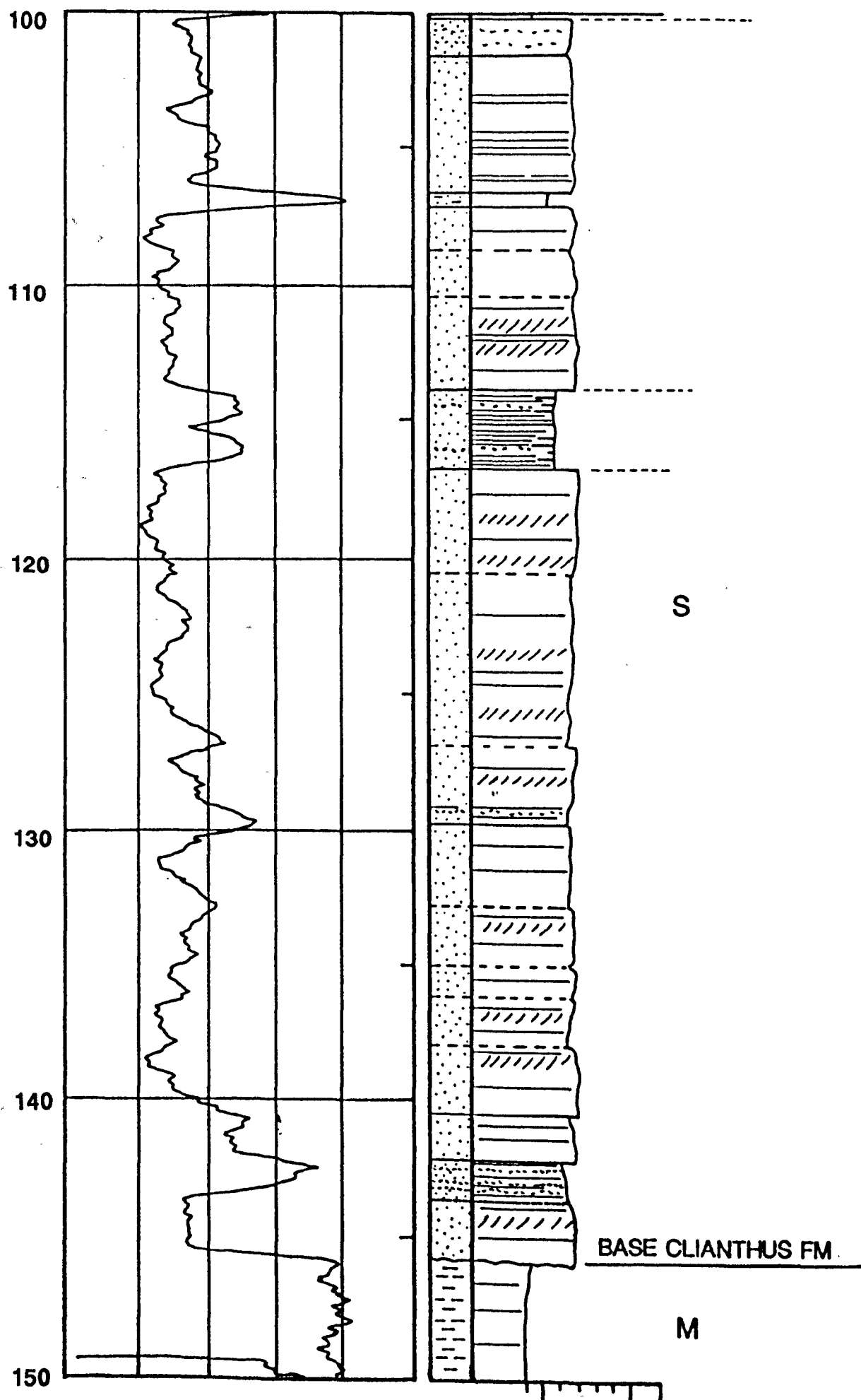
300

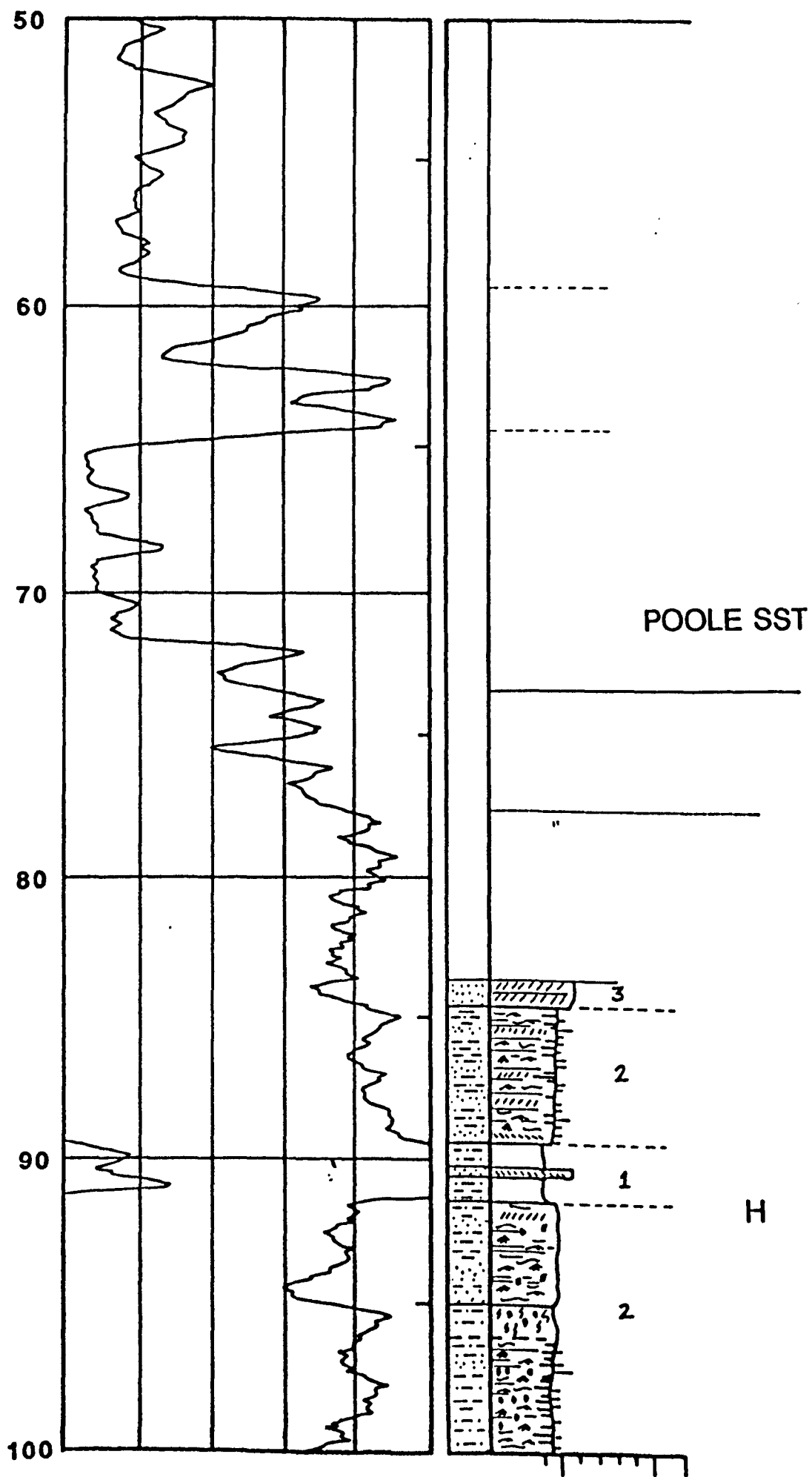




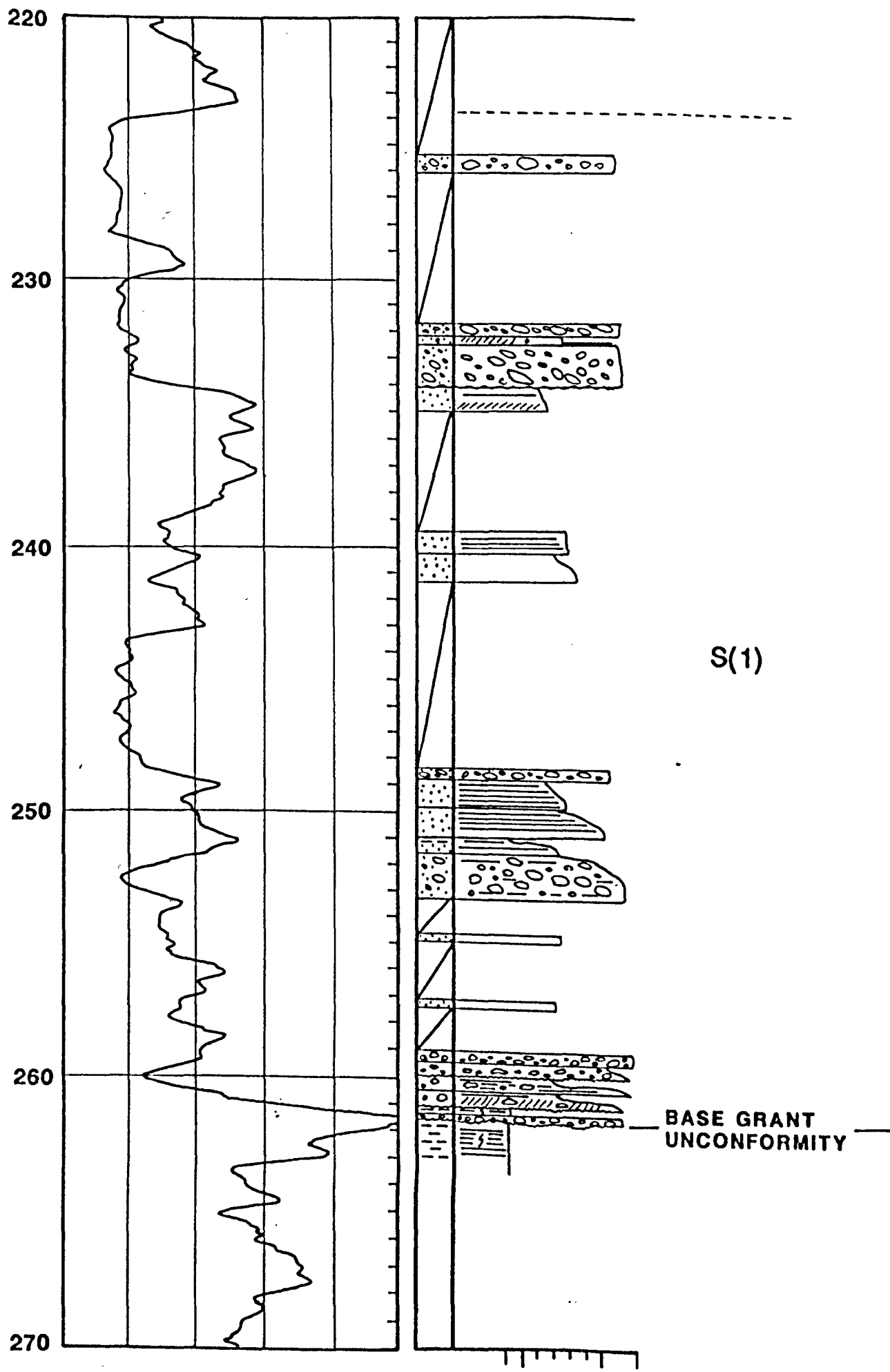


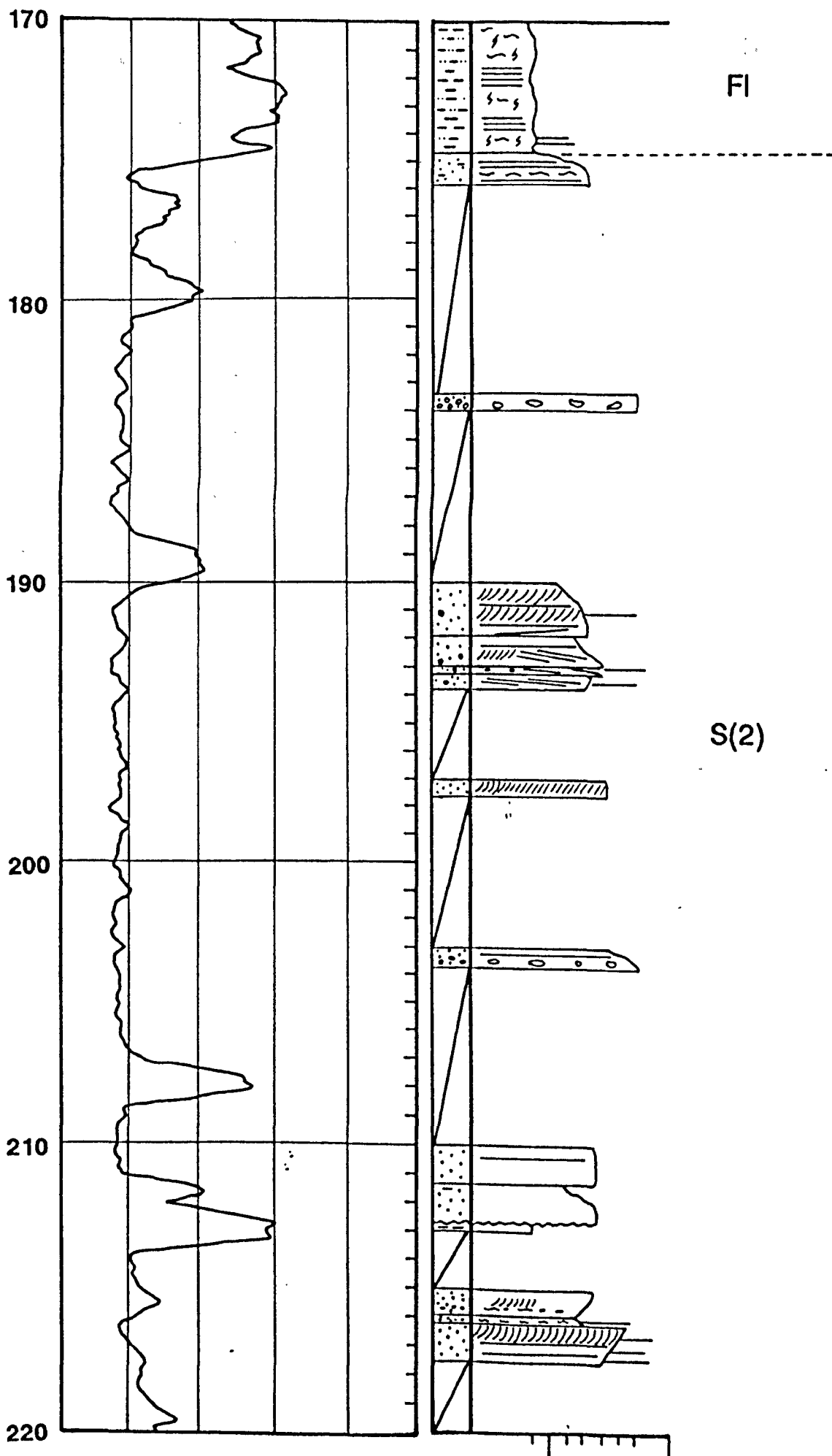
M

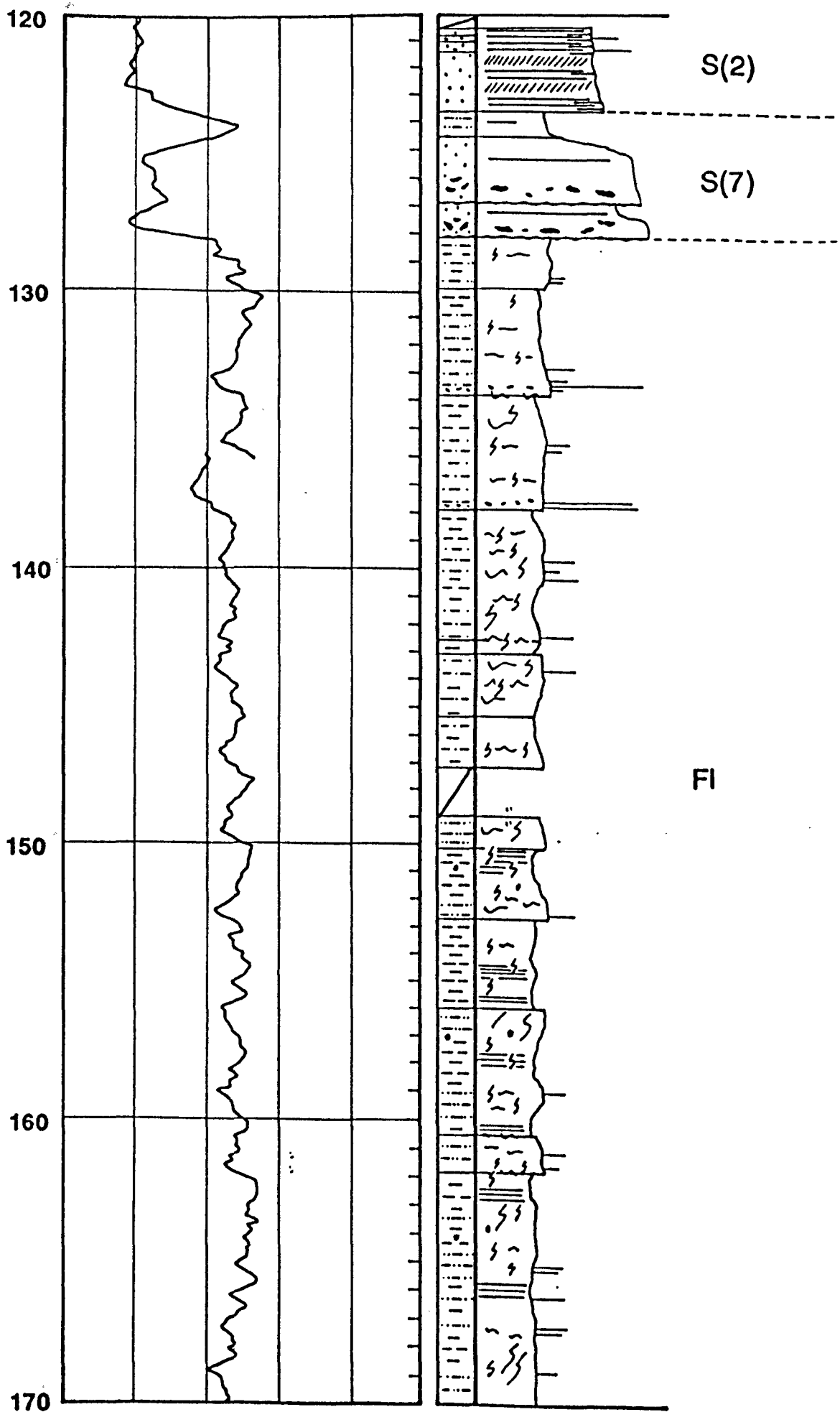


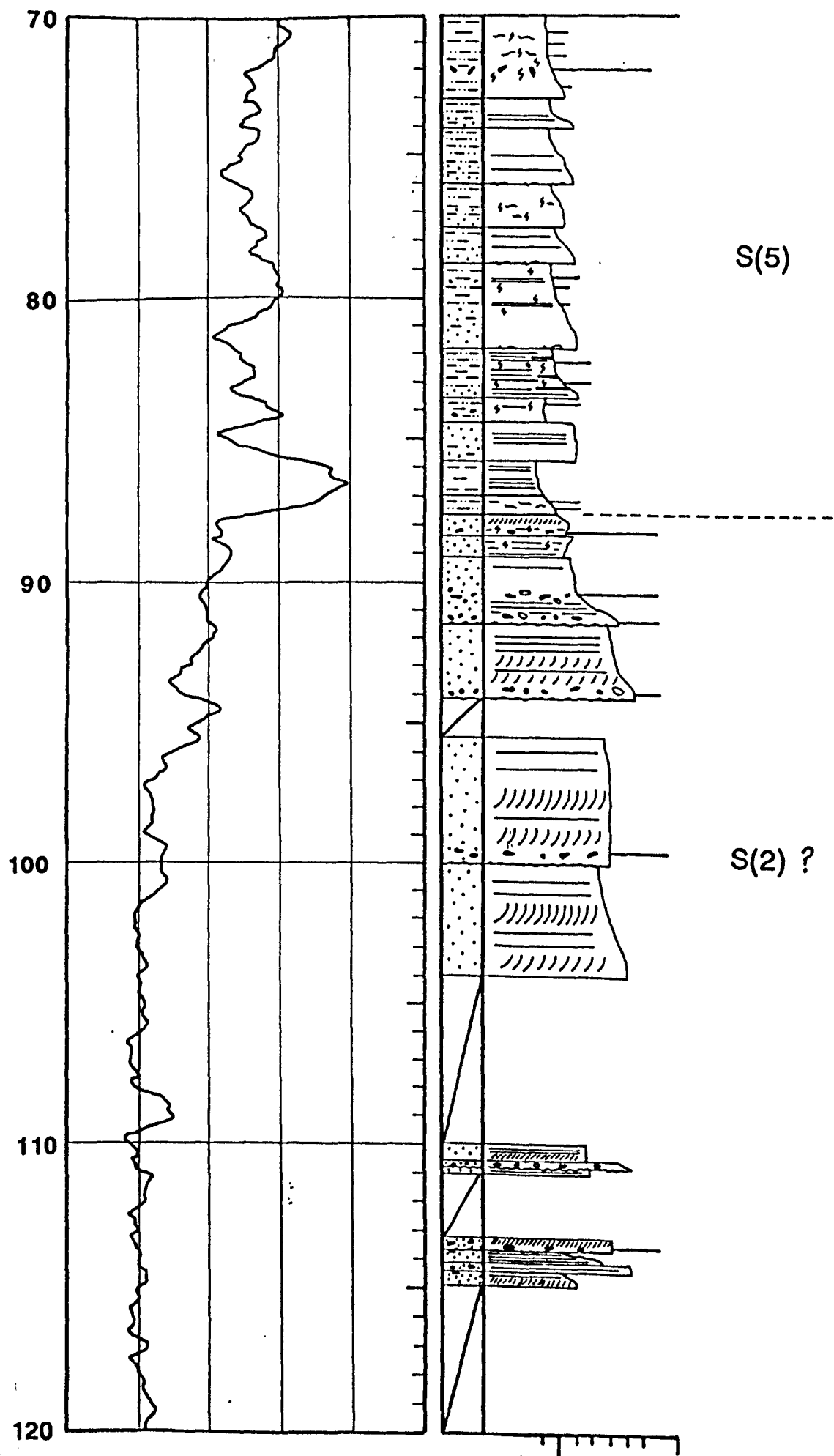


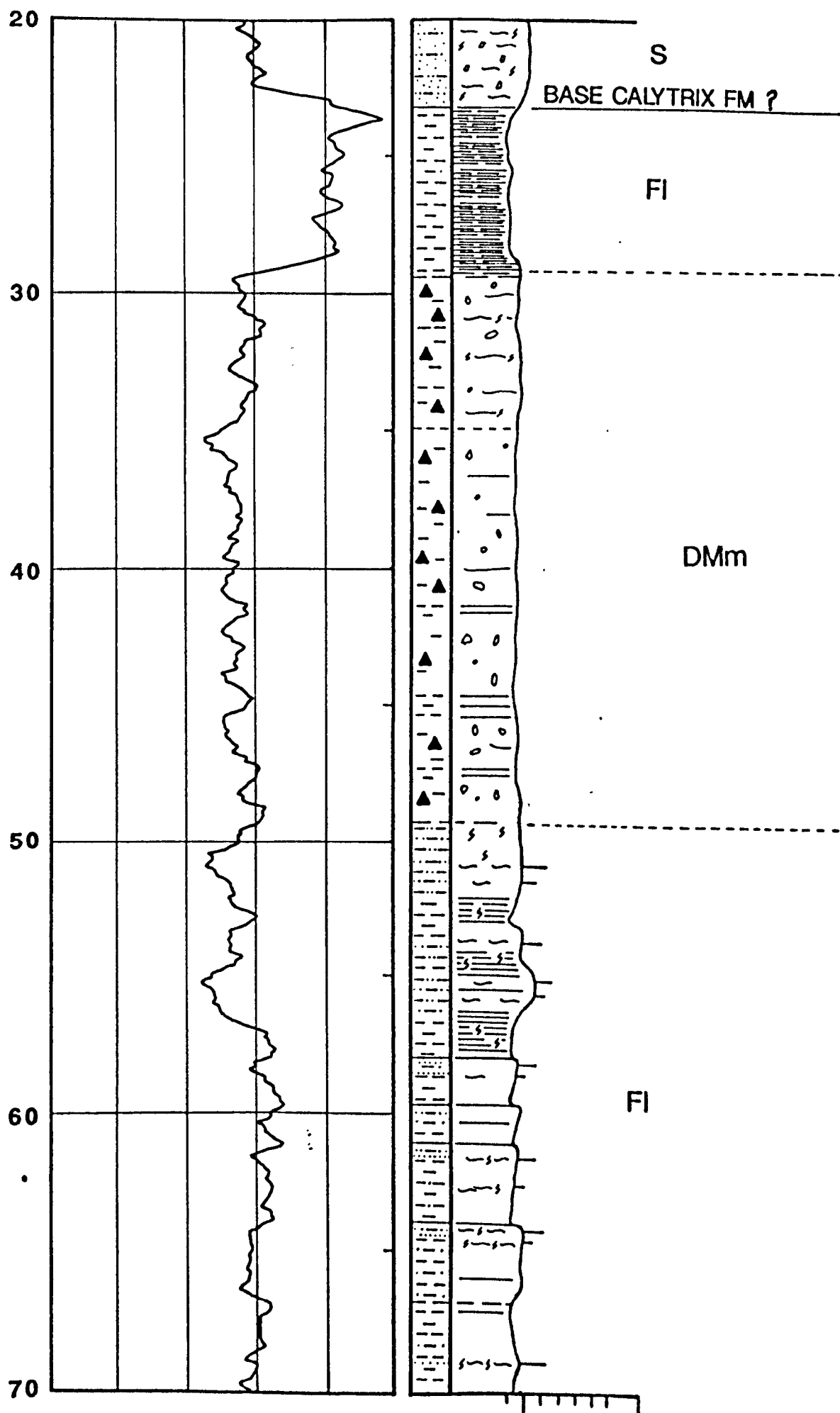
KUNZEA 1



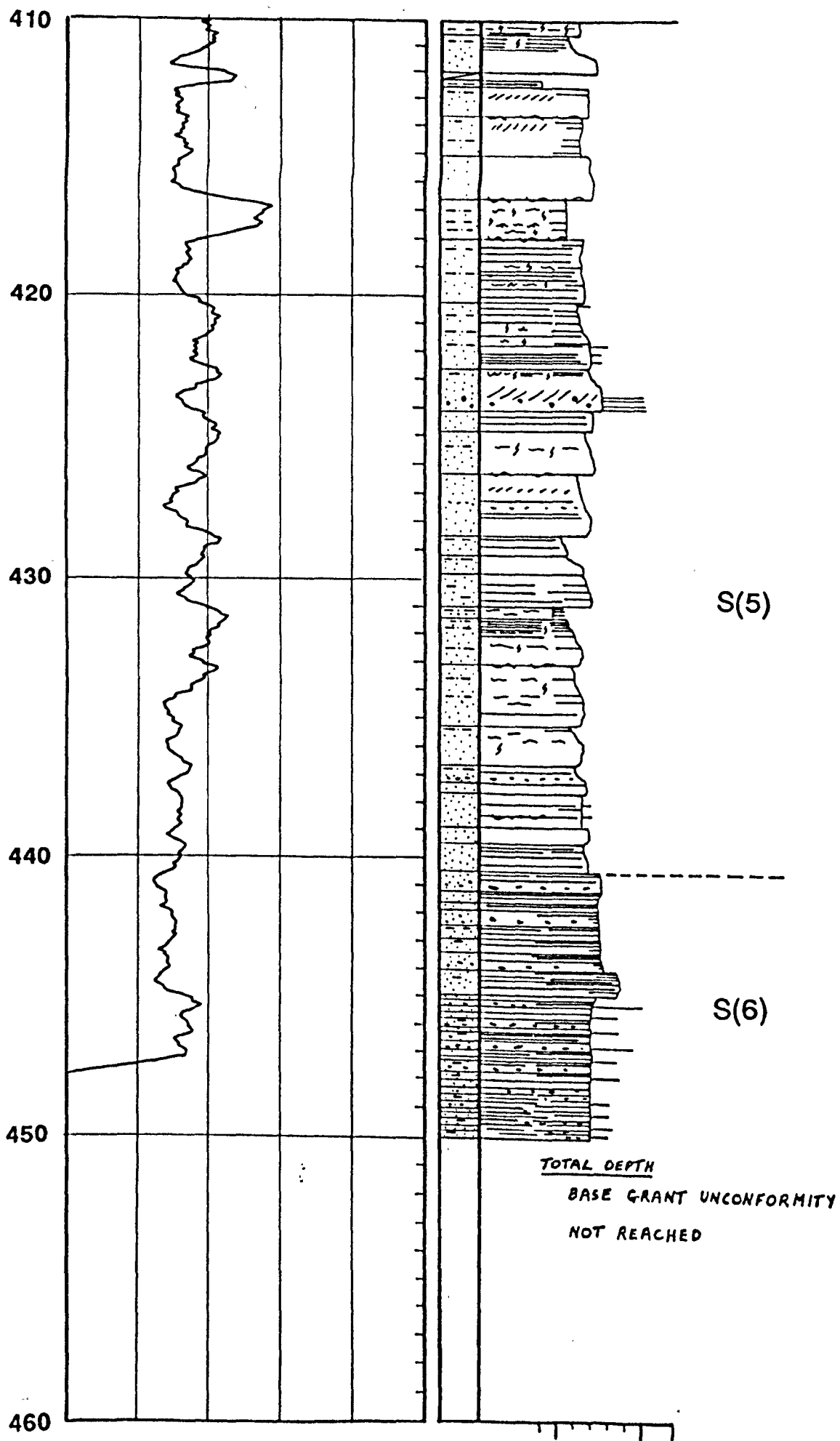


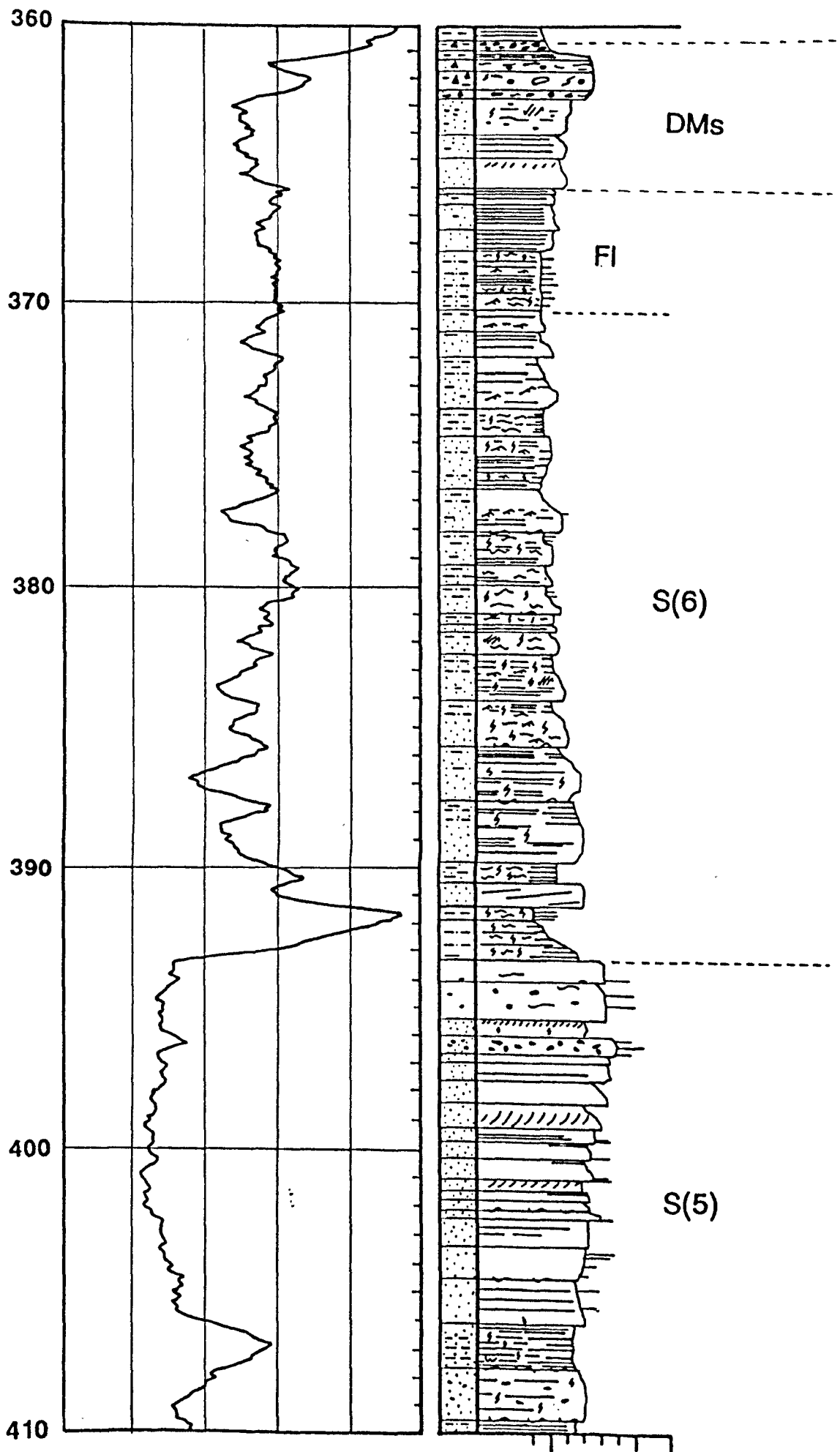


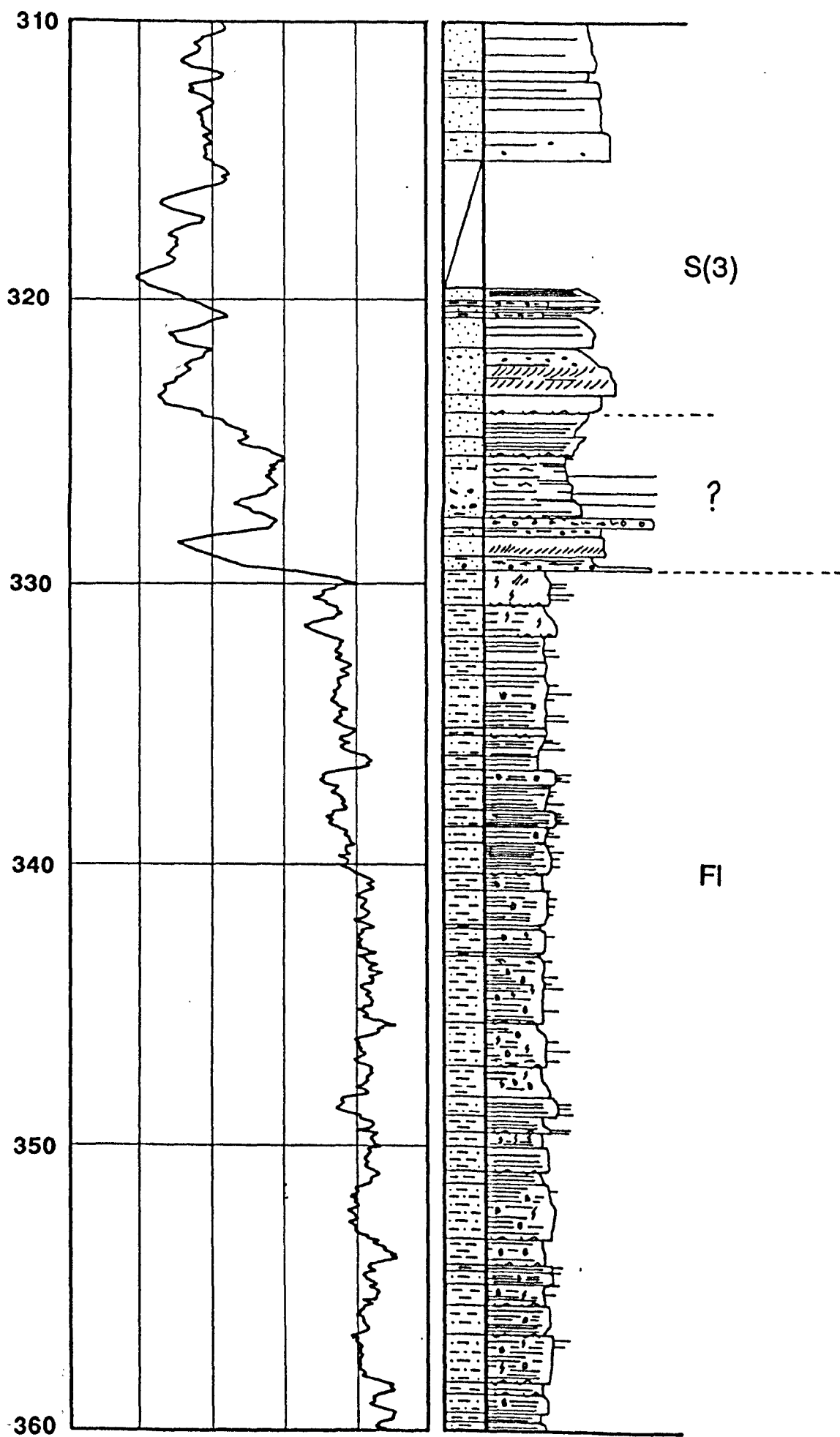




MELALEUCA 1







260

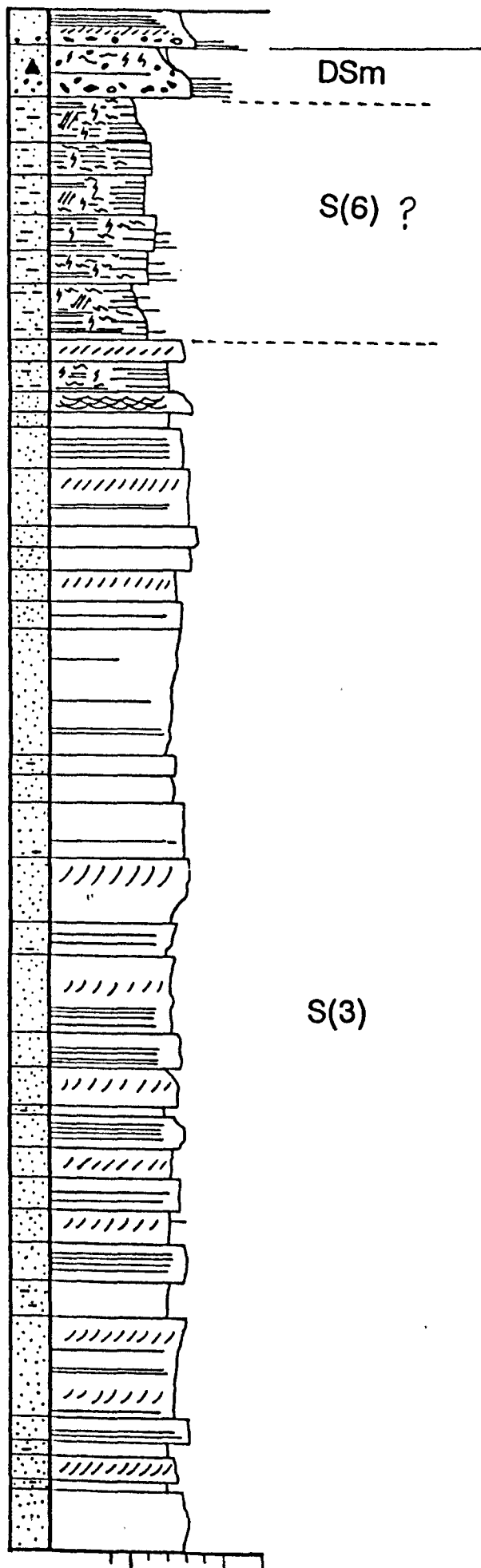
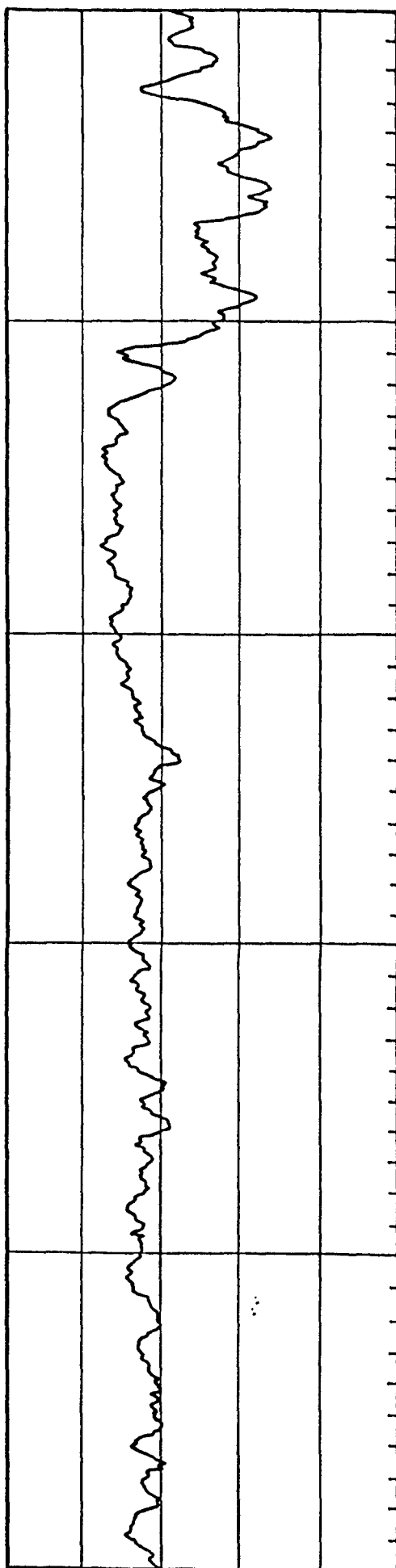
270

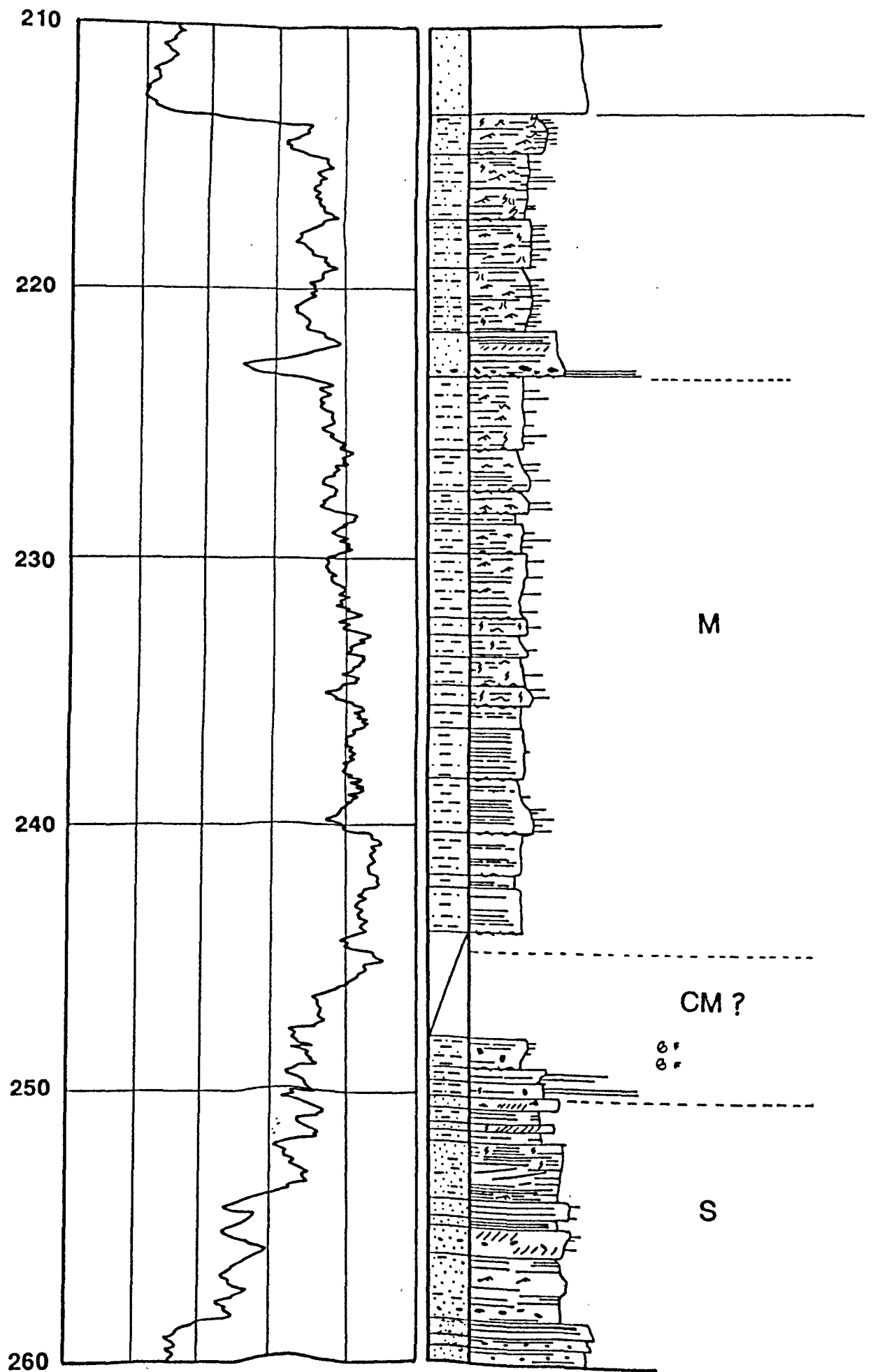
280

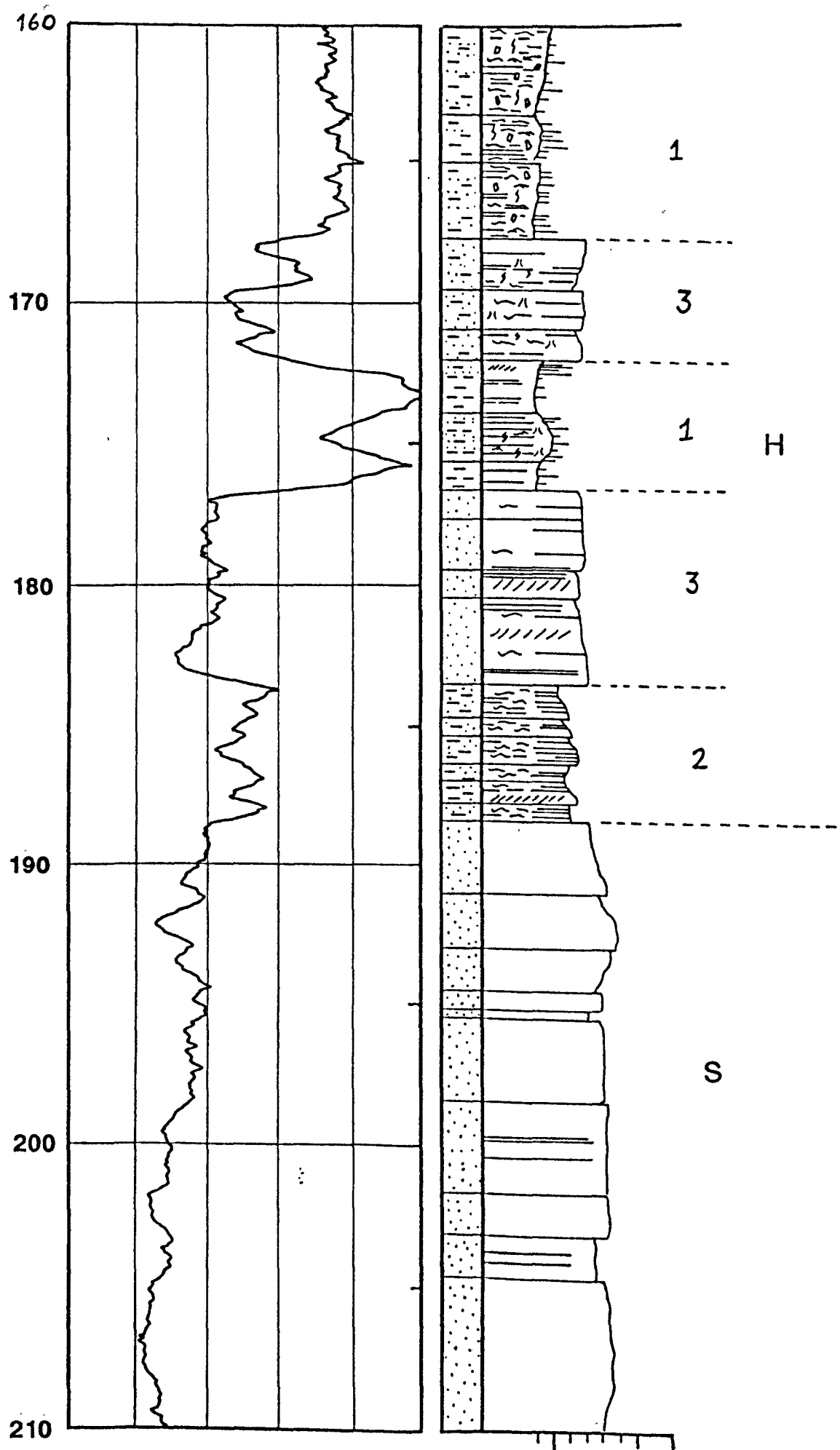
290

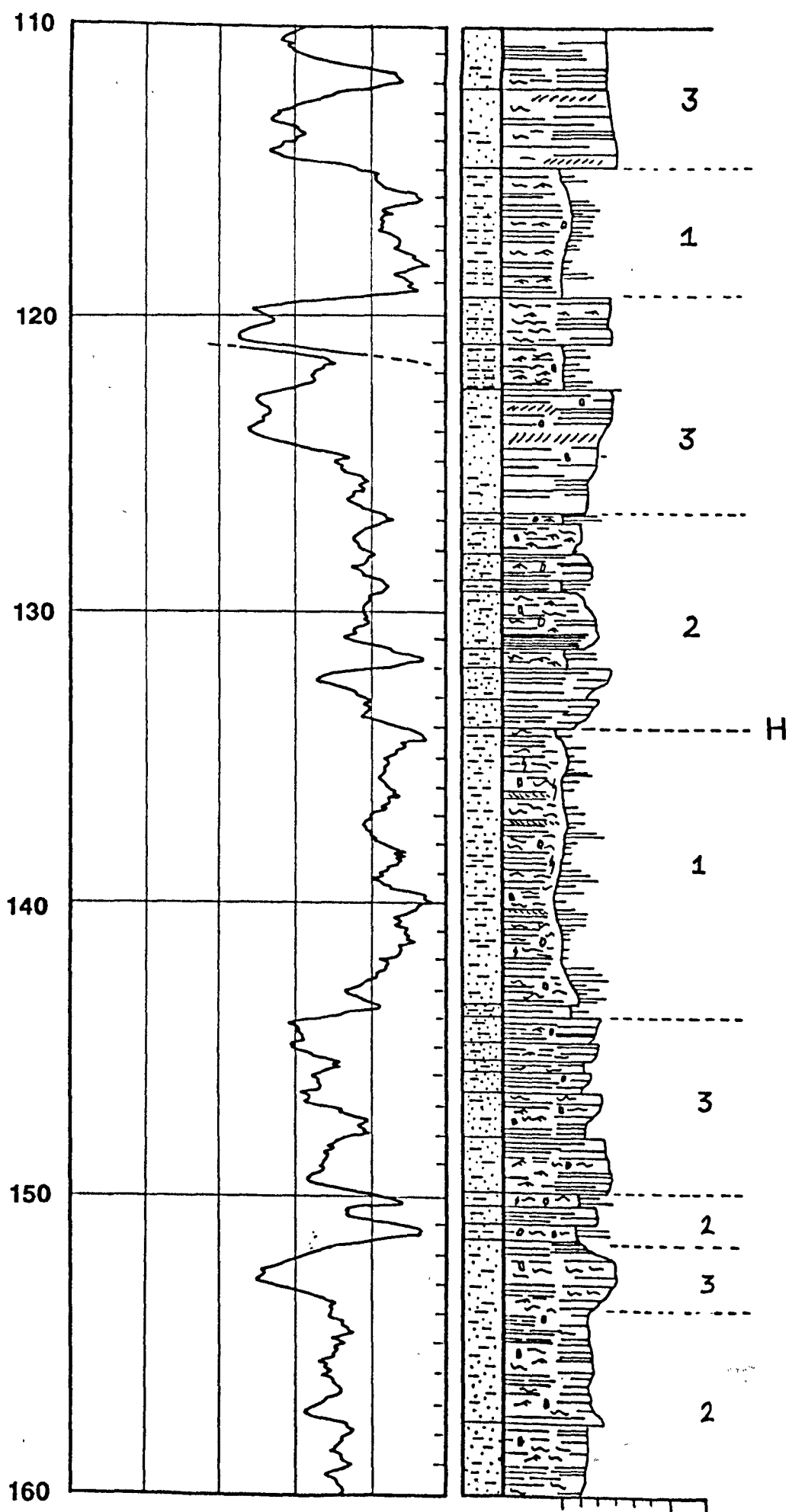
300

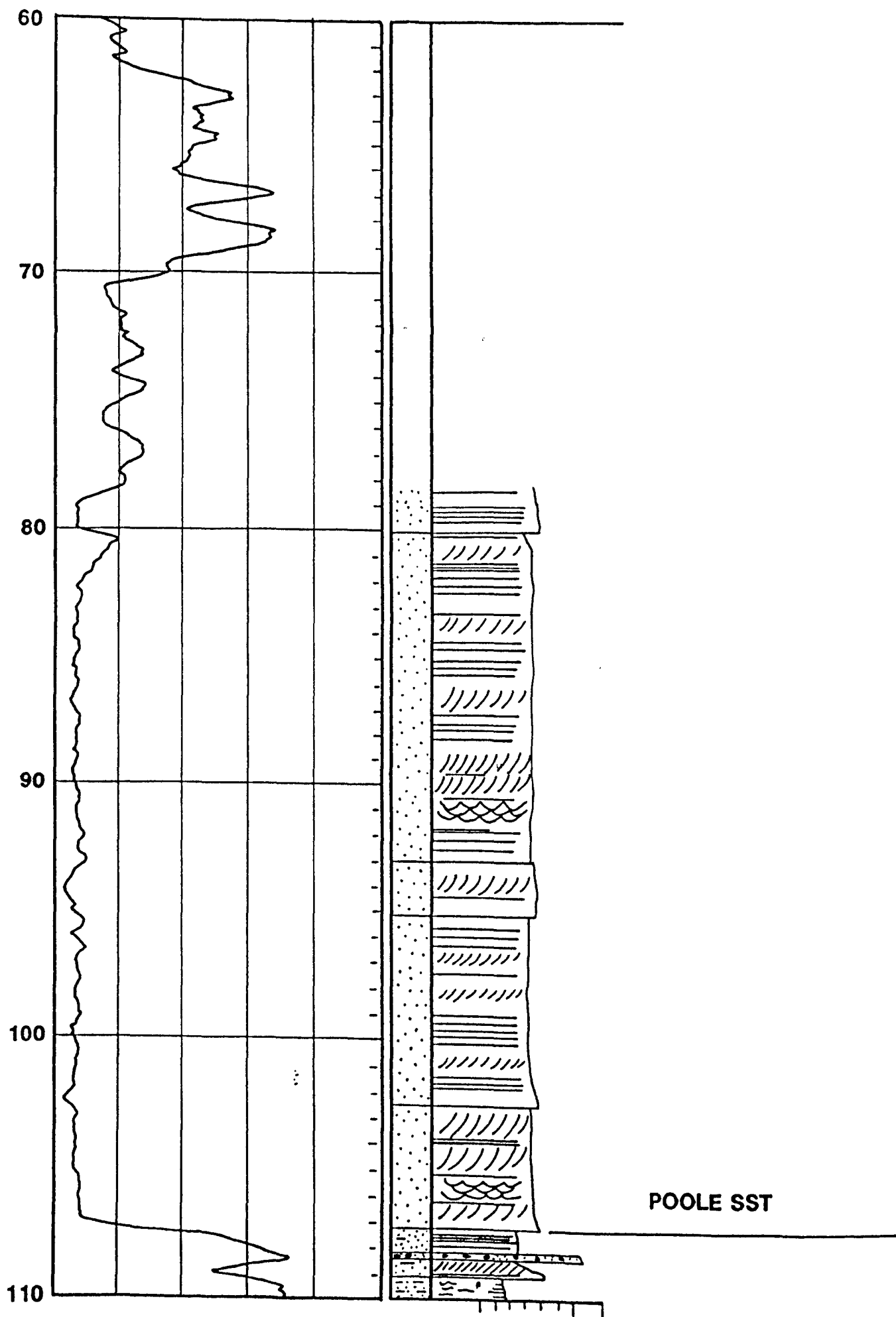
310





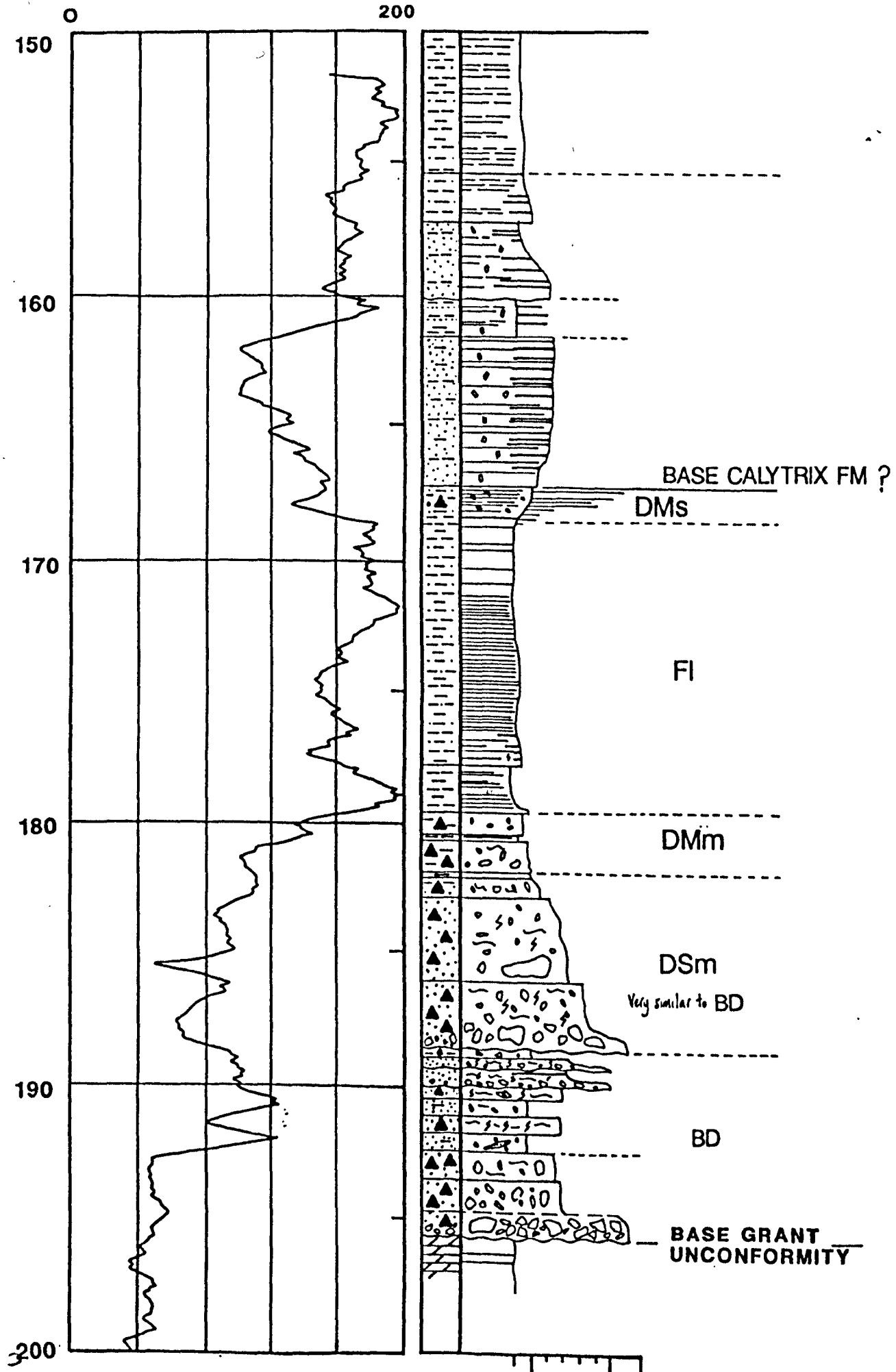






TRIODIA 1

200



APPENDIX 2

WELL NAME		ARISTIDA 1		LOCATION		Lat. 19 53' 55"S Long 125 19' 36"E					
SPUD DATE		18 . 10 . 83		SEISMIC		Line 82-23B SP 602					
ELEV.		177m		TD.		216m		CORED INTERVAL		112 - 216m	
BASE GRANT				206.00m				TWT		N / A	
TOP GRANT				?				SUBCROP		Nullara Lmst Equiv	
THICKNESS				102m+				CORE METERAGE			
BASE HOYA FM				206.00m				NET SANDSTONE		0m	
TOP HOYA FM				153.60m ?				NET / GROSS		N / A	
THICKNESS				52.40m ?				NET DIAMICTITES		47.40m	
BASE CALYTRIX				153.60m?				NET SANDSTONE			
TOP CALYTRIX								NET / GROSS			
THICKNESS											
BASE CLIANTHUS								NET SANDSTONE			
TOP CLIANTHUS								NET / GROSS			
THICKNESS											

WELL NAME		ARISTIDA 1A		LOCATION		Lat. 19 53' 55"S Long 125 19' 36"E	
SPUD DATE		28. 10. 83		SEISMIC		Line 82-23B SP 602	
ELEV.	177m ASL	TD.	734m	CORED INTERVAL		154 -734m	
BASE GRANT		205.15m		TWT			
TOP GRANT		?		SUBCROP		NULLARA LMST EQUIV	
THICKNESS		70m +		CORE METERAGE			
BASE HOYA FM		205.15m		NET SANDSTONE			1m
TOP HOYA FM		151.40m?		NET / GROSS			1 : 154
THICKNESS		53.75m		NET DIAMICTITES			44.95m
BASE CALYTRIX		151.40m?		NET SANDSTONE			
TOP CALYTRIX		145.20m?		NET / GROSS			
THICKNESS		6.2m					
BASE CLIANTHUS		145.20m?		NET SANDSTONE			
TOP CLIANTHUS				NET / GROSS			
THICKNESS							

WELL NAME	CALADENIA 1	LOCATION	Lat. 19 40' 46" Long. 125 06' 26"	
SPUD DATE	5 . 9 . 83	SEISMIC	Line 82-24 SP 322	
ELEV.	170m ASL	TD.	296.5m	CORED INTERVAL 80 - 296.5m
BASE GRANT	139.18m	TWT	Base 126ms	
TOP GRANT	NR	SUBCROP	Nullara Lmst Equiv	
THICKNESS	139.18m +	CORE METERAGE	59.18m	
BASE HOYA FM	139.18m	NET SANDSTONE	1m	
TOP HOYA FM	109.55m	NET / GROSS	1 : 30	
THICKNESS	29.63m	NET DIAMICTITES	20m	
BASE CALYTRIX	109.55m	NET SANDSTONE		
TOP CALYTRIX	35.80m	NET / GROSS		
THICKNESS	73.75m			
BASE CLIANTHUS	35.80m	NET SANDSTONE	35.80m	
TOP CLIANTHUS		NET / GROSS	1 : 1	
THICKNESS				

WELL NAME	CALYTRIX 1	LOCATION	Lat. 20 21' 22.3"S Long. 126 05' 17.5"E	
SPUD DATE	29 . 4 . 84	SEISMIC	Line 84-41 SP 838	
ELEV.	283m ASL	TD.	450m	CORED INTERVAL 84.5 - 450m
BASE GRANT	396m	TWT	Base 199ms	
TOP GRANT	78m	SUBCROP	Nullara Lmst Equiv	
THICKNESS	318m	CORE METERAGE	311.50m	
BASE HOYA FM	396m	NET SANDSTONE	25.60m	
TOP HOYA FM	222m	NET / GROSS	1 : 7	
THICKNESS	174m	NET DIAMICTITES	62m	
BASE CALYTRIX	222m	NET SANDSTONE		
TOP CALYTRIX	143.50m	NET / GROSS		
THICKNESS	78.50m			
BASE CLIANTHUS	143.50m	NET SANDSTONE	32.50	
TOP CLIANTHUS	78m	NET / GROSS	1 : 2	
THICKNESS	65.5m			

WELL NAME	CLIANTHUS 1	LOCATION	Lat. 20 18' 16.6"S Long. 126 05' 19.7"E	
SPUD DATE	14 . 5 . 84	SEISMIC	Line 84-41 SP 1381	
ELEV.	258M ASL	TD.	450m	CORED INTERVAL 112 - 450m
BASE GRANT		NR 450m+	TWT	Base 277ms+ Top 70ms
TOP GRANT		148.50m	SUBCROP	NR Nullara Lmst Equiv
THICKNESS		301.5m +	CORE METERAGE	301.5m
BASE HOYA FM		NR 450m +	NET SANDSTONE	13.50m
TOP HOYA FM		324m	NET / GROSS	1 : 9
THICKNESS		126m	NET DIAMICTITES	30m +
BASE CALYTRIX		324m	NET SANDSTONE	
TOP CALYTRIX		224m	NET / GROSS	
THICKNESS		100m	"	
BASE CLIANTHUS		224m	NET SANDSTONE	38.50m
TOP CLIANTHUS		148.50m	NET / GROSS	1 : 2
THICKNESS		75.5m		

WELL NAME	DROSER 1	LOCATION	Lat. 19 40' 46"S Long. 125 02' 22"E	
SPUD DATE	30 . 3 . 84	SEISMIC	Line 82-24 SP 144	
ELEV.	165m ASL	TD.	450m	CORED INTERVAL 46-450m

BASE GRANT	440.55m	TWT	Base 351ms Top 93ms	
TOP GRANT	? 60m	SUBCROP	Carribuddy Fm	
THICKNESS	380.55m +	CORE METERAGE	380.55m	

BASE HOYA FM	440.55m	NET SANDSTONE	271.35m
TOP HOYA FM		NET / GROSS	1 : 1.4
THICKNESS	380.55m+	NET DIAMICTITES	14m

BASE CALYTRIX		NET SANDSTONE	
TOP CALYTRIX		NET / GROSS	
THICKNESS			

BASE CLIANTHUS		NET SANDSTONE	
TOP CLIANTHUS		NET / GROSS	
THICKNESS			

WELL NAME	EREMOPHILA 1	LOCATION	Lat. 19 46' 49.985"S Long. 125 12' 12.710"	
SPUD DATE	6 . 4 . 82	SEISMIC	Line 82-20A SP	
ELEV.	173.60 ASL	TD.	1252m	CORED INTERVAL 115.6-1252m

BASE GRANT	195.60m	TWT	
TOP GRANT	43m ?	SUBCROP	Nullara Lmst Equiv.
THICKNESS	152.60m	CORE METERAGE	80m

BASE HOYA FM	195.60m	NET SANDSTONE	
TOP HOYA FM	174.30m	NET / GROSS	
THICKNESS	21.30m	NET DIAMICTITES	5m

BASE CALYTRIX	174.30m	NET SANDSTONE	
TOP CALYTRIX	97m ?	NET / GROSS	
THICKNESS	77.30m ?		

BASE CLIANTHUS	97m?	NET SANDSTONE	40m
TOP CLIANTHUS	43m?	NET / GROSS	1 : 1.35
THICKNESS	54m?		

WELL NAME		EREMOPHILA 2		LOCATION		Lat. 19 46' 49" S. Long. 125 13' 05"E					
SPUD DATE		1 . 12 . 83		SEISMIC		Line 82 - 20A SP 655					
ELEV.		173m ASL		TD.		360m		CORED INTERVAL		91 - 360m	
BASE GRANT		228.16m		TWT		Base 232ms					
TOP GRANT		33m?		SUBCROP		Nullara Lmst Equiv					
THICKNESS		195.16m		CORE METERAGE				173.16m			
BASE HOYA FM		228.16m		NET SANDSTONE							
TOP HOYA FM		177m		NET / GROSS							
THICKNESS		51.16m		NET DIAMICTITES				36.50m			
BASE CALYTRIX		177m		NET SANDSTONE							
TOP CALYTRIX		85m		NET / GROSS							
THICKNESS		92m									
BASE CLIANTHUS		85m		NET SANDSTONE				40m			
TOP CLIANTHUS		33m ?		NET / GROSS				1 : 1.3			
THICKNESS		52m?									

WELL NAME	EREMOPHILA 3	LOCATION	Lat. 19 46' 46"S Long. 125 14' 13"E	
SPUD DATE	7 . 12 . 83	SEISMIC	Line 82-20A SP 705	
ELEV.	176m	TD.	464m	CORED INTERVAL 75 - 464m
BASE GRANT		295m	TWT	Base 276ms
TOP GRANT		19m ?	SUBCROP	Nullara Lmst Equiv
THICKNESS		276m ?	CORE METERAGE	219m
BASE HOYA FM		295m	NET SANDSTONE	23m
TOP HOYA FM		193m	NET / GROSS	1 : 2.5
THICKNESS		102m	NET DIAMICTITES	38.50m
BASE CALYTRIX		193m	NET SANDSTONE	
TOP CALYTRIX		78.30m	NET / GROSS	
THICKNESS		114.70		
BASE CLIANTHUS		78.30	NET SANDSTONE	
TOP CLIANTHUS		19	NET / GROSS	
THICKNESS		59.30		

WELL NAME	FICUS 1		LOCATION	Lat. 19 49' 08" S Long. 125 17' 53" E	
SPUD DATE	5 . 1 . 82		SEISMIC	Line 84 - 20 SP 1250	
ELEV.	185m ASL	TD.	1083.7m	CORED INTERVAL	39-52 90-TD
BASE GRANT	474.30m	TWT	Base 348ms		
TOP GRANT	50m ?	SUBCROP	Fairfield Fm		
THICKNESS	424.30m	CORE METERAGE	384.30m		
BASE HOYA FM	474.30m	NET SANDSTONE	99.50m		
TOP HOYA FM	313.40m	NET / GROSS	1 : 1.6		
THICKNESS	160.90m	NET DIAMICTITES	16m		
BASE CALYTRIX	313.40m	NET SANDSTONE			
TOP CALYTRIX	171.20m	NET / GROSS			
THICKNESS	142.20m				
BASE CLIANTHUS	171.20m	NET SANDSTONE			
TOP CLIANTHUS	50m ?	NET / GROSS			
THICKNESS	121.20m				

WELL NAME	GOODENIA 1		LOCATION	Lat. 19 51' 52" S Long. 125 13' 44" E	
SPUD DATE	21 . 11 . 83		SEISMIC	Line 82 - 49 SP 890	
ELEV.	176m	TD.	464m	CORED INTERVAL	75 - 464m
BASE GRANT	105.20m	TWT	Base 130ms		
TOP GRANT	50m ?	SUBCROP	Nullara Lmst Equiv		
THICKNESS	55.20m??	CORE METERAGE	5.20m		
BASE HOYA FM	105.20m	NET SANDSTONE			
TOP HOYA FM	?	NET / GROSS			
THICKNESS	?	NET DIAMICTITES			
BASE CALYTRIX	?	NET SANDSTONE			
TOP CALYTRIX	?	NET / GROSS			
THICKNESS	?				
BASE CLIANTHUS		NET SANDSTONE			
TOP CLIANTHUS		NET / GROSS			
THICKNESS					

WELL NAME	HALGANIA 1		LOCATION	Lat. 19 41' 28"S Long 125 23' 44"E	
SPUD DATE	17 . 8 . 83		SEISMIC	Line 82-24 SP 1079	
ELEV.	200m ASL	TD.	500m	CORED INTERVAL	133 - 500m
BASE GRANT	309.17m	TWT	Base 284ms Nr Top 38ms		
TOP GRANT	26m	SUBCROP	Fairfield/Nullara Lmst		
THICKNESS	283.17m	CORE METERAGE	176.17m		
BASE HOYA FM	309.17m	NET SANDSTONE	32m		
TOP HOYA FM	228.55m	NET / GROSS	1 : 2.5		
THICKNESS	80.62m	NET DIAMICTITES	19m		
BASE CALYTRIX	228.55m	NET SANDSTONE	4.5m		
TOP CALYTRIX	104m ?	NET / GROSS	1 : 27.6		
THICKNESS	124.55m				
BASE CLIANTHUS	104m ?	NET SANDSTONE	N / A		
TOP CLIANTHUS	26m ?	NET / GROSS	N / A		
THICKNESS	78m ?				

WELL NAME	HOYA 1		LOCATION	Lat. 20 23' 37.2"S Long. 126 05' 18.6"E	
SPUD DATE	7 . 5 . 84		SEISMIC	Line 84 - 41 SP 450	
ELEV.	285m ASL	TD.	450m	CORED INTERVAL	85 - 450m
BASE GRANT	434.40m	TWT	Base 249ms Top -3ms		
TOP GRANT	71.80m	SUBCROP	Nullara Lmst Equiv		
THICKNESS	362.60	CORE METERAGE	362.60m		
BASE HOYA FM	434.40m	NET SANDSTONE	26m		
TOP HOYA FM	214.40m	NET / GROSS	1 : 8.5		
THICKNESS	220m	NET DIAMICTITES	60m		
BASE CALYTRIX	214.40m	NET SANDSTONE			
TOP CALYTRIX	145.50m	NET / GROSS			
THICKNESS	68.90m				
BASE CLIANTHUS	145.50m	NET SANDSTONE	41.50m		
TOP CLIANTHUS	72m	NET / GROSS	1 : 1.77		
THICKNESS	73.50m				

WELL NAME	KUNZEA 1		LOCATION	Lat. 19 32' 06.4"S Long. 124 59' 22.9"E	
SPUD DATE	27.5.84		SEISMIC	Line 83-1 SP 4551	
ELEV.	180m ASL	TD.	450m	CORED INTERVAL	8 - 450m
BASE GRANT		260.40m	TWT	Base 254ms Top 70ms	
TOP GRANT		29.50m ?	SUBCROP	Carribuddy Fm	
THICKNESS		230.90m	CORE METERAGE		230.90m
BASE HOYA FM		260.40m	NET SANDSTONE		116.5m
TOP HOYA FM		? 29.50m	NET / GROSS		1 : 2
THICKNESS		? 230.90m	NET DIAMICTITES		19.8m
BASE CALYTRIX			NET SANDSTONE		
TOP CALYTRIX			NET / GROSS		
THICKNESS					
BASE CLIANTHUS			NET SANDSTONE		
TOP CLIANTHUS			NET / GROSS		
THICKNESS					

WELL NAME		MELALEUCA		LOCATION		Lat. 19 41' 17.88"S Long. 125 32' 44.52"E	
SPUD DATE		11 . 4 . 84		SEISMIC		Line 82-24 SP 1472	
ELEV.	198m ASL	TD.	450m	CORED INTERVAL		78 - 450m	
BASE GRANT		450m +		TWT	Base 360ms Top 106ms		
TOP GRANT		107.68m		SUBCROP	Not cored, Fairfield ?		
THICKNESS		342.32m +		CORE METERAGE		372m	
BASE HOYA FM		450m +		NET SANDSTONE		101.30m	
TOP HOYA FM		261.66m		NET / GROSS		1 : 1.85	
THICKNESS		188.34m+		NET DIAMICTITES		4.25m	
BASE CALYTRIX		261.66m		NET SANDSTONE		0	
TOP CALYTRIX		213.91m		NET / GROSS			
THICKNESS		47.75m					
BASE CLIANTHUS		213.91m		NET SANDSTONE		42.6m	
TOP CLIANTHUS		107.68m		NET / GROSS		1 : 2.5	
THICKNESS		106.23m					

WELL NAME	TRIODIA 1	LOCATION	Lat. 19 38' 17"S Long 125 13' 57"E	
SPUD DATE	6 . 1 . 84	SEISMIC	Line 82 - 16 SP 750	
ELEV.	178m	TD.	631m	CORED INTERVAL 139 - 631m
BASE GRANT	195.60m	TWT	Base 192ms	
TOP GRANT	NR	SUBCROP	Nullara Lmst Equiv	
THICKNESS	195.60m+	CORE METERAGE	56m	
BASE HOYA FM	195.60m	NET SANDSTONE	1.5m	
TOP HOYA FM	167.25m	NET / GROSS	1 : 19	
THICKNESS	28.35m	NET DIAMICTITES	28.35m	
BASE CALYTRIX	167.25m	NET SANDSTONE		
TOP CALYTRIX	49m ?	NET / GROSS		
THICKNESS	118.25m?			
BASE CLIANTHUS	49m?	NET SANDSTONE		
TOP CLIANTHUS	At Surface	NET / GROSS		
THICKNESS	49m+?			

APPENDIX 3

MICROPALAEONTOLOGICAL EXAMINATION OF SAMPLES FROM WMC FICUS 1 AND EREMOPHILA 2

V. PALMIERI
Geological Survey of Queensland

FICUS 1

305.06 - 290.00m (7 samples)

Grey sandy mudstones (305-302m); grey mudstones to shales (varvate mud) (301-290m). Pyritic aggregates and pyritic replacement of organic matter (305-296m); hydrocarbon stain (305-302m); rounded quartz grains at 290m; calcite present (305-302m). Immature brachiopods (*Chonetes*) at 305 and 302.9m; gastropods (*Warthia*) at 302.9m, and (*Paraplatyschisma*) at 296m.

Agglutinating foraminifers throughout. The fauna is characterised by textulariid and verneulinid foraminifers in a quite diverse assemblage, probably achieving its acme at 304m.

Within a periglacial marine environment it represents a small transgressive - regressive cycle. The environment is also, overall, a reducing one.

This is believed to be the first Permian transgressive episode of the region and can be correlated, on faunal basis and allowing for facies variation, to: Calytrix 1 220m (base of transgression?) to 199m (acme of marine episode, with relatively more temperate climate); Dampiera 1A at 295.4m (possibly acme of transgression); Eremophila 2 at 205m (base of transgression), 200m and 175m (two acmes of transgression?), 173m (regressive episode).

221 - 209m (11 samples)

Grey silty mudstones, micaceous (muscovite mica flakes).

An agglutinating foraminiferal fauna is present and is dominated by saccamminid and hyperamminid individuals. The fauna represent a small periglacial marine episode and part of it can be correlated to Dampiera 1A at 207m and Eremophila 2 at 152 to 149m.

121 - 118m (5 samples)

Grey claystones and mudstones, laminated, rare silty laminae, abundant plant remains (megaspores). A reducing environment of deposition is suggested by the strong reaction of the samples with oxidising agents. Rare agglutinating foraminifers are present, mostly hyperamminid and subsequently saccamminid and reophacid.

The fauna seems to indicate a very restricted environment, possibly of a fjord-type, with abundant megaspores, which are in general well preserved. It can be correlated to Eremophila 2 at 128 - 125m.

- 2 -

EREMOPHILA 2 205 - 200m (5 samples)

Grey, indurated, silty to sandy mudstones, with rounded or polished quartz and lithic grains at 205 - 201m, some pyritic aggregates at 201 and 200m and some bituminous aggregates at 200m.

Rare crinoid fragments at 200m.

The foraminiferal fauna is represented by the agglutinating hyperamminid, textulariid, ammodiscid and saccamminid forms, complemented by calcareous foraminifers and typified by syzraniiid and protonodosariid (nodosinellid) species at 200.1m; the presence of *Tezaquina clivuli* in this sample indicates its relationship with Calytrix 1 at 199m and subsequently with Dampiera 1A at 295m, and Ficus 1 at 304m.

A periglacial transgressive episode (205m near base of transgression) is indicated, with a more open marine environment at 200.1m.

177 - 173m (5 samples)

Grey silty mudstones, rare pyritic aggregates, some sandy lenses. Small fragments of bryozoans and echinoids at 177-175m. The foraminiferal fauna is represented by hyperamminid, textulariid, ammodiscid, and saccamminid forms, complemented at 175m by calcareous perforate and imperforate foraminifers, suggesting an overall similarity with the sample at 200m. Accordingly another brief transgressive episode is indicated (base of transgression at 177m, base of regression at 173.25). The marine environment seems to be less restricted at 177 to 175m. The fauna can be correlated as the preceding one.

153.40 - 152.40m (2 samples)

Grey varvate clay with mica flakes and common plant remains. Rare megaspores. Some pyritic aggregates and sideritic(?) crystals. No foraminifers. A glacial (lacustrine?) environment is suggested.

151.85 - 149.5m (3 samples)

Grey mudstones, silty at 150.1m; relatively abundant plant remains; some mica flakes. The fauna is represented by rare hyperamminid, saccamminid and trochamminid forms. A correlation seems to be possible with part of Ficus 1 at 220 - 209m and Dampiera 1A at 207m. A small periglacial marine episode with an overall cold, restricted, reducing environment is suggested.

- 3 -

128.6 - 125.4m (4 samples)

Grey silty mudstones with abundant plant remains, common megaspores, common mica flakes. The fauna is represented by hyperamminid and saccamminid forms. It indicates a periglacial environment and can be correlated with Ficus 1 at 121 - 118m.

AGE OF THE FAUNAS

By comparison with and as a complement of the faunas already retrieved from Calytrix 1 and Dampiera 1A, an Early Permian (Asselo-Sakmarian) age is attributed to the assemblages contained in these glacio-marine sediments.

TABLE 1

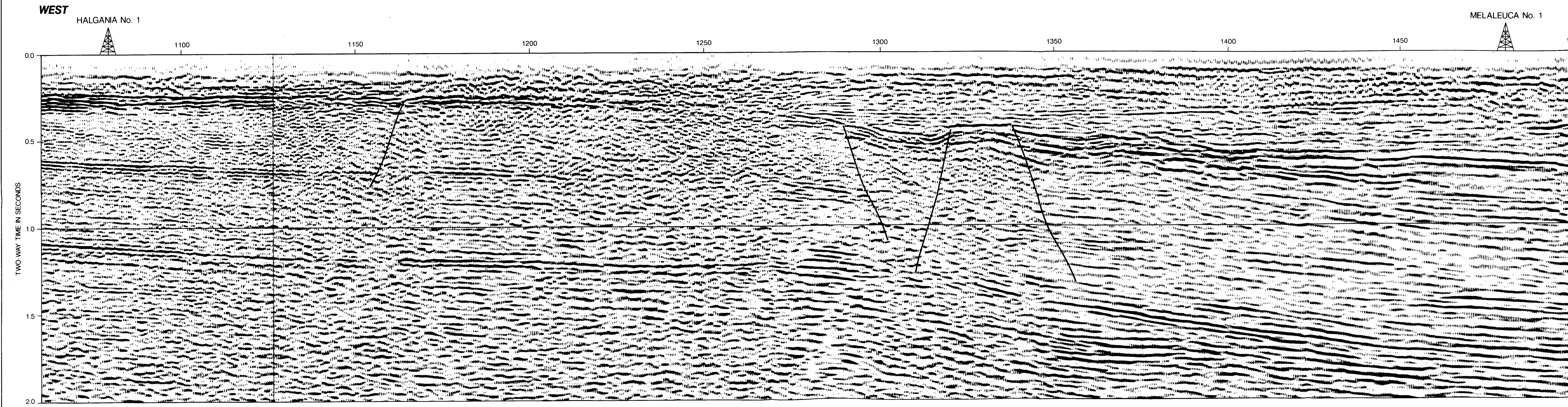
UNIVERSITY
OF BRISTOL
LIBRARY

WELL NAME	DATE	TD	CORED INTERVAL	BASE GRANT	TWT	TOP GRANT	TWT	THICK- NESS	TOP HOYA	THICK- NESS	TOP CALYTRIX	THICK- NESS	TOP CLIANTHUS	THICK- NESS	SUBCROP
ACACIA 1	19.8.81	1208.7	39 - 1208.7	361.6	312	41.50	38	320.10	215	146.60	139	76	41.50	97.50	TS
ARISTIDA 1	18.10.83	216	112 - 216	206.0				102+	153.60	52.40					NLE
ARISTIDA 1A	28.10.83	734	154 - 734	205.15				70+	151.40	53.75	145.20	6.2			NLE
BOAB 1	23.9.81	1033.4	141 - 1033.4	209.50				209.50+							
CALADENIA 1	5.9.83	296.5	80 - 296.5	139.18	126			139.18+	109.55	29.63	35.80	73.75		35.80+	NLE
CALYTRIX 1	29.4.84	450	84.5 - 450	396	199	78		318	222	174	143.5	78.5	78	65.5	NLE
CASSIA 1	2.11.81	850.3	129 - 850.3	549.9		45.8		504.1							F
CAPPARIS 1	21.1.84	521	19 - 521	212.40	158	23?	0	189	168	44.4			23?		PLE
CLIANTHUS 1	14.5.84	450	112 - 450	450+		148.5	70	301.5	324	126	224	100	148.50	75.5	NLE
DAMPIERA 1A	10.2.82	1856.9	129 - 1856.9	377.95	348	75		302.95	298.25	79.70	135 ?	163.25	75	60	F
DROSSERA 1	30.3.84	450	46 - 450	440.55	351	60?	93	380.55?	60?	380.55?					C
EREMOPHILA 1	6.4.82	1252	115.5 - 1252	195.60	184	43?	48	152.60	174.30	21.30	97?	77.30	43?	54	NLE
EREMOPHILA 2	1.12.83	360	91 - 360	228.16	232	33?		195.16	177	51.16	85	92	33	52	NLE
EREMOPHILA 3	7.12.83	464	75 - 464	295	276			295+	193	102	78.30	114.70			NLE
FRANKENIA 1	1.2.84	479	42 - 479	248.25	226	42	57	206.25	192	56.25	162	30	42	120	NLE
FICUS 1	5.1.82	1083.7	90 - 1083.7	474.30	348	50?		424.30	313.40	160.90	171.20	142.20	50?	121.20	F
GOODENIA 1	21.11.83	163.3	102 - 163.3	105.20	130	50?		105.20?							NLE - F?
HALGANIA 1	17.8.83	500	133 - 500	309.17	284	26	38	283.17	228.55	80.62	104?	124.55	26?	78	F
HOYA 1	7.5.84	450	85 - 450	434.40	249	71.80	-3	362.60	214.40	220	145.50	68.9	72	73.50	NLE
KUNZEA 1	27.5.84	450	8 - 450	261.40	254	29.50	70	230.90	?						C
MELALEUCA 1	11.4.84	450	78 - 450	450+		107.68	106	342.32	261.66	188.34	213.91	47.75	107.68	106.23	F
PANICUM 1	21.3.84	278	108 - 278	179.34	160	33?	41	146.34?							PLE
PRATIA 1	12.2.84	464	22.5 - 464	299.62	262	46?	38	253.62	232	67.62	152	80?	46?	106	PLE
SANTALUM 1A	24.9.83	629.30	252.75 - 629.3	321	256	110	83	211	196	125	173.50	22.50	110	63.50	C
SOLANUM 1	22.2.84	834	6-47 93-834	137	141			137+							C
TRIODIA 1	6.1.84	631	139 - 631	195.60	192			195.60+	167.25	28.35	49	118.25		49+	NLE
TYPHA 1	11.3.84	395	106.5 - 395	225.53	208	30	48	195.53	123?	102.53					F

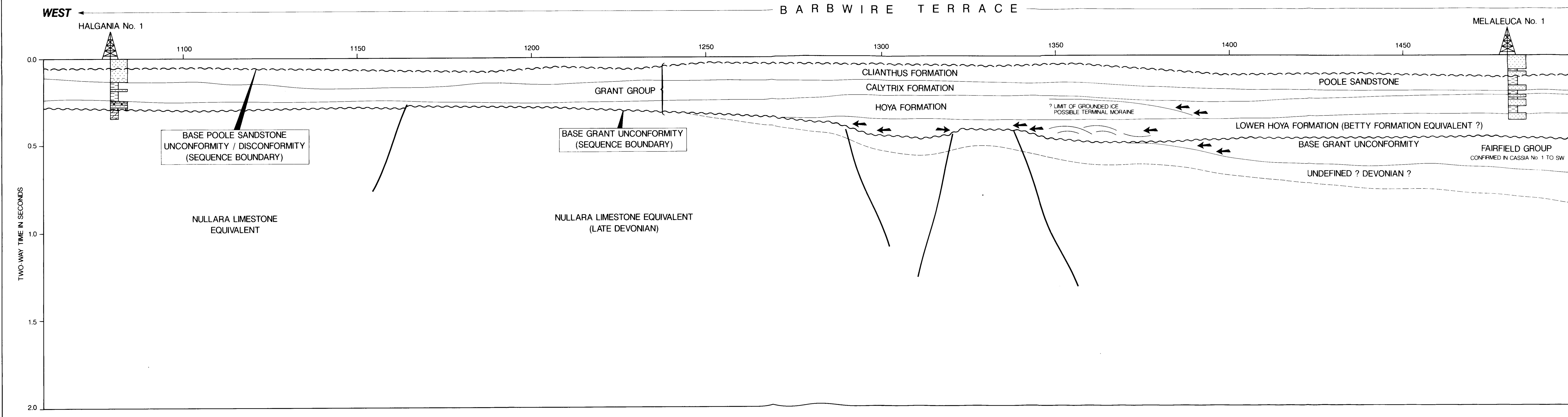
NOTES: 1. All depths and thicknesses are given in metres. 2. Two-Way Time (TWT) given in milliseconds. 3. + Indicates top or base not recorded.
4. Bold typeface = cores examined Normal typeface = boundaries log picks and preliminary. 5. ? uncertain boundary.
6. SUBCROP TS = Tandalgoo Sst. NLE Nullara lmst Equiv. PLE = Pillara Lmst Equiv. C = Carribuddy Fm F = Fairfield Group
7. Date = spud date for well.

ENCLOSURE

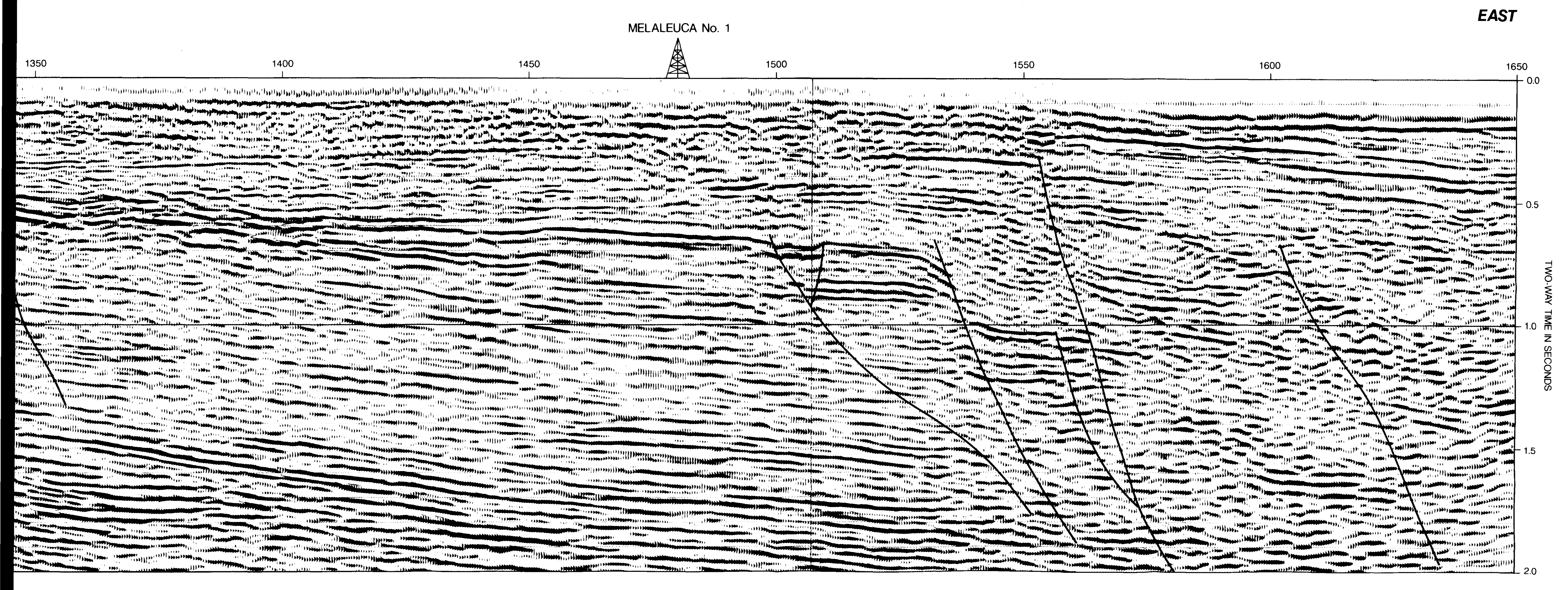
SEISMIC SECTION



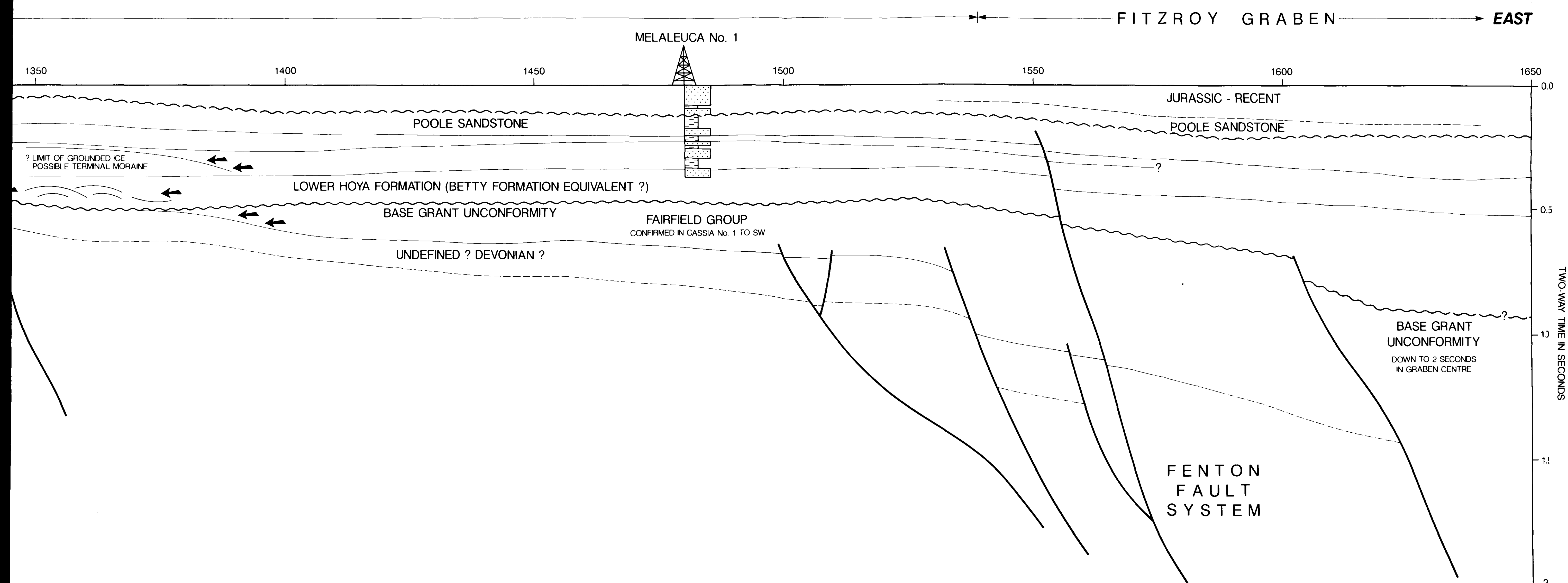
GEOSEISMIC INTERPRETATION



IC SECTION



C INTERPRETATION



CANNING BASIN
WESTERN AUSTRALIA

LINE W82 - 24
SP 1060 - 1650
SEISMIC SECTION AND
INTERPRETATION

ENCLOSURE 1

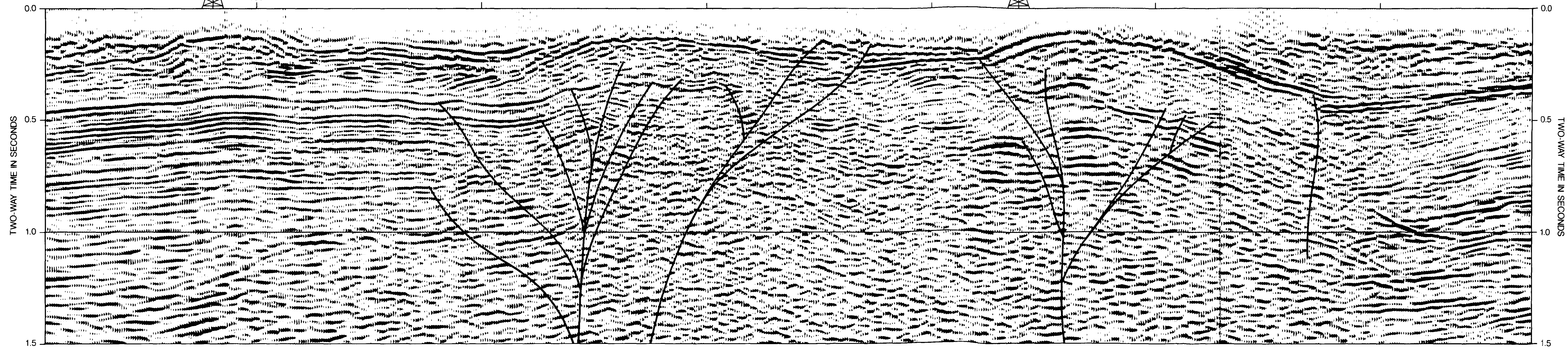
SEISMIC SECTION

WEST

EAST

DROSERA No.1

CALADENIA No.1



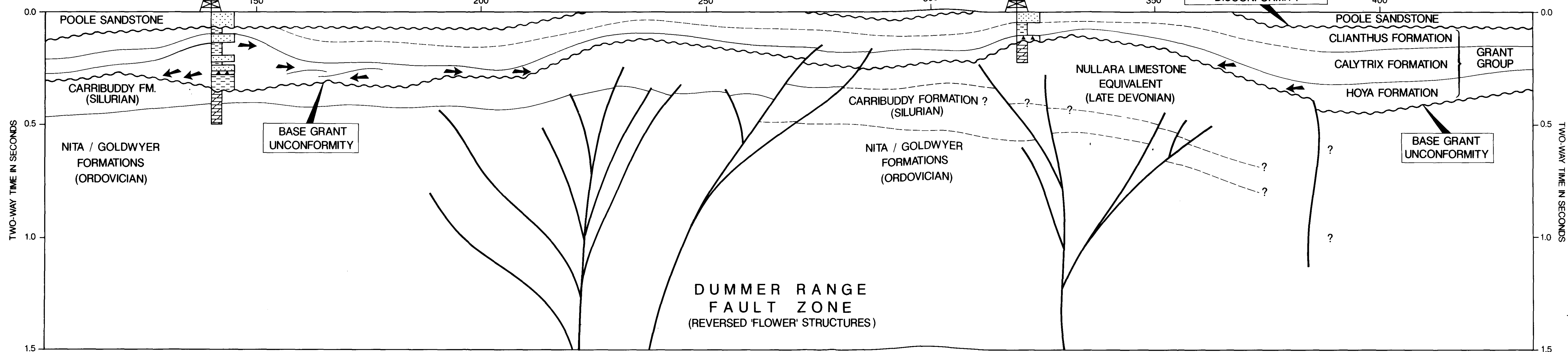
GEOSEISMIC INTERPRETATION

WEST

EAST

DROSERA No.1

CALADENIA No.1



1 KILOMETRE

CANNING BASIN
WESTERN AUSTRALIA

LINE W82 - 24
SP 110 - 440
SEISMIC SECTION AND
INTERPRETATION

ENCLOSURE 2